OFDM-Based Relay Systems for Next Generation Networks



Shuping Dang

Harris Manchester College

Department of Engineering Science, University of Oxford

Supervised by Prof. Justin P. Coon and Prof. Dominic O'Brien

A thesis submitted to the University of Oxford for the degree of Doctor of Philosophy in Engineering Science

November 2017

Abstract

Thesis Title: OFDM-Based Relay Systems for Next Generation Networks
Name: Shuping Dang
College: Harris Manchester College
Degree: Doctor of Philosophy
Term and Year of Submission: Michaelmas 2017

The performance of four newly proposed orthogonal frequency-division multiplexing (OFDM)-based relay systems with different application scenarios are analyzed in this thesis. The first scenario that is studied relates to the bulk and per-subcarrier relay selections, which can be regarded as two extremes of the performance-complexity trade-off in multi-carrier relay selection. Specifically, the outage performance yielded by these two selection schemes is analyzed in spatially random networks where relays are randomly distributed. Subsequently, a novel selection scheme for OFDM-based relay systems is proposed by combining conventional bulk and per-subcarrier selections. The asymptotic outage performance of the combined selection scheme in the high signal-to-noise (SNR) region is analyzed, and it is found that the combined selection can achieve the optimal outage probability without using the full set of available relays for selection. Hence, a satisfactory solution to the performance-complexity trade-off can be obtained. Apart from conventional application scenarios, OFDM-based relay systems with relay selections are also analyzed in more practical scenarios, e.g., device-to-device (D2D) communications. However, due to the adoption of underlay D2D communication protocol, power control mechanisms are thereby necessary to be applied to mitigate the interference to conventional cellular communications, which lead to a series of new analytical challenges. Meanwhile, to incorporate with new modulation techniques, OFDM-based relay systems are also combined with index modulation (IM). Then, an adaptive OFDM-IM is proposed for two-hop relay networks to enhance the system reliability when there is only one relay, and relay selection is thereby infeasible. Specifically, in this proposed adaptive OFDM-IM, the mapping schemes between a bit stream and indices of active subcarriers are adaptively selected by a certain criterion. All these analyses for a variety of cases given in this thesis constitute a comprehensive analytical framework for OFDM-based relay systems in next generation networks.

Acknowledgments

First and foremost, I express my sincere gratitude to my supervisor Prof. Justin P. Coon for his continuous support of my study and related research in Oxford, as well as his patience, motivation, and immense knowledge. His guidance and detailed comments help me in all the time of research and writing of this thesis. Without his support, it would not be possible to conduct my research smoothly in these years.

Also, I specially thank Dr. Gaojie Chen and Dr. David E. Simmons, who recommended a tremendous number of relevant papers for my research and are always patient to answer my questions. Meanwhile, as my regular collaborators, they also provided a huge number of helpful suggestions and comments on our publications and pointed out the right directions for my technical works.

Meanwhile, my sincere thanks also go to Mr. Hachem Yassine, Mr. Dene A. Hedges, Dr. Shahriar E. Tajbakhsh and Mr. Jinchuan Tang as well as other colleagues, who provided me an opportunity to learn from them and widen my horizon. Besides, I would also like to say 'thank you' to the reviewers of my publications and the examiners of my works, who provided indispensable comments to improve the quality of my research.

In addition, I express the gratitude toward China Scholarship Council (CSC), which awarded me a full scholarship (No. 201508060323) covering tuition fee, college fee and living expenses for my D.Phil study in the UK. Thanks also go to other funds supporting my study during the three years in Oxford, which include funds from EU FP7 DIWINE Project (CNET-ICT-318177) and EPSRC SEN Project (EPSRC EP/NN002350/1), Edgell Sheppee Fund, Harris Manchester College Fund, IARU-Santander GSP Scholarship, Oxford Alumni Association Bursary and Siew-Sngiem Award.

Most importantly, to my beloved parents, grandparents, and wife, I thank you all for your unconditional support and encouragement throughout my study period in Oxford.

List of Publications

Journal Publications

1. **S. Dang**, G. Chen and J. P. Coon, "Outage Performance of Two-Hop OFDM with Index Modulation and Multi-Carrier Relay Selections," in *IEEE Wireless Communications Letters* (under review).

2. **S. Dang**, G. Chen and J. P. Coon, "Multicarrier Relay Selection for Full-Duplex Relay-Assisted OFDM D2D Systems," in *IEEE Transactions on Vehicular Technology* (under review).

3. **S. Dang**, J. P. Coon and G. Chen, "Adaptive OFDM with Index Modulation for Two-Hop Relay-Assisted Networks," in *IEEE Transactions on Wireless Communications*, 2017.

4. **S. Dang**, J. P. Coon and G. Chen, "Outage Performance of Two-Hop OFDM Systems with Spatially Random Decode-and-Forward Relays," in *IEEE Access*, 2017.

5. **S. Dang**, G. Chen and J. P. Coon, "Outage Performance Analysis of Full-Duplex Relay-Assisted Device-to-Device Systems in Uplink Cellular Networks," in *IEEE Transactions on Vehicular Technology*, vol. 66, no. 5, pp. 4506-4510, May 2017.

6. **S. Dang**, J. P. Coon and G. Chen, "Resource Allocation for Full-Duplex Relay-Assisted Device-to-Device Multicarrier Systems," in *IEEE Wireless Communications Letters*, vol. 6, no. 2, pp. 166-169, Apr. 2017.

7. **S. Dang**, J. P. Coon and G. Chen, "An Equivalence Principle for OFDM-Based Combined Bulk/Per-Subcarrier Relay Selection Over Equally Spatially Correlated Channels," in *IEEE Transactions on Vehicular Technology*, vol. 66, no. 1, pp. 122-133, Jan. 2017.

Conference Publications

1. **S. Dang**, G. Chen and J. P. Coon, "Power Allocation for Adaptive OFDM Index Modulation in Cooperative Networks," *Proc. IEEE GLOBECOM*, Singapore, 2017.

2. **S. Dang**, J. P. Coon, G. Chen and D. E. Simmons, "Outage performance Analysis of Multicarrier Relay Selection for Cooperative Networks," *Proc. IEEE ISCC*, Heraklion, Greece, 2017.

3. **S. Dang**, J. P. Coon and D. E. Simmons, "Combined Bulk/Per-Subcarrier Relay Selection in Two-Hop OFDM Systems," *Proc. IEEE VTC Spring*, Nanjing, China, 2016.

4. **S. Dang**, D. E. Simmons and J. P. Coon "Comparison of Multicarrier Relay Selection Schemes in Super Dense Networks," *Proc. IEEE CAMAD*, Guildford, UK, 2015.

5. **S. Dang**, J. P. Coon and D. E. Simmons, "Combined Bulk and Per-Tone Relay Selection in Super Dense Wireless Networks," *Proc. IEEE ICC*, London, UK, 2015.

Acronyms

AF	Amplify-and-forward
AP	Access point
APM	Amplitude and phase modulation
AWGN	Additive white Gaussian noise
A/D	Analog-to-digital (conversion)
BER	Bit error rate
bpcu	Bit per channel use
BPP	Binomial point process
BS	Base station
CDF	Cumulative distribution function
CDMA	Code-division multiple access
CP	Cyclic prefix
CSI	Channel state information
CR	Cognitive radios
CUE	Cellular user equipment
dB	Decibel
DF	Decode-and-forward
DUE	Device-to-device user equipment
D2D	Device-to-device
D/A	Digital-to-analog (conversion)
FBMC	Filter-bank based multi-carrier
FDMA	Frequency-division multiple access
FFT	Fast Fourier transform
FG	Fixed-gain
FPSK	frequency and phase shift keying
GFDM	Generalized frequency-division multiplexing
ICI	Inter-channel interference
IEEE	Institute of Electrical and Electronics Engineers
IFFT	Inverse fast Fourier transform
i.i.d.	Independent and identically distributed
IM	Index modulation
IMT-A	International Mobile Telecommunications Advanced
IoT	Internet of Things

IP	Internet protocol
ISI	Inter-symbol interference
LTE	Long-Term Evolution
LTE-A	Long-Term Evolution Advanced
MIMO	Multiple-input and multiple-output
ML	Maximum-likelihood
M2M	Machine-to-machine
nG	nth generation (network)
ni.i.d.	Non-independent and identically distributed
NOMA	Non-orthogonal multiple access
OFDM	Orthogonal frequency-division multiplexing
OFDM-IM	Orthogonal frequency-division multiplexing with index modulation
OOK	On-off keying
PAPR	Peak-to-average power ratio
PCP	Poisson cluster process
PDF	Probability density function
PEP	Pairwise error probability
PGFL	Probability generating functional
PHY	Physical (layer)
PMF	Probability mass function
PPP	Poisson point process
PSK	Phase-shift keying
QAM	Quadrature amplitude modulation
QoS	Quality of service
QPSK	Quadrature phase shift keying
SC-FDMA	Single-carrier frequency-division multiple access
SER	Symbol error rate
SI	Self-interference
SIC	Successive interference cancellation
SINR	Signal-to-interference-plus-noise ratio
SIR	Signal-to-interference ratio
SM	Spatial modulation
SNR	Signal-to-noise ratio
SWIPT	Simultaneous wireless information and power transfer
TAS	Transmit antenna selection
TDMA	Time-division multiple access
TD-SCDMA	Time-division synchronous code-division multiple access
VG	Variable-gain
VR	Virtual reality
WCDMA	Wideband code-division multiple access
WiMAX	Worldwide Interoperability for Microwave Access
WLAN	Wireless local area networks

WSN	Wireless sensor networks
3GPP	Third Generation Partnership Project

Contents

Abstract i

Acknowledgments ii

List of Publications iii

Acronyms v

List of Figures xi

List of Tables xiv

List of Mathematical Notations xvi

1 Introduction 1
- 1.1 Evolution of Wireless Communication Networks 1
- 1.2 Motivation for Applying OFDM-Based Relay Systems 3
- 1.3 Thesis Contributions and Organization 5

2 Research Overview 9
- 2.1 Relay-Assisted Cooperative Communications 11
  - 2.1.1 Cooperative Networks and Relay Networks 12
  - 2.1.2 Half- and Full-Duplex Relaying 14
  - 2.1.3 Amplify-and-Forward Relaying 15
  - 2.1.4 Decode-and-Forward Relaying 16
- 2.2 OFDM 18
- 2.3 OFDM-Based Relay Systems: Pros and Cons 21
  - 2.3.1 Merits of OFDM-Based Relay Systems 22
    - 2.3.1.1 Diversity 22
    - 2.3.1.2 Energy Efficiency 23
    - 2.3.1.3 Spectrum Efficiency 23
    - 2.3.1.4 Network Coverage Extension 25
    - 2.3.1.5 Load Balancing among Base Stations 25
    - 2.3.1.6 Cost Efficiency 26
    - 2.3.1.7 Scalability and Flexibility 27
  - 2.3.2 Drawbacks of OFDM-Based Relay Systems 27
    - 2.3.2.1 Transmission Delay 27

2.3.2.2 Complexity and Signaling Overhead 28
2.3.2.3 PAPR and Nonlinear Distortion 29
2.4 Multi-Carrier Relay Selections 29
2.4.1 Bulk Relay and Per-Subcarrier Selections 30
2.4.2 Combined Relay Selection 31
2.5 Summary 34

3 OFDM-Based Relay Selection with Spatially Random Relays 36
3.1 System Framework and Channel Model 37
3.2 Outage Performance Analysis with Multi-Carrier Relay Selections . 39
3.2.1 Bulk Relay Selection 41
3.2.1.1 Finite Relay Distribution Region 41
3.2.1.2 Infinite Relay Distribution Region 42
3.2.2 Per-Subcarrier Relay Selection 42
3.2.2.1 Finite Relay Distribution Region 42
3.2.2.2 Infinite Relay Distribution Region 43
3.3 Discussion of Important System Properties 43
3.3.1 Cooperative Diversity Analysis 44
3.3.2 Comparison of Outage Performance between Bulk and Per-Subcarrier Selections 45
3.3.3 Optimization of the Number of Subcarriers for Bulk Selection 46
3.4 Numerical Simulations and Discussion 49
3.4.1 Outage Performance of Bulk and Per-Subcarrier Selections . 49
3.4.2 Relation between Relay Node Density and Multi-Relay Performance Advantage 50
3.4.3 Relation between the Number of Subcarriers and System Throughput 53
3.4.4 Numerical Study of Combined Selection in Random Networks 54
3.5 Summary 55
3.6 Appendices 57
3.6.1 Proof of Diversity Gain in Infinite Poisson Random Networks 57
3.6.2 Proof of the Approximation of $\phi(\lambda)$ for Small λ 58
3.6.3 Proof of the Concavity of $\kappa(\tilde{K}, \lambda)$ in Terms of $\tilde{K}$ 59

4 OFDM-Based Relay Systems with Combined Relay Selection over Spatially Correlated Channels 61
4.1 System Framework 62
4.2 Outage Performance Analysis with Combined Relay Selection . . . 64
4.2.1 Conditionally Independent Variable Transformation 64
4.2.2 Asymptotic Outage Performance: a Generalized Theorem . . 66
4.3 Asymptotic Outage Performance Analysis with Different Forwarding Protocols 69
4.3.1 Decode-and-Forward Relaying 69
4.3.2 Fixed-Gain Amplify-and-Forward Relaying 70
4.3.3 Variable-Gain Amplify-and-Forward Relaying 71
4.4 Numerical Simulations and Discussion 72

4.4.1 Verification of Analytical Results . . . 72
4.4.2 Comparison among Different Forwarding Protocols . . . 75
4.4.3 Effects of Outage Threshold . . . 75
4.5 Summary . . . 76
4.6 Appendices . . . 78
4.6.1 Derivation of Asymptotic Outage Probability of Decode-and-Forward Relaying . . . 78
4.6.2 Derivation of Asymptotic Outage Probability of Fixed-Gain Amplify-and-Forward Relaying . . . 80
4.6.3 Derivation of Asymptotic Outage Probability of Variable-Gain Amplify-and-Forward Relaying . . . 83

5 Full-Duplex Relay-Assisted OFDM D2D Systems 84
5.1 System Framework . . . 86
5.2 Decode-and-Forward Relaying in D2D Communication Networks . . 88
5.3 Definitions of Outage Probability with Multi-Carrier Relay Selections 89
5.3.1 Full-Duplex Systems . . . 89
5.3.2 Half-Duplex Systems . . . 89
5.4 Outage Performance Analysis . . . 90
5.4.1 Bulk Relay Selection . . . 92
5.4.2 Per-Subcarrier Relay Selection . . . 97
5.5 Outage Performance Optimization . . . 98
5.5.1 Dynamic Power Control Mechanism . . . 99
5.5.2 Static Power Control Mechanism . . . 100
5.6 Numerical Simulations and Discussion . . . 100
5.6.1 Verification of Analytical Results . . . 100
5.6.2 Performance Benefits by Relay Selections and Comparisons . 103
5.6.2.1 Effects of μ_{SR} and μ_{RD} . . . 103
5.6.2.2 Effects of μ_{SB} and μ_{RB} . . . 104
5.6.2.3 Effects of μ_{CR} and μ_{CD} . . . 105
5.6.3 Comparison between Dynamic and Static Power Control Mechanisms . . . 106
5.6.4 Comparison between Full-Duplex and Half-Duplex Transmissions . . . 108
5.6.5 Verification of Outage Performance Optimization Strategies 110
5.7 Summary . . . 110
5.8 Appendices . . . 112
5.8.1 Proof of Equivalence of Optimization Problems Formulated in (5.45) and (5.46) . . . 112
5.8.2 Proof of Quasi-Concavity of the Optimization Problem Formulated in (5.47) . . . 113
5.8.3 Proof of Quasi-Concavity of the Optimization Problem Formulated in (5.49) . . . 115

6 Adaptive OFDM with Index Modulation for Relay Networks 117
6.1 System Framework . . . 118
6.2 Mapping Scheme Selections and Performance Evaluation Metrics . . 121
6.2.1 Signal Model and Dual-Mode Transmission Protocol 122
6.2.2 Decentralized Mapping Scheme Selection . . . 124
6.2.3 Centralized Mapping Scheme Selection . . . 125
6.2.4 Performance Evaluation Metrics . . . 127
6.2.4.1 Average Outage Probability . . . 127
6.2.4.2 Average End-to-End Capacity . . . 128
6.2.4.3 Average Symbol Error Rate . . . 128
6.2.5 Comparison Benchmarks . . . 129
6.2.5.1 Conventional OFDM-IM . . . 129
6.2.5.2 FPSK . . . 130
6.3 Performance Analysis for Decentralized Mapping Scheme Selection . 132
6.3.1 Outage Performance Analysis . . . 132
6.3.2 End-to-End Capacity Analysis . . . 133
6.3.3 Error Performance Analysis . . . 135
6.4 Performance Analysis for Centralized Mapping Scheme Selection . . 137
6.4.1 Outage Performance Analysis . . . 137
6.4.2 End-to-End Capacity Analysis . . . 138
6.4.3 Error Performance Analysis . . . 139
6.5 Numerical Simulations and Discussion . . . 139
6.5.1 Outage Performance . . . 139
6.5.2 End-to-End Capacity . . . 143
6.5.3 Error Performance . . . 144
6.5.4 Effects of CSI accuracy on Error Performance . . . 144
6.6 Summary . . . 148
6.7 Appendices . . . 149
6.7.1 Proof of Lemma 6 . . . 149
6.7.2 Proof of Lemma 7 . . . 150

7 Conclusions 151
7.1 Thesis Summary . . . 151
7.2 Outlook on OFDM-Based Relay Technology . . . 152
7.3 Future Work . . . 153
7.3.1 Incentives for OFDM-Based Cooperative Communications . 153
7.3.2 Novel Multi-Carrier Relay Selection Criterion Design . . . 154
7.3.3 OFDM-Based Relay Systems in Spatially Random Networks 156
7.3.4 Relay-Assisted OFDM with Index Modulation . . . 156
7.3.5 OFDM-Based Relay Systems with Energy Harvesting . . . 157
7.3.6 NOMA-OFDM Relay Systems . . . 158
7.3.7 Relay Systems Using New Waveforms . . . 158

References 159

List of Figures

2.1 Cooperation protocols: (a) full-duplex relaying; (b) two-phase relaying: mode 1; (c) two-phase relaying: mode 2; (d) three-phase two-way relaying; (e) four-phase two-way relaying; (f) two-phase two-way relaying using network coding. 12
2.2 Classic application scenarios of relays integrated with conventional cellular networks: (a) coverage extension; (b) cell-edge performance enhancement; (c) alternative to incompetent direct transmission; (d) load balancing; (e) diversity provision; (f) easy-to-implement hotspot for rural areas, temporary dense areas and/or emergency/disaster recovery. 13
2.3 Illustrations of half- and full-duplex relaying protocols. 15
2.4 Illustrations of AF and DF relaying protocols. 18
2.5 Outage performance of different forwarding protocols in normalized Raleigh fading channels vs. the ratio of transmit power P_t to the noise power N_0, given the outage threshold $s = 1$. 18
2.6 Snapshot of a frequency-selective channel partitioned into 16 frequency-flat subchannels. 20
2.7 Amplitudes of orthogonal subcarriers generated by OFDM in the frequency domain with four subcarriers. 20
2.8 System diagram of a typical OFDM system. 21
2.9 Illustration of the topology for demonstrating the energy efficiency advantage brought by cooperative communications. 24
2.10 Isotropic interference areas: a comparison between cases (a) without and (b) with relays. 24
2.11 Illustration of the selection process of combined relay selection with three subcarriers and four relays. The green boxes indicate the minimum SXRs of subcarriers performing per-subcarrier selection over the two-relay pairs and the red figure is the lowest SXR among all subcarriers after performing per-subcarrier selection. 33
2.12 Illustration of (a) bulk, (b) per-subcarrier and (c) combined relay selection schemes for a single source, single destination and multiple relays. The numbers in boxes are corresponding to the sequence numbers of subcarriers. 33

2.13 Outage performance of different multi-carrier relay selection schemes in normalized Raleigh fading channels vs. the ratio of transmit power P_t to the noise power N_0 for DF relaying, given the number of subcarriers $K = 8$, the outage threshold $s = 1$ and the number of relays $M \in \{3, 4\}$. 34

3.1 Illustration of (a) bulk and (b) per-subcarrier relay selection schemes for single source, single destination and multiple spatially randomly distributed relays, given $K = 8$. The numbers in boxes are the sequence numbers of subcarriers. 40
3.2 Relation among $\kappa(K, \lambda)$, K and λ for bulk selection in free space ($\alpha = 2$), when $s = 1$, $P_t/N_0 = 100$, $r_{SD} = 5$ and $\varsigma = 5$. 47
3.3 Bulk selection case: outage probability vs. P_t/N_0, when $\lambda = 1$, $\varsigma = 5$ and $r_{SD} = 5$. 50
3.4 Per-subcarrier selection case: outage probability vs. P_t/N_0, when $\lambda = 1$, $\varsigma = 5$ and $r_{SD} = 5$. 51
3.5 Connection probability vs. relay node density λ, when $P_t/N_0 = 100$, $\varsigma = 5$, $r_{SD} = 5$ and $K = 4$. 52
3.6 $\bar{\epsilon}$ vs. relay node density λ, when $\varsigma = 5$, $r_{SD} = 5$ and $K = 4$. 52
3.7 Relation between relay node density λ and the optimal number of subcarriers K_{opt} as well as the maximum system throughput characterized by $\kappa(K_{\text{opt}}, \lambda)$, when $s = 1$, $P_t/N_0 = 100$, $\varsigma = 5$ and $r_{SD} = 5$. 54
3.8 Relation between relay node density λ and the optimal number of subcarriers K_{opt} for a given outage probability $\Psi \in \{10^{-2}, 10^{-3}, 10^{-5}\}$, when $\alpha = 2$, $s = 1$, $P_t/N_0 = 100$, $\varsigma = 5$ and $r_{SD} = 5$. 55
3.9 Two-hop DF relay selection case: outage performance comparison among bulk, per-subcarrier and combined selections in random networks 56

4.1 Two-hop DF relay selection case: outage probability vs. SNR for per-subcarrier and combined selection systems. 73
4.2 Two-hop FG AF relay selection case: outage probability vs. SNR for per-subcarrier and combined selection systems. 73
4.3 Two-hop VG AF relay selection case: outage probability vs. SNR for per-subcarrier and combined selection systems. 74
4.4 Two-hop DF relay selection case: outage probability vs. SNR for per-subcarrier and combined selection systems. 76
4.5 Outage performance of combined selection corresponding to DF relays, given $s \in \{1, 2, 4, 8\}$. 77

5.1 Network model for the proposed full-duplex relay-assisted D2D system, containing one BS, K CUEs in a CUE cluster, M relays in a relay cluster, one DUE transmitter (source) and one DUE receiver (destination). 86
5.2 Outage probability of D2D communications vs. $\bar{P}_S$ for bulk and per-subcarrier selection schemes, given $\bar{P}_R = \bar{P}_S$. 102

5.3 Outage probability of D2D communications vs. the average channel power gain μ_{SR}, given $\mu_{RD} = \mu_{SR}$ and $M = K = 4$. 104
5.4 Outage probability of D2D communications vs. the average channel power gain μ_{SB}, given $\mu_{RB} = \mu_{SB}$ and $M = K = 4$. 105
5.5 Outage probability of D2D communications vs. the average channel power gain μ_{CR}, given $\mu_{CD} = \mu_{CR}$ and $M = K = 4$. 106
5.6 Outage probability vs. μ_{CB} for D2D and cellular communications, given $M = K = 4$. 107
5.7 Outage probability of D2D communications vs. $\bar{\varphi}$ for bulk and per-subcarrier selection schemes, given $M = K = 4$. 109
5.8 Outage probability of D2D communications vs. α for bulk and per-subcarrier selection schemes, given $M = K = 4$. 111

6.1 System block diagram of the source (similar to the transmission part of the relay). 120
6.2 An example of (a): a two-hop system with the decentralized mapping scheme selection; (b): a two-hop system with the centralized mapping scheme selection, when $N_T = 4$, $N_S = 3$ and $N_A(k) = 2$. 126
6.3 An example of mapping scheme selection process from $\mathcal{N}$ to $\mathcal{N}_S(c)$, when $N_T = 8$ and $N_S = 4$. 126
6.4 Activation patterns for the proposed adaptive OFDM-IM, conventional OFDM-IM and FPSK with $N_T = 4$ and $B_S = 2$. The numbers in boxes are corresponding to the sequence numbers of subcarriers. The grey boxes are corresponding to subcarriers are selected by the adaptive mechanism and red numbers indicate the corresponding subcarriers are active. 131
6.5 Transmission rates of different schemes vs. N_S. 131
6.6 Average outage probability vs. ratio of transmit power to noise power P_t/N_0 for different schemes. 141
6.7 Exact expressions and asymptotic expressions of outage probability for decentralized and centralized mapping scheme selections. 142
6.8 Average end-to-end capacity vs. ratio of transmit power to noise power P_t/N_0 for different schemes. 145
6.9 Threshold power ratio ratio vs. the number of selected subcarriers N_S with different N_T for decentralized and centralized mapping scheme selections. 146
6.10 Average SER vs. ratio of transmit power to noise power P_t/N_0 for different schemes. 147
6.11 Average SER vs. ratio of transmit power to noise power P_t/N_0 with different δ_S, δ_R and δ_D. 148

List of Tables

1.1 Quantitative forecasting for next generation networks [1, 2]. 3

6.1 An example of the OFDM-IM mapping table when $B_M = 1$ and $B_S = N_S = 2$. 127

List of Mathematical Notations

d_o	Diversity gain
$\mathbb{E}\{\cdot\}$	Expectation of the event enclosed
$\mathrm{E_i}(\cdot)$	Exponential integral function: type I
$E_n(\cdot)$	Exponential integral function: type II
f_k	Central frequency of the kth subcarrier
H	Number of hops
$I_v(\cdot)$	The vth order modified Bessel function of the first kind
$K_v(\cdot)$	The vth order modified Bessel function of the second kind
$\mathcal{L}_{bulk}$	Set of selected relays by bulk selection
$\mathcal{L}_{ps}$	Set of selected relays by per-subcarrier selection
$\mathcal{L}_{comb}$	Set of selected relays by combined selection
$\mathcal{M}$	Full set of relays
M	Number of relays
N_0	Noise power
$O(\cdot)$	Bachmann-Landau notation
$\mathbb{P}\{\cdot\}$	Probability of the event enclosed
P_t	Transmit power
$Q(\cdot)$	Q-function
$Q(\cdot,\cdot)$	Marcum Q-function
r_h	Distance between two adjacent nodes in the hth hop
r_{SD}	Distance between source and destination
s	Preset outage threshold
$\mathsf{SIR}(m,k)$	Signal-to-interference ratio of the kth subcarrier forwarded by the mth relay
$\mathsf{SNR}(m,k)$	Signal-to-noise ratio of the kth subcarrier forwarded by the mth relay
T_s	OFDM symbol time
$\Gamma(\cdot)$	Gamma function
$\underline{\Gamma}(\cdot,\cdot)$	Lower incomplete gamma function
$\bar{\gamma}$	Average SNR/SINR/SIR
$\binom{\cdot}{\cdot}$	Binomial coefficient
μ_{AB}	The average channel gain from node A to node B
μ_h	The average channel gain in the ith hop

Chapter 1

Introduction

1.1 Evolution of Wireless Communication Networks

Wireless communication enjoys a long history dating back to Marconi's pioneering demonstration of wireless telegraphy more than a hundred years ago. Theoretical analysis of modern communications started from information theory originally proposed by Claude E. Shannon in 1948 [1]. The industrialization and evolution of modern wireless communication networks commenced around the 1970s and hitherto have experienced four generations. The evolutions of wireless communication networks not only depend on the progress of communication technologies, but also the development of communication hardware. In the 1980s, first generation (1G) networks utilized analog signals and were dedicated to voice communications by frequency-division multiple access (FDMA) without considering security. Because of the low spectrum efficiency and unsatisfactory service provided by 1G networks, second generation networks (2G) utilizing digital signals were proposed and employed around the 1990s. In 2G networks, in addition to voice communications, basic data services for short message and e-mail were also supported. Benefiting from digital communication technologies, time-division multiple access (TDMA)

and code-division multiple access (CDMA) emerged to enhance spectrum and energy efficiencies in 2G networks. Coming to the 21st century, the number of mobile users boosted and third generation (3G) networks employing packet switching technology replaced 2G networks. Also, in 3G networks, a variety of sophisticated data services are supported by applying wideband CDMA (WCDMA), CDMA2000, time-division synchronous CDMA (TD-SCDMA), Long-Term Evolution (LTE), and Worldwide Interoperability for Microwave Access (WiMAX). However, people soon noticed that 3G networks would be saturated by a fast and ever increasing data requirement, and fourth generation (4G) networks involving all-Internet protocol (IP) technology and orthogonal frequency-division multiplexing (OFDM) are being widely used [1, 3]. In the meantime, fifth generation (5G) networks are in preparation for large-scale implementation in 2020 [4].

It can be seen that wireless communication networks have evolved in every decade in order to accomplish new service requirements. Therefore, it is pertinent to ask the following questions: what are researchers trying to achieve in 5G networks and why is it challenging? To answer these two questions, we need to have a glimpse of today's communication market and its future forecast first. Currently, the penetration rate of mobile communications has been already high and almost saturated, especially in developed regions, and most users are basically satisfied with the mobile service currently provided [5]. On the other hand, researchers have firm evidence that the wireless data explosion will continue into the next decade, which will ultimately lead to a crisis without major technical breakthroughs in wireless communications. Mobile data traffic will increase seven-fold from 2016 to 2021 and exceed 500 exabytes (1 exabyte=10^{18} bytes) driven by more than 50 billion connected devices by 2020 [1,2]. These tremendous data increases come from live streaming videos, the Internet of Things (IoT), and potentially virtual reality (VR) technology [6, 7]. To satisfy these new service demands, it is expected that 5G networks will be capable of providing unbounded access to information and

Table 1.1: Quantitative forecasting for next generation networks [1, 2].

Performance indicators	Quantitative forecasting (compared to 4G)
Data volume	1000 times higher
Number of connected devices	10 to 100 times higher
Data rate	10 to 100 times higher
Energy efficiency	10 times higher
Latency	20 percent of 4G

sharing of data everywhere and every time for everyone and every device [1]. To show the difficulty of evolving from 4G to 5G networks, some quantitative clues are provided in Table 1.1 [1, 2].

1.2 Motivation for Applying OFDM-Based Relay Systems

From Table 1.1, it is a consensus that the above requirements cannot be accomplished by incremental improvements of 4G networks, and a novel network architecture with state-of-the-art communication technologies must be jointly applied to overcome the serious crisis just around the corner [8]. So what technologies should be employed? For signaling and multiple access, multi-carrier modulation schemes, especially OFDM, dominate and are believed to continue this domination for the next decade, owing to the highest spectrum efficiency among other mature signaling technologies [1, 2].

To further enhance the network performance, the multiple-input multiple-output (MIMO) technology, as perhaps the most important breakthrough in wireless communications at the beginning of the 21st century, can provide spatial diversity and satisfactory quality of service (QoS). Meanwhile, MIMO technology is mature and suited to cooperate with OFDM as well as a large number of emerging paradigms. However, there are three factors handicapping the use of MIMO systems in prac-

tice: physical size, processing capability and battery life of a communication device. First, the installation of multiple antennas requires a large space in a communication device, which is only possible for large and full-fledged base stations (BSs), and contradictory to the miniaturization design guidelines of household communication devices, e.g., mobile phones and tablets. Second, MIMO systems need to have a high processing capability, since the coordination among multiple antennas would be complicated. The requirement of high processing capability will result in a high complexity in devices, which may not always be affordable, especially for wireless sensor networks (WSNs), in which nodes are very simple. Third, the power consumption of MIMO systems is high, which could lead to frequent battery charging and decrease the user experience. Even worse, sometimes devices are simple and non-rechargeable, and the high power consumption will decrease the network lifetime sharply [9].

One of the most promising technologies to overcome the drawbacks of the MIMO technology is physical (PHY) layer relaying, in which an intermediate communication node termed a *relay* conveys a message from the source to the destination. Fortunately, the relay technology as a good alternative to the MIMO technology can cope with these drawbacks, and still ensures most merits of the MIMO technology, including spatial diversity. Specifically, a large number of devices with a single antenna can be organized in a cooperative manner to form a *virtual* or *distributed* MIMO system. By integrating the antennas mounted in these cooperative devices, the spatial diversity is still obtainable, whereas the three main drawbacks of MIMO systems vanish [10]. Most importantly, the implementation of relays can provide much higher design flexibility for 5G networks. As a consequence, the OFDM-based relay technology is expected to play a crucial role and have a substantial impact on the performance improvement in 5G networks. In addition, the standardization of OFDM-based relay technology has been ongoing for years and relatively full-fledged at present, which paves the way for its implementation in 5G networks. [11]. We

hereby choose to analyze OFDM-based relay systems for next generation networks in this thesis.

1.3 Thesis Contributions and Organization

In the previous sections, we presented the status quo of the wireless communication networks and clarified the motivation for applying OFDM-based relay systems. Based on the above discussions, we mainly propose and analyze four different OFDM-based relay systems in this thesis, which have different system models and are suitable for different scenarios. To provide a logic roadmap for readers, we introduce the organization of the rest of this thesis as well as the technical contributions of each chapter infra. Note that most nomenclatures and mathematical notations are independently defined and used in each chapter for clarity. Meanwhile, most of the analytical results given throughout this thesis are derived by Mathematica or manually, otherwise special notes and/or references are provided. Numerical results are generated by Monte Carlo simulations via MATLAB.

In **Chapter 2**, we provide a research overview of the OFDM-based relay technology aiming at providing preliminary knowledge and giving a full picture of this technology to readers. First, we provide a retrospective of the preliminaries relevant to the OFDM-based relay technology, in which a series of key concepts, two basic forwarding protocols and the principles of OFDM are introduced. Then, we briefly discuss the advantages and disadvantages of OFDM-based relay systems. The third part of this overview consists of brief reviews of multi-carrier relay selections.

As the most fundamental multi-carrier relay selection schemes, in **Chapter 3**, we analyze the outage performance of bulk and per-subcarrier relay selections for two-hop OFDM systems in a Poisson field of decode-and-forward (DF) relays. The stochastic network model adopted in this chapter is different from the conventional network model assuming relays are deterministic and stationary in terms of

topological positions. By the analysis provided in this chapter, the gap between OFDM-based relay systems and stochastic networks can be filled up. Specifically, the exact expressions for outage probability for bulk and per-subcarrier selections are derived in integral forms for general cases. In addition, for some special cases, closed-form expressions for outage probability are also obtained. Based on these derived results, it is proven that the cooperative diversity gain in Poisson random networks can either be zero, one or infinite, which is termed the *ternary property*. Except for these main findings, some crucial properties related to OFDM-based relay systems in random networks are also investigated and discussed in this chapter. This chapter is a joint study with Prof. Justin P. Coon, Dr. Gaojie Chen and Dr. David E. Simmons. The main contents of this chapter have been published in *IEEE Access* and *Proc. 2017 IEEE ISCC* [12, 13].

To provide a satisfactory solution to the performance-complexity trade-off in multi-carrier relay selection, in **Chapter 4**, we analyze the outage performance of the combined relay selection scheme over spatially correlated channels for OFDM-based relay systems. This combined selection scheme can be regarded as a compromise between bulk and per-subcarrier selections, but interestingly, can still achieve the optimal performance at high signal-to-noise ratio (SNR). To be convincing, we rigorously prove a generalized theorem termed the *equivalence principle*, which states that the combined selection can achieve an optimal outage probability equivalent to the per-subcarrier selection at high SNR without using the full set of available relays for selection. To provide quantitative analysis, we derive generic asymptotic expressions for outage probability at high SNR when applying combined selection, which are subsequently applied to and verified by a number of applications. This chapter is a joint study with Prof. Justin P. Coon, Dr. Gaojie Chen and Dr. David E. Simmons. The main contents of this chapter have been published in *IEEE Transactions on Vehicular Technology*, *Proc. 2016 IEEE VTC Spring*, *Proc. 2015 IEEE CAMAD* and *Proc. 2015 IEEE ICC* [14–17].

To supplement the practicality analysis of OFDM-based relay systems, in **Chapter 5**, we focus on multi-carrier relay selections for OFDM-based relay systems in a more realistic and complicated application scenario. Particularly, we propose an OFDM device-to-device (D2D) system in two-hop networks, where multiple full-duplex DF relays assist the transmission from D2D user equipment (DUE) transmitter to DUE receiver. By such a transmission mechanism, the signal transmitted by the DUE transmitter does not need to go through a BS. Meanwhile, due to the adoption of underlay D2D communication protocols, power control mechanisms are thereby necessary to be applied to mitigate the interference to conventional cellular communications. Based on these considerations, we analyze the outage performance of the proposed system, and derive the exact expressions of outage probabilities when bulk and per-subcarrier relay selections are applied. Subsequently, we also investigate the outage performance optimization problems by coordinating transmit power among DUE transmitter and relays, and provide suboptimal solutions, which are capable of improving the outage performance. This chapter is a joint study with Prof. Justin P. Coon and Dr. Gaojie Chen. The main contents of this chapter have been published in *IEEE Transactions on Vehicular Technology*, *IEEE Wireless Communications Letters* [18, 19], and submitted for possible publication in *IEEE Transactions on Vehicular Technology* [20].

Furthermore, in **Chapter 6**, to consider state-of-the-art modulation schemes and provide an approach to enhance reliability when there is only one relay and relay selection is thereby impossible, we propose an adaptive OFDM scheme with index modulation (OFDM-IM) for two-hop relay networks. In contrast to the traditional OFDM-IM, in this proposed adaptive OFDM-IM, the mapping schemes between a bit stream and indices of active subcarriers for the first and second hops are adaptively selected by a certain criterion. As a result, the active subcarriers for the same bit stream in the first and second hops can be varied in order to combat slow frequency-selective fading. Additionally, considering the fact that a relay device

is normally a simple node, which may not always be able to perform mapping scheme selection due to limited processing capability, we also propose an alternative adaptive methodology in which the mapping scheme selection is only performed at the source. The analyses of average outage probability, end-to-end capacity and symbol error rate (SER) are given in closed form for DF relaying. This chapter is a joint study with Prof. Justin P. Coon and Dr. Gaojie Chen. The main contents of this chapter have been submitted to *IEEE Wireless Communication Letters* [21], and published in *IEEE Transactions on Wireless Communications* [22] as well as *Proc. 2017 IEEE GLOBECOM* [23].

Finally, in **Chapter 7**, the thesis is concluded and several potential directions for future work are pointed out.

Chapter 2

Research Overview

Relay-assisted communications were first published in 1971 under the moniker 'three-terminal communications', in which a triangle topology consisting of three nodes was constructed and analyzed in terms of mutual information rate [24]. This marks the inception of the long march of cooperative communications, which has lasted for more than 40 years towards 5G networks. However, due to the user demands and limitations on infrastructure and hardware design, relay-assisted communications had been nothing more than a purely mathematical concept and out of the consideration of engineering practice in the 20th century. With a rapidly increasing demand for data service in the early 21st century, traditional communication technologies based on point-to-point paradigms were less able to cope with the tremendous amount of data and diverse communication service requirements [25]. Meanwhile, considering the maturity of hardware design and implementation of the relay, relay-assisted communications returned to researchers' view as one of the most promising candidates to accommodate such an ever increasing demand for data service [26, 27]. The most important milestone of the modern research of relay-assisted communications was Laneman, Tse and Wornell's work published in 2004 [28]. In this work, the first practical cooperative diversity system was proposed and analyzed in terms of outage performance, which is proven to be capable

of efficiently combating multi-path fading. This work, not surprisingly, boosted the research of relay-assisted communications in many aspects lasting for the next two decades until now [29].

The fundamental principle of relay-assisted communications (a.k.a. cooperative communications, which will be used interchangeably in this thesis) is relatively simple. Different from point-to-point communication paradigms, relay-assisted communications require multiple communication nodes to collaborate, and a multi-hop cooperative transmission scenario is thus formed. By such a multi-hop transmission scenario, a so-called *virtual* MIMO system is constructed and the network reliability can be enhanced by exploiting *spatial diversity* [10]. This spatial diversity is brought by relaying multiple replicas of the signal originally generated by the source node, which allows the destination node to process redundant received signals experiencing different channel impairments [28]. Meanwhile, employing relays can also increase energy efficiency, since a long-distance single-hop transmission link can be split into a number of short-distance multi-hop transmission links [30]. According to the radio wave propagation mechanism [31], a short transmission distance could save a great amount of transmit power and reduce the interference to other users. Apart from these technological advantages, the cost efficiency of relay nodes is another attraction for implementing cooperative networks [32].

On the other hand, researchers also found it difficult to support the ever increasing communication demand solely by applying relay-assisted communications, and thereby the combinations of relay-assisted communications and other communication technologies are indispensable [33]. One of the most successful cases is the alliance between relay-assisted communications and OFDM. OFDM, as a multiplexing technology, allows parallel signal transmissions over mutually orthogonal channels via different subcarriers. OFDM not only increases the spectrum efficiency by subcarrier orthogonality, but also enables one to partition a frequency-selective fading channel into a number of frequency-flat fading channels. This transformation

makes the system robust against frequency-selective fading, and eases the processing of received signals in a per-subcarrier manner at receivers [34].

The pioneering works incorporating fixed relay systems with OFDM in the PHY layer were published in [35,36], in which numerical and analytical studies of network capacity were shown. Then, the first system model of an amplify-and-forward (AF) OFDM relay network was proposed in [37]. Following that, in the early stage, the research on OFDM-based relay systems is mainly focused on resource allocations and performance optimizations. The first resource allocation work of OFDM-based relay systems dedicated to multi-user scenarios was presented in [38], and was developed by considering fairness-related issues in [39]. Resource allocation algorithms jointly considering power and subcarriers were given in [40–42]. Performance analysis of OFDM-based relay systems was done for both AF and DF relaying in [43–46]. Some practical issues including synchronization, channel estimation, coding and forwarding protocol design were taken into consideration by [47–50]. All these achievements in the early years construct basic research frameworks for OFDM-based relay systems. In addition, the analytical and numerical results demonstrated in these primary works also confirm the satisfactory characteristics as well as a great potential of OFDM-based relay systems for enhancing network reliability, energy efficiency and spectrum efficiency at a relatively low cost.

Based on these preliminaries, not surprisingly, the OFDM-based relay technology is progressing at a rapid pace in recent years. In this regard, we carry out a research overview of related topics of OFDM-based relay systems in this chapter.

2.1 Relay-Assisted Cooperative Communications

In this section, we introduce a series of basic concepts related to relaying and cooperative networks, which are prerequisites for understanding the technical contributions of this thesis.

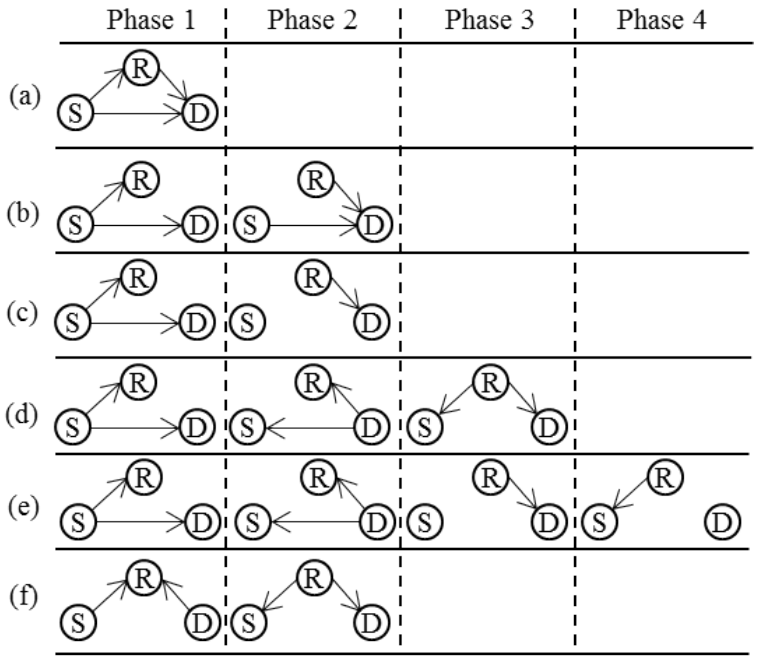


Figure 2.1: Cooperation protocols: (a) full-duplex relaying; (b) two-phase relaying: mode 1; (c) two-phase relaying: mode 2; (d) three-phase two-way relaying; (e) four-phase two-way relaying; (f) two-phase two-way relaying using network coding.

2.1.1 Cooperative Networks and Relay Networks

Different from conventional point-to-point networks only utilizing direct transmission links, *cooperative networks* employ relays to assist transmissions between source and destination, and a multi-hop transmission scenario is thereby yielded. The simplest and primitive cooperative network proposed in [24] consists of three nodes, i.e., source, relay and destination. The source broadcasts a signal to both relay and destination. The relay receives, processes and forwards the signal to the destination by a certain protocol. As a result, the destination can receive two replicas of the original signal, which would help the reception and estimation at the destination [51]. The advantageous effects brought by deploying cooperative networks are subject to the designs of cooperation protocols, e.g., half-duplex/full-duplex and one-way/two-way as well as coding schemes. We depict several common cooperation protocols in Figure 2.1, and more details can be found in [29, 52–54].

This cooperative network paradigm is particularly useful when the direct trans-

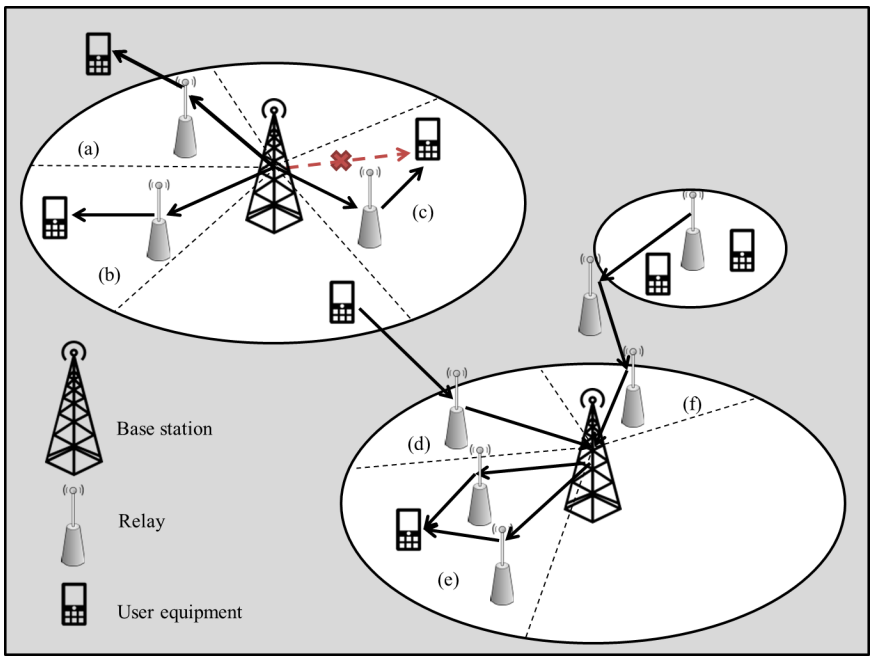


Figure 2.2: Classic application scenarios of relays integrated with conventional cellular networks: (a) coverage extension; (b) cell-edge performance enhancement; (c) alternative to incompetent direct transmission; (d) load balancing; (e) diversity provision; (f) easy-to-implement hotspot for rural areas, temporary dense areas and/or emergency/disaster recovery.

mission link between source and destination is in deep fading, but source-relay and relay-destination links (a.k.a. *relay link* and *access link* [55]) are viable [56]. Meanwhile, if the direct transmission link is always much weaker than the source-relay and relay-destination links in terms of received power[1], it is negligible and a complete transmission from the source to the destination requires two orthogonal phases when the half-duplex forwarding protocol is adopted. To show the usefulness of cooperative networks, we demonstrate some classic application scenarios of relay systems integrated with conventional cellular networks in Figure 2.2. More information regarding applications of cooperative networks and relay systems can be found in [25, 55, 57–59].

It must be clarified that the relay is more a functional concept than a special kind of device, and any mobile user equipment can be regarded as a relay if it not only transmits its own message, but also helps others when it is idle. In this regard,

[1]This is common for mobile cellular networks, e.g., WiMAX networks [30].

we can distinguish two similar concepts: cooperative network and relay network. Strictly speaking, the cooperative network, in which relay nodes are exclusively designed for relaying purposes without transmitting their own messages is called a *relay network* [60]. In other words, the relay network can be viewed as a special case of the cooperative network. However, in most research without special notification, these two concepts are viewed as equivalent and used interchangeably.

2.1.2 Half- and Full-Duplex Relaying

A relay can adopt half-duplex or full-duplex relaying protocol when forwarding a received signal, which is highly relevant to the network efficiency and performance. As we will compare the performance of both forwarding cases in **Chapter 5**, we provide the fundamentals in this subsection.

As shown in Figure 2.3, full-duplex relaying allows relay nodes to transmit and receive simultaneously, while half-duplex relaying only allows a node to either transmit or receive at a time. Researchers have shown that the capacity as well as the outage probability would be enhanced if full-duplex relaying is applied [61,62]. However, because normally in-band resources are utilized in cooperative networks [30], self-interference (SI) is generated by full-duplex transmissions, which would degrade the system performance. A comprehensive performance comparison between full-duplex and half-duplex AF relaying is given in [61]. In general, it has been demonstrated that if the SI can be suppressed at least 3 dB lower than the noise level, its deleterious effects on full-duplex cooperative systems are negligible [63]. Fortunately, with the development of interference cancellation techniques [64, 65], the residual SI processed by analog and digital cancellations can be mitigated below the noise level, and full-duplex relaying currently becomes realistic [66].

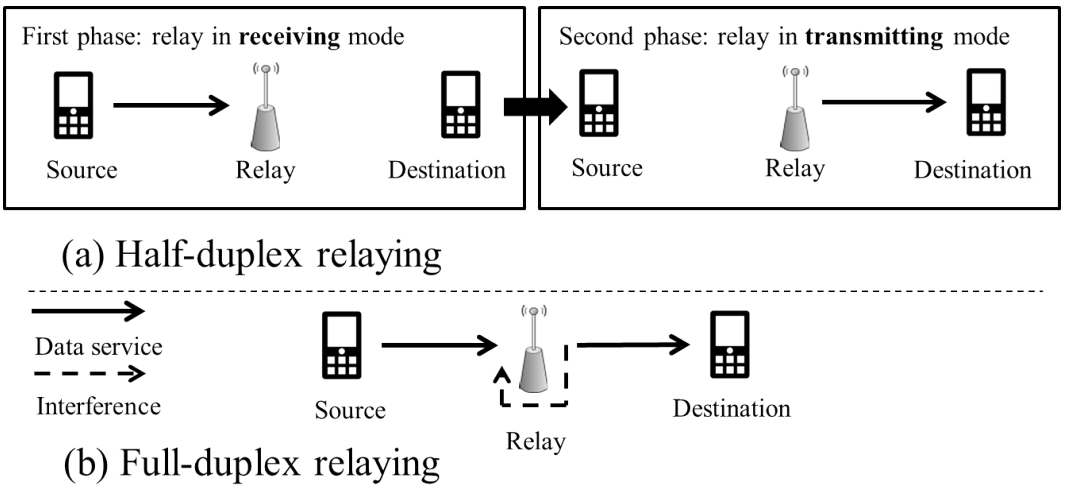


Figure 2.3: Illustrations of half- and full-duplex relaying protocols.

2.1.3 Amplify-and-Forward Relaying

The way to process the received signal at the relay node is also highly associated with the system performance. There exist numerous relaying protocols suited for different applications. In this thesis, we mainly focus on the AF and DF relaying. AF relaying (a.k.a. non-regenerative relaying[2]) is the simplest forwarding protocol. The AF relay amplifies the received signal by a certain gain and retransmits the processed signal to the destination. Though AF relaying is simple so that the signaling overhead and caused delay would be relatively low, the drawbacks of AF relaying are also obvious. First, the AF relay not only amplifies the received signal, but also the received noise, which would greatly distort the retransmitted signal when noise power is large [67]. Second, the amplification saturation problem should also be taken into consideration, which will result in more severe nonlinear distortion in the retransmitted signal [68].

From a taxonomic point of view, AF relaying can be further classified into two categories depending on the different designs of amplification gains, which are fixed-gain (FG) AF and variable-gain (VG) AF relaying. In FG AF relaying, the received signal and noise will always be amplified by a fixed and uniform gain regardless of

[2]This term comes from the feature of AF relaying that it does not decode and re-encode the received signal.

instantaneous channel conditions and the amplification saturation problem [25]. We can express the end-to-end SNR of a two-hop FG AF relay network as

$$\mathsf{SNR}_{\mathsf{FG-AF}} = \frac{G_F^2 G_1 G_2 P_t}{(G_F^2 G_2 + 1) N_0}, \tag{2.1}$$

where P_t and N_0 denote the transmit and noise power[3]; G_i represents the channel gain for the ith hop with average power μ_i, $\forall i \in \{1, 2\}$; $G_F = \sqrt{\frac{P_t}{P_t \mu_1 + N_0}}$ is the fixed amplification gain.

On the contrary, VG AF relaying requires the instantaneous CSI and adjusts the amplification gain according to the channel conditions [25]. Because of its dynamic nature, VG AF relaying enjoys better performance than that of FG AF relaying, whereas the performance gain comes at the price of a higher channel estimation overhead and system complexity. We can express the end-to-end SNR of a two-hop VG AF relay network as

$$\mathsf{SNR}_{\mathsf{VG-AF}} = \frac{G_V^2 G_1 G_2 P_t}{(G_V^2 G_2 + 1) N_0}, \tag{2.2}$$

where $G_V = \sqrt{\frac{P_t}{P_t G_1 + N_0}}$ is the variable amplification gain.

2.1.4 Decode-and-Forward Relaying

Different from AF relaying, DF relaying (a.k.a. regenerative relaying) performs a series of complicated processes to the received signal before retransmitting it. In particular, the DF relay also requires the instantaneous CSI and uses this information to estimate the received signal first. Then, the DF relay re-encodes the decoded bit stream carried by the received signal to a new signal and retransmits this new signal to the destination [25]. In the meantime, from an analytical point of

[3] Note that as we normalize bandwidth throughout the thesis and thereby the noise power quantitatively equals the noise spectral density. Therefore, we use N_0 to represent the noise power throughout the thesis.

view, DF relaying has a much better mathematical tractability than AF relaying[4], which makes DF relaying an appropriate option for theoretical research and serves as a tractable benchmark for AF relaying. We can express the end-to-end SNR of a two-hop DF relay network as

$$\mathsf{SNR}_{\mathsf{DF}} = \frac{P_t}{N_0} \min\{G_1, G_2\}. \tag{2.3}$$

On the other hand, as we can observe from (2.3), even though the noise can be eliminated by DF relaying, there exists another drawback diminishing the system performance: if the first hop is in deep fading or the separation between the source and relay is large, it is highly likely that the received signal at the relay would be erroneously decoded, and the re-encoded signal will be different from the originally transmitted signal at the source. This is termed the *error propagation* and could lead to a poorer system performance than AF relaying, especially when the source-relay link is much worse than the relay-destination link [30]. Also, considering practical issues, DF relaying would cause a relatively large transmission delay due to the complex processing performed at the relay node. Meanwhile, secrecy and security must be taken into consideration, as a DF relay can decode the original message.

For clarity and comparison purposes, we draw a diagram in Figure 2.4 to pictorially demonstrate the AF and DF forwarding protocols and present the numerical results of outage probability, i.e. the probability that the SNR falls below a threshold s for different forwarding protocols in Figure 2.5.

[4]The mathematical tractability of DF relaying comes from the fact that the transmission over multiple hops can be regarded as independent and analyzed separately when DF relaying is applied, while this must be considered as a whole for AF relaying [30].

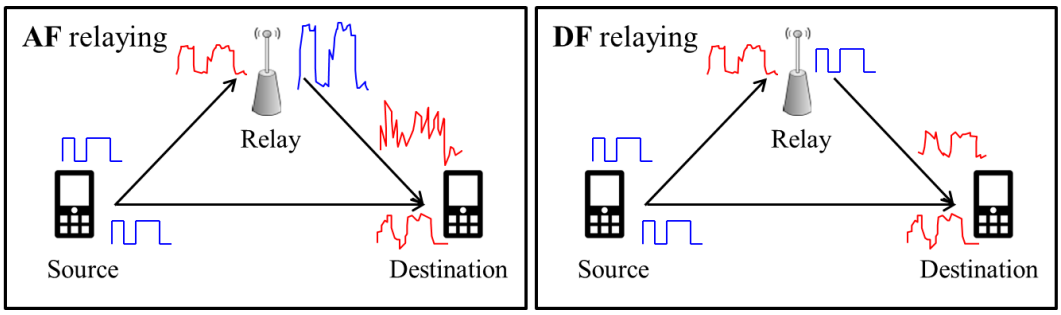


Figure 2.4: Illustrations of AF and DF relaying protocols.

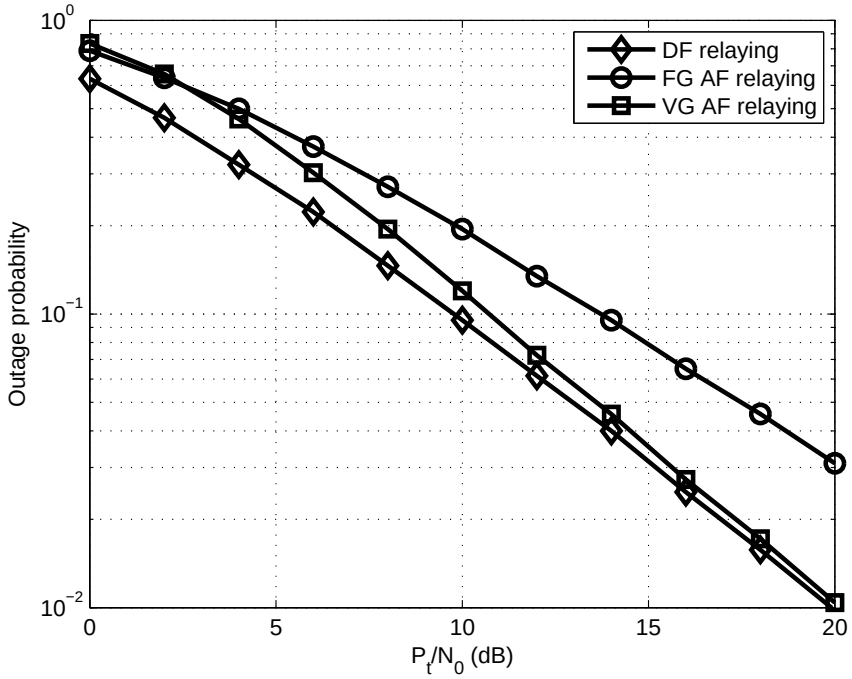


Figure 2.5: Outage performance of different forwarding protocols in normalized Raleigh fading channels vs. the ratio of transmit power P_t to the noise power N_0, given the outage threshold $s = 1$.

2.2 OFDM

OFDM can be regarded as one of the most important breakthroughs in modulation technology, and has been adopted as the kernel of 4G networks [30]. Specifically, OFDM utilizes a set of subcarriers with different *orthogonal frequencies* to split a frequency-selective channel into a number of frequency-flat subchannels (depicted in Figure 2.6). Because of the orthogonality of subcarrier frequencies, the subchannels can be regarded as independent and the inter-channel interference (ICI) shall

be mitigated or even eliminated [67]. Meanwhile, OFDM has a high spectrum efficiency, as it does not require guard bands inserted among subcarriers. Moreover, different subcarriers can overlap in the frequency domain but still maintain orthogonality, as long as certain quantitative relations among their central frequencies can be satisfied. In particular, assuming the cosine waveform is used to modulate signals, the quantitative relations among central frequencies can be expressed as [56]

$$\begin{cases} f_k = m/(2T_s) \\ \Delta(k_1, k_2) = |f_{k_1} - f_{k_2}| = n/T_s \end{cases} \tag{2.4}$$

where f_k, f_{k_1} and f_{k_2} are the central frequencies of the kth, k_1th and k_2th subcarriers; T_s is the symbol period; n and m are positive integers. From (2.4), we can also see that the minimum frequency separation between two adjacent subcarriers is $\Delta_{\min} = 1/T_s$, which substantially increases the spectrum efficiency. To reveal this important characteristic of OFDM, we plot an example of OFDM with normalized symbol period and four subcarriers in Figure 2.7. From this figure, it is obvious that instead of inserting guard bands between subcarriers, OFDM allows overlap of subcarriers, but still maintains orthogonality, since at the central frequency of one subcarrier, the amplitudes of other subcarriers drop to zero. On the other hand, we can also find that OFDM is sensitive to frequency deviation, which could be caused by the Doppler effect and error in the frequency synchronization [48].

Another attractive feature of OFDM is that it allows independent and different processing on each subcarrier, and provides a higher flexibility for system-level design. From a practical point of view, OFDM is also easy to be modulated and demodulated by inverse fast Fourier transform (IFFT) and fast Fourier transform (FFT), respectively [30]. To provide an overview and more technical details of OFDM, we illustrate its completed system diagram in Figure 2.8. From this figure, it is clear that there exist one-to-one relations between the processing blocks at

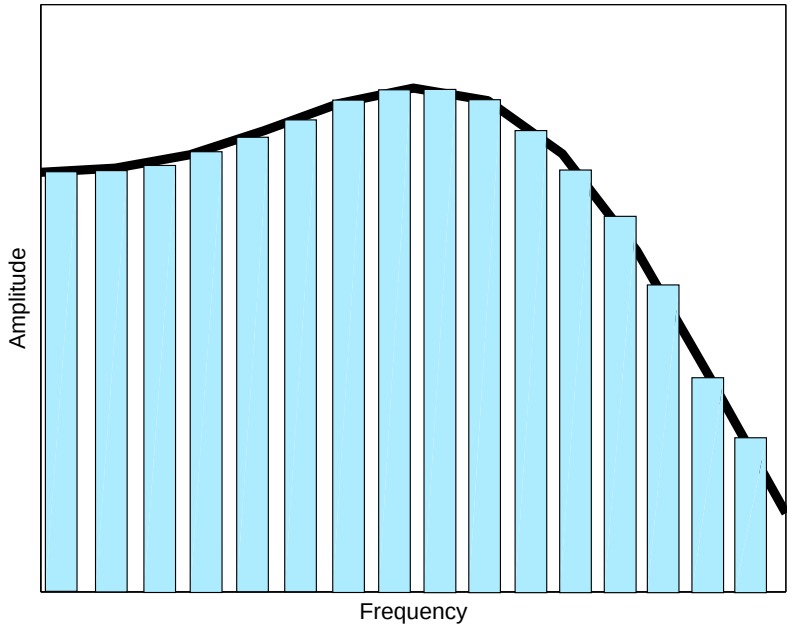


Figure 2.6: Snapshot of a frequency-selective channel partitioned into 16 frequency-flat subchannels.

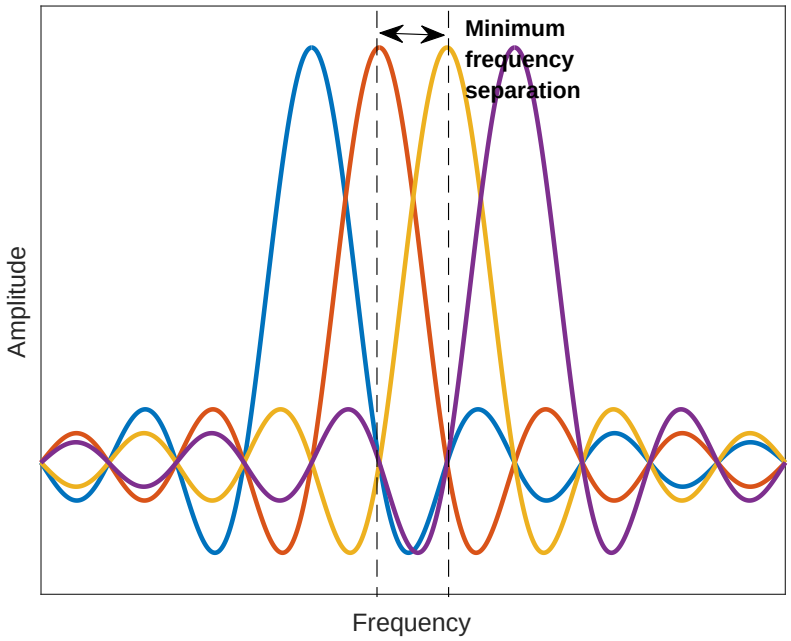


Figure 2.7: Amplitudes of orthogonal subcarriers generated by OFDM in the frequency domain with four subcarriers.

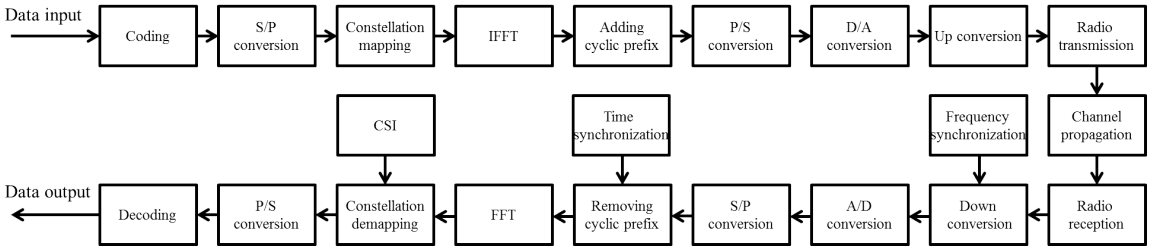


Figure 2.8: System diagram of a typical OFDM system.

the transmitter and receiver. First, 'input data' refers to the bit stream intended to transmit by the transmitter, which would be encoded to be a new bit stream (normally with a longer length), so that a better robustness is obtained. Then, this bit stream is split into a number of small fragments and mapped to complex symbols by M-quadrature amplitude modulation (QAM) or M-phase-shift keying (PSK) etc. After that, these modulated symbols are processed by IFFT and the cyclic prefix (CP) is added as a guard interval to prevent inter-symbol interference (ISI) and converts the linear convolution to the circular convolution for frequency-selective multi-path fading channels. Subsequently, all parallel signals are summed up and converted to analog for radio transmission. The reception process is simply the inverse of the transmission process with channel estimation and synchronization. By such a process in OFDM, the complex symbol transmitted on each subcarrier experiences independent fading during the radio propagation process and can be processed independently, so that the frequency-selective fading can be efficiently overcome [67].

2.3 OFDM-Based Relay Systems: Pros and Cons

All technologies are double-edged swords, which have pros and cons, and the OFDM-based relay technology is not exceptional. As we have more or less mentioned in previous contents, the merits and drawbacks of the OFDM-based relay technology are summarized in this section to provide a full picture of this technology. One should note that the pros and cons referred in this section is not unique for OFDM-

based relay technology only, but originally come from both cooperative relaying and OFDM.

2.3.1 Merits of OFDM-Based Relay Systems

2.3.1.1 Diversity

Diversity advantage would be the most obvious merit of OFDM-based relay technology. Without considering source coding techniques, the diversity gain brought by an uncoded OFDM-based relay system comes from two parts: spatial diversity and frequency diversity. Considering the three-node case with one source, one relay and one destination, there exist two possible routes to transmit a signal from the source to the destination, i.e., the direct link (source-destination) and two-hop link (source-relay-destination). As a result, the spatial diversity has been raised from one to two by such a network architecture, which improves the system reliability. The spatial diversity brought by the cooperative relay is also termed the *cooperative diversity*. The cooperative diversity can be further increased by involving multiple relays, and performing relay selection and reception combining. When multiple relays and relay selections are involved, the cooperative diversity is also known as *selection diversity* [10]. Meanwhile, in some special cases requiring high reliability, OFDM can also be utilized to provide frequency diversity, although parallel subcarriers normally carry different symbols for multiplexing purposes. In particular, identical symbols can be carried by more than one subcarrier and as long as the subcarrier with the highest SNR can be correctly estimated, the corresponding symbol can be reproduced, which provides the frequency diversity [69]. Moreover, space-frequency coding techniques can be used to integrate both spatial and frequency diversities and provide a joint diversity equal to the product of the numbers of relays and subcarriers [70].

2.3.1.2 Energy Efficiency

The energy efficiency is increased by OFDM-based relay systems, because the radio wave propagation length can be effectively reduced by deploying relays. Assuming a single isotropic antenna is installed in all communication nodes in a relay network, temporarily without considering small-scale fading, the average required transmit power can be expressed by the Friis transmission equation as $\mathbb{E}\{P_t\} = \xi r^{\alpha}$ [71], where ξ is a fixed coefficient determined by antenna gain, reception threshold and radio frequency etc.; r is the distance between transmitter and receiver; $2 \leq \alpha \leq 7$ is the path loss exponent depending on the propagation environment and terrain. To simplify the analysis and provide an intuitive comparison, we can take an ideal case where $H-1$ relays (i.e., H hops) are deployed in a straight line connecting the source and destination, and all nodes are homogeneous as shown in the example illustrated in Figure 2.9. Then, we can easily derive the following relation by the multinomial expansion as[5]

$$\mathbb{E}\{P_{t:d}\} = \xi r_{SD}^{\alpha} = \xi \left(\sum_{h=1}^{H} r_h \right)^{\alpha} > \xi \left(\sum_{h=1}^{H} r_h^{\alpha} \right) = \mathbb{E}\{P_{t:c}\} \tag{2.5}$$

where $\mathbb{E}\{P_{t:d}\}$ and $\mathbb{E}\{P_{t:c}\}$ denote the average required transmit power for non-cooperative and cooperative transmissions; r_{SD} represents the distance between source and destination; r_h represents the radio wave propagation distance in the hth hop. The derived relation above guarantees a higher energy efficiency by involving multi-hop transmissions. Although in practice relay nodes are not necessarily placed in such an ideal manner, the inequality is still valid for most cases [72].

2.3.1.3 Spectrum Efficiency

The spectrum efficiency enhancement brought by OFDM-based relay systems is from two aspects: cooperative communications and OFDM. First, as we mentioned

[5] Here, we assume perfect detection at each relay node.

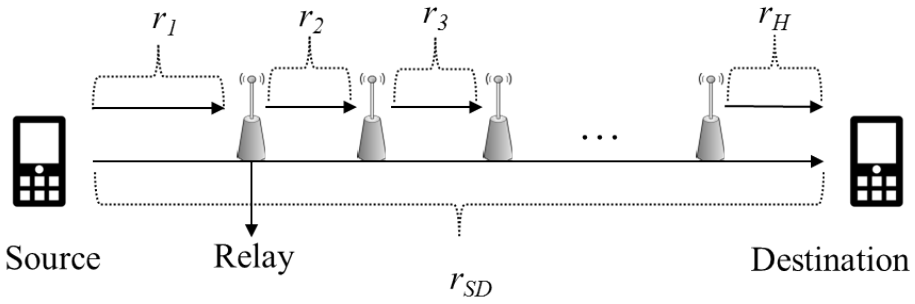


Figure 2.9: Illustration of the topology for demonstrating the energy efficiency advantage brought by cooperative communications.

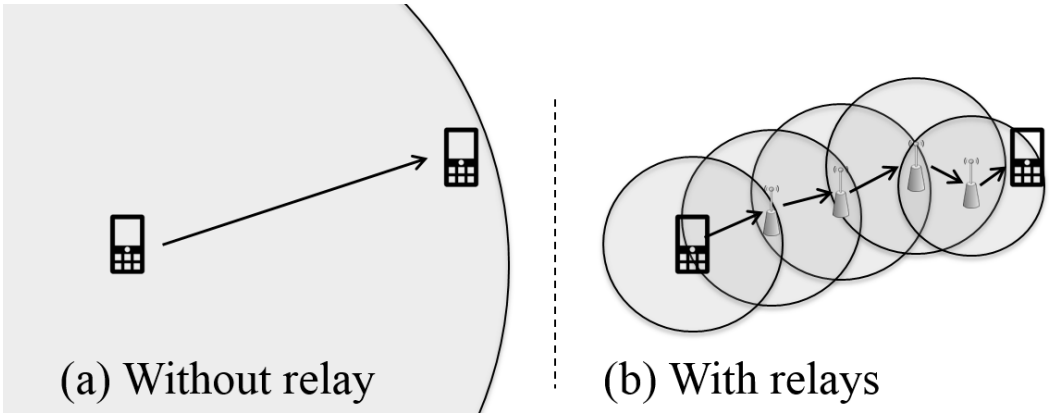


Figure 2.10: Isotropic interference areas: a comparison between cases (a) without and (b) with relays.

in the previous parts, the transmit power can be reduced by involving relays and cooperative transmissions. Therefore, the reuse of the same spectrum resource among multiple users in close proximity becomes possible [57]. We can demonstrate the difference of interference areas for the case without and with relays in Figure 2.10. Second, due to the unique orthogonality among subcarriers provided by OFDM, the overall required bandwidth decreases by the overlap of subcarriers (c.f. Figure 2.7), which facilitates using less spectrum resource to obtain the same performance gains. Consequently, the spectrum efficiency can be enhanced by OFDM(A) compared to conventional single-carrier FDMA (SC-FDMA) [73].

2.3.1.4 Network Coverage Extension

It has been proven that relaying is a powerful tool to extend the network coverage [58,59,74]. This is particularly useful when the installation of a new BS is prohibited for economic and environmental reasons. For example, the deployment of a BS in less populous areas might not be economically feasible, since the number of user equipments is limited, which cannot even support the routine maintenance cost of a BS. In this scenario, a relay station could be a good alternative to take the BS's job, since in LTE Advanced (LTE-A) framework, a relay is also allowed to form a small cell to support the communication service [75]. The advantage of coverage extension by relays can also be demonstrated when user equipments are inside buildings or in other dead spots, in which direct communications to a BS are not possible. In these cases, a relay can be deployed at the top of a building or some higher places so that a line-of-sight path between BS and relay can be constructed. Then, the service provisions from the BS to user equipments are assisted by the relay, so that the network coverage can be extended to these dead spots [59]. Another reason to utilize relays for network coverage extension is because of the rise of environmental awareness in recent years. Since the last decade, fully-fledged BSs are not very welcome in residential areas and there were even protests against the installation of BSs for health and environmental concerns [76]. Therefore, the argumentation process and installation assignment of a BS would be much more complicated than deploying a relay. Due to these reasons, with the miniaturization of service cells, relays are more commonly used to extend network coverage nowadays.

2.3.1.5 Load Balancing among Base Stations

It has been proven that load balancing plays a crucial role for providing system capacity enhancement and satisfactory user experience. Fortunately, another useful function of the relay node is that it could be used to balance the load among BSs. For example, when a BS is fully loaded with a great number of service subscribers, new

communication requests can be relayed to other neighboring BSs, which still own spare resources to cope with these requests [25]. The load balancing can enhance the global infrastructure efficiency as well as the QoS for service subscribers, which can hardly be realized without a relay, because of the severe signal attenuation caused by a long propagation distance among different cells.

2.3.1.6 Cost Efficiency

An important feature of OFDM-based relay systems that is attractive to commercial operators is the cost efficiency. Compared to traditional point-to-point communications supported by BSs with costly backhaul infrastructure, cooperative communications show a superior cost efficiency in three areas: implementation, operation and maintenance. For the aspect of implementation, the brute solution to solve the ever increasing demands in communications without a relay is to implement a large number of BSs, which has been proven not to be economically sustainable as the already high penetration rate of mobile users cannot be further increased to compensate the implementation cost. The main cost advantage of relay network implementation is due to the lack of backhaul infrastructure [59]. The cost caused by connecting BSs to core networks can thus be reduced by 8 percent to 20 percent [75]. Meanwhile, in terms of the physical size, a relay is much smaller than a BS, which will ease the site selection and reduce the corresponding cost [25]. For the aspect of operation, involving relays in cellular networks will increase the frequency reuse efficiency. As the frequency resource is the most expensive part of operating cellular networks, relay networks can also help decrease the operation cost. Also, because the service area of a relay station is smaller, the transmit power can be reduced accordingly and the cost of electricity for operating relay networks thereby become less [30, 75]. For the aspect of maintenance, a dedicated relay is mainly a transceiver with simple processing units or amplifiers, and replacing components in a relay does not cost too much [25].

2.3.1.7 Scalability and Flexibility

As we mentioned above, a relay is a relatively simple transceiver, which allows rapid deployment. Therefore, with relays, the network topology is dynamic. As a result, networks with relays can be adapted fast and easily depending on the service requests. For example, the network can be easily scaled by deploying *nomadic* relays, which suits emergency communications without sufficient time to build up permanent facilities [55]. Also, such a dynamic topology will ease implementations of resource allocation algorithms and interference management [58,77]. In addition, as we explained above, any device capable of transmitting and receiving electromagnetic signals can work as a relay. Such a flexibility enables relay networks to be defined in a broad way, and suits the trends of the IoT and machine-to-machine (M2M) communications. Another side effect of this flexibility is that the backward compatibility is relatively easy to deal with and the update of relay networks becomes simpler [78]. Besides, OFDM can also bring an extra flexibility, since the asymmetric transmission in uplink and downlink can be easily supported by the subcarrier coordination [79].

2.3.2 Drawbacks of OFDM-Based Relay Systems

The benefits of OFDM-based relay systems are also brought at the cost of a series of drawbacks, which sometimes could lead to severe performance degradation without precautionary measures. To provide a fair comparison, we elucidate these drawbacks as follows.

2.3.2.1 Transmission Delay

To decouple the transmissions in multiple hops and provide a high capacity, orthogonal phases are needed for a complete transmission in cooperative networks. As a consequence, if the half-duplex forwarding protocol is adopted, an increasing trans-

mission delay will be inevitable to prevent cross-hop interference. What is worse, when adopting DF relaying protocol, an even longer delay would be expected, as the decoding process will take much more time than simply amplifying [59]. Besides, another large portion of the transmission delay is contributed by the routing process. When multiple relays constitute a mesh network with multiple hops, the multi-hop routing problem shares the same mathematical model with the famous route inspection problem and is NP-hard [53]. As a consequence, it would take a long delay to calculate an optimal or suboptimal route to transmit the signal from the source to the destination.

2.3.2.2 Complexity and Signaling Overhead

An increasing complexity and signaling overhead at the transmitter and receiver will be caused when non-transparent relays are involved in a network. First, a more complicated time synchronization over multiple relays is needed. The employment of OFDM will worsen the situation and generate more signaling overhead for strict frequency synchronization, as the signal modulated by OFDM is sensitive to the frequency offset. Meanwhile, if DF relays are in use, the transmission security and confidentiality should be concerned, as DF relays are also capable of decoding the transmitted signal [30]. Also, to perform relay selection or determine an optimal/-suboptimal transmission route from the source to the destination, the cooperative network needs to be estimated and instantaneous or statistical CSI is required. This requirement results in enormous signaling overhead. An extra feedback channel exclusively used for selected relay/route indication further contributes to the system complexity [80]. Furthermore, at the receiving side, multiple replicas from parallel channels need to be combined to assist the estimation, which requires an extra combining process at the receiver [33].

2.3.2.3 PAPR and Nonlinear Distortion

The high peak-to-average power ratio (PAPR) problem is mainly caused by the use of OFDM, and the negative impact of the high PAPR can be reinforced by the amplifier's nonlinear distortion in AF relay networks. In the time domain, an aggregate OFDM block is generated by summing up modulated signals on K independent subcarriers. Because of the unique frequency relations among OFDM subcarriers (c.f. (2.4)), it is more likely that peaks of several subcarriers will appear at the same time, so that the resultant amplitude of the aggregate OFDM symbol will be overlarge at some instants compared to its average over the entire symbol period. This phenomenon is termed the *high PAPR problem* and will be more serious with an increasing number of subcarriers [81]. The high PAPR problem will result in difficulties in analog-to-digital (A/D) and digital-to-analog (D/A) conversions as well as signal amplification. This is because most electronic components can only function well within a limited power region. Therefore, a signal with high PAPR is more likely to be distorted [68]. The presence of such a nonlinear distortion would cause severe ICI and has a deleterious impact on OFDM symbol estimation at the receiver [82].

2.4 Multi-Carrier Relay Selections

After reviewing the fundamentals related to relay technology and OFDM, we can now move a bit forward to some specific and relevant research topics. The most frequent and important research topic related to relay systems would be relay selection (a.k.a. relay assignment). Relay selection has the potential to provide full diversity and has thus been investigated since the proposal of cooperative diversity systems in 2004. However, the extension of relay selection technologies designed for single-carrier systems to multi-carrier systems is not straightforward, because the system performance (e.g., outage and error) over different subcarriers must be con-

sidered as a whole [83]. In this section, we introduce two intuitive and commonly used multi-carrier relay selection schemes as well as a compromise scheme termed the *combined relay selection*.

2.4.1 Bulk Relay and Per-Subcarrier Selections

The primary work proposing multi-carrier relay selections is presented in [84], in which two basic selection criteria are given. The simplest multi-carrier relay selection scheme is called *bulk relay selection*, and this selection scheme selects only *one* relay to forward signals transmitted on all subcarriers. In contrast, another basic multi-carrier relay selection scheme is called *per-subcarrier relay selection*, and it selects multiple relays in a per-subcarrier manner. Obviously, the per-subcarrier relay selection outperforms bulk relay selection in terms of outage and error performance, but its signaling overhead and system complexity are much higher. We can mathematically express the sets of selected relay(s) by both schemes as[6]

$$\mathcal{L}_{bulk} = \arg \max_{m \in \mathcal{M}} \min_{k \in \mathcal{K}} \mathsf{SXR}(m,k) \tag{2.6}$$

and

$$\mathcal{L}_{ps} = \bigcup_{k=1}^{K} \left\{ \arg \max_{m \in \mathcal{M}} \mathsf{SXR}(m,k) \right\}, \tag{2.7}$$

where K denotes the number of subcarriers; $\mathcal{M}$ is the set of all M relays; $\mathsf{SXR}(m,k)$ denotes the SNR/signal-to-interference-plus-noise ratio (SINR)/signal-to-interference ratio (SIR) of the kth subcarrier forwarded by the mth relay.

In [84], the outage performance for both bulk and per-subcarrier relay selection schemes is analyzed for DF relaying in multi-hop cooperative networks. First, this work explains the mechanism of reducing processing complexity and transmission delay for OFDM-based relay systems by involving relay selections. In particular, it shows that multi-carrier relay selection would be a good approach to achieve the

[6] For bulk relay selection, it has been proven that the outage event at high SNR/SINR/SIR is dominated by the deepest faded subcarrier [85]. As a result of this dominance, the best way to improve the reliability of OFDM-based systems by selecting only one relay is to *maximize* the *minimum* SNR/SINR/SIR over all subcarriers.

full diversity by the minimum cooperation among relays and can be easily implemented in a decentralized manner without centralized control and coordination. This work meanwhile explores the bottleneck effect of multi-hop networks in multi-carrier scenarios, and defines end-to-end performance metrics for evaluating multi-carrier multi-hop systems. Also, a timer-based distributed implementing scheme is proposed to further reduce signaling overhead. However, as a primary work, the analysis of outage performance for multi-hop cooperative networks is given in multiple integrals and cannot provide much insight into the proposed systems.

To provide a better mathematical tractability, the number of hops is fixed to two and the definition of the outage event for uncoded OFDM-based relay systems is given in [86]:

Definition 1. An outage occurs when the end-to-end SNR/SINR/SIR of any subcarrier falls below a preset outage threshold s.

■

As a consequence, we can express the system outage probability for a generic OFDM-based relay system by

$$P_{out}(s) = 1 - \prod_{k=1}^{K} (1 - P_{out}(s,k)) \tag{2.8}$$

where $P_{out}(s,k)$ is the outage probability of the kth subcarrier.

2.4.2 Combined Relay Selection

As shown in **Section 2.4.1**, bulk and per-subcarrier relay selections can be regarded as two extreme cases in the performance-complexity trade-off. Bulk relay selection is the simplest selection scheme involving only one relay, while the outage/error performance is far from optimal. On the contrary, per-subcarrier relay selection has the optimal performance, albeit incurring a much higher system complexity as well as signaling overheads by involving multiple relays [84].

To provide a satisfactory solution to this performance-complexity trade-off, another selection criterion termed the *combined selection* originally proposed for OFDM-based transmit antenna selection (TAS) would be useful [85]. In [87], the combined selection criterion is transferred to DF relay selection scenarios. Specifically, by combined relay selection, relays are selected by two steps. In the first step, a subset of two relays are selected in a similar manner to bulk selection by the criterion

$$\mathcal{L}_{comb} = \arg \max_{\mathcal{L}_2 \subseteq \mathcal{M}} \min_{k \in \mathcal{K}} \max_{m \in \mathcal{L}_2} \mathsf{SXR}(m, k), \tag{2.9}$$

where $\mathcal{L}_2$ identifies a pair of relays that can be employed to carry out per-subcarrier selection and[7] $|\mathcal{L}_2| = 2$; Obviously, we have $M(M-1)/2$ available options of $\mathcal{L}_2$ in total.

After that, per-subcarrier selection is performed over the two relays in $\mathcal{L}_{comb}$ in a per-subcarrier manner by

$$l_{comb}(k) = \arg \max_{l \in \mathcal{L}_{comb}} \mathsf{SXR}(l, k), \tag{2.10}$$

where $l_{comb}(k)$ denotes the index of the relay forwarding the kth subcarrier after applying combined relay selection. To illustrate the selection process, we give an example with three subcarriers and four relays in Figure 2.11.

To be more clear, the proposed combined selection scheme as well as the conventional bulk and per-subcarrier selection schemes are illustrated in Figure 2.12.

Surprisingly, by such a selection set shrinking, the full diversity is still obtainable. Also, the size of the subset (i.e., the number of relays involved for forwarding) only has an impact on the performance convergence rate, and does not affect the diversity gain. Therefore, we can set the size of subset to *two* (i.e., only two relays are active

[7]We can alternatively employ a three-relay subset $\mathcal{L}_3$ or even a $(M-1)$-relay subset $\mathcal{L}_{M-1}$ in this step. All cases will be the same at high SNR, just with a different convergence rate. However, $\mathcal{L}_2$ is the most representative case, since it is the closest to bulk selection. Therefore, we can later show that as long as one more relay is selected compared to bulk selection (the worst case), the outage performance given by combined selection is asymptotic to the per-subcarrier selection's (the best case).

Original subcarrier-relay SXR matrix

	Relay 1	Relay 2	Relay 3	Relay 4
Subcarrier 1	0.0438	1.9527	0.2329	3.3323
Subcarrier 2	0.7228	0.8633	0.414	0.1635
Subcarrier 3	0.2228	0.0881	0.422	0.0683

Generate six relay pairs and perform per-subcarrier selection within the relays in a pair

	Relay 1	Relay 2
Subcarrier 1	0.0438	1.9527
Subcarrier 2	0.7228	0.8633
Subcarrier 3	0.2228	0.0881

	Relay 1	Relay 3
Subcarrier 1	0.0438	0.2329
Subcarrier 2	0.7228	0.414
Subcarrier 3	0.2228	0.422

	Relay 1	Relay 4
Subcarrier 1	0.0438	3.3323
Subcarrier 2	0.7228	0.1635
Subcarrier 3	0.2228	0.0683

	Relay 2	Relay 3
Subcarrier 1	1.9527	0.2329
Subcarrier 2	0.8633	0.414
Subcarrier 3	0.0881	0.422

	Relay 2	Relay 4
Subcarrier 1	1.9527	3.3323
Subcarrier 2	0.8633	0.1635
Subcarrier 3	0.0881	0.0683

	Relay 3	Relay 4
Subcarrier 1	0.2329	3.3323
Subcarrier 2	0.414	0.1635
Subcarrier 3	0.422	0.0683

Yield the best pair by selecting the maximum among all minumum SXRs

	Relay 2	Relay 3
Subcarrier 1	1.9527	0.2329
Subcarrier 2	0.8633	0.414
Subcarrier 3	0.0881	0.422

Figure 2.11: Illustration of the selection process of combined relay selection with three subcarriers and four relays. The green boxes indicate the minimum SXRs of subcarriers performing per-subcarrier selection over the two-relay pairs and the red figure is the lowest SXR among all subcarriers after performing per-subcarrier selection.

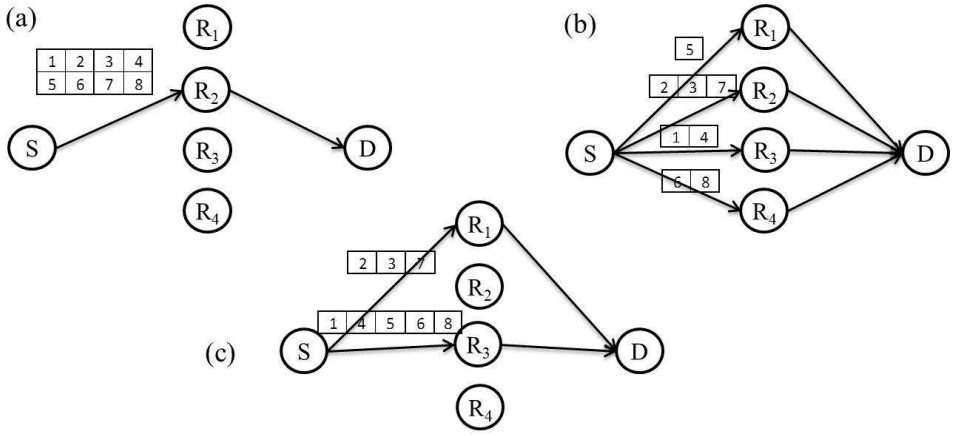


Figure 2.12: Illustration of (a) bulk, (b) per-subcarrier and (c) combined relay selection schemes for a single source, single destination and multiple relays. The numbers in boxes are corresponding to the sequence numbers of subcarriers.

to forward signals), and still obtain the same optimal performance at high SNR as the per-subcarrier selection. We illustrate this behavior by a numerical simulation shown in Figure 2.13 for DF relaying. Unfortunately, all these observations are based on numerical simulations and no analytical result has been presented so far to explain this behavior. In this regard, we carry out the relevant analysis and give a rigorous proof in **Chapter 4**.

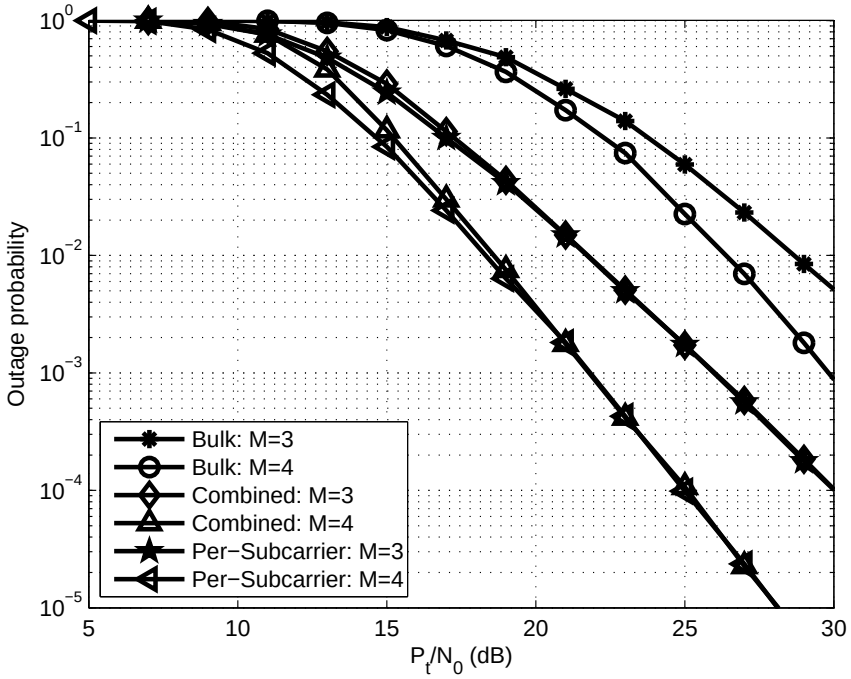


Figure 2.13: Outage performance of different multi-carrier relay selection schemes in normalized Raleigh fading channels vs. the ratio of transmit power P_t to the noise power N_0 for DF relaying, given the number of subcarriers $K = 8$, the outage threshold $s = 1$ and the number of relays $M \in \{3, 4\}$.

2.5 Summary

In this chapter, we reviewed a number of important aspects of OFDM-based relay systems. First, the preliminary knowledge for understanding the technical contents in this thesis and fundamentals of OFDM-based relay systems are expatiated. Following these fundamentals, we briefly discussed the multi-carrier relay selections, which are commonly applied in cooperative systems to obtain diversity. Based on this overview and current research achievements related to the OFDM-based relay technology, we carry out investigations in this thesis mainly around the four questions raised below:

1. Can we analyze OFDM-based relay systems with multi-carrier relay selections in stochastic networks where the number and locations of relays are random?

2. Can we analytically prove the performance equivalence between per-subcarrier

and combined relay selections?

3. Can we integrate OFDM-based relay systems into a practical setting, such as those that should be considered in 5G networks?

4. Can we achieve a diversity gain when there is only one relay and relay selection is not feasible?

In order to address these four questions, relevant technical works are presented in the following four chapters respectively.

Chapter 3

OFDM-Based Relay Selection with Spatially Random Relays

Following the two pioneering works presented in [84, 86], detailed analysis of bulk relay selection is presented in [88]. In this work, DF relay systems performing bulk relay selection with local CSI is considered, and six selection metrics are analyzed. The first work dedicated to OFDM-based AF relaying is presented in [89]. Both bulk and per-subcarrier relay selections are analyzed in OFDM-based AF relay networks, and several bounds of outage probabilities are given. However, all of the above achievements of bulk and per-subcarrier selections do not consider the randomness of relays[1]. The conventional network model employed in these works assumes the number and locations of all nodes are deterministic and stationary, which form a stationary network topology. In practice, however, the dynamic nature of communication nodes is common and should be considered in order to provide a more general and meaningful analysis [90]. Hence, a more realistic way to model a communication network is to assume the location of a node is a random variable. To perform the analysis effectively, Poisson point processes (PPPs) would be used to model the location distribution of relay nodes. However, so far, the link between

[1] The randomness here mainly refers to the number and locations of relays.

OFDM systems and randomly distributed networks is lacking. This motivates us to construct a framework for analyzing the outage performance of OFDM-based relay systems with spatially random relays.

Therefore, in this chapter, we analyze the outage performance of bulk and per-subcarrier relay selection schemes for two-hop OFDM systems in a Poisson field of relays. In particular, special emphasis is placed on DF relay systems. The exact expressions for outage probability are derived in integrals for general cases. In addition, asymptotic expressions for outage probability in the high SNR region in the finite circle relay distribution region are determined in closed form for both relay selection schemes. Meanwhile, a series of important properties related to cooperative systems in random networks are investigated, including diversity, outage probability ratio of two selection schemes and optimization of the number of subcarriers in terms of system throughput. Additionally, we numerically study and discuss the performance of combined relay selection in random networks.

3.1 System Framework and Channel Model

We consider a network with a single source located at the origin denoted by $\mathbf{p}_S = (0, 0)$ and a destination node located at $\mathbf{p}_D = (r_{SD}, 0)$ in a two-dimensional polar coordinate system. The locations of source and destination are deterministic and stationary. Then, we assume the relays are homogeneously Poisson distributed over a two-dimensional region $\mathcal{C} \subseteq \mathbb{R}^2$ with a constant density λ, which form a homogeneous PPP denoted as $\Pi(\mathcal{C})$. In particular, a finite circle distribution region centered at the source node with a radius ς and an infinite distribution region are considered and employed to analyze the system performance in this chapter, which are denoted by $\mathcal{C}_\varsigma$ and $\mathcal{C}_{\text{inf}}$, respectively. Besides, for a typical OFDM system, we assume the number of subcarriers is K, which is deterministic. The set of all subcarriers is denoted as $\mathcal{K}$. Furthermore, it is assumed that the CSI can be

perfectly estimated without any delay and overhead by the source node, so that relay selection can be effectively performed[2]. We further suppose that the entire network operates in a half-duplex protocol and there is not a direct transmission link between source and destination due to deep fading. Therefore, two orthogonal phases are required for one complete transmission from the source to the destination. In particular, the source broadcasts the signal to all relays at the first phase and relays decode and forward the received signal to the destination. For the noise, it is assumed to be independent and identically distributed (i.i.d.) additive white Gaussian noise (AWGN) at all nodes with noise power N_0.

Meanwhile, two signal degradation mechanisms encountered in transmission are considered, which are signal attenuation and multi-path fading. Assuming randomly distributed relays are organized in the set $\mathcal{M}$, for the mth relay located at $\mathbf{p}_m = (r_{Sm}, \theta_m)$ (r_{Sm} and θ_m are the distance and angle between the mth relay to the source), $\forall\ m \in \mathcal{M}$, if an equal power allocation scheme is applied over all communication nodes with transmit power P_t, the received instantaneous SNR on the kth subcarrier is[3]

$$\mathsf{SNR}_1(m,k) = P_t G_1(m,k) r_{Sm}^{-\alpha}/N_0, \tag{3.1}$$

where α is the path loss exponent; $G_i(m,k)$ is the ith hop channel gain on the kth subcarrier due to multi-path fading and is modeled as an i.i.d. exponentially distributed random variable with unit mean. Therefore, for $i \in \{1,2\}$, $m \in \mathcal{M}$ and $k \in \mathcal{K}$, the probability density function (PDF) and cumulative distribution function (CDF) of $G_i(m,k)$ are given by

$$f_G(\zeta) = e^{-\zeta} \ \Leftrightarrow\ F_G(\zeta) = 1 - e^{-\zeta}. \tag{3.2}$$

[2]For an infinite distribution region, the perfect CSI assumption can be justified by implementing a distributed channel estimation method, by which the relays far away from the source and/or destination will not be perceived. As a consequence, a centralized coordinator for channel estimation and relay selection is not required, and the signaling overhead can be reduced to a reasonable level [91].

[3] Here we assume a high-frequency spectrum is in use, so that the distance between any transmitter and receiver is much larger than the radio wavelength and all propagations are thereby in the far field. As a consequence, we may choose a small reference distance, so that the constant path loss term at the reference distance can be neglected for simplicity [92].

For the second phase, because of the DF forwarding protocol, the received instantaneous SNR at the destination is

$$\mathsf{SNR}_2(m,k) = P_t G_2(m,k) r_{mD}^{-\alpha}/N_0, \tag{3.3}$$

where r_{mD} is the distance between the mth relay and destination; however, it should be noted that because we assume the locations of all relays are unchanged during a complete transmission process, r_{mD} is a dependent random variable on r_{Sm} and θ_m, which can be expressed by the law of cosines as

$$r_{mD} = \sqrt{r_{SD}^2 + r_{Sm}^2 - 2 r_{SD} r_{Sm} \cos\theta_m}. \tag{3.4}$$

Finally, the equivalent end-to-end SNR in DF relaying network can be regarded as[4]

$$\mathsf{SNR}(m,k) = \min\{\mathsf{SNR}_1(m,k), \mathsf{SNR}_2(m,k)\}. \tag{3.5}$$

3.2 Outage Performance Analysis with Multi-Carrier Relay Selections

Replacing $\mathsf{SXR}(m,k)$ in (2.6) and (2.7) by $\mathsf{SNR}(m,k)$ obtained in (3.5), we can obtain the sets of selected relays by bulk and per-subcarrier relay selections[5]. For clarity, these two selection schemes are illustrated in Figure 3.1.

To consider the outage performance of multiple subcarriers as an entity, let the superscript $\Xi \in \{bulk, ps\}$ stand for different relay selection schemes and define the

[4]An outage in DF relaying networks depends on the minimum channel coefficient among the source-relay and the relay-destination links. Hence, we can employ the minimum single-hop channel SNR as the equivalent end-to-end SNR here.

[5]Note that here it is allowed that $\arg\max_{m\in\mathcal{M}} \mathsf{SNR}(m,k) = \arg\max_{m\in\mathcal{M}} \mathsf{SNR}(m,n)$ for $k \neq n$. In other words, the relay is capable of forwarding two or more subcarriers simultaneously. Because we do not consider a transmit power limit in all nodes, the power imbalance problem among relays is out of the scope of this chapter.

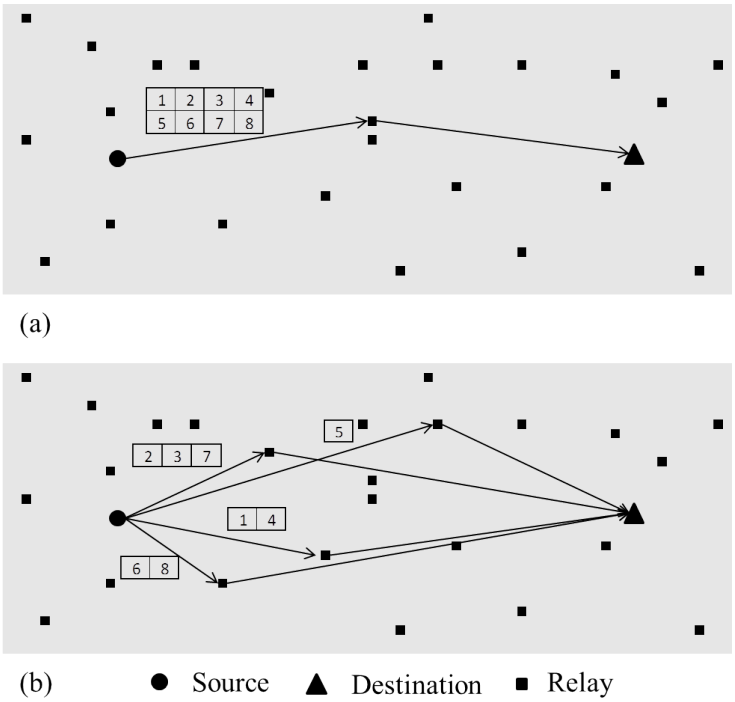


Figure 3.1: Illustration of (a) bulk and (b) per-subcarrier relay selection schemes for single source, single destination and multiple spatially randomly distributed relays, given $K = 8$. The numbers in boxes are the sequence numbers of subcarriers.

a posteriori outage probability after selection as[6]

$$\Phi^{\Xi}(s) = \mathbb{P}\left\{\left\{\min_{k\in\mathcal{K}} \max_{m_k\in\mathcal{L}_{\Xi}} \mathsf{SNR}(m_k, k) < s\right\} \bigcup \{\mathcal{M} = \varnothing\}\right\}, \tag{3.6}$$

where $\mathbb{P}\{\cdot\}$ denotes the probability of the random event enclosed; s is a predefined and fixed target SNR threshold ; m_k is the index of the selected relay forwarding the kth subcarrier. In this chapter, we will take the outage probability defined above as a metric to evaluate the outage performance of the proposed OFDM-based relay system.

[6] $\mathcal{M} = \varnothing$ is possible when the area of relay distribution region $|\mathcal{C}| < \infty$ and this special scenario should be regarded as outage as well [93]. This is because the relay nodes are distributed according to PPP with a constant and bounded density λ. Consequently, as long as the distribution region is finite, there is always a possibility that the number of relay within that distribution region becomes zero and the transmission between source and destination is disabled in this scenario, as we assume a deeply faded direct transmission link.

3.2.1 Bulk Relay Selection

By (3.2) and (3.5), the CDF of the end-to-end SNR $\mathsf{SNR}(m,k)$ can be derived as

$$F(s) = 1 - \exp\left(-\frac{sN_0}{P_t}\left(r_{Sm}^{\alpha} + r_{mD}^{\alpha}\right)\right), \tag{3.7}$$

and by (2.6) the *a posteriori* outage probability after performing bulk relay selection can be determined by[7]

$$\Phi^{bulk}(s) = \mathop{\mathbb{E}}_{\Pi(\mathcal{C})}\left\{\prod_{m\in\mathcal{M}}\left[1-(1-F(s))^K\right]\right\} \overset{\text{(a)}}{=} \exp\left(-\lambda\int_{\mathcal{C}}(1-F(s))^K \mathrm{d}\mathbf{p}_m\right), \tag{3.8}$$

where $\mathbb{E}\{\cdot\}$ denotes the average of the enclosed; (a) holds from the probability generating functional (PGFL) of the homogeneous PPP [94].

3.2.1.1 Finite Relay Distribution Region

Due to the symmetry of the finite circle region $\mathcal{C}_\varsigma$, we transform the surface integral given in (3.8) to a double integral and obtain the outage probability in the finite circle region as:

$$\Phi_\varsigma^{bulk}(s) = \exp\left(-2\lambda u(\varsigma)\right), \tag{3.9}$$

where $u(\varsigma) = \int_0^{\pi}\int_0^{\varsigma}\mathcal{H}(K)\mathrm{d}r_{Sm}\,\mathrm{d}\theta_m$ and $\mathcal{H}(K) = r_{Sm}\exp\left(-\frac{KsN_0}{P_t}\left(r_{Sm}^{\alpha}+r_{mD}^{\alpha}\right)\right)$.

Although there is no closed-form expression of (3.9) because of the double integral in $u(\varsigma)$, we can employ a power series expansion at $\frac{P_t}{N_0}\to\infty$ and obtain the asymptotic expressions of $\Phi_\varsigma^{bulk}(s)$ for an arbitrary α:

$$\Phi_\varsigma^{bulk}(s) \sim \tilde{\Phi}_\varsigma^{bulk}(s) = \exp\left(-\lambda\pi\varsigma^2\left(1-\frac{KsN_0\tau_\alpha}{P_t}\right)\right), \tag{3.10}$$

where

$$\tau_\alpha = \begin{cases} r_{SD}^2+\varsigma^2, & \alpha = 2 \\ r_{SD}^4 + 2r_{SD}^2\varsigma^2 + \frac{2}{3}\varsigma^4, & \alpha = 4 \\ \frac{1}{2}\left(2r_{SD}^2+\varsigma^2\right)\left(r_{SD}^4+4r_{SD}^2\varsigma^2+\varsigma^4\right), & \alpha = 6 \end{cases}. \tag{3.11}$$

[7]The average over $\Pi(\mathcal{C})$ includes the case of $\mathcal{M}=\varnothing$ when $|\mathcal{C}|$ is finite; The surface integral given in the second line of the equation can be converted to a double integral by adopting a certain coordinate system (Cartesian, polar or biangular) and thus numerically calculated.

From (3.10), it can be seen that with an increasing $\frac{P_t}{N_0}$, $\Phi_{\varsigma}^{bulk}(s)$ will converge to the outage floor given by

$$\underline{\Phi}_{\varsigma}^{bulk}(s) = \exp(-\lambda\pi\varsigma^2), \tag{3.12}$$

which is caused by the scenario where there is no relay existing in the finite circle distribution region (c.f. (3.6)).

3.2.1.2 Infinite Relay Distribution Region

Due to the symmetry of the infinite region $\mathcal{C}_{\text{inf}}$, we can obtain

$$\Phi_{\text{inf}}^{bulk}(s) = \exp\left(-2\lambda \int_0^{\pi} \int_0^{\infty} \mathcal{H}(K)\mathrm{d}r_{Sm}\,\mathrm{d}\theta_m\right). \tag{3.13}$$

Unfortunately, there does not exist a closed form of (3.13) for an arbitrary α. However, for a special case when $\alpha = 2$ (free space), we can obtain

$$\Phi_{\text{inf}}^{bulk}(s)|_{\alpha=2} = \exp\left(-\frac{\lambda\pi P_t}{2KsN_0}\exp\left(-\frac{r_{SD}^2 KsN_0}{2P_t}\right)\right). \tag{3.14}$$

3.2.2 Per-Subcarrier Relay Selection

Similarly to the case of bulk relay selection, by (2.7) and the binomial expansion, the *a posteriori* outage probability after performing per-subcarrier relay selection can be determined by

$$\begin{aligned}
\Phi^{ps}(s) &= \mathop{\mathbb{E}}_{\Pi(\mathcal{C})}\left\{1 - \left(1 - \prod_{m\in\mathcal{M}} F(s)\right)^K\right\} \\
&= \sum_{k=1}^{K}\left[\binom{K}{k}(-1)^{k+1}\mathop{\mathbb{E}}_{\Pi(\mathcal{C})}\left\{\prod_{m\in\mathcal{M}} F^k(s)\right\}\right] \\
&= \sum_{k=1}^{K}\left[\binom{K}{k}(-1)^{k+1}\exp\left(-\lambda\int_{\mathcal{C}}\left(1 - F^k(s)\right)\mathrm{d}\mathbf{p}_m\right)\right].
\end{aligned} \tag{3.15}$$

3.2.2.1 Finite Relay Distribution Region

We can obtain the outage probability of per-subcarrier selection scheme over finite relay distribution region by

$$\Phi_{\varsigma}^{ps}(s) = \sum_{k=1}^{K}\left[\binom{K}{k}(-1)^{k+1}\exp\left(-2\lambda\sum_{n=1}^{k}\binom{k}{n}(-1)^{n+1}u(\varsigma,n)\right)\right], \tag{3.16}$$

where $u(\varsigma, n) = \int_0^{\pi} \int_0^{\varsigma} \mathcal{H}(n) \mathrm{d}r_{Sm} \, \mathrm{d}\theta_m$.

Meanwhile, by power series expansion on (3.16) at $\frac{P_t}{N_0} \to \infty$, we also obtain the asymptotic expression of $\Phi_{\varsigma}^{ps}(s)$ as

$$\Phi_{\varsigma}^{ps}(s) \sim \tilde{\Phi}_{\varsigma}^{ps}(s) = \exp\left(-\lambda\pi\varsigma^2\right) \left[1 - K\left(1 - \exp\left(\frac{\lambda\pi\varsigma^2 s N_0 \tau_{\alpha}}{P_t}\right)\right)\right], \tag{3.17}$$

from which we can observe that the outage floor given by

$$\underline{\Phi}_{\varsigma}^{ps}(s) = \exp(-\lambda\pi\varsigma^2) = \underline{\Phi}_{\varsigma}^{bulk}(s), \tag{3.18}$$

is exactly the same as the case of bulk selection. As expected, the outage event at high SNR within a finite circle distribution region is dominated by the case where there is no relay candidate for selection (i.e., $\mathcal{M} = \varnothing$). As a result, it is irrelevant to the selection schemes and/or forwarding protocols and only dependent on the relay node density λ and the radius ς. In general, the outage floor for an arbitrary finite distribution region $\mathcal{C}$ can be derived by

$$\underline{\Phi}(\mathcal{C}) = \exp\left(-\lambda|\mathcal{C}|\right). \tag{3.19}$$

3.2.2.2 Infinite Relay Distribution Region

Similarly, substituting $\mathcal{C} = \mathcal{C}_{\text{inf}}$ into (3.15) yields

$$\Phi_{\text{inf}}^{ps}(s) = \sum_{k=1}^{K} \left[\binom{K}{k} (-1)^{k+1} \exp\left(-2\lambda \sum_{n=1}^{k} \binom{k}{n} (-1)^{n+1} \int_0^{\pi} \int_0^{\infty} \mathcal{H}(n) \mathrm{d}r_{Sm} \, \mathrm{d}\theta_m \right) \right]. \tag{3.20}$$

Again, there is no closed form of (3.20) for an arbitrary α. When $\alpha = 2$, we can obtain

$$\Phi_{\text{inf}}^{ps}(s)|_{\alpha=2} = \sum_{k=1}^{K} \left[\binom{K}{k} (-1)^{k+1} \exp\left(-\lambda\pi \sum_{n=1}^{k} \binom{k}{n} (-1)^{n+1} \frac{P_t}{2nsN_0} \exp\left(-\frac{r_{SD}^2 nsN_0}{2P_t} \right) \right) \right]. \tag{3.21}$$

3.3 Discussion of Important System Properties

In this section, based on the outage performance analysis given in the previous section, we first discuss the diversity gain of OFDM-based relay systems in random

networks, which then leads to an important finding: the ternary property. After that, we also focus on the comparison between bulk and per-subcarrier selections in random networks as well as the optimization on the number of subcarriers K.

3.3.1 Cooperative Diversity Analysis

For deterministic networks, in which the number of relays and/or their locations are stationary, diversity gain is an all-important metric to measure the cooperative performance advantage [28]. However, we show as follows that this metric is not appropriate anymore for cooperative systems in random networks where relays are Poisson distributed. Subsequently we prove the *ternary property* of diversity gain in Poisson random networks.

For cooperative systems in finite Poisson random networks, the binary property of diversity gain has already been proven and it states that the diversity gain $d_o(\mathcal{C})$ can only be either one or zero[8] depending on whether there is a direct transmission link between source and destination or not [93]. Following the discussion of outage floor in **Section 3.2**, this binary property related to diversity gain is straightforward. Without a direct transmission link, an increasing power would not affect the outage performance at high SNR and this leads to a *zero-diversity-order system*.

However, when considering an infinite distribution region, there does not exist such an outage floor, because if the region is infinite, as long as the relay node density λ is positive, there are always an infinite number of relays distributed over region $\mathcal{C}_{\text{inf}}$. As a result, with a *sufficiently* large transmit power (considering the asymptotic region), the two-hop transmission can always be successful, because there must exist a 'satisfactory' two-hop link among an infinite number of relays. This indicates the diversity gain of cooperative systems in infinite random networks

[8] A zero diversity indicates an outage/error floor at high SNR, which does not change by increasing the transmit power.

is infinity. Mathematically, for an arbitrary and bounded α, we can prove that[9]

$$d_o^{\Xi}(\mathcal{C}_{\text{inf}}) = -\lim_{\frac{P_t}{N_0}\to\infty} \frac{\log(\Phi_{\text{inf}}^{\Xi}(s))}{\log(P_t/N_0)} = \infty. \tag{3.22}$$

Therefore, unlike the situations in deterministic networks, it would be impossible to derive a linear relation among $d_o(\mathcal{C})$, λ and α in random networks. Instead, the diversity gain can only be either zero, one or infinity. We term this *ternary property* of diversity gain in Poisson random networks. In the meantime, (3.22) also indicates that any high but bounded path loss attenuation does not counter the constructive effects of infinite distribution region on asymptotic outage performance. Although we will not have the infinite distribution region in practice, this property reminds us that one must be careful when employing the diversity order in spatially random models.

3.3.2 Comparison of Outage Performance between Bulk and Per-Subcarrier Selections

By (3.8) and (3.15), we can quantify the outage performance advantage of per-subcarrier selection over bulk selection via the outage probability ratio given by

$$\phi(\lambda) = \frac{\Phi^{ps}(s)}{\Phi^{bulk}(s)} = \sum_{k=1}^{K} \left[\binom{K}{k} (-1)^{k+1} \exp\left(-\lambda \Delta(k)\right) \right], \tag{3.23}$$

where $\Delta(k) = \int_{\mathcal{C}} \left[1 - F^k(s) - (1 - F(s))^K \right] \mathrm{d}\mathbf{p}_m$.

Considering the case of sparse networks with small λ, the outage probability ratio $\phi(\lambda)$ can be approximated by[10]

$$\phi(\lambda) \approx 1 + \frac{\lambda^2}{2} \sum_{k=1}^{K} \left[\binom{K}{k} (-1)^{k+1} \Delta^2(k) \right]. \tag{3.24}$$

Eq. (3.24) indicates that the outage performance advantage brought by per-subcarrier selection over bulk selection will become negligible with a decreasing λ, because the number of relays for selection is small and employing multiple relays to

[9] See Appendix 3.6.1 for a proof.
[10] See Appendix 3.6.2 for a proof.

perform per-subcarrier selection becomes less likely. Meanwhile, if we would like to ensure the performance advantage by letting the outage probability ratio $\phi(\lambda) \leq \epsilon$ (i.e., the outage probability of per-subcarrier selection is ϵ times lower than that of bulk selection, where $0 < \epsilon < 1$), an approximation of the required minimum density λ can be derived as

$$\lambda \geq \underline{\lambda}(\epsilon) \approx \sqrt{2(\epsilon - 1) / \sum_{k=1}^{K} \left[\binom{K}{k} (-1)^{k+1} \Delta^2(k) \right]}, \tag{3.25}$$

which would provide an efficient switching mechanism between bulk and per-subcarrier selections when the relay node density λ is known[11].

3.3.3 Optimization of the Number of Subcarriers for Bulk Selection

With the development of index modulation (IM) and frequency resource allocation, OFDM systems with a varying number of active subcarriers become common in practice [95–98]. Therefore, it is meaningful to investigate the effects of adopting different numbers of subcarriers K on the system throughput. For simplicity, we assume that equal numbers of bits are carried by each subcarrier. Hence, the average system throughput can be characterized by the average number of successfully decoded subcarriers per transmission at the destination [99], which can be determined by

$$\kappa(K, \lambda) = K \left(1 - \Phi^{\Xi}(s)\right). \tag{3.26}$$

According to (3.6), a large K will lead to a large $\Phi^{\Xi}(s)$, since all signals transmitted on these K subcarriers need to be successfully decoded at the destination, or an outage will occur otherwise. Consequently, for a given λ, there exists an optimal number of subcarriers denoted by K_{opt}, by which the system throughput can be

[11] Although per-subcarrier selection scheme has the optimal outage performance, it is not always preferable if the performance advantage is not significant, because the selection and synchronization processes among multiple relays and destination node are complicated and thus will require more overheads [87].

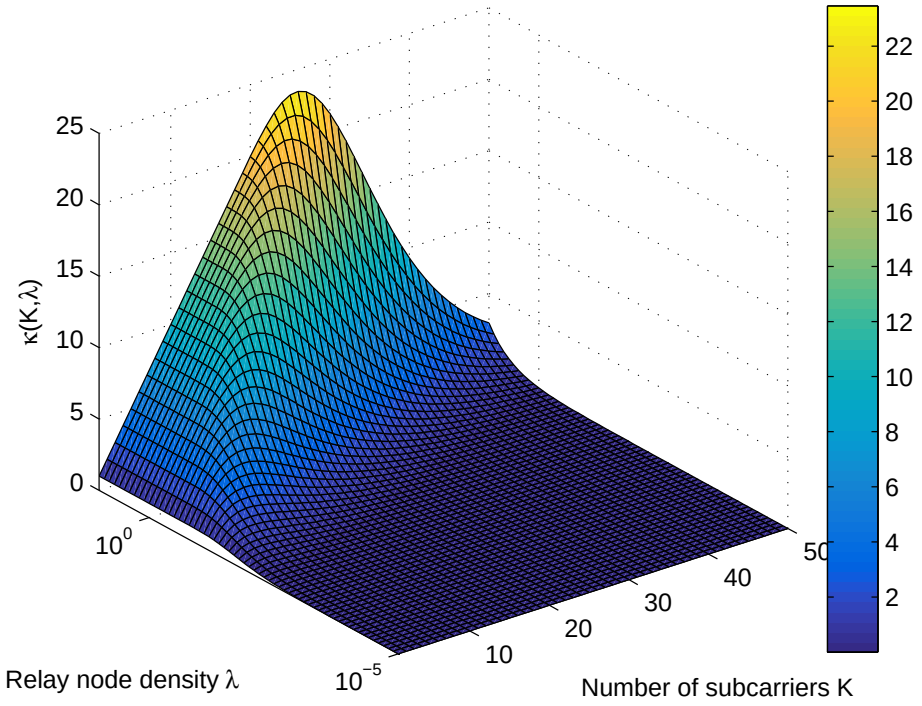


Figure 3.2: Relation among $\kappa(K, \lambda)$, K and λ for bulk selection in free space ($\alpha = 2$), when $s = 1$, $P_t/N_0 = 100$, $r_{SD} = 5$ and $\varsigma = 5$.

maximized. Also, because relay node density λ is varying in practice due to the dynamic on/off switching mechanisms and node mobility [100, 101], it is intuitive that we can dynamically adjust the number of subcarriers K to offset the adverse effects of relay node density λ, so that the system throughput can always be maximized. To be clear, the relation among $\kappa(K, \lambda)$, K and λ is plotted in Figure 3.2 for the case of bulk selection in free space.

Now, let us focus on the method to determine K_{opt}. First, we relax the integer K to a positive real number[12] $\tilde{K}$, so that some optimization tools can be applied. Then, it can be proven that $\kappa(\tilde{K}, \lambda)$ is a concave function of[13] $\tilde{K}$. Therefore, the

[12]Currently, this method is only applicable for bulk selection, since K can be regarded as a product factor in $\Phi^{bulk}(s)$ and thus can be relaxed to $\tilde{K}$. On the other hand, because K is the upper limit of the summation in $\Phi^{ps}(s)$, this relaxing relation is not feasible, and thus the following optimization is not possible for per-subcarrier selection.

[13]See Appendix 3.6.3 for a proof.

optimal solution to $\tilde{K}$ can be obtained via a concave problem formulated by

$$\begin{aligned} \tilde{K}_{\text{opt}} &= \arg\max_{\tilde{K}} \kappa(\tilde{K}, \lambda) \\ &\text{s.t.} \quad \tilde{K} > 0, \end{aligned} \tag{3.27}$$

which can be solved efficiently using standard optimization techniques (e.g., CVX in MATLAB). Then, K_{opt} is determined by

$$K_{\text{opt}} = \begin{cases} \lceil \tilde{K}_{\text{opt}} \rceil, & \text{if } \kappa(\lceil \tilde{K}_{\text{opt}} \rceil, \lambda) \geq \kappa(\lfloor \tilde{K}_{\text{opt}} \rfloor, \lambda) \\ \lfloor \tilde{K}_{\text{opt}} \rfloor, & \text{if } \kappa(\lceil \tilde{K}_{\text{opt}} \rceil, \lambda) < \kappa(\lfloor \tilde{K}_{\text{opt}} \rfloor, \lambda), \end{cases} \tag{3.28}$$

where $\lceil \cdot \rceil$ and $\lfloor \cdot \rfloor$ denote ceiling and floor functions, respectively.

However, the optimization of $\kappa(K, \lambda)$ given above would not always be applicable, since the chosen K_{opt} would lead to an inappropriate outage probability beyond a threshold Ψ, which should be maintained for a prescribed QoS. Unlike networks for real-time streaming media, in which throughput is the key [102], this reliability requirement is particularly crucial for some special networks, e.g., the IoT [103] and military WSNs [104]. In this context, K_{opt} is dependent on λ and Ψ. Therefore, with this constraint on outage probability Ψ, the concave optimization problem formulated in (3.27) becomes[14]

$$\begin{aligned} \tilde{K}_{\text{opt}} &= \arg\max_{\tilde{K}} \kappa(\tilde{K}, \lambda) \\ &\text{s.t.} \quad \tilde{K} > 0 \ \text{ and } \ \Phi^{\Xi}(s)|_{K=\tilde{K}} \leq \Psi. \end{aligned} \tag{3.29}$$

Then K_{opt} will be determined by

$$K_{\text{opt}} = \lfloor \tilde{K}_{\text{opt}} \rfloor. \tag{3.30}$$

On the other hand, because $K \geq 1$ must be ensured in order to provide transmission service, it is impossible to always maintain a given outage probability Ψ by reducing K when λ keeps decreasing. Consequently, there is a cut-off relay node density λ_c, below which the outage probability Ψ cannot be maintained by reducing K. By substituting $K = 1$ into (3.8), the cut-off density can be numerically

[14]This formulated problem is also concave, due to the monotonous relation between K and $\Phi^{\Xi}(s)$.

evaluated by

$$\lambda_c = -\frac{\ln \Psi}{\int_{\mathcal{C}}(1 - F(s))\mathrm{d}\mathbf{p}_m}. \tag{3.31}$$

By (3.14), the cut-off relay node density for bulk selection in free space can be approximated by

$$\lambda_c|_{\alpha=2} \approx -\frac{2sN_0 \ln \Psi}{\pi P_t \exp\left(-\frac{r_{SD}^2 sN_0}{2P_t}\right)}. \tag{3.32}$$

3.4 Numerical Simulations and Discussion

3.4.1 Outage Performance of Bulk and Per-Subcarrier Selections

First of all, we need to verify the correctness of the analytical results of outage probabilities. To do so, we normalize $s = 1$, $N_0 = 1$ and set $\lambda = 1$, $\varsigma = 5$ and[15] $r_{SD} = 5$. Also, it should be noted that by using OFDM as the modulation scheme, we are able to pack subcarriers close to each other, and thereby convert a frequency-selective fading channel into K frequency-flat fading sub-channels without interference. As a result, we assume the fading conditions of all subcarriers are independent in simulations throughout this thesis. Then, we simulate the relation between the outage probability and the transmit power with spatially random relays distributed over a finite circle region. The simulation results for bulk and per-subcarrier selections are presented in Figure 3.3 and Figure 3.4, respectively. From the results shown in these two figures, our analysis of the outage performance corresponding to finite circle region has been verified. Meanwhile, we can also see that the variation of the number of subcarriers K has a significant impact on the outage performance for bulk selection, while it is relatively trivial for per-subcarrier selection. This is because bulk selection can only employ one relay to satisfy transmission requirements of all subcarriers, which is more 'K-sensitive' than the case of per-subcarrier

[15]The lengths given here are relative and thus dimensionless, since other parameters have been normalized.

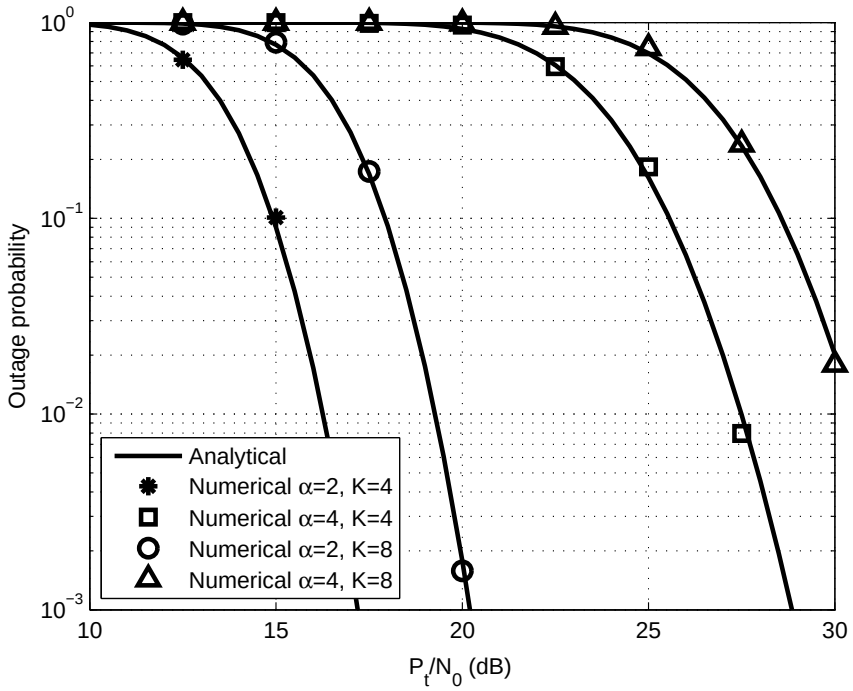


Figure 3.3: Bulk selection case: outage probability vs. P_t/N_0, when $\lambda = 1$, $\varsigma = 5$ and $r_{SD} = 5$.

selection, which is capable of employing multiple relays. Both selection schemes are affected by path loss exponent on a large but similar scale, which aligns with our expectation.

3.4.2 Relation between Relay Node Density and Multi-Relay Performance Advantage

In order to investigate the effects of the relay node density λ on outage probability ratio $\phi(\lambda)$, we define the *connection probability* as $\bar{\Phi}^{\Xi}(s) = 1 - \Phi^{\Xi}(s)$, which eases the illustration of some crucial properties of spatially random networks in logarithmic plots when λ is small[16]. Then, we set $P_t/N_0 = 100$ and $K = 4$ and plot the relation between connection probability and λ in Figure 3.5. From Figure 3.5, it is obvious that when λ is small (i.e., in sparse networks), the multi-relay

[16] When λ is small, the outage probability will approach one and the logarithmic scale is a nonlinear scale in terms of the power of ten, which cannot show the details around one.

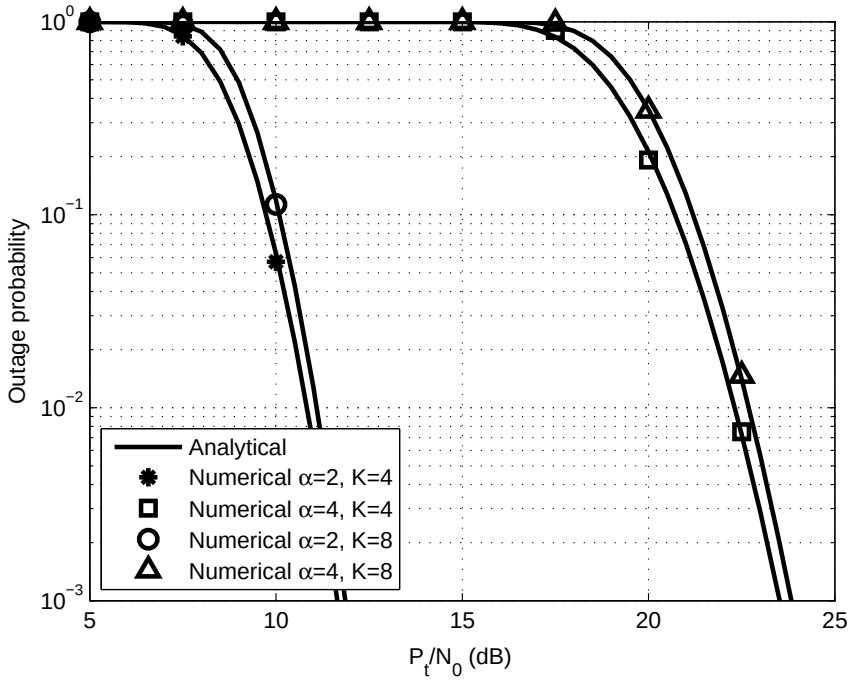


Figure 3.4: Per-subcarrier selection case: outage probability vs. P_t/N_0, when $\lambda = 1$, $\varsigma = 5$ and $r_{SD} = 5$.

performance advantage brought by per-subcarrier selection over bulk selection will become negligible, because the number of relays for selection is small and employing multiple relays to perform per-subcarrier selection becomes less likely. Also, in order to show the properties for small λ in logarithmic plots, we specify $\bar{\epsilon} = 1 - \epsilon$ and plot the relation between $\bar{\epsilon}$ and λ to verify the proposed approximation (3.25) in Figure 3.6[17]. From this figure, it is verified that the proposed approximation on $\underline{\lambda}(\epsilon)$ is tight for small λ and can thereby provide an efficient metric for evaluating the performance advantage brought by per-subcarrier selection over bulk selection in sparse networks.

[17] For the same reason that we define connection probability, when λ is small, ϵ will approach to one and the details cannot be shown on a logarithmic scale based on the power of ten. In Figure 3.6, the exact λ is produced by numerically inversely solving (3.23) for $\phi(\lambda) = 1 - \bar{\epsilon}$, while the approximate λ is produced by calculating $\underline{\lambda}(1 - \bar{\epsilon})$, as given in (3.25).

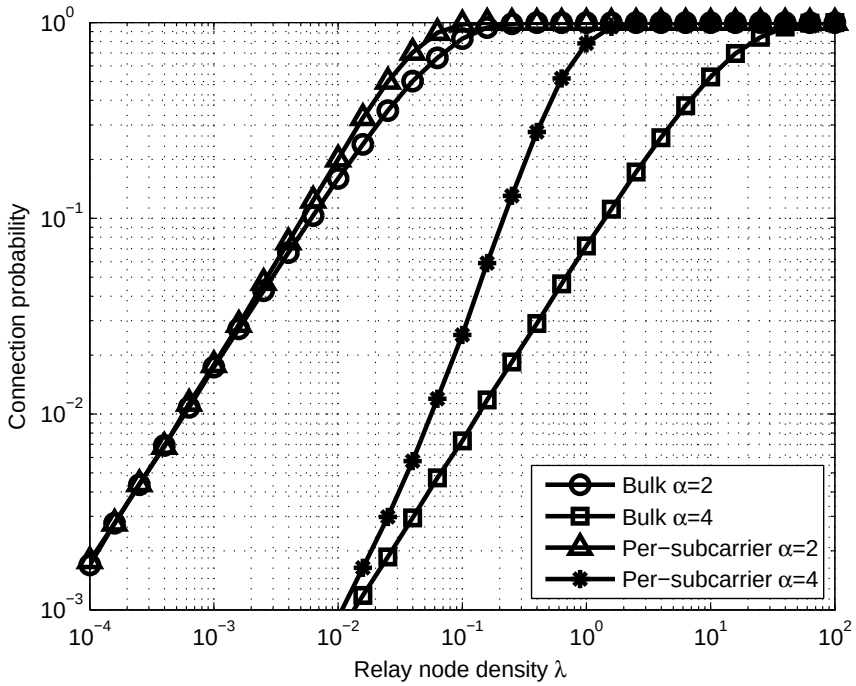


Figure 3.5: Connection probability vs. relay node density λ, when $P_t/N_0 = 100$, $\varsigma = 5$, $r_{SD} = 5$ and $K = 4$.

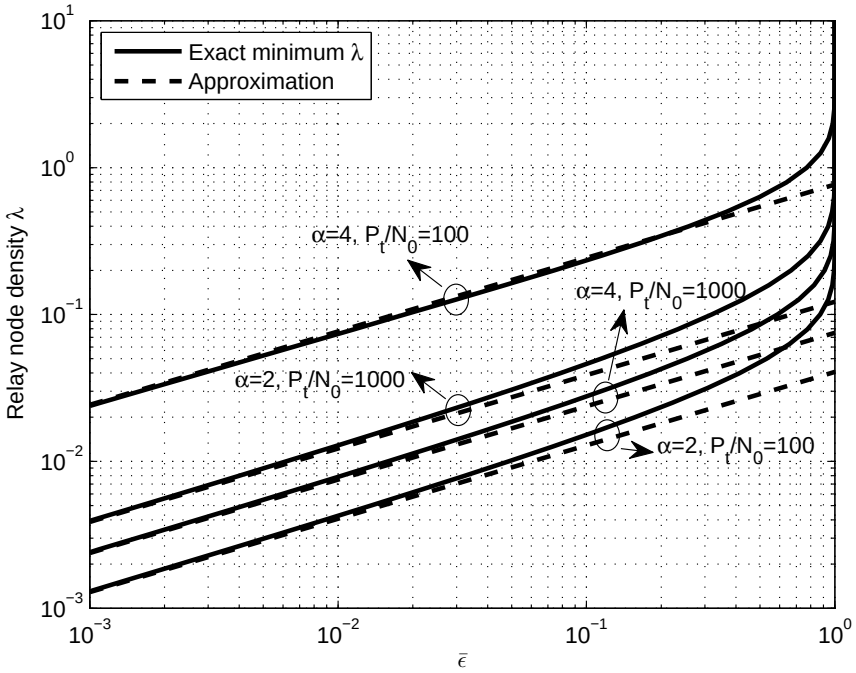


Figure 3.6: $\bar{\epsilon}$ vs. relay node density λ, when $\varsigma = 5$, $r_{SD} = 5$ and $K = 4$.

3.4.3 Relation between the Number of Subcarriers and System Throughput

To verify the solutions to the optimal number of subcarriers produced by the concave problem formulated in (3.27), we set $r_{SD} = 5$, $\varsigma = 5$ and $P_t/N_0 = 100$ and plot the simulation results in Figure 3.7. The jagged nature of K_{opt} reflects K, as the number of subcarriers can only take discrete values in practice. Meanwhile, from this figure, the solutions produced by the concave problem exactly match the numerical results, which verifies the accuracy of the proposed solution. It also aligns with our expectation that with an increasing λ, both K_{opt} and the maximum $\kappa(K, \lambda)$ will increase, since the signal propagation environment has been improved with more 'appropriate' relays. Also, a higher path loss exponent will greatly degrade the system throughput, which can be observed by comparing the results shown for $\alpha = 2$ and $\alpha = 4$. The degradation due to high path loss exponent is obvious especially when λ is large.

Besides, to verify the constrained solution to the optimal number of subcarriers K_{opt} for a given outage probability Ψ, the simulation results are presented in Figure 3.8. Here, we specify $K_{\text{opt}} = 0$ when λ is lower than the cut-off density λ_c for simplicity and frequency resource saving purposes. Again, both numerical and analytical results match each other and these results verify the feasibility of the proposed solution for the scenario with an outage constraint. Also, in comparison with the results illustrated in Figure 3.7, the constraint on outage probability will result in a lower optimal number of subcarriers. Furthermore, by comparing the cases for different Ψ, it can be found that the optimal number of subcarriers reduces with the constraint on outage.

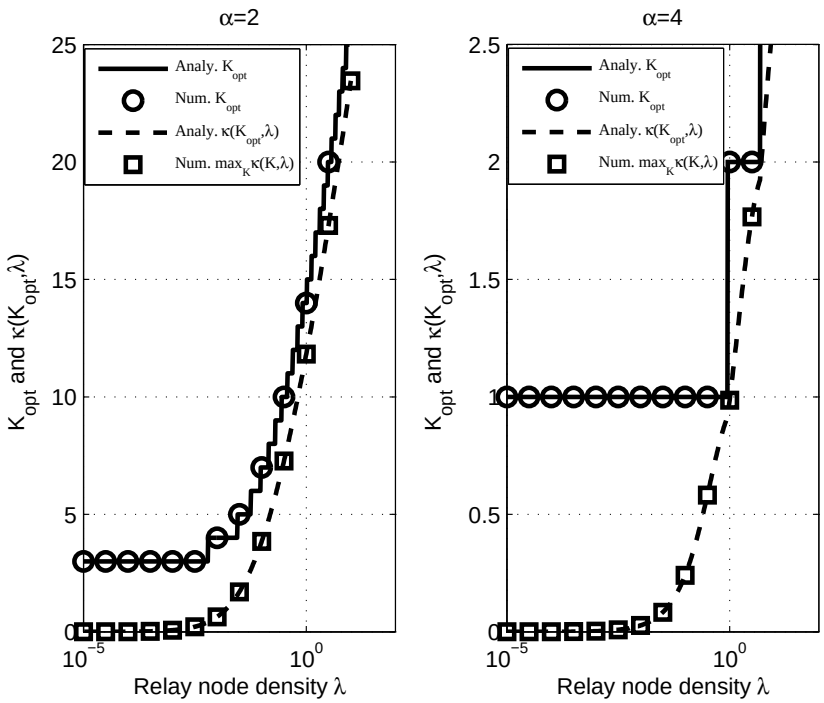


Figure 3.7: Relation between relay node density λ and the optimal number of subcarriers K_{opt} as well as the maximum system throughput characterized by $\kappa(K_{\text{opt}}, \lambda)$, when $s = 1$, $P_t/N_0 = 100$, $\varsigma = 5$ and $r_{SD} = 5$.

3.4.4 Numerical Study of Combined Selection in Random Networks

As introduced in **Section 2.4.2**, the combined relay selection can be regarded as a satisfactory solution to the performance-complexity trade-off in multi-carrier relay selection. Although the analytical methodology adopted in this chapter might not be applicable to combined selection, it would be of interest to observe the performance of combined selection in random networks by numerical simulations. We thereby carry out the simulation in this subsection. The simulation results are illustrated in Figure 3.9. From these results, it can be observed that the combined selection cannot enjoy the same performance as per-subcarrier selection in random networks, but a significant performance improvement exhibits with one more extra relay compared to bulk selection. The disappearance of this performance equivalence is caused by the randomness of the network topology. Therefore, the diversity

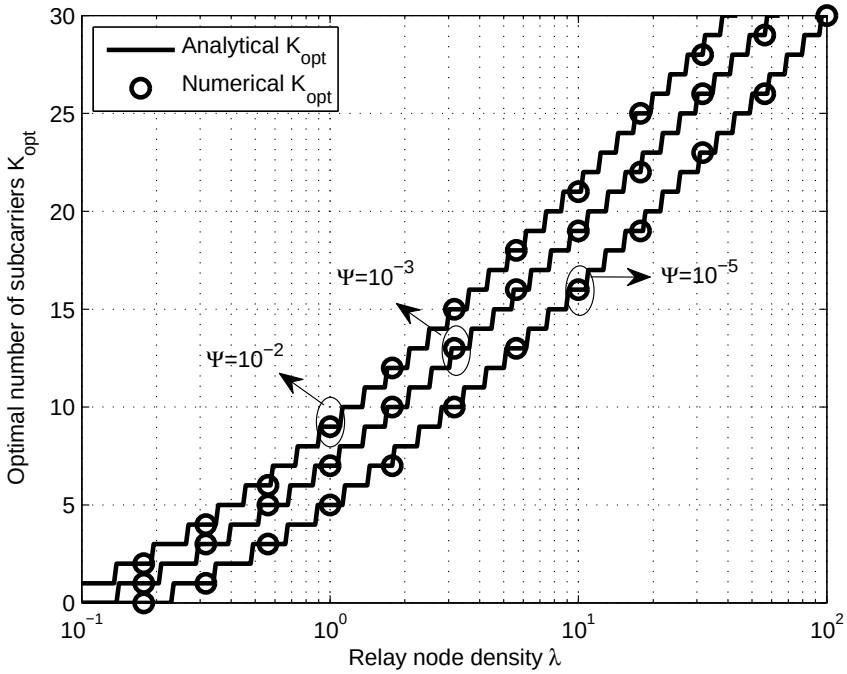


Figure 3.8: Relation between relay node density λ and the optimal number of subcarriers K_{opt} for a given outage probability $\Psi \in \{10^{-2}, 10^{-3}, 10^{-5}\}$, when $\alpha = 2$, $s = 1$, $P_t/N_0 = 100$, $\varsigma = 5$ and $r_{SD} = 5$.

cannot be used to characterize the asymptotic performance at high SNR anymore, which is the foundation of the performance equivalence between per-subcarrier and combined relay selections in stationary networks.

3.5 Summary

In this chapter, we analyzed the outage performance of OFDM-based relay systems with spatially random DF relays, which adopt bulk and per-subcarrier selection schemes, respectively. Also, a series of important properties related to cooperative systems in random networks were investigated, including diversity, outage probability ratio of two selection schemes and the optimization of the number of subcarriers. All analyses have been verified by simulations and some key properties of the proposed OFDM-based relay system over finite and infinite random networks have been revealed and discussed. Additionally, we numerically studied the outage per-

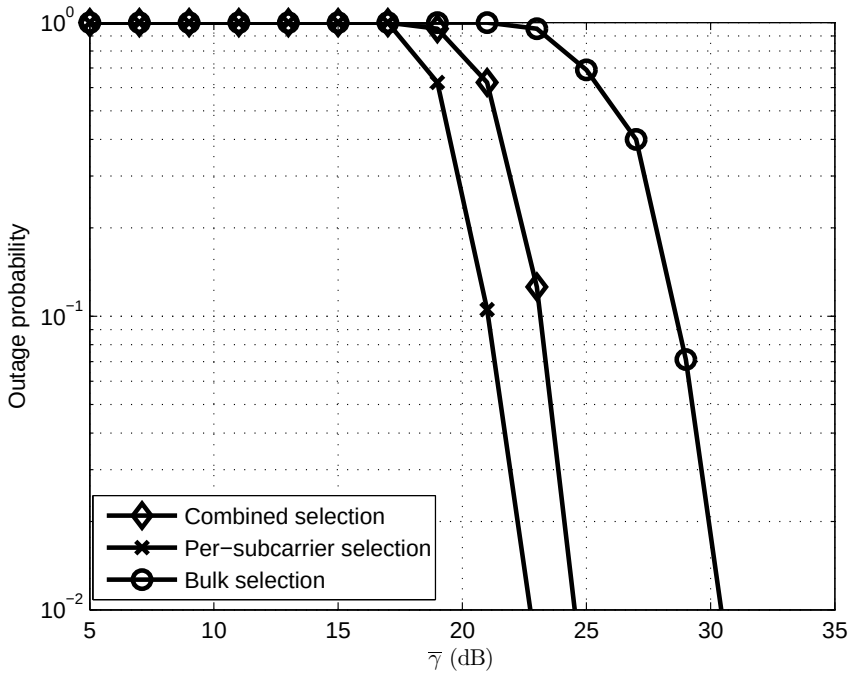


Figure 3.9: Two-hop DF relay selection case: outage performance comparison among bulk, per-subcarrier and combined selections in random networks

formance of combined relay selection in random networks and briefly discussed the results. Moreover, with (3.8) and (3.15), an analytical framework for OFDM-based relay systems applying multi-carrier relay selections over randomly distributed relays has been constructed in this chapter, which can be easily modified to analyze other similar cases for different forwarding protocols, location distributions and/or channel conditions.

3.6 Appendices

3.6.1 Proof of Diversity Gain in Infinite Poisson Random Networks

To determine the diversity gain in infinite Poisson random networks for bulk selection, we first have the relation

$$\begin{aligned} d_o^{bulk}(\mathcal{C}_{\inf}) &= -\lim_{\frac{P_t}{N_0}\to\infty} \frac{\log\left(\Phi_{\inf}^{bulk}(s)\right)}{\log\left(P_t/N_0\right)} \\ &\overset{\text{(b)}}{>} \lim_{\frac{P_t}{N_0}\to\infty} \frac{2\pi\lambda\int_0^\infty r_{Sm}\exp\left(-\frac{KsN_0}{P_t}\left(r_{Sm}^\alpha+(r_{Sm}+r_{SD})^\alpha\right)\right)\mathrm{d}r_{Sm}}{\ln 10\log(P_t/N_0)} \\ &> \mathcal{T}_2 = \lim_{\frac{P_t}{N_0}\to\infty} \frac{2\pi\lambda\mathcal{T}_1}{\ln 10\log(P_t/N_0)}, \end{aligned} \tag{3.33}$$

where (b) holds because of the trigonometric relation among r_{mD}, r_{Sm} and θ_m expressed in (3.4); $\mathcal{T}_1$ is given by

$$\begin{aligned} \mathcal{T}_1 &= \int_0^\infty r_{Sm}\exp\left(-\frac{KsN_0}{P_t}\left(r_{Sm}^\alpha+(2\max(r_{Sm},r_{SD}))^\alpha\right)\right)\mathrm{d}r_{Sm} \\ &= \int_0^{r_{SD}} r_{Sm}\exp\left(-\frac{KsN_0}{P_t}\left(r_{Sm}^\alpha+(2r_{SD})^\alpha\right)\right)\mathrm{d}r_{Sm} + \int_{r_{SD}}^\infty r_{Sm}\exp\left(-\frac{KsN_0}{P_t}\left(r_{Sm}^\alpha+(2r_{Sm})^\alpha\right)\right)\mathrm{d}r_{Sm} \\ &= \left(\frac{P_t}{KsN_0}\right)^{\frac{2}{\alpha}}\exp\left(-\frac{KsN_0(2r_{SD})^\alpha}{P_t}\right)\underline{\Gamma}\left(\frac{2}{\alpha},\frac{KsN_0r_{SD}^\alpha}{P_t}\right)+\frac{r_{SD}^2}{\alpha}E_{\frac{\alpha-2}{\alpha}}\left(\frac{(1+2^\alpha)KsN_0r_{SD}^\alpha}{P_t}\right), \end{aligned} \tag{3.34}$$

where $\underline{\Gamma}(n,x)=\int_0^x t^{n-1}e^{-t}\mathrm{d}t$ is the lower incomplete gamma function and $E_n(x)=\int_1^\infty e^{xt}/t^n\mathrm{d}t$ is the exponential integral function.

Substituting (3.34) into the last line of (3.33) yields

$$\mathcal{T}_2 = \lim_{\frac{P_t}{N_0}\to\infty} \frac{2\pi\lambda\mathcal{T}_1}{\ln 10\log(P_t/N_0)} = \infty. \tag{3.35}$$

As a consequence of $d_o^{bulk}(\mathcal{C}_{\inf}) > \mathcal{T}_2$, we have $d_o^{bulk}(\mathcal{C}_{\inf}) = \infty$. Meanwhile, as different selection schemes will not affect diversity gain, which is only related to relay's distribution [86], we can also have $d_o^{ps}(\mathcal{C}_{\inf}) = d_o^{bulk}(\mathcal{C}_{\inf}) = \infty$. Therefore, considering an infinite distribution region $\mathcal{C}_{\inf}$, for $\Xi \in \{bulk, ps\}$, (3.22) has been proven.

3.6.2 Proof of the Approximation of $\phi(\lambda)$ for Small λ

First, we propose a lemma below and this is the prerequisite for applying power series expansion on $\exp(-\lambda\Delta(k))$ for small λ:

Lemma 1. $\Delta(k) = \int_{\mathcal{C}} \left[1 - F^k(s) - (1 - F(s))^K\right] \mathrm{d}\mathbf{p}_m$ is positive and bounded for $k \in \mathbb{N}^+$ and $k \leq K$.

■

Proof. Because $k \leq K$ and $F(s)$ is a CDF and thus satisfies $0 < F(s) < 1$, there exists a relation of the integrand in $\Delta(k)$:

$$1 - F^k(s) - (1 - F(s))^K \geq 1 - F^k(s) - (1 - F(s))^k . \tag{3.36}$$

For $1 - F^k(s) - (1 - F(s))^k$, we can employ mathematical induction as below to prove $1 - F^k(s) - (1 - F(s))^k \geq 0$:

For $k = 1$, $1 - F^1(s) - (1 - F(s))^1 = 0$ and the statement is true. Then for $k = n > 1$, assuming $1 - F^n(s) - (1 - F(s))^n \geq 0$ holds, we can have $1 - F^n(s) \geq (1 - F(s))^n$. Because $0 < F(s) < 1$, we can further obtain

$$1 - F^{n+1}(s) > 1 - F^n(s) \geq (1 - F(s))^n > (1 - F(s))^{n+1} . \tag{3.37}$$

Therefore, the statement for $k = n + 1$ is true and we thus prove the statement $1 - F^k(s) - (1 - F(s))^k \geq 0$ for $k \in \mathbb{N}^+$. Due to (3.36) and $K \geq 2$ (basic assumption of multi-carrier systems), we thereby prove $1 - F^k(s) - (1 - F(s))^K > 0$ for $k \in \mathbb{N}^+$ and $k \leq K$. Meanwhile, because $F(s)$ will decrease exponentially with an increasing transmission distance, the surface integral of the integrand $1 - F^k(s) - (1 - F(s))^K$ over the region $\mathcal{C}$ is positive and bounded. As a result, the lemma is proven.

■

By Lemma 1, $\exp(-\lambda\Delta(k))$ is proven to be expandable for small λ [105]. We can employ a power series expansion on $\exp(-\lambda\Delta(k))$ for small λ and obtain

$$\exp(-\lambda\Delta(k)) = 1 - \lambda\Delta(k) + \frac{\lambda^2\Delta^2(k)}{2} + O(\lambda^3). \tag{3.38}$$

We can truncate $\exp(-\lambda\Delta(k))$ by its second order term and substitute $\exp(-\lambda\Delta(k)) \approx 1-\lambda\Delta(k)+\lambda^2\Delta^2(k)/2$ into (3.23), which yields

$$\begin{aligned}\phi(\lambda) &\approx \sum_{k=1}^{K}\left[\binom{K}{k}(-1)^{k+1}\left(1-\lambda\Delta(k)+\frac{\lambda^2\Delta^2(k)}{2}\right)\right] \\ &= \sum_{k=1}^{K}\left[\binom{K}{k}(-1)^{k+1}\right]-\lambda\sum_{k=1}^{K}\left[\binom{K}{k}(-1)^{k+1}\Delta(k)\right]+\frac{\lambda^2}{2}\sum_{k=1}^{K}\left[\binom{K}{k}(-1)^{k+1}\Delta(k)^2\right].\end{aligned} \tag{3.39}$$

Furthermore, for $K \in \mathbb{N}^+$ and $K \geq 2$, by the binomial expansion, we can derive

$$\sum_{k=1}^{K}\left[\binom{K}{k}(-1)^{k+1}\right] = 1-\sum_{k=0}^{K}\binom{K}{k}(-1)^k = 1-(1-1)^K = 1. \tag{3.40}$$

For the first order term, we can use the additivity property of integrals and swap the order of summation and integral by

$$\sum_{k=1}^{K}\left[\binom{K}{k}(-1)^{k+1}\Delta(k)\right] = \int_{\mathcal{C}}\sum_{k=1}^{K}\left\{\binom{K}{k}(-1)^{k+1}\left[1-F^k(s)-(1-F(s))^K\right]\right\}\mathrm{d}\mathbf{p}_m. \tag{3.41}$$

Subsequently, the integrand can be determined by

$$\begin{aligned}&\sum_{k=1}^{K}\left\{\binom{K}{k}(-1)^{k+1}\left[1-F^k(s)-(1-F(s))^K\right]\right\} \\ &= \sum_{k=1}^{K}\left[\binom{K}{k}(-1)^{k+1}\right]-\sum_{k=1}^{K}\left[\binom{K}{k}(-1)^{k+1}F^k(s)\right]-(1-F(s))^K\sum_{k=1}^{K}\left[\binom{K}{k}(-1)^{k+1}\right] \\ &= 1-[1-(1-F(s))^K]-(1-F(s))^K = 0.\end{aligned} \tag{3.42}$$

As a result, the corresponding surface integral of this zero integrand given in (3.41) is also zero. Finally, the approximation of $\phi(\lambda)$ for small λ given in (3.24) has been proven.

3.6.3 Proof of the Concavity of $\kappa(\tilde{K},\lambda)$ in Terms of $\tilde{K}$

According to the expressions of outage probability for bulk and per-subcarrier selections given in (3.8) and (3.15), it is obvious that $\Phi^{\Xi}(s)$ is a monotonically deceasing

function of $\tilde{K}$. Therefore, $\forall\ \beta \in [0,1]$, $\tilde{K}_1 > 0$ and $\tilde{K}_2 > 0$, we have

$$\Phi^{\Xi}(s)|_{K=(1-\beta)\tilde{K}_1+\beta\tilde{K}_2} \geq \Phi^{\Xi}(s)|_{K=(1-\beta)\tilde{K}_1} \tag{3.43}$$

and

$$\Phi^{\Xi}(s)|_{K=(1-\beta)\tilde{K}_1+\beta\tilde{K}_2} \geq \Phi^{\Xi}(s)|_{K=\beta\tilde{K}_2}. \tag{3.44}$$

As a result, it can be derived that

$$\kappa((1-\beta)\tilde{K}_1 + \beta\tilde{K}_2, \lambda) \geq (1-\beta)\kappa((1-\beta)\tilde{K}_1, \lambda) + \beta\kappa(\beta\tilde{K}_2, \lambda). \tag{3.45}$$

This proves the concavity of $\kappa(\tilde{K}, \lambda)$ in terms of $\tilde{K}$, according to the definition of a concave function [106].

Chapter 4

OFDM-Based Relay Systems with Combined Relay Selection over Spatially Correlated Channels

As shown in **Chapter 3**, bulk and per-subcarrier relay selections can be regarded as two extreme cases in the performance-complexity trade-off. Bulk relay selection is the simplest selection scheme involving only one relay, while the outage/error performance is far from optimal. On the contrary, per-subcarrier relay selection has the optimal performance, albeit incurring a much higher system complexity as well as signaling overheads by involving multiple relays [84]. As a result, the performance-complexity trade-off immediately comes with the proposals of bulk and per-subcarrier relay selections. As we briefly discussed and observed in the numerical simulation given in Section 2.4.2, combined relay selection can provide the optimal outage performance as per-subcarrier relay selection at high SNR with a shrinking subset of two relays, which results in a much lower complexity. However, the optimal performance yielded by the combined relay selection has not been rigorously proven. Moreover, most previous works on relay selections assume i.i.d. fading channels, which are practically rare owing to the insufficient physical sepa-

rations among relays [107]. The performance analysis of combined selection over spatially correlated fading channels is still an open issue. To perform the analysis smoothly, we can employ the spatially correlated channel model given in [108], in which a set of channel gains produced by equally correlated channels can be transferred to a set of conditionally independent channel gains. As a result, we are able to analyze the outage performance using conventional analytical tools, e.g., order statistics[1].

Specifically, in this chapter, we analyze the outage performance of OFDM relay systems employing combined relay selection over equally spatially correlated channels. Specifically, We analyze the asymptotic outage performance of the combined selection scheme in the high SNR region, and prove a generalized theorem. This theorem states that the combined selection can achieve an optimal outage probability equivalent to the per-subcarrier selection at high SNR without using the full set of available relays for selection. This unique property is termed the *equivalence principle*, and it holds for all correlation conditions when the network topology is stationary.

4.1 System Framework

We consider a typical two-hop OFDM system with K *orthogonal subcarriers* and M relays from the single source to the single destination. Hence, MK channels in total are constructed at each hop and for a given subcarrier k, the M channels are equally correlated in space. For the mth relay, the end-to-end SNR transmitted on the kth subcarrier is denoted by $\mathsf{SNR}(m,k)$, $\forall m \in \mathcal{M} = \{1, 2, \cdots, M\}$ and $\forall k \in \mathcal{K} = \{1, 2, \cdots, K\}$. Accordingly, the *a priori* outage probability without

[1]In this chapter, we only analyze a stationary network where the number and locations of relays are given and fixed, so that the diversity can still be employed to characterize the system reliability and the performance equivalence between per-subcarrier and combined relay selections exists.

conditioning on any selection can be defined as

$$F(s) = \mathbb{P}\left\{\mathsf{SNR}(m,k) < s\right\}, \tag{4.1}$$

where s is the end-to-end SNR threshold; $\mathbb{P}(\cdot)$ denotes the probability of the enclosed.

For a two-hop system, there are M channels for a given subcarrier in each hop, denoted as $h_i(m,k)$, $i \in \{1,2\}$. We assume that the channels are mutually correlated with the common cross-correlation coefficient denoted as ρ_i ($0 \leq \rho_i \leq 1$). Therefore, we can construct the equally correlated Rayleigh fading channel by [108]

$$h_i(m,k) = [\sqrt{1-\rho_i}x_i(m,k) + \sqrt{\rho_i}x_{i0}(k)] + j[\sqrt{1-\rho_i}y_i(m,k) + \sqrt{\rho_i}y_{i0}(k)], \tag{4.2}$$

where $j = \sqrt{-1}$; $x_i(m,k)$, $y_i(m,k) \sim \mathcal{N}(0, \mu_i/2)$ are i.i.d. and μ_i is the average channel gain at each hop; $x_{i0}(k)$, $y_{i0}(k) \sim \mathcal{N}(0, \mu_i/2)$ are i.i.d. and serve as references to correlate all channels. Hence, $\forall m \neq n$ we have $\frac{\mathbb{E}\{h_i(m,k)h_i^*(n,k)\}}{\sqrt{\mathbb{E}\{|h_i(m,k)|^2\}\mathbb{E}\{|h_i(n,k)|^2\}}} = \rho_i$. Also, by the fundamental theory of statistics, we have $h_i(m,k) \sim \mathcal{CN}(0,\mu_i)$. As a result, $|h_i(m,k)|^2 \sim \chi_2(0,\mu_i)$. Meanwhile, how both $h_1(m,k)$ and $h_2(m,k)$ are organized in $\mathsf{SNR}(m,k)$ depends on the adopted forwarding protocol, i.e., DF, FG AF and VG AF relaying protocols. Specific relations among $\mathsf{SNR}(m,k)$, $h_1(m,k)$ and $h_2(m,k)$ are detailed in **Section 4.3**.

Besides, we assume that the CSI is perfectly estimated and shared among all communication nodes[2], and the relaying network operates in a half-duplex protocol so that two orthogonal time slots are required for one complete transmission from the source to the destination. All noises are assumed to be independent AWGN with the noise power N_0. Meanwhile, we further suppose that equal bit and power allocation schemes are applied, so that the average transmit power per subcarrier

[2]The CSI is usually estimated through pilots and feedback (e.g., [109]) and the CSI estimation without feedback may also be applied (e.g., [110]).

at the source and at each utilized relay is denoted by P_t.

4.2 Outage Performance Analysis with Combined Relay Selection

Replacing $\mathsf{SXR}(m,k)$ in (2.9) and (2.10) by $\mathsf{SNR}(m,k)$, we can obtain the set of selected relays by combined selection. Therefore, when combined selection is employed, the *a posteriori* outage probability depending on selection can be defined as

$$F_{comb}(s) = \mathbb{P}\{\min_{k\in\mathcal{K}} \max_{l\in\mathcal{L}_{comb}} \mathsf{SNR}(l,k) < s\}. \tag{4.3}$$

Per-subcarrier selection scheme selects multiple relays (up to K) from M relays in a per-subcarrier manner so that all subcarriers can be forwarded via their optimal relays and thus the optimal outage performance is attainable. We can similarly obtain the set of selected relays by replacing $\mathsf{SXR}(m,k)$ in (2.7) by $\mathsf{SNR}(m,k)$, and the *a posteriori* outage probability when per-subcarrier selection is employed can be defined as

$$F_{ps}(s) = \mathbb{P}\{\min_{k\in\mathcal{K}} \max_{m\in\mathcal{M}} \mathsf{SNR}(m,k) < s\}. \tag{4.4}$$

Note that the equivalence principle potentially exists between combined and per-subcarrier selections [85]. Therefore, we adopt the per-subcarrier relay selection as the comparison benchmark in this chapter.

4.2.1 Conditionally Independent Variable Transformation

As detailed in [108], we take a similar approach to transform a set of equally correlated random variables to a set of conditionally independent random variables, so that conventional analytical tools, e.g., order statistics can be applied to analyze them effectively. To do so, we first assume that two references for each subcarrier $x_{i0}(k)$ and $y_{i0}(k)$ are fixed and have $x_{i0}(k) = X_{i0}(k)$ and $y_{i0}(k) = Y_{i0}(k)$. There-

fore, the conditional distribution of $h_i(m,k)$ is $\mathcal{CN}(\sqrt{\rho_i}[X_{i0}(k)+jY_{i0}(k)], \mu_i(1-\rho_i))$. Consequently, given $x_{i0}(k) = X_{i0}(k)$ and $y_{i0}(k) = Y_{i0}(k)$, $|h_i(m,k)|^2 \sim \chi_2(\sqrt{\rho_i[X_{i0}^2(k)+Y_{i0}^2(k)]}, \mu_i(1-\rho_i))$. If we denote $T_i(k) = X_{i0}^2(k) + Y_{i0}^2(k)$, the conditional PDF and the conditional CDF of $|h_i(m,k)|^2$ are given by [71]

$$f_{h_i}(s|T_i(k)) = \frac{1}{\mu_i(1-\rho_i)} e^{-\frac{s+\rho_i T_i(k)}{\mu_i(1-\rho_i)}} I_0\left(\frac{2\sqrt{\rho_i T_i(k) s}}{\mu_i(1-\rho_i)}\right) \tag{4.5}$$

and

$$F_{h_i}(s|T_i(k)) = 1 - Q\left(\sqrt{\frac{2\rho_i T_i(k)}{\mu_i(1-\rho_i)}}, \sqrt{\frac{2s}{\mu_i(1-\rho_i)}}\right), \tag{4.6}$$

where $I_0(\cdot)$ is the zero order modified Bessel function of the first kind; $Q(\cdot,\cdot)$ is the first order Marcum Q function. Meanwhile, the PDF and CDF of $T_i(k)$ can be obtained as:

$$f_{T_i}(T_i(k)) = \frac{1}{\mu_i} e^{-\frac{T_i}{\mu_i}} \quad \Leftrightarrow \quad F_{T_i(k)}(T_i(k)) = 1 - e^{-\frac{T_i(k)}{\mu_i}}. \tag{4.7}$$

Denote $\mathbf{T}_1 = \{T_1(1), T_1(2), \ldots, T_1(K)\}$ and $\mathbf{T}_2 = \{T_2(1), T_2(2), \ldots, T_2(K)\}$. Because $\forall i \in \{1,2\}$ and $k \in \mathcal{K}$, $T_i(k)$ are mutually independent, we thereby can derive the joint PDF corresponding to $\mathbf{T}_1$ and $\mathbf{T}_2$ by

$$f_{\mathbf{T}}(\mathbf{T}_1, \mathbf{T}_2) = \left(\frac{1}{\mu_1\mu_2}\right)^K \prod_{k=1}^{K} \left(e^{-\frac{T_1(k)}{\mu_1}} e^{-\frac{T_2(k)}{\mu_2}}\right). \tag{4.8}$$

Accordingly, for the kth subcarrier, we can denote the conditional *a priori* outage probability as $F(s|T_1(k), T_2(k))$. We can also denote the conditional *a posteriori* outage probabilities for combined selection and per-subcarrier selection as $F_{comb}(s|\mathbf{T}_1, \mathbf{T}_2)$ and $F_{ps}(s|\mathbf{T}_1, \mathbf{T}_2)$ respectively.

4.2.2 Asymptotic Outage Performance: a Generalized Theorem

We present the all-important contribution of this chapter in this subsection: a generalized equivalence principle, which corresponds to when relays are close to each other and spatial correlation exists. Before presenting the equivalence principle, we first propose a lemma for the *a posteriori* outage performance of combined selection in the high SNR region for relay systems, which is also valid over correlated channels:

Lemma 2. Consider a generic two-hop OFDM system performing combined selection over K orthogonal subcarriers and M relays. By applying the combined relay selection scheme so that the minimum SNR over all subcarriers can be maximized, the worst possible SNR has been improved to the Mth smallest out of the total MK SNRs in the subcarrier-relay grid (c.f. Figure 2.11 for an example).

■

Proof. We can prove this lemma by contradiction: as specified in Section 2.4, two relays will be first selected from M relays, when combined relay selection is performed. Assume the worst possible end-to-end SNR for a certain orthogonal subcarrier, say kth subcarrier, contained in the subset $\mathcal{L}_{comb}$ is produced by the mth relay and is ranked lower than the Mth worst in the total MK end-to-end SNRs. This assumption indicates that the end-to-end SNR of the mth relay for the kth subcarrier is always larger than the end-to-end SNR for the kth subcarrier provided by its partner relay contained in $\mathcal{L}_2$. However, the number of the total two-relay combination $\mathcal{L}_2$ formed by the mth relay and any of the remaining $M-1$ relays is $\binom{M-1}{1} = M-1$, which means that the worst end-to-end SNR of the mth relay for the kth subcarrier should be larger than at least $M-1$ end-to-end SNRs. This is contradictory to our initial assumption and thus proves that the initial assumption is incorrect. Hence, we equivalently prove that by combined relay selection, the worst possible end-to-end SNR has at least the Mth smallest value out of the total

MK end-to-end SNRs. Moreover, by the proof elaborated above, one should note that this lemma does not rely on the channel correlation situation.

■

Subsequently, we can state and prove the generalized equivalence principle as follows.

Theorem 1. If the conditional CDF of the end-to-end SNR for an arbitrary subcarrier, $F(s|T_1(k), T_2(k))$, can be expanded in the variable $\bar{\gamma} = P_t/N_0$ as[3]

$$\begin{aligned} F(s|T_1(k), T_2(k)) &= \sum_{i=i_0}^{\infty} c_i(s|T_1(k), T_2(k)) \left(\frac{1}{\bar{\gamma}}\right)^{\frac{i}{\theta}} [\ln(\bar{\gamma})]^r \\ &\sim c_{i_0}(s|T_1(k), T_2(k)) \left(\frac{1}{\bar{\gamma}}\right)^{\frac{i_0}{\theta}} [\ln(\bar{\gamma})]^r , \end{aligned} \tag{4.9}$$

where i_0 is an integer given by $i_0 = \arg\min_{n\in\mathbb{N}} \{c_n(s|T_1(k), T_2(k)) \neq 0\}$; θ is a nonzero natural number; $\{c_i(s|T_1(k), T_2(k))\}$ represents a series of functions of s, given $T_1(k), T_2(k)$; $r \in \mathbb{N}$, then the combined selection is able to achieve an outage probability equivalent to conventional per-subcarrier selection as $\bar{\gamma} \to \infty$.

■

Proof. By **Lemma 2**, it is clear that once an outage event occurs, there must exist at least one subcarrier, on which all M end-to-end SNRs via M relays drop below the outage threshold. Also, it is well known that the outage event is dominated by the deepest fade at high SNR and is asymptotic to the case where only one subcarrier, on which all M end-to-end SNRs via M relays drop below the outage threshold at high SNR [111]. Consequently, we have

$$F_{comb}(s|\mathbf{T}_1, \mathbf{T}_2) = \sum_{k=1}^{K} [F(s|T_1(k), T_2(k))]^M + O\left([F(s|T_1(k), T_2(k))]^{M+1}\right). \tag{4.10}$$

[3] This is a general form and fits most of end-to-end wireless fading channels in OFDM systems, MIMO systems and multi-hop systems.

Therefore, according to (4.9), the asymptotic expression for $F_{comb}(s|\mathbf{T}_1, \mathbf{T}_2)$ at $\bar{\gamma} \to \infty$ can be determined by

$$F_{comb}(s|\mathbf{T}_1, \mathbf{T}_2) \sim \sum_{k=1}^{K} \left\{ c_{i_0}(s|T_1(k), T_2(k)) \left(\frac{1}{\bar{\gamma}}\right)^{\frac{i_0}{\theta}} [\ln(\bar{\gamma})]^r \right\}^M. \tag{4.11}$$

Similar to the derivation performed for combined selection, according to (4.4), the conditional outage probability of per-subcarrier selection can be asymptotically expressed by

$$\begin{aligned} F_{ps}(s|\mathbf{T}_1, \mathbf{T}_2) &= 1 - \prod_{k=1}^{K} \left\{1 - [F(s|T_1(k), T_2(k))]^M\right\} \\ &\sim \sum_{k=1}^{K} \left\{ c_{i_0}(s|T_1(k), T_2(k)) \left(\frac{1}{\bar{\gamma}}\right)^{\frac{i_0}{\theta}} [\ln(\bar{\gamma})]^r \right\}^M, \end{aligned} \tag{4.12}$$

where $O(\cdot)$ is the Bachmann-Landau notation (a.k.a. asymptotic notation); mathematically, for real functions $f(x)$ and $g(x)$, if $f(x) = O(g(x))$ as $x \to a$, where a is an arbitrary real constant or infinity, then $\limsup_{x \to \infty} |f(x)/g(x)| < \infty$ [112].

Comparing the same asymptotic expressions given in (4.11) and (4.12), it is clear that when both multiply (4.8) and are integrated by $\mathbf{T}_1$ and $\mathbf{T}_2$ from zero to infinity, they will produce the same asymptotic outage performance as

$$\begin{aligned} &\{F_{comb}(s), F_{ps}(s)\} \\ &\sim K \left(\frac{1}{\mu_1 \mu_2}\right) \left\{ \left(\frac{1}{\bar{\gamma}}\right)^{\frac{i_0}{\theta}} [\ln(\bar{\gamma})]^r \right\}^M \int_0^\infty \int_0^\infty \{c_{i_0}(s|T_1, T_2)\}^M \left(e^{-\frac{T_1}{\mu_1}} e^{-\frac{T_2}{\mu_2}}\right) \mathrm{d}T_1 \, \mathrm{d}T_2. \end{aligned} \tag{4.13}$$

By (4.13), **Theorem 1** is proven.

■

4.3 Asymptotic Outage Performance Analysis with Different Forwarding Protocols

After proving the generalized equivalence principle in the previous section, we apply the combined relay selection to three specific cases for different relaying protocols and derive the asymptotic expressions of outage probability at high SNR for all cases in this section.

4.3.1 Decode-and-Forward Relaying

According to [88], the equivalent instantaneous end-to-end SNR corresponding to the kth subcarrier and the mth relay using a DF protocol can be expressed as

$$\mathsf{SNR}(m,k) = \frac{P_t}{N_0} \min\left\{|h_1(m,k)|^2, |h_2(m,k)|^2\right\}. \tag{4.14}$$

By series expansion, we can determine the asymptotic expression for the conditional CDF of the equivalent instantaneous end-to-end SNR for the kth subcarrier at high SNR[4]

$$F(s|T_1(k),T_2(k)) \sim \left[\frac{s}{2}\left(e^{-\frac{\rho_1 T_1(k)}{2\psi_1}}/\psi_1 + e^{-\frac{\rho_2 T_2(k)}{2\psi_2}}/\psi_2\right)\right]\frac{1}{\bar{\gamma}}, \tag{4.15}$$

where we denote $\psi_i = \mu_i(1-\rho_i)/2$ for brevity. Hence, by (4.9), $c_{i_0}(s|T_1(k),T_2(k))$ can be determined by

$$c_{i_0}(s|T_1(k),T_2(k)) = \frac{s}{2}\left(e^{-\frac{\rho_1 T_1(k)}{2\psi_1}}/\psi_1 + e^{-\frac{\rho_2 T_2(k)}{2\psi_2}}/\psi_2\right). \tag{4.16}$$

[4]See Appendix 4.6.1 for a proof.

Then, by (4.13), the unconditional outage probabilities for both selection schemes are determined by

$$\{F_{comb}(s), F_{ps}(s)\} \sim K(1-\rho_1)(1-\rho_2)\left(\frac{s}{2\bar{\gamma}}\right)^M \sum_{m=0}^{M}\binom{M}{m}\frac{\left(\frac{1}{\psi_1}\right)^{M-m}\left(\frac{1}{\psi_2}\right)^m}{[1+\rho_1(M-m-1)][1+\rho_2(m-1)]}. \tag{4.17}$$

4.3.2 Fixed-Gain Amplify-and-Forward Relaying

It is also well known that for FG AF relay systems, the instantaneous end-to-end SNR can be expressed as [113]

$$\mathsf{SNR}(m,k) = \frac{|h_1(m,k)|^2|h_2(m,k)|^2P_t^2}{(\mu_1 P_t + |h_2(m,k)|^2 P_t + N_0)N_0}. \tag{4.18}$$

By (4.5) and (4.6), we can derive the asymptotic expression for the conditional CDF at $\bar{\gamma} \to \infty$ by[5]

$$F(s|T_1(k), T_2(k)) \sim \left(\frac{\mu_1 s}{4\psi_1\psi_2}e^{-\frac{\rho_1 T_1(k)}{2\psi_1}}e^{-\frac{\rho_2 T_2(k)}{2\psi_2}}\right)\frac{\ln(\bar{\gamma})}{\bar{\gamma}}. \tag{4.19}$$

Consequently, $c_{i_0}(s|T_1(k), T_2(k))$ is given by

$$c_{i_0}(s|T_1(k), T_2(k)) = \frac{\mu_1 s}{4\psi_1\psi_2}e^{-\frac{\rho_1 T_1(k)}{2\psi_1}}e^{-\frac{\rho_2 T_2(k)}{2\psi_2}}. \tag{4.20}$$

Therefore, according to (4.13), we have

$$\{F_{comb}(s), F_{ps}(s)\} \sim \frac{K(1-\rho_1)(1-\rho_2)}{[1+\rho_1(M-1)][1+\rho_2(M-1)]}\left[\frac{\mu_1 s}{4\psi_1\psi_2\bar{\gamma}}\ln(\bar{\gamma})\right]^M. \tag{4.21}$$

[5]See Appendix 4.6.2 for a proof.

4.3.3 Variable-Gain Amplify-and-Forward Relaying

Similarly, the instantaneous end-to-end SNR for VG AF relaying can be given by [113]

$$\mathsf{SNR}(m,k) = \frac{|h_1(m,k)|^2|h_2(m,k)|^2P_t^2}{(|h_1(m,k)|^2P_t + |h_2(m,k)|^2P_t + N_0)N_0}. \tag{4.22}$$

Again, performing series expansion at $\bar{\gamma} \to \infty$ yields the asymptotic expression for $F(s|T_1(k), T_2(k))$ for VG AF relay systems[6]

$$F(s|T_1(k), T_2(k)) \sim \left[\frac{s}{2}\left(e^{-\frac{\rho_1 T_1(k)}{2\psi_1}}/\psi_1 + e^{-\frac{\rho_2 T_2(k)}{2\psi_2}}/\psi_2\right)\right]\frac{1}{\bar{\gamma}}. \tag{4.23}$$

Obviously, $c_{i_0}(s|T_1(k), T_2(k))$ for VG AF relay system is exactly the same as given in (4.16). Likewise, by (4.13), the unconditional outage probability in VG AF relaying network can be determined by

$$\{F_{comb}(s), F_{ps}(s)\} \sim K(1-\rho_1)(1-\rho_2)\left(\frac{s}{2\bar{\gamma}}\right)^M \sum_{m=0}^{M}\binom{M}{m}\frac{\left(\frac{1}{\psi_1}\right)^{M-m}\left(\frac{1}{\psi_2}\right)^m}{[1+\rho_1(M-m-1)][1+\rho_2(m-1)]}. \tag{4.24}$$

Note, the unconditional outage probability of VG AF relay systems (c.f. (4.24)) is exactly the same as that given in DF relay systems (c.f. (4.17)), which aligns with the numerical results presented in [114]. Also, by the definition of the diversity gain

$$d_o = -\lim_{\bar{\gamma}\to\infty}\frac{\log F_{comb}(s)}{\log \bar{\gamma}}, \tag{4.25}$$

we can see that for all three kinds of relays, the diversity gain is the same value given by the number of relays M. That is, the diversity advantage of combined selection will not be shadowed by different forwarding protocols and channel correlations and is only related to the number of available relays.

[6]See Appendix 4.6.3 for a proof.

4.4 Numerical Simulations and Discussion

4.4.1 Verification of Analytical Results

First, to verify our analysis in **Section 4.2** and **Section 4.3**, we employ Monte Carlo simulation methods to numerically study the outage performance of OFDM systems employing per-subcarrier and combined selection schemes with three forwarding protocols. Meanwhile, the asymptotic outage performance at high SNR is also taken into account in our simulations. In particular, we let $K = 8$, $s = 1$ (i.e., 0 dB), $\mu_1 = \mu_2 = 2$, for all simulations. Meanwhile, we vary $M \in \{3, 5\}$ and $\rho_1 = \rho_2 \in \{0, 0.8\}$ to observe the effects of M and ρ_i on the outage performance. The simulation results corresponding to the three relay protocols are presented in Figure 4.1, 4.2 and 4.3, respectively[7]. The outage performance produced by our proposed combined selection scheme is compared with the benchmark outage performance produced by the conventional per-subcarrier selection scheme. Also, the asymptotic curves are given to illustrate the trends of numerical results. One should note that the concave asymptotic curves for FG AF relay selection is mainly due to the logarithmic terms in the asymptotic expression of outage probability (c.f. (4.21)).

From these three figures, we can summarize some key points with respect to the combined selection scheme. Most importantly, it has been verified that the equivalence principle holds for all three types of relay networks over equally spatially correlated channels. That is, the relay systems employing combined selection can achieve the optimal outage performance as those employing per-subcarrier selection at high SNR. Meanwhile, the increase in the number of relays M will yield a better outage performance, since a larger diversity can be provided. Note, however, that an increase in M does not indicate that the number of *utilized* relays increases for the combined selection system since $|\mathcal{L}_{comb}| = 2$, whereas only the range of

[7]Here, higher order terms for FG AF case are kept in order to illustrate the convergence between numerical and asymptotic results within a reasonable SNR range.

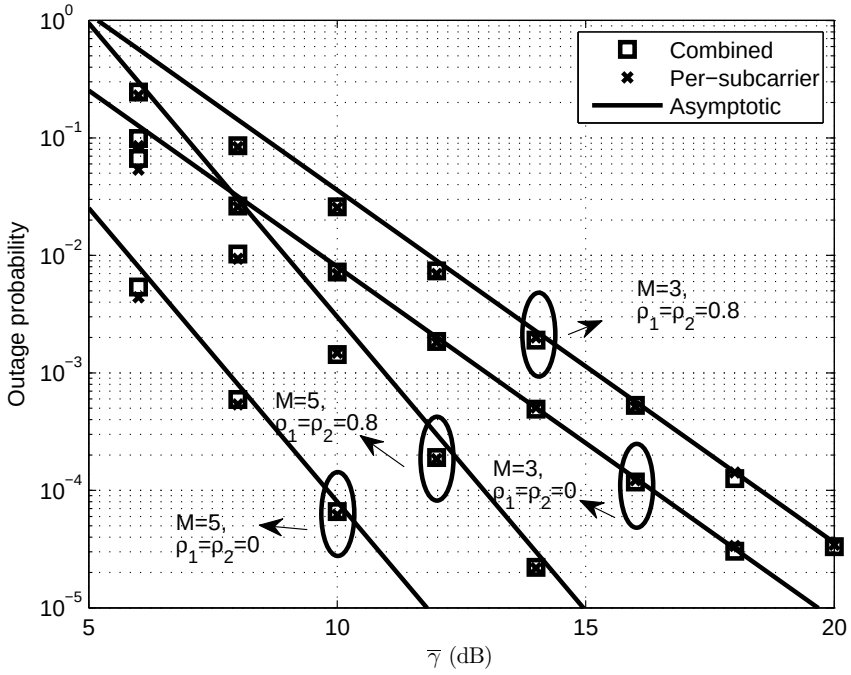


Figure 4.1: Two-hop DF relay selection case: outage probability vs. SNR for per-subcarrier and combined selection systems.

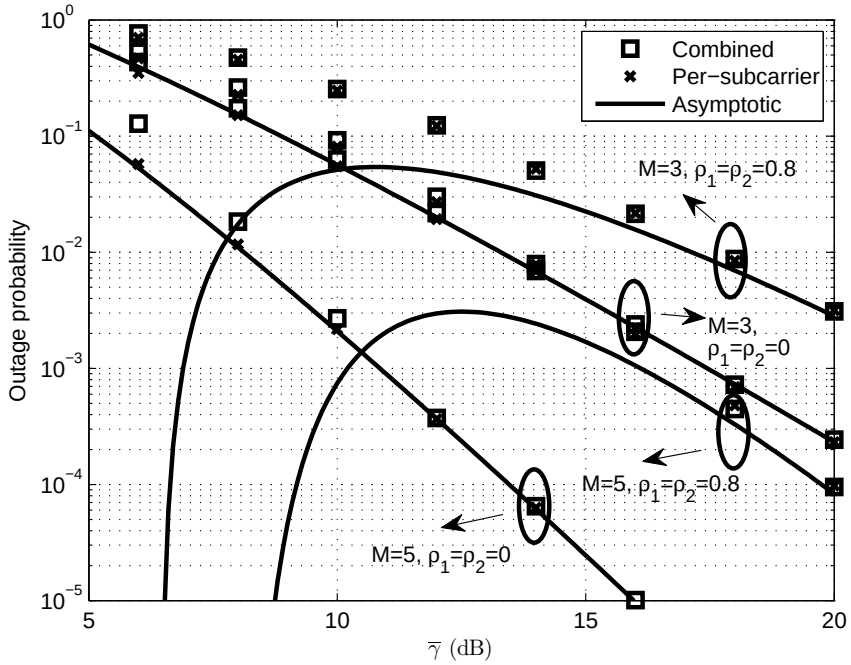


Figure 4.2: Two-hop FG AF relay selection case: outage probability vs. SNR for per-subcarrier and combined selection systems.

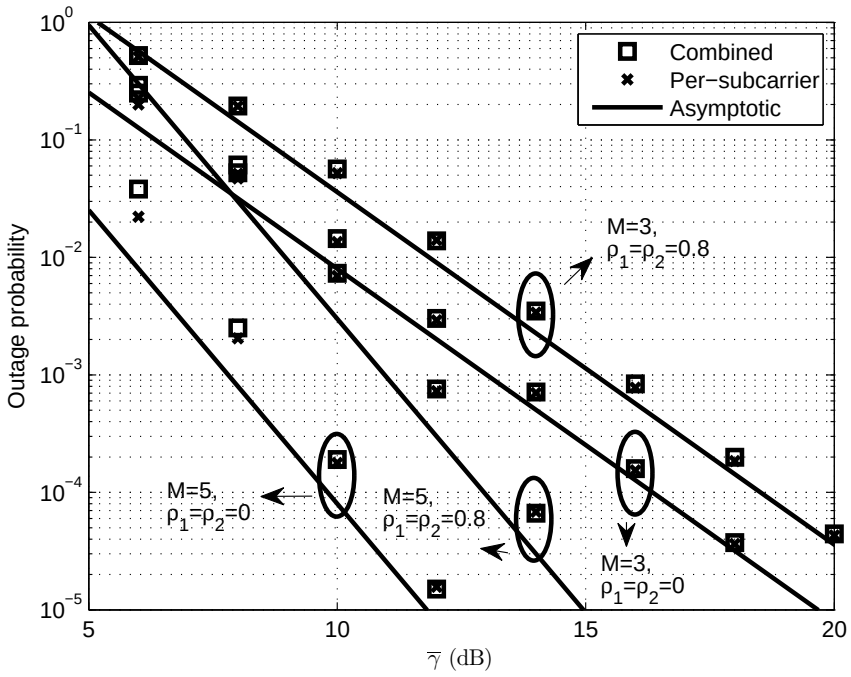


Figure 4.3: Two-hop VG AF relay selection case: outage probability vs. SNR for per-subcarrier and combined selection systems.

selection is enlarged. As for channel correlation, it is apparent that the diversity advantage of cooperative systems brought by relay selection will not be shadowed by channel correlation, as long as $\rho_1\rho_2 \neq 1$. On the other hand, a higher cross-correlation coefficient, whichever in the first hop or second hop, will result in a higher outage probability. In other words, channel correlation has a detrimental impact on the coding gain of a cooperative network. Although we mainly analyze the outage performance in the high SNR region, some important features of combined selection in the low SNR region can also be observed from these figures. First, there exists a gap between combined and per-subcarrier selections, which is caused by the difference in the numbers of selected relays and the fact that fading at low SNR is not dominated by the worst channel. Therefore, a smaller M will lead to a smaller gap at low SNR, and in particular it is expected that the gap will be eliminated when $M = 2$. Also, there is no evident impact by choosing different ρ_i on the performance gap at low SNR, because channel correlation does not affect

the number of selected relays and thus equivalent to both selection schemes.

4.4.2 Comparison among Different Forwarding Protocols

In comparison with the outage performance shown in these three figures, we can also have a rough insight into the merits and drawbacks corresponding to three types of relays. First, the outage performance given by DF and VG AF relaying is close to each other at high SNR, which aligns with our expectation, because both have the same asymptotic outage performance (c.f. (4.17) and (4.24)). Outage performance yielded by both DF and VG AF relaying is better than that of FG AF relaying. On the other hand, the superiority in outage performance is paid by a higher system complexity. The former needs to decode received signals at relay nodes, and the latter needs to estimate the channel in the first hop in a real-time manner. While the FG AF relay system is relatively simple and retransmits all received signals by a specified and fixed mechanism, which only needs to estimate the average channel gain in the first hop once. Therefore, there exists a trade-off between outage performance and system complexity among all three types of relays, which should be considered carefully when implementing cooperative networks. To clearly illustrate the outage performance of these three relays, we also simulate the case $\rho_1 = \rho_2 = 0.4$ for all three types of relays and plot the results in Figure 4.4. Additionally, compared to the results generated by such a static network model to those generated by dynamic network model in Figure 3.9, we can also discover the difference between these two network models and find diversity gain only appropriate to be used as a reliability measure in static networks.

4.4.3 Effects of Outage Threshold

Meanwhile, to reveal the effects of different s on the outage performance, we can take the DF relay case as an example with fixed $M = 3$ and $\rho_1 = \rho_2 = 0.4$. Then, we vary $s \in \{1, 2, 4, 8\}$ and plot the outage performance in Figure 4.5. As expected,

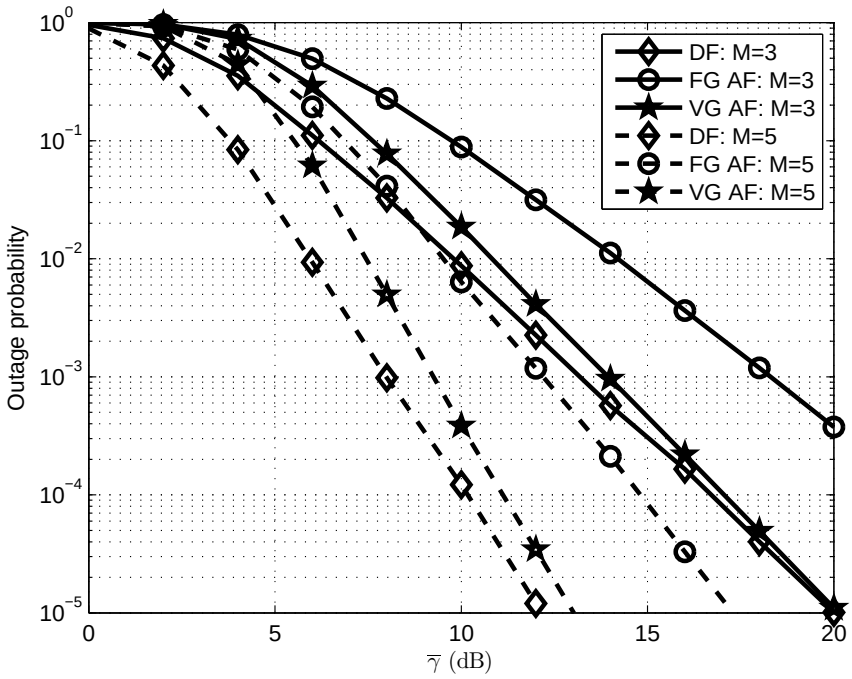


Figure 4.4: Two-hop DF relay selection case: outage probability vs. SNR for per-subcarrier and combined selection systems.

a larger s will lead to a worse outage performance (a coding gain shift to the right). In addition, s has an obvious impact on the convergence rate of combined selection to per-subcarrier selection; a larger s indicates a higher $\bar{\gamma}$ is required in order to obtain the equivalent performance.

4.5 Summary

In conclusion, we proved the optimality of a novel relay selection scheme for OFDM-based relay systems by combining conventional bulk and per-subcarrier selection schemes, and analyzed its outage performance over spatially correlated channels. Specifically, we carried out the asymptotic outage performance analysis of the combined selection scheme in the high SNR region, and proved a generalized theorem stating that if the conditional CDF of the end-to-end SNR, $F(s|T_1(k), T_2(k))$, can be expanded as a certain series in the variable $\bar{\gamma}$, combined selection is able to achieve an outage probability equivalent to conventional per-subcarrier selection in the high

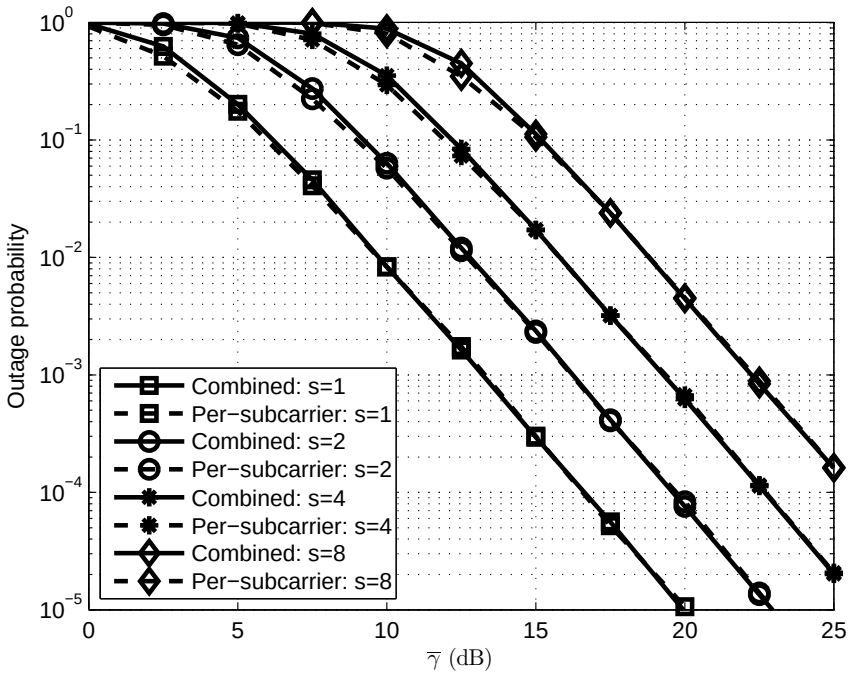


Figure 4.5: Outage performance of combined selection corresponding to DF relays, given $s \in \{1, 2, 4, 8\}$.

SNR region. To specify the generalized theorem, we also took three examples of DF, FG AF and VG AF relay systems to analyze and obtained their asymptotic outage probabilities. By Monte Carlo simulations, our analysis was verified by numerical results. The proposed combined relay selection and the proven theorem in this chapter provide a satisfactory solution to the trade-off between system complexity and outage performance when multi-carrier relay selection is applied. As a result, the optimal outage probability is achievable at high SNR without using the full set of available relays for selection.

4.6 Appendices

4.6.1 Derivation of Asymptotic Outage Probability of Decode-and-Forward Relaying

According to (4.14), we can approximate $F(s|T_1(k), T_2(k))$ at high SNR by

$$\begin{aligned} F(s|T_1(k), T_2(k)) &= \mathbb{P}\left\{ \frac{P_t}{N_0} \min(\gamma_1, \gamma_2) < s \right\} \\ &= 1 - \left[1 - F_{h_1}\left(\frac{s}{\bar{\gamma}} \middle| T_1(k) \right) \right] \left[1 - F_{h_2}\left(\frac{s}{\bar{\gamma}} \middle| T_2(k) \right) \right] \\ &= F_{h_1}\left(\frac{s}{\bar{\gamma}} \middle| T_1(k) \right) + F_{h_2}\left(\frac{s}{\bar{\gamma}} \middle| T_2(k) \right) - F_{h_1}\left(\frac{s}{\bar{\gamma}} \middle| T_1(k) \right) F_{h_2}\left(\frac{s}{\bar{\gamma}} \middle| T_2(k) \right) \\ &\approx F_{h_1}\left(\frac{s}{\bar{\gamma}} \middle| T_1(k) \right) + F_{h_2}\left(\frac{s}{\bar{\gamma}} \middle| T_2(k) \right), \end{aligned} \tag{4.26}$$

where we denote $\gamma_i = |h_i(m,k)|^2$ for brevity.

By (4.6), we can further obtain

$$F(s|T_1(k), T_2(k)) = \sum_{i=1}^{2} \left[1 - Q\left(\sqrt{\frac{\rho_i T_i(k)}{\psi_i}}, \sqrt{\frac{s}{\psi_i \bar{\gamma}}} \right) \right]. \tag{4.27}$$

Also, we can express $Q\left(\sqrt{\rho_i T_i(k)/\psi_i}, \sqrt{s/(\psi_i \bar{\gamma})} \right)$ by [71]

$$Q\left(\sqrt{\frac{\rho_i T_i(k)}{\psi_i}}, \sqrt{\frac{s}{\psi_i \bar{\gamma}}} \right) = e^{-\frac{\rho_i T_i(k)}{2\psi_i}} e^{-\frac{s}{2\psi_1 \bar{\gamma}}} \sum_{p=0}^{\infty} \left(\sqrt{\frac{\rho_i T_i(k) \bar{\gamma}}{s}} \right)^p I_p\left(\frac{1}{\psi_i} \sqrt{\frac{\rho_i T_i(k) s}{\bar{\gamma}}} \right). \tag{4.28}$$

Also, we can expand the pth order modified Bessel function of the first kind by [71]

$$I_p\left(\frac{1}{\psi_i} \sqrt{\frac{\rho_i T_i(k) s}{\bar{\gamma}}} \right) = \left(\frac{1}{2\psi_i} \sqrt{\frac{\rho_i T_i(k) s}{\bar{\gamma}}} \right)^p \sum_{q=0}^{\infty} \frac{\left(\frac{\rho_i T_i(k) s}{4\psi_i^2 \bar{\gamma}} \right)^q}{q! \Gamma(q+p+1)}, \tag{4.29}$$

where $\Gamma(\cdot)$ is the Gamma function.

Therefore, the summation part can be alternatively expressed by

$$\sum_{p=0}^{\infty}\left(\sqrt{\frac{\rho_i T_i(k)\bar{\gamma}}{s}}\right)^p I_p\left(\frac{1}{\psi_i}\sqrt{\frac{\rho_i T_i(k)s}{\bar{\gamma}}}\right)=\sum_{q=0}^{\infty}\sum_{p=0}^{\infty}\frac{\left(\frac{\rho_i T_i(k)}{2\psi_i}\right)^p\left(\frac{\rho_i T_i(k)s}{4\psi_i^2\bar{\gamma}}\right)^q}{q!\Gamma(q+p+1)}. \quad (4.30)$$

Meanwhile, $e^{-\frac{s}{2\psi_i\bar{\gamma}}}$ can also be expanded in terms of $\bar{\gamma}$ by [115]

$$e^{-\frac{s}{2\psi_i\bar{\gamma}}}=\sum_{p=0}^{\infty}\frac{1}{p!}\left(-\frac{s}{2\psi_i\bar{\gamma}}\right)^p. \quad (4.31)$$

Therefore, substituting (4.30) and (4.31) into (4.28) yields

$$\begin{aligned}Q\left(\sqrt{\frac{\rho_i T_i(k)}{\psi_i}},\sqrt{\frac{s}{\psi_i\bar{\gamma}}}\right)&=e^{-\frac{\rho_i T_i(k)}{2\psi_i}}\left[\sum_{p=0}^{\infty}\frac{1}{p!}\left(-\frac{s}{2\psi_i\bar{\gamma}}\right)^p\right]\left[\sum_{q=0}^{\infty}\sum_{p=0}^{\infty}\frac{\left(\frac{\rho_i T_i(k)}{2\psi_i}\right)^p\left(\frac{\rho_i T_i(k)s}{4\psi_i^2\bar{\gamma}}\right)^q}{q!\Gamma(q+p+1)}\right]\\&\sim 1-e^{-\frac{\rho_i T_i(k)}{2\psi_i}}\frac{s}{2\psi_i\bar{\gamma}}.\end{aligned} \quad (4.32)$$

Subsequently, substituting (4.32) into (4.27) yields the asymptotic expression for $F(s|T_1(k),T_2(k))$ at $\bar{\gamma}\to\infty$:

$$F(s|T_1(k),T_2(k))\sim\left[\frac{s}{2}\left(e^{-\frac{\rho_1 T_1(k)}{2\psi_1}}/\psi_1+e^{-\frac{\rho_2 T_2(k)}{2\psi_2}}/\psi_2\right)\right]\frac{1}{\bar{\gamma}}. \quad (4.33)$$

4.6.2 Derivation of Asymptotic Outage Probability of Fixed-Gain Amplify-and-Forward Relaying

We can adopt a similar method to the one proposed in [116] to derive the CDF of end-to-end SNR over correlated channels and determine $F(s|T_1(k), T_2(k))$ by

$$\begin{aligned} F(s|T_1(k), T_2(k)) &= \mathbb{P}\left\{\frac{\gamma_1\gamma_2 P_t^2}{(\mu_1 P_t + \gamma_2 P_t + N_0)N_0} < s\right\} \\ &= \mathbb{P}\left\{\gamma_1 < \frac{s\left(\mu_1 + \gamma_2 + \frac{1}{\bar{\gamma}}\right)}{\gamma_2\bar{\gamma}}\right\} \qquad (4.34) \\ &= \int_0^\infty F_{h_1}\left(\frac{s\left(\mu_1 + \gamma_2 + \frac{1}{\bar{\gamma}}\right)}{\gamma_2\bar{\gamma}}\middle| T_1(k)\right) f_{h_2}(\gamma_2|T_2(k))\mathrm{d}\gamma_2. \qquad (4.35) \end{aligned}$$

Considering $\bar{\gamma} \to \infty$, we can approximate the outage condition by omitting the higher order terms corresponding to $1/\bar{\gamma}$ and obtain

$$\frac{s\left(\mu_1 + \gamma_2 + \frac{1}{\bar{\gamma}}\right)}{\gamma_2\bar{\gamma}} \approx \frac{s\left(\mu_1 + \gamma_2\right)}{\gamma_2\bar{\gamma}}, \qquad (4.36)$$

and thereby have

$$F(s|T_1(k), T_2(k)) \approx \int_0^\infty F_{h_1}\left(\frac{s(\gamma_2 + \mu_1)}{\gamma_2\bar{\gamma}}\middle| T_1(k)\right) f_{h_2}(\gamma_2|T_2(k))\mathrm{d}\gamma_2. \qquad (4.37)$$

Now, let us take a close look at the conditional CDF $F_{h_1}\left(\frac{s(\gamma_2+\mu_1)}{\gamma_2\bar{\gamma}}\middle|T_1(k)\right)$. Again, by (4.6), we can express this conditional CDF by

$$F_{h_1}\left(\frac{s(\gamma_2 + \mu_1)}{\gamma_2\bar{\gamma}}\middle| T_1(k)\right) = 1 - Q\left(\sqrt{\frac{\rho_1 T_1(k)}{\psi_1}}, \sqrt{\frac{s(\gamma_2 + \mu_1)}{\psi_1\gamma_2\bar{\gamma}}}\right). \qquad (4.38)$$

Therefore, we can perform the similar derivation to DF relaying and the Marcum

Q function can be alternatively expressed as

$$\begin{aligned} &Q\left(\sqrt{\frac{\rho_1 T_1(k)}{\psi_1}}, \sqrt{\frac{s(\gamma_2+\mu_1)}{\psi_1\gamma_2\bar{\gamma}}}\right) \\ &= e^{-\frac{\rho_1 T_1(k)}{2\psi_1}} \sum_{q=0}^{\infty}\sum_{p=0}^{\infty} \frac{\left(\frac{\rho_1 T_1(k)}{2\psi_1}\right)^p \left(\frac{\rho_1 T_1(k)}{4\psi_1^2}\right)^q}{q!\Gamma(q+p+1)} \left[\frac{s(\gamma_2+\mu_1)}{\bar{\gamma}}\right]^q \left(\frac{1}{\gamma_2}\right)^q e^{-\frac{s(\gamma_2+\mu_1)}{2\psi_1\gamma_2\bar{\gamma}}}. \end{aligned} \tag{4.39}$$

Meanwhile, we can also expand $f_{h_2}(\gamma_2|T_2(k))$ by [71]

$$f_{h_2}(\gamma_2|T_2(k)) = \frac{1}{2\psi_2} e^{-\frac{\rho_2 T_2(k)}{2\psi_2}} e^{-\frac{\gamma_2}{2\psi_2}} \sum_{u=0}^{\infty} \frac{\left(\frac{\rho_2 T_2(k)\gamma_2}{4\psi_2^2}\right)^u}{(u!)^2}. \tag{4.40}$$

Therefore, we can obtain

$$\begin{aligned} &\int_0^{\infty} Q\left(\sqrt{\frac{\rho_1 T_1(k)}{\psi_1}}, \sqrt{\frac{s(\gamma_2+\mu_1)}{\psi_1\gamma_2\bar{\gamma}}}\right) f_{h_2}(\gamma_2|T_2(k))\mathrm{d}\gamma_2 \\ &= \frac{1}{2\psi_2} e^{-\frac{\rho_1 T_1(k)}{2\psi_1}} e^{-\frac{\rho_2 T_2(k)}{2\psi_2}} \sum_{q=0}^{\infty}\sum_{p=0}^{\infty}\sum_{u=0}^{\infty} \mathcal{C}(q,p,u)\mathcal{H}(q,u), \end{aligned} \tag{4.41}$$

where

$$\mathcal{C}(q,p,u) = \frac{\left(\frac{\rho_1 T_1(k)}{2\psi_1}\right)^p \left(\frac{\rho_1 T_1(k)}{2\psi_1}\right)^q \left(\frac{\rho_2 T_2(k)}{2\psi_2}\right)^u}{q!\Gamma(q+p+1)(u!)^2} \tag{4.42}$$

and

$$\mathcal{H}(q,u) = \int_0^{\infty} \left[\frac{s(\gamma_2+\mu_1)}{2\psi_1\gamma_2\bar{\gamma}}\right]^q \left(\frac{\gamma_2}{2\psi_2}\right)^u e^{-\frac{s(\gamma_2+\mu_1)}{2\psi_1\gamma_2\bar{\gamma}}} e^{-\frac{\gamma_2}{2\psi_2}} \mathrm{d}\gamma_2. \tag{4.43}$$

Because we are only interested in the high SNR region, i.e., $\bar{\gamma} \to \infty$, we can approximate (4.41) by considering $q = 0$ and $q = 1$ only:

$$\begin{aligned} &\int_0^{\infty} Q\left(\sqrt{\frac{\rho_1 T_1(k)}{\psi_1}}, \sqrt{\frac{s(\gamma_2+\mu_1)}{\psi_1\gamma_2\bar{\gamma}}}\right) f_{h_2}(\gamma_2|T_2(k))\mathrm{d}\gamma_2 \\ &\approx \frac{1}{2\psi_2} e^{-\frac{\rho_1 T_1(k)}{2\psi_1}} e^{-\frac{\rho_2 T_2(k)}{2\psi_2}} \sum_{u=0}^{\infty} \left[\sum_{p=0}^{\infty} \mathcal{C}(0,p,u)\right] \mathcal{H}(0,u) \\ &\quad + \frac{1}{2\psi_2} e^{-\frac{\rho_1 T_1(k)}{2\psi_1}} e^{-\frac{\rho_2 T_2(k)}{2\psi_2}} \sum_{u=0}^{\infty} \left[\sum_{p=0}^{\infty} \mathcal{C}(1,p,u)\right] \mathcal{H}(1,u) \end{aligned} \tag{4.44}$$

Then, the closed-form expressions for $\mathcal{H}(0,u)$ and $\mathcal{H}(1,u)$ are now obtainable

and given by

$$\mathcal{H}(0,u) = 4\psi_2 e^{-\frac{s}{2\psi_1\bar{\gamma}}} \left(\frac{\mu_1 s}{4\psi_1\psi_2\bar{\gamma}}\right)^{\frac{u+1}{2}} K_{u+1}\left(\sqrt{\frac{\mu_1 s}{\psi_1\psi_2\bar{\gamma}}}\right) \tag{4.45}$$

and

$$\begin{aligned}\mathcal{H}(1,u) = {} & 2\psi_2 e^{-\frac{s}{2\psi_1\bar{\gamma}}} \left(\frac{s}{\psi_1\bar{\gamma}}\right)\left(\frac{\mu_1 s}{4\psi_1\psi_2\bar{\gamma}}\right)^{\frac{u+1}{2}} K_{u+1}\left(\sqrt{\frac{\mu_1 s}{\psi_1\psi_2\bar{\gamma}}}\right) \\ & + e^{-\frac{s}{2\psi_1\bar{\gamma}}} \left(\frac{\mu_1 s}{\psi_1\bar{\gamma}}\right)\left(\frac{\mu_1 s}{4\psi_1\psi_2\bar{\gamma}}\right)^{\frac{u}{2}} K_u\left(\sqrt{\frac{\mu_1 s}{\psi_1\psi_2\bar{\gamma}}}\right),\end{aligned} \tag{4.46}$$

where $K_v(\cdot)$ is the vth order modified Bessel function of the second kind.

Meanwhile, we can also obtain

$$\sum_{p=0}^{\infty} \mathcal{C}(0,p,u) = \frac{\left(\frac{\rho_2 T_2(k)}{2\psi_2}\right)^u e^{\frac{\rho_1 T_1(k)}{2\psi_2}}}{(u!)^2} \tag{4.47}$$

and

$$\sum_{p=0}^{\infty} \mathcal{C}(1,p,u) = \frac{\left(\frac{\rho_2 T_2(k)}{2\psi_2}\right)^u \left(e^{\frac{\rho_1 T_1(k)}{2\psi_2}} - 1\right)}{(u!)^2}. \tag{4.48}$$

Now, we can perform series expansion at $\bar{\gamma} \to \infty$ and obtain the asymptotic expressions for (4.41) by

$$\int_0^{\infty} Q\left(\sqrt{\frac{\rho_1 T_1(k)}{\psi_1}}, \sqrt{\frac{s(\gamma_2+\mu_1)}{\psi_1\gamma_2\bar{\gamma}}}\right) f_{h_2}(\gamma_2|T_2(k))\mathrm{d}\gamma_2 \sim 1 - \left(\frac{\mu_1 s}{4\psi_1\psi_2} e^{-\frac{\rho_1 T_1(k)}{2\psi_1}} e^{-\frac{\rho_2 T_2(k)}{2\psi_2}}\right)\frac{\ln(\bar{\gamma})}{\bar{\gamma}} \tag{4.49}$$

Also, due to the property of a PDF, it is obvious that $\int_0^{\infty} f_{h_2}(\gamma_2|T_2(k))\mathrm{d}\gamma_2 = 1$. As a result, by (4.38) and (4.49) the asymptotic expression for (4.37) can be given by

$$F(s|T_1(k),T_2(k)) \sim \left(\frac{\mu_1 s}{4\psi_1\psi_2} e^{-\frac{\rho_1 T_1(k)}{2\psi_1}} e^{-\frac{\rho_2 T_2(k)}{2\psi_2}}\right)\frac{\ln(\bar{\gamma})}{\bar{\gamma}}. \tag{4.50}$$

4.6.3 Derivation of Asymptotic Outage Probability of Variable-Gain Amplify-and-Forward Relaying

Similar to the analysis of the FG AF case, we can express $F(s|T_1(k), T_2(k))$ by

$$\begin{aligned}
F(s|T_1(k), T_2(k)) &= \mathbb{P}\left\{\frac{\gamma_1\gamma_2 P_t^2}{(\gamma_1 P_t + \gamma_2 P_t + N_0)N_0} < s\right\} \\
&= \mathbb{P}\left\{\gamma_1 < \frac{s\left(\gamma_2 + \frac{1}{\bar{\gamma}}\right)}{\gamma_2\bar{\gamma} - s} | \gamma_2 > \frac{s}{\bar{\gamma}}\right\} + \mathbb{P}\left\{\gamma_1 > \frac{s\left(\gamma_2 + \frac{1}{\bar{\gamma}}\right)}{\gamma_2\bar{\gamma} - s} | 0 < \gamma_2 < \frac{s}{\bar{\gamma}}\right\} \\
&= \int_{\frac{s}{\bar{\gamma}}}^{\infty} F_{h_1}\left(\left.\frac{s\left(\gamma_2 + \frac{1}{\bar{\gamma}}\right)}{\gamma_2\bar{\gamma} - s}\right| T_1(k)\right) f_{h_2}(\gamma_2|T_2(k))\mathrm{d}\gamma_2 \\
&\quad + \int_0^{\frac{s}{\bar{\gamma}}} \left[1 - F_{h_1}\left(\left.\frac{s\left(\gamma_2 + \frac{1}{\bar{\gamma}}\right)}{\gamma_2\bar{\gamma} - s}\right| T_1(k)\right)\right] f_{h_2}(\gamma_2|T_2(k))\mathrm{d}\gamma_2.
\end{aligned}$$

Again, we first need to expand $s(\gamma_2 + 1/\bar{\gamma})/(\gamma_2\bar{\gamma} - s)$ at $\bar{\gamma} \to \infty$ in order to derive the asymptotic expression. Here we have

$$\frac{s\left(\gamma_2 + \frac{1}{\bar{\gamma}}\right)}{\gamma_2\bar{\gamma} - s} \approx \frac{s}{\bar{\gamma}}. \tag{4.51}$$

Therefore, we can approximate $F(s|T_1(k), T_2(k))$ at high SNR by

$$\begin{aligned}
&F(s|T_1(k), T_2(k)) \\
&\approx \int_{\frac{s}{\bar{\gamma}}}^{\infty} F_{h_1}\left(\left.\frac{s}{\bar{\gamma}}\right| T_1(k)\right) f_{h_2}(\gamma_2|T_2(k))\mathrm{d}\gamma_2 + \int_0^{\frac{s}{\bar{\gamma}}} \left[1 - F_{h_1}\left(\left.\frac{s}{\bar{\gamma}}\right| T_1(k)\right)\right] f_{h_2}(\gamma_2|T_2(k))\mathrm{d}\gamma_2 \\
&= F_{h_1}\left(\left.\frac{s}{\bar{\gamma}}\right| T_1(k)\right) + F_{h_2}\left(\left.\frac{s}{\bar{\gamma}}\right| T_1(k)\right) - 2F_{h_1}\left(\left.\frac{s}{\bar{\gamma}}\right| T_1(k)\right) F_{h_2}\left(\left.\frac{s}{\bar{\gamma}}\right| T_1(k)\right) \\
&\approx F_{h_1}\left(\left.\frac{s}{\bar{\gamma}}\right| T_1(k)\right) + F_{h_2}\left(\left.\frac{s}{\bar{\gamma}}\right| T_1(k)\right).
\end{aligned} \tag{4.52}$$

Then, the analysis follows the case derived for DF relay and the asymptotic expression is given by the same one in (4.33).

Chapter 5

Full-Duplex Relay-Assisted OFDM D2D Systems

Apart from the ideal network models and conditions provided in **Chapter 3** and **Chapter 4**, OFDM-based relay systems shall be considered and analyzed in more realistic and complicated scenarios in order to integrate practical factors in next generation networks. Specifically, D2D networks would be a good example in next generation networks to consider. D2D communications have been a hot topic in both academia and industry for years and regarded as a potential supplement for conventional cellular communications in next generation networks, owing to the high spectral efficiency, high energy efficiency and low transmission delay [117–119]. D2D communications allow transmission among devices in close proximity without the direct involvement of a BS or access point (AP), and have been employed in a number of applications, e.g., proximity-aware social networking, content sharing, VR gaming and WiFi as well as Bluetooth [117, 120, 121]. On the other hand, conventional D2D communications requiring a strong direct link between DUEs might not always be feasible in practice, as the direct link could experience deep fading and shadowing of obstacles due to the existence of physical obstacles. In this scenario, D2D communications will become impractical or require a huge amount

of transmit power, which will result in severe interference to cellular communications and greatly degrade the overall system performance [122]. To further enhance the performance of D2D communications and mitigate the interference to cellular communications, cooperative architectures are also integrated with D2D communication paradigms. Cooperative architectures in D2D networks can either be used to enhance the D2D transmission link, or provide coverage extension for cellular communications [120]. Meanwhile, OFDM has been involved in D2D communications to provide a more flexible resource scheduling scheme, which has been shown to bring a substantial performance gain for D2D communications, especially when the distance between D2D transmitter and the receiver is short [123]. To further enhance the performance of relay-assisted D2D systems, recent research also focuses on the employment of full-duplex relays, as it would double the transmission rate, as long as the SI can be dealt with appropriately [124, 125].

Therefore, to fill the gap between full-duplex relay-assisted D2D communications and multi-carrier paradigms and provide a direct performance analysis, we propose a full-duplex relay-assisted OFDM D2D system in this chapter. Then, we analyze the outage performance of the proposed system, and derive the exact expressions of outage probabilities when bulk and per-subcarrier relay selections are applied for DF relaying. Furthermore, closed-form expressions of outage probabilities are also obtained for special cases when the instantaneous CSI between BS and cellular user equipments (CUEs) is not accessible, so that a static power control mechanism is applied. Subsequently, we also investigate the outage performance optimization problems by coordinating transmit power among DUE transmitter and relays, and provide suboptimal solutions, which are capable of improving the outage performance.

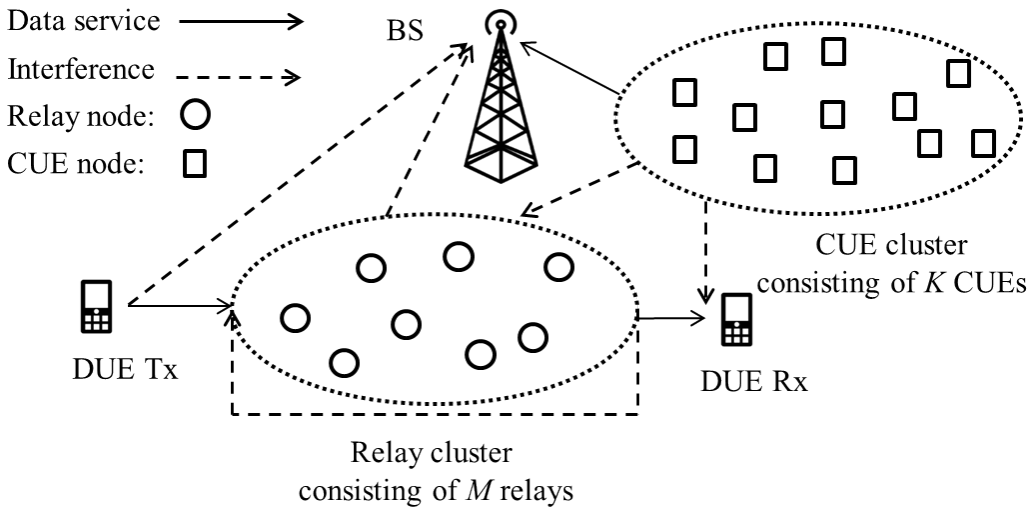


Figure 5.1: Network model for the proposed full-duplex relay-assisted D2D system, containing one BS, K CUEs in a CUE cluster, M relays in a relay cluster, one DUE transmitter (source) and one DUE receiver (destination).

5.1 System Framework

The framework of the proposed system is presented in Figure 5.1, where one BS, a pair of DUE transmitter and receiver, a cluster of M full-duplex DF relays and a cluster of K CUEs are considered. Their shorthand notations are B, S, D, R_m and C_k, respectively, $\forall\ m \in \mathcal{M} = \{1, 2, \ldots, M\}$ and $\forall\ k \in \mathcal{N} = \{1, 2, \ldots, K\}$. Meanwhile, by employing OFDM, it is supposed that there exist K independent subcarriers allocated to K CUEs and used by CUEs and DUEs in an underlay manner. The set of these K subcarriers is denoted as $\mathcal{K} = \{1, 2, \ldots, K\}$. In other words, there is a unique bijective mapping relation between $\mathcal{N}$ and $\mathcal{K}$, in order to mitigate the interference among CUEs and optimize the multiplexing gain of the cellular network[1].

From Figure 5.1, it is obvious that the signal and interference transmissions are in an uplink scenario. Note that most D2D communication systems are designed to utilize uplink cellular resources, because D2D users can monitor the received power

[1]Here, we omit the subcarrier allocation process for CUEs, and assume it is a *fait accompli* as a system configuration in this chapter. Details of OFDM subcarrier allocation for multi-user scenarios can be found in [96–98].

of the downlink control signals to estimate the channel between the DUE transmitter and the BS [117]. Therefore, this will help maintain the transmit power of the DUE transmitter below a SIR outage threshold, so that the interference caused by D2D communications to cellular systems can be mitigated effectively [126]. Another reason to use the uplink resource for D2D transmission is to avoid the severe interference caused by the transmission from BS, as BS normally transmits by a much larger power than CUEs'. Following this common design guideline, we also assume that D2D communication utilizes uplink spectrum resources. Therefore, the existing interference can be classified into three categories: 1) interference from active CUEs to DUE receiver and selected relay(s); 2) interference from DUE transmitter and selected relay(s) to BS; 3) SI at selected relay(s) because of the adoption of the full-duplex transmission protocol. According to the basic design guidelines of D2D communication networks [117], the cellular communications should be ensured with transmission priority, and the first interference is thereby inevitable in the proposed system. In order to deal with the second interference, we have to make sure that for the kth subcarrier, the received aggregate interference from the DUE transmitter and selected relay(s) is mitigated below a certain level. Therefore, considering an interference-limited environment [127], a dynamic power control mechanism is applied at the DUE transmitter and selected relay(s) on the kth subcarrier, which can be written as:

$$P_S(k) = \min\left\{\frac{\alpha P_C G_{CB}(k)}{\xi G_{SB}(k)}, \bar{P}_S\right\} \tag{5.1}$$

and

$$P_{R_m}(k) = \min\left\{\frac{(1-\alpha) P_C G_{CB}(k)}{\xi G_{R_m B}(k)}, \bar{P}_R\right\}, \tag{5.2}$$

where P_C is the CUE transmit power and assumed to be the same for all CUEs; $\alpha \in (0, 1)$ is a preset power coordination factor, which is used to coordinate the transmit power of DUE transmitter and relays and is the same among all subcarriers and relays; ξ is a preset SIR outage threshold for cellular communications; $\bar{P}_S$ and

$\bar{P}_R$ are the maximum allowed transmit power corresponding to DUE transmitter and relays on each subcarrier; $G_{ij}(k)$ denotes the channel power gain for the kth subcarrier, given $i \neq j$ and $i, j \in \{B, S, D\} \bigcup \mathcal{M} \bigcup \mathcal{N}$, and obeys the exponential distribution with the PDF and CDF given by

$$f_{G_{ij}}(g) = e^{-g/\mu_{ij}}/\mu_{ij} \quad \Leftrightarrow \quad F_{G_{ij}}(g) = 1 - e^{-g/\mu_{ij}}, \tag{5.3}$$

where μ_{ij} is the average channel power gain[2].

5.2 Decode-and-Forward Relaying in D2D Communication Networks

Because of the interference-limited environment, we can neglect the effects of additive noise at the receivers and express the instantaneous SIR from DUE transmitter to the mth relay (i.e., the first hop) on the kth subcarrier by

$$\mathsf{SIR}_1(m,k) = \frac{G_{SR_m}(k)P_S(k)}{P_C G_{CR_m}(k) + \varphi_m(k)}, \tag{5.4}$$

where $\varphi_m(k)$ denotes the power of the residual SI at the mth relay for the kth subcarrier, and we assume that $\varphi_m(k)$ obeys the exponential distribution with PDF and CDF written in the same form in (5.3) with the average power of residual SI $\bar{\varphi}$.

Further assuming that there does not exist a direct transmission link between DUE transmitter and receiver due to deep fading, and the DF forwarding protocol is applied at all relays, we can express the SIR from the mth relay to the DUE receiver (i.e., the second hop) by

$$\mathsf{SIR}_2(m,k) = \frac{G_{R_m D}(k)P_{R_m}(k)}{P_C G_{CD}(k)}. \tag{5.5}$$

[2]Because of relay and CUE clusters, we can further assume that the sizes of clusters are relatively small compared to the scale of the network. As a result, we can have uniform μ_{SR}, μ_{RD}, μ_{CR}, μ_{CD}, μ_{RB}, μ_{CB} for all relays and CUEs [128].

Subsequently, we can express the equivalent end-to-end instantaneous SIR for full-duplex DF relay systems by

$$\mathsf{SIR}(m,k) = \min\left\{\mathsf{SIR}_1(m,k), \mathsf{SIR}_2(m,k)\right\}. \tag{5.6}$$

5.3 Definitions of Outage Probability with Multi-Carrier Relay Selections

Replacing $\mathsf{SXR}(m,k)$ in (2.6) and (2.7) by $\mathsf{SIR}(m,k)$ obtained in (5.6), we can obtain the sets of selected relays by bulk and per-subcarrier relay selections in D2D networks. To facilitate the following analysis, we denote $\tilde{l}(k)$ as the index of the selected relay forwarding the kth subcarrier after performing a certain selection criterion.

5.3.1 Full-Duplex Systems

The full-duplex transmission would potentially have an outage performance benefit, if the power of residual SI can be managed below a certain level by a series of SI cancellation technologies [129]. Consequently, we adopt the full-duplex transmission protocol in this chapter for relay forwarding. As a result, for full-duplex systems, we can express the outage probability after relay selection by **Definition 1** as

$$P_{out}(s) = \mathbb{P}\left\{\min_{k\in\mathcal{K}}\left\{\mathsf{SIR}(\tilde{l}(k),k)\right\} < s\right\}, \tag{5.7}$$

where $\mathbb{P}\{\cdot\}$ denotes the probability of the event enclosed.

5.3.2 Half-Duplex Systems

As an important comparison benchmark of full-duplex systems, we also give the outage probability for half-duplex systems as follows

$$P_{out}^{half}(s) = \mathbb{P}\left\{\min_{k\in\mathcal{K}}\left\{\mathsf{SIR}^{half}(\tilde{l}(k),k)\right\} < s(s+2)\right\}, \tag{5.8}$$

where $\mathsf{SIR}^{half}(\tilde{l}(k),k) = \mathsf{SIR}(\tilde{l}(k),k)|_{\varphi_{\tilde{n}(k)}=0}$.

Proof. Considering the original definition of the outage probability in terms of capacity, for full-duplex OFDM systems, we have

$$P_{out}(s) = \mathbb{P}\left\{\log\left(1+\min_{k\in\mathcal{K}}\left\{\mathsf{SIR}(\tilde{l}(k),k)\right\}\right) < \mathsf{T}\right\} = \mathbb{P}\left\{\min_{k\in\mathcal{K}}\left\{\mathsf{SIR}(\tilde{l}(k),k)\right\} < e^{\mathsf{T}}-1\right\}, \tag{5.9}$$

so that we can define

$$s = e^{\mathsf{T}} - 1 \tag{5.10}$$

as the preset SIR outage threshold.

Similarly, for half-duplex OFDM systems, we have

$$\begin{aligned} P_{out}^{half}(s) &= \mathbb{P}\left\{\log\left(1+\min_{k\in\mathcal{K}}\left\{\mathsf{SIR}^{half}(\tilde{l}(k),k)\right\}\right) < \mathsf{T}\right\} \\ &= \mathbb{P}\left\{\min_{k\in\mathcal{K}}\left\{\mathsf{SIR}^{half}(\tilde{l}(k),k)\right\} < e^{2\mathsf{T}}-1\right\}, \end{aligned} \tag{5.11}$$

and by (5.10) we can derive the preset SIR outage threshold of half-duplex OFDM systems as

$$e^{2\mathsf{T}} - 1 = (s+1)^2 - 1 = s(s+2). \tag{5.12}$$

■

5.4 Outage Performance Analysis

By observing (5.1), (5.2) and (5.6), we can find that $G_{CB}(k)$ is a common term in the first and second hops and will result in a correlation between two hops. Moreover, $G_{CD}(k)$ and $G_{SB}(k)$ will lead to correlations among relays when performing relay selections. In order to carry out analysis without considering these correlation terms, we can temporarily let them be fixed values, say $G_{CB}(k) = \bar{g}(k)$, $G_{CD}(k) = \bar{h}(k)$ and $G_{SB}(k) = \bar{l}(k)$. As a consequence, the SIRs corresponding to different relays and subcarriers can be regarded as independent. Now we can define the conditional *a priori* outage probability, (i.e., the outage probability not conditioned

on any form of relay selection having taken place) for the kth subcarrier forwarded by an arbitrary relay in the first and second hops as

$$\Xi_1\left(k|\bar{g}(k),\bar{l}(k)\right)=\mathbb{P}\left\{\mathsf{SIR}_1(m,k)<s|\bar{g}(k),\bar{l}(k)\right\}, \tag{5.13}$$

and

$$\Xi_2\left(k|\bar{g}(k),\bar{h}(k)\right)=\mathbb{P}\left\{\mathsf{SIR}_2(m,k)<s|\bar{g}(k),\bar{h}(k)\right\}. \tag{5.14}$$

Consequently, due to the bottleneck effect of two-hop DF relay networks (c.f. (5.6)), the conditional end-to-end *a priori* outage probability can be determined by

$$\Xi(k|\bar{g}(k),\bar{h}(k),\bar{l}(k))=\Xi_1(k|\bar{g}(k),\bar{l}(k))+\Xi_2(k|\bar{g}(k),\bar{h}(k))-\Xi_1(k|\bar{g}(k),\bar{l}(k))\Xi_2(k|\bar{g}(k),\bar{h}(k)). \tag{5.15}$$

To carry out further analysis, we should now focus on the derivations of $\Xi_1\left(k|\bar{g}(k),\bar{l}(k)\right)$ and $\Xi_2\left(k|\bar{g}(k),\bar{h}(k)\right)$. Because we have temporarily fixed $G_{CB}(k)=\bar{g}(k)$ and $G_{SB}(k)=\bar{l}(k)$, $P_S(k)$ can be viewed as a fixed coefficient, instead of a random variable (c.f. (5.1)). Therefore, to derive $\Xi(k|\bar{g}(k),\bar{h}(k),\bar{l}(k))$, we first need to determine the distribution of $Z(k)=P_C G_{CR_m}(k)+\varphi_m(k)$, which can be written as

$$F_Z(z)=\begin{cases}\frac{\bar{\varphi}\left(1-e^{-\frac{z}{\bar{\varphi}}}\right)-P_C\mu_{CR}\left(1-e^{-\frac{z}{P_C\mu_{CR}}}\right)}{\bar{\varphi}-P_C\mu_{CR}}, & \bar{\varphi}\neq P_C\mu_{CR}\\ 1-\frac{z+\bar{\varphi}}{\bar{\varphi}}e^{-\frac{z}{\bar{\varphi}}}, & \bar{\varphi}=P_C\mu_{CR}\end{cases} \tag{5.16}$$

Consequently, we can determine the PDF of $Z(k)$ by

$$f_Z(z)=\frac{\mathrm{d}F_Z(z)}{\mathrm{d}z}=\begin{cases}\frac{e^{-\frac{z}{\bar{\varphi}}}-e^{-\frac{z}{P_C\mu_{CR}}}}{\bar{\varphi}-P_C\mu_{CR}}, & \bar{\varphi}\neq P_C\mu_{CR}\\ \frac{z}{\bar{\varphi}^2}e^{-\frac{z}{\bar{\varphi}}}, & \bar{\varphi}=P_C\mu_{CR}\end{cases} \tag{5.17}$$

Denoting $W(k)=G_{SR_m}(k)/Z(k)$, we further determine the CDF of $W(k)$ by

$$F_W(w)=1-\frac{\mu_{SR}^2}{(\mu_{SR}+P_C\mu_{CR}w)(\mu_{SR}+\bar{\varphi}w)}. \tag{5.18}$$

Subsequently, by (5.4) and (5.18), it is straightforward to obtain

$$\Xi_1(k|\bar{g}(k),\bar{l}(k))=1-\frac{P_S^2(k)\mu_{SR}^2}{(P_S(k)\mu_{SR}+P_C\mu_{CR}s)(P_S(k)\mu_{SR}+\bar{\varphi}s)}. \tag{5.19}$$

Then, by (5.2), (5.5) and (5.14), $\Xi_2(k|\bar{g}(k),\bar{h}(k))$ can be written and reduced to

$$\begin{aligned}\Xi_2(k|\bar{g}(k),\bar{h}(k)) &= \mathbb{P}\left\{G_{R_mD}(k) < \frac{P_C\bar{h}(k)s}{P_{R_m}(k)}\right\} = \mathop{\mathbb{E}}_{P_{R_m}(k)}\left\{F_{G_{RD}}\left(\frac{P_C\bar{h}(k)s}{P_{R_m}(k)}\right)\right\} \\ &= 1 - e^{-\frac{P_C\bar{h}(k)s}{P_R\mu_{RD}}}\left[1 - e^{-\frac{(1-\alpha)P_C\bar{g}(k)}{P_R\mu_{RB}\xi}} + \frac{(1-\alpha)\mu_{RD}\bar{g}(k)e^{-\frac{(1-\alpha)P_C\bar{g}(k)}{P_R\mu_{RB}\xi}}}{(1-\alpha)\mu_{RD}\bar{g}(k) + \mu_{RB}\bar{h}(k)\xi s}\right],\end{aligned} \tag{5.20}$$

where $\mathbb{E}\{\cdot\}$ denotes the expectation of the argument. Subsequently, substituting (5.19) and (5.20) into (5.15) yields the expression of $\Xi(k|\bar{g}(k),\bar{h}(k),\bar{l}(k))$.

5.4.1 Bulk Relay Selection

Subsequently, by **Definition 1** and order statistics, we can obtain the conditional *a posteriori* outage probability for bulk relay selection and reduce it with the binomial expansion to be

$$\begin{aligned}P_{out}(s|\bar{\mathbf{g}},\bar{\mathbf{h}},\bar{\mathbf{l}}) &= \left[1 - \prod_{k=1}^{K}(1 - \Xi(k|\bar{g}(k),\bar{h}(k),\bar{l}(k)))\right]^M \\ &= \sum_{m=0}^{M}\binom{M}{m}(-1)^m\prod_{k=1}^{K}(1 - \Xi(k|\bar{g}(k),\bar{h}(k),\bar{l}(k)))^m.\end{aligned} \tag{5.21}$$

where $\bar{\mathbf{g}} = \{\bar{g}(1),\bar{g}(2),\ldots,\bar{g}(K)\}$, $\bar{\mathbf{h}} = \{\bar{h}(1),\bar{h}(2),\ldots,\bar{h}(K)\}$ and $\bar{\mathbf{l}} = \{\bar{l}(1),\bar{l}(2),\ldots,\bar{l}(K)\}$; $\binom{\cdot}{\cdot}$ represents the binomial coefficient. To remove the conditions and obtain the final expression, we have to average $P_{out}(s|\bar{\mathbf{g}},\bar{\mathbf{h}},\bar{\mathbf{l}})$ over $\bar{\mathbf{g}}$, $\bar{\mathbf{h}}$ and $\bar{\mathbf{l}}$, which will result in a $3K$-fold integral and can be written as

$$P_{out}(s) = \iiint_{\bar{\mathbf{g}},\bar{\mathbf{h}},\bar{\mathbf{l}}} P_{out}(s|\bar{\mathbf{g}},\bar{\mathbf{h}},\bar{\mathbf{l}})f_{\bar{\mathbf{G}}}(\bar{\mathbf{g}})f_{\bar{\mathbf{H}}}(\bar{\mathbf{h}})f_{\bar{\mathbf{L}}}(\bar{\mathbf{l}})\mathrm{d}\bar{\mathbf{g}}\,\mathrm{d}\bar{\mathbf{h}}\,\mathrm{d}\bar{\mathbf{l}} = \sum_{m=0}^{M}\binom{M}{m}(-1)^m\left(\prod_{k=1}^{K}\Phi(k)\right), \tag{5.22}$$

where

$$f_{\bar{\mathbf{G}}}(\bar{\mathbf{g}}) = \prod_{k=1}^{K}F_{G_{CB}}(\bar{g}(k)) = \left(\frac{1}{\mu_{CB}}\right)^K\prod_{k=1}^{K}e^{-\frac{\bar{g}(k)}{\mu_{CB}}}, \tag{5.23}$$

$$f_{\bar{\mathbf{H}}}(\bar{\mathbf{h}}) = \prod_{k=1}^{K}F_{G_{CD}}(\bar{h}(k)) = \left(\frac{1}{\mu_{CD}}\right)^K\prod_{k=1}^{K}e^{-\frac{\bar{h}(k)}{\mu_{CD}}}, \tag{5.24}$$

and

$$f_{\bar{\mathbf{L}}}(\bar{\mathbf{l}}) = \prod_{k=1}^{K} F_{G_{SB}}(\bar{l}(k)) = \left(\frac{1}{\mu_{SB}}\right)^{K} \prod_{k=1}^{K} e^{-\frac{\bar{l}(k)}{\mu_{SB}}}, \tag{5.25}$$

denoting the joint PDFs corresponding to $\bar{\mathbf{g}}$, $\bar{\mathbf{h}}$ and $\bar{\mathbf{l}}$, respectively; $\Phi(k)$ is a triple integral, which is defined and simplified by the multinomial expansion as follows [130]:

$$\begin{aligned}\Phi(k) &= \iiint_{\bar{g},\bar{h},\bar{l}} (1 - \Xi(k|\bar{g},\bar{h},\bar{l}))^{m} F_{G_{CB}}(\bar{g}) F_{G_{CD}}(\bar{h}) F_{G_{SB}}(\bar{l}) \mathrm{d}\bar{g}\, \mathrm{d}\bar{h}\, \mathrm{d}\bar{l} \\ &= \iiint_{\bar{g},\bar{h},\bar{l}} \sum_{\mathsf{C}(m,4)} \frac{m!(-1)^{m_2+m_3}}{\prod_{\tau=1}^{4} m_\tau!} \Xi_1(k|\bar{g},\bar{l})^{m_2+m_4} \Xi_2(k|\bar{g},\bar{h})^{m_3+m_4} F_{G_{CB}}(\bar{g}) F_{G_{CD}}(\bar{h}) F_{G_{SB}}(\bar{l}) \mathrm{d}\bar{g}\, \mathrm{d}\bar{h}\, \mathrm{d}\bar{l},\end{aligned} \tag{5.26}$$

where $\mathsf{C}(m,T) = \left\{ m_1, m_2, \ldots, m_T | \sum_{\tau=1}^{T} m_\tau = m,\ \forall\ 0 \le m_\tau \le m \right\}$, denoting the executive condition of the summation operation; $\bar{g}$, $\bar{h}$ and $\bar{l}$ are the shorthand notations of variables of integration $\bar{g}(k)$, $\bar{h}(k)$ and $\bar{l}(k)$, as all subcarriers are i.i.d.. Then, we can utilize the interchangeability between summation and integration operations and the independence among $\bar{g}$, $\bar{h}$ and $\bar{l}$ to further reduce $\Phi(k)$ to

$$\Phi(k) = \sum_{\mathsf{C}(m,4)} \frac{m!(-1)^{m_2+m_3}}{\prod_{\tau=1}^{4} m_\tau!} \int_0^\infty \phi_1(k, m_2+m_4) \phi_2(k, m_3+m_4) F_{G_{CB}}(\bar{g}) \mathrm{d}\bar{g}, \tag{5.27}$$

where

$$\phi_1(k,m) = \int_0^\infty \Xi_1(k|\bar{g},\bar{l})^{m} F_{G_{SB}}(\bar{l}) \mathrm{d}\bar{l}, \tag{5.28}$$

and

$$\phi_2(k,m) = \int_0^\infty \Xi_2(k|\bar{g},\bar{h})^{m} F_{G_{CD}}(\bar{h}) \mathrm{d}\bar{h}. \tag{5.29}$$

Now, let us focus on the derivations of $\phi_1(k, m_2+m_4)$ and $\phi_2(k, m_3+m_4)$. For $\phi_1(k, m_2+m_4)$, we can similarly employ the binomial expansion and obtain

$$\phi_1(k, m_2+m_4) = \sum_{p=0}^{m_2+m_4} \binom{m_2+m_4}{p} (-1)^p \vartheta(k), \tag{5.30}$$

where $\vartheta(k)$ is determined by

$$\begin{aligned}\vartheta(k) &= \int_0^\infty \left[\frac{P_S^2(k)\mu_{SR}^2}{(P_S(k)\mu_{SR}+P_C\mu_{CR}s)(P_S(k)\mu_{SR}+\bar{\varphi}s)}\right]^p F_{G_{SB}}(\bar{l})\mathrm{d}\bar{l} \\ &= \left(1-e^{-\frac{\alpha P_C\bar{g}}{\bar{P}_S\mu_{SB}\xi}}\right)\left[\frac{\bar{P}_S^2\mu_{SR}^2}{(\bar{P}_S\mu_{SR}+P_C\mu_{CR}s)(\bar{P}_S\mu_{SR}+\bar{\varphi}s)}\right]^p \\ &\quad + \frac{1}{\mu_{SB}}\left(\frac{\alpha^2P_C\bar{g}^2\mu_{SR}^2}{\mu_{CR}\bar{\varphi}\xi^2s^2}\right)^p \chi^{(p)}_{\frac{\alpha P_C\bar{g}}{\bar{P}_S\xi}}\left(\left\{\frac{\alpha\bar{g}\mu_{SR}}{\mu_{CR}\xi s}, \frac{\alpha P_C\bar{g}\mu_{SR}}{\bar{\varphi}\xi s}\right\}, \frac{1}{\mu_{SB}}\right),\end{aligned} \tag{5.31}$$

and $\chi_u^{(p)}(\mathbf{a}, b)$ is a defined function given by

$$\chi_u^{(p)}(\mathbf{a}, b) = \int_u^\infty \frac{e^{-bx}}{\prod_{\mathbf{a}}(x+a_i)^p}\mathrm{d}x, \tag{5.32}$$

$\mathbf{a} = \{a_1, a_2, \ldots, a_{N_a}\}$ denotes a set of N_a positive numbers; b and u are positive numbers; p is a nonnegative integer. When $p = 0$, we can easily obtain

$$\chi_u^{(0)}(\mathbf{a}, b) = e^{-bu}/b. \tag{5.33}$$

When $p > 0$, by partial fraction decomposition [131], we can determine the closed-form expression of $\chi_u^{(p)}(\mathbf{a}, b)$ by

$$\begin{aligned}\chi_u^{(p)}(\mathbf{a}, b) &= \int_u^\infty \sum_{q=1}^{p}\sum_{i=1}^{N_a}\left[\frac{A(q,i)}{(x+a_i)^q}\right]e^{-bx}\mathrm{d}x = \sum_{q=1}^{p}\sum_{i=1}^{N_a}A(q,i)\int_u^\infty \frac{e^{-bx}}{(x+a_i)^q}\mathrm{d}x \\ &= \sum_{q=1}^{p}\sum_{i=1}^{N_a}A(q,i)e^{a_ib}\Gamma\left(1-q, b(a_i+u)\right),\end{aligned} \tag{5.34}$$

where $\{A(q,i)\}$ is a unique and real constant set, which can be derived by a recursive algorithm for any given $\mathbf{a}$ and p [132]; $\Gamma(a,x) = \int_x^\infty t^{a-1}e^{-t}\mathrm{d}t$ is the incomplete gamma function.

For $\phi_2(k, m_3+m_4)$, we can derive its closed-form expression by applying the binomial expansion twice and exchanging the order of summation and integration, and obtain

$$\phi_2(k, m_3+m_4) = \sum_{p=0}^{m_3+m_4}\sum_{q=0}^{p}\binom{m_3+m_4}{p}\binom{p}{q}(-1)^p\left[1-e^{-\frac{(1-\alpha)P_C\bar{g}}{P_R\mu_{RB}\xi}}\right]^{p-q}\theta(k), \tag{5.35}$$

where $\theta(k)$ is defined and reduced to

$$\theta(k) = \int_0^\infty \left[\frac{(1-\alpha)\mu_{RD}\bar{g}e^{-\frac{(1-\alpha)P_C\bar{g}}{\bar{P}_R\mu_{RB}\xi}}}{(1-\alpha)\mu_{RD}\bar{g} + \mu_{RB}\bar{h}\xi s} \right]^q e^{-\left(\frac{pP_C s}{\bar{P}_R\mu_{RD}} + \frac{1}{\mu_{CD}}\right)\bar{h}} \mathrm{d}\bar{h}$$

$$= \left[\frac{(1-\alpha)\mu_{RD}\bar{g}e^{-\frac{(1-\alpha)P_C\bar{g}}{\bar{P}_R\mu_{RB}\xi}}}{\mu_{RB}\xi s} \right]^q \left(\frac{pP_C s}{\bar{P}_R\mu_{RD}} + \frac{1}{\mu_{CD}} \right)^{q-1} e^{\frac{(1-\alpha)\mu_{RD}\bar{g}}{\mu_{RB}\xi s}\left(\frac{pP_C s}{\bar{P}_R\mu_{RD}} + \frac{1}{\mu_{CD}}\right)} \quad (5.36)$$

$$\times \Gamma\left(1-q, \frac{(1-\alpha)\mu_{RD}\bar{g}}{\mu_{RB}\xi s}\left(\frac{pP_C s}{\bar{P}_R\mu_{RD}} + \frac{1}{\mu_{CD}}\right)\right).$$

Consequently, by substituting the single integral expression of $\Phi(k)$ into (5.22), we can reduce $P_{out}(s)$ from a $3K$-fold integral to a summation of multiplications of a series of single integrals, which can be easily evaluated by standard numerical approaches. However, there does not exist a closed-form expression of $P_{out}(s)$ when the dynamic power control mechanism is applied.

In addition, because of the demanding estimation of instantaneous CSI, the BS might not always be able to get access to $\bar{g}$, and therefore a static power control mechanism will be applied in this scenario. Specifically, the static power control mechanism will not take $\bar{g}$ into account, but replace it with a preset static power control factor κ, which is determined by the statistical features of the network [133]. However, one should note that the static power control mechanism cannot always eliminate the deleterious effects of the interference from D2D communications to cellular communications. Although it could bring a better outage performance to D2D communications by releasing power control, this performance gain at the D2D side comes at the price of the performance loss of cellular communications [133]. As a consequence, the higher κ is, the better the outage performance in D2D communications will be, and vice versa. In other words, this provides a performance trade-off between cellular communications and D2D communications, when both coexist in an underlay manner. Then, we can derive the closed-form expression of

outage probability for bulk selection by

$$P_{out}(s) = \sum_{m=0}^{M} \binom{M}{m} (-1)^m \prod_{k=1}^{K} \left[\sum_{\mathsf{C}(m,4)} \left(\frac{m!(-1)^{m_2+m_3}}{\prod_{\tau=1}^{4} m_\tau!} \phi_1(k, m_2+m_4)|_{\bar{g}=\kappa} \phi_2(k, m_3+m_4)|_{\bar{g}=\kappa} \right) \right]. \tag{5.37}$$

Albeit useful, the expression given in (5.37) is still complicated and it is not easy to observe the relations among outage performance and system parameters, as $\phi_1(k,m)$ and $\phi_2(k,m)$ are involved. To further simplify the expression and provide an insight into the proposed system, we release the hardware constraints on transmit power at DUE transmitter and relays and assume the residual SI is eliminated by advanced SI cancellation technologies. Then, mathematically, we have $\bar{P}_S \to \infty$, $\bar{P}_R \to \infty$ and $\bar{\varphi} \to 0$. Consequently, we can derive the outage floor in a neat expression for relay-assisted OFDM D2D systems applying bulk selection and static power control mechanism by

$$\tilde{P}_{out} = \sum_{m=0}^{M} \binom{M}{m} (-1)^m \left[\mathscr{E}_m \left(\frac{\alpha \mu_{SR} \kappa}{\mu_{SB} \mu_{CR} \xi s} \right) \mathscr{E}_m \left(\frac{(1-\alpha) \mu_{RD} \kappa}{\mu_{RB} \mu_{CD} \xi s} \right) \right]^K, \tag{5.38}$$

where $\mathscr{E}_m(x) = xe^x E_m(x)$ and $E_m(x) = \int_1^\infty e^{-xt}/t^m \mathrm{d}t$ denotes the exponential integral function.

By (5.38), the potential of the proposed relay-assisted OFDM D2D system in idealized conditions can be shown, and the relations among outage performance and system parameters are revealed. Meanwhile, it can be observed that because of the summation over multiple terms with opposite signs, increasing the number of relays M might not be an efficient way to enhance outage performance when applying bulk selection.

5.4.2 Per-Subcarrier Relay Selection

In a similar manner to bulk relay selection, we can derive the conditional *a posteriori* outage probability for per-subcarrier relay selection to be

$$P_{out}(s|\bar{\mathbf{g}},\bar{\mathbf{h}},\bar{\mathbf{l}}) = 1 - \prod_{k=1}^{K}\left[1 - \left(\Xi(k|\bar{g},\bar{h},\bar{l})\right)^{M}\right]. \tag{5.39}$$

In a similar manner to bulk selection, we remove the conditions by averaging $P_{out}(s|\bar{\mathbf{g}},\bar{\mathbf{h}},\bar{\mathbf{l}})$ over $\bar{\mathbf{g}}$, $\bar{\mathbf{h}}$ and $\bar{\mathbf{l}}$, which leads to a $3K$-fold integral and can be expressed as

$$P_{out}(s) = \iiint_{\bar{\mathbf{g}},\bar{\mathbf{h}},\bar{\mathbf{l}}} P_{out}(s|\bar{\mathbf{g}},\bar{\mathbf{h}},\bar{\mathbf{l}}) f_{\bar{\mathbf{G}}}(\bar{\mathbf{g}}) f_{\bar{\mathbf{H}}}(\bar{\mathbf{h}}) f_{\bar{\mathbf{L}}}(\bar{\mathbf{l}}) \mathrm{d}\bar{\mathbf{g}}\,\mathrm{d}\bar{\mathbf{h}}\,\mathrm{d}\bar{\mathbf{l}} = 1 - \prod_{k=1}^{K}\left(1 - \Psi(k)\right), \tag{5.40}$$

where $\Psi(k)$ is defined and can be simplified by the multinomial expansion as follows [130]:

$$\begin{aligned}\Psi(k) &= \iiint_{\bar{g},\bar{h},\bar{l}} \left(\Xi(k|\bar{g},\bar{h},\bar{l})\right)^{M} F_{G_{CB}}(\bar{g}) F_{G_{CD}}(\bar{h}) F_{G_{SB}}(\bar{l}) \mathrm{d}\bar{g}\,\mathrm{d}\bar{h}\,\mathrm{d}\bar{l} \\ &= \iiint_{\bar{g},\bar{h},\bar{l}} \sum_{\mathsf{C}(M,3)} \frac{M!(-1)^{m_3}}{\prod_{\tau=3}^{3} m_\tau!} \Xi_1(k|\bar{g},\bar{l})^{m_1+m_3} \Xi_2(k|\bar{g},\bar{h})^{m_2+m_3} F_{G_{CB}}(\bar{g}) F_{G_{CD}}(\bar{h}) F_{G_{SB}}(\bar{l}) \mathrm{d}\bar{g}\,\mathrm{d}\bar{h}\,\mathrm{d}\bar{l}.\end{aligned} \tag{5.41}$$

Because of the interchangeability between summation and integration operations and the independence among $\bar{g}$, $\bar{h}$ and $\bar{l}$, we can simplify the triple integral in $\Psi(k)$ to a summation of a series of single integrals as

$$\Psi(k) = \sum_{\mathsf{C}(M,3)} \frac{M!(-1)^{m_3}}{\prod_{\tau=1}^{3} m_\tau!} \int_0^{\infty} \phi_1(k, m_1+m_3)\phi_2(k, m_2+m_3) F_{G_{CB}}(\bar{g}) \mathrm{d}\bar{g}. \tag{5.42}$$

Finally, substituting (5.42) into (5.40) yields the single integral expression of the outage probability for per-subcarrier selection when the dynamic power control mechanism is applied. Again, if the static power control mechanism is applied, we can express the closed-form expression of outage probability for per-subcarrier

selection by

$$P_{out}(s) = 1 - \prod_{k=1}^{K} \left[1 - \sum_{\mathsf{C}(M,3)} \left(\frac{M!(-1)^{m_3}}{\prod_{\tau=1}^{3} m_\tau!} \phi_1(k, m_1 + m_3)|_{\bar{g}=\kappa} \phi_2(k, m_2 + m_3)|_{\bar{g}=\kappa} \right) \right]. \tag{5.43}$$

To provide an insight into systems applying per-subcarrier selection and static power control mechanism, we can simplify (5.43) by assuming $\bar{P}_S \to \infty$, $\bar{P}_R \to \infty$ and $\bar{\varphi} \to 0$ and obtain the outage floor in a neat expression as

$$\tilde{P}_{out}(s) = 1 - \left[1 - \sum_{m=0}^{M} \binom{M}{m} (-1)^m \mathscr{E}_m \left(\frac{\alpha \mu_{SR} \kappa}{\mu_{SB} \mu_{CR} \xi s} \right) \mathscr{E}_m \left(\frac{(1-\alpha) \mu_{RD} \kappa}{\mu_{RB} \mu_{CD} \xi s} \right) \right]^K. \tag{5.44}$$

By (5.44), the potential of the per-subcarrier selection in relay-assisted OFDM D2D networks under these two idealized conditions can be quantified.

5.5 Outage Performance Optimization

Because of the joint power control mechanism at DUE transmitter and relays, there exists a trade-off in α in the outage performance of relay-assisted D2D communications, which is associated with channel statistics. That is to say, there exists an optimal $\alpha^* \in (0, 1)$, which is capable of minimizing the outage probability. Following this thought, we can then formulate an outage performance optimization problem infra

$$\begin{aligned} &\min_{\alpha} \{P_{out}(s)\} \\ &\text{s.t. } 0 < \alpha < 1. \end{aligned} \tag{5.45}$$

Because all subcarriers are i.i.d., this formulated optimization problem can be equivalently transferred to an optimization problem of maximizing the average end-to-end SIR regarding an individual subcarrier, written as[3]

$$\begin{aligned} &\max_{\alpha} \{\mathbb{E}\{\mathsf{SIR}(m,k)\}\} \\ &\text{s.t. } 0 < \alpha < 1. \end{aligned} \tag{5.46}$$

[3]The equivalence of these two optimization problems can be proven in a general manner in Appendix 5.8.1.

5.5.1 Dynamic Power Control Mechanism

Because $\mathbb{E}\{\mathsf{SIR}(m,k)\}$ is mathematically intractable, we must find another alternative objective function to approximate $\mathbb{E}\{\mathsf{SIR}(m,k)\}$ and provide a suboptimal solution instead. Therefore, for the dynamic power control mechanism, we formulate an alternative optimization problem to approximate the original problem formulated in (5.46) by

$$\begin{aligned} &\max_{\alpha}\{\Omega(\alpha)\} \\ &\text{s.t. } 0<\alpha<1, \end{aligned} \tag{5.47}$$

where $\Omega(\alpha)$ is constructed by replacing all instantaneous channel power gains by their averages in $\mathsf{SIR}(m,k)$ except for $\bar{g}(k)$, and averaging over $\bar{g}(k)$; $\Omega(\alpha)$ can be explicitly expressed as

$$\begin{aligned} \Omega(\alpha) &= \mathop{\mathbb{E}}_{\bar{g}(k)}\left\{\min\left\{\frac{\mu_{SR}\min\left\{\frac{\alpha P_C\bar{g}(k)}{\xi\mu_{SB}},\bar{P}_S\right\}}{P_C\mu_{CR}+\bar{\varphi}},\frac{\mu_{RD}\min\left\{\frac{(1-\alpha)P_C\bar{g}(k)}{\xi\mu_{RB}},\bar{P}_R\right\}}{P_C\mu_{CD}}\right\}\right\} \\ &= \begin{cases}\omega_1(\alpha), & \frac{\bar{P}_S\mu_{SR}}{P_C\mu_{CR}+\bar{\varphi}}>\frac{\bar{P}_R\mu_{RD}}{P_C\mu_{CD}}\\ \omega_2(\alpha), & \frac{\bar{P}_S\mu_{SR}}{P_C\mu_{CR}+\bar{\varphi}}\le\frac{\bar{P}_R\mu_{RD}}{P_C\mu_{CD}}\end{cases} \end{aligned} \tag{5.48a}$$

$$\omega_1(\alpha)=\begin{cases}\frac{\alpha P_C\mu_{SR}\mu_{CB}}{\xi\mu_{SB}(P_C\mu_{CR}+\bar{\varphi})}\left[1-e^{-\frac{\xi\bar{P}_R\mu_{SB}\mu_{RD}(P_C\mu_{CR}+\bar{\varphi})}{\alpha P_C^2\mu_{SR}\mu_{CB}\mu_{CD}}}\right], & 0<\alpha<\varrho\\ \frac{(1-\alpha)P_C\mu_{RD}\mu_{CB}}{P_C\xi\mu_{RB}\mu_{CD}}\left[1-e^{-\frac{\bar{P}_R\xi\mu_{RB}}{(1-\alpha)P_C\mu_{CB}}}\right], & \varrho\le\alpha<1\end{cases} \tag{5.48b}$$

$$\omega_2(\alpha)=\begin{cases}\frac{\alpha P_C\mu_{SR}\mu_{CB}}{\xi\mu_{SB}(P_C\mu_{CR}+\bar{\varphi})}\left[1-e^{-\frac{\bar{P}_S\xi\mu_{SB}}{\alpha P_C\mu_{CB}}}\right], & 0<\alpha<\varrho\\ \frac{(1-\alpha)P_C\mu_{RD}\mu_{CB}}{P_C\xi\mu_{RB}\mu_{CD}}\left[1-e^{-\frac{\bar{P}_SP_C\xi\mu_{SR}\mu_{RB}\mu_{CD}}{(1-\alpha)P_C\mu_{RD}\mu_{CB}(P_C\mu_{CR}+\bar{\varphi})}}\right], & \varrho\le\alpha<1\end{cases} \tag{5.48c}$$

$$\varrho=\frac{\mu_{SB}\mu_{RD}(P_C\mu_{CR}+\bar{\varphi})}{P_C\mu_{SR}\mu_{RB}\mu_{CD}+\mu_{SB}\mu_{RD}(P_C\mu_{CR}+\bar{\varphi})} \tag{5.48d}$$

Then, we prove the quasi-concavity of the formulated problem in Appendix 5.8.2, which enables it to be efficiently solved by standard optimization techniques (e.g., CVX in MATLAB), and a suboptimal $\alpha^{\&}$ can be yielded to improve the outage performance when the dynamic power control mechanism is applied.

5.5.2 Static Power Control Mechanism

Again, because it is difficult to analyze $\mathbb{E}\{\mathsf{SIR}(m,k)\}$ directly, we propose an alternative optimization problem for the static power control case. This new optimization problem can be written as

$$\begin{aligned} &\max_{\alpha}\{\gamma(\alpha)\} \\ &\text{s.t. } 0<\alpha<1, \end{aligned} \tag{5.49}$$

where $\gamma(\alpha)=\min\{\gamma_1(\alpha),\gamma_2(\alpha)\}$; $\gamma_1(\alpha)$ and $\gamma_2(\alpha)$ are given below:

$$\gamma_1(\alpha)=\frac{\mu_{SR}\min\left\{\frac{\alpha P_C\kappa}{\xi\mu_{SB}},\bar{P}_S\right\}}{P_C\mu_{CR}+\bar{\varphi}}, \tag{5.50}$$

and

$$\gamma_2(\alpha)=\frac{\mu_{RD}\min\left\{\frac{(1-\alpha)P_C\kappa}{\xi\mu_{RB}},\bar{P}_R\right\}}{P_C\mu_{CD}}, \tag{5.51}$$

which are produced by replacing all instantaneous channel power gains in $\mathsf{SIR}(m,k)$ by their averages. Subsequently, we can prove this alternative optimization problem to be quasi-concave in Appendix 5.8.3. As a result, this optimization problem can be efficiently solved by using standard optimization techniques, and a suboptimal $\alpha^{\&}$ can be yielded to improve the outage performance when the static power control mechanism is applied.

5.6 Numerical Simulations and Discussion

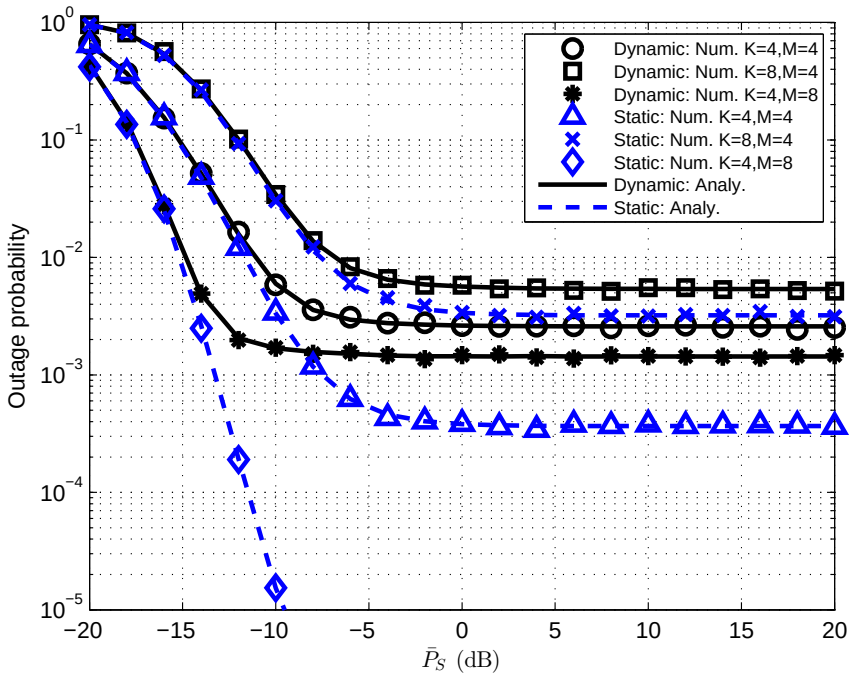
5.6.1 Verification of Analytical Results

To verify the analysis presented in **Section 5.4** for different relay selection schemes and power control mechanisms, we carried out Monte Carlo simulations in this section. First, we set $\mu_{SR}=\mu_{RD}=30$ dB, $\mu_{SB}=\mu_{RB}=10$ dB, $\mu_{CR}=\mu_{CD}=2$ dB, $\mu_{CB}=20$ dB and $\bar{\varphi}=5$ dB; also, we normalize $s=\xi=P_C=1$ and let $\alpha=0.5$ (without considering power coordination for the time being) and $\kappa=4$ for implementing the static power control mechanism. We further suppose $\bar{P}_R=\bar{P}_S$

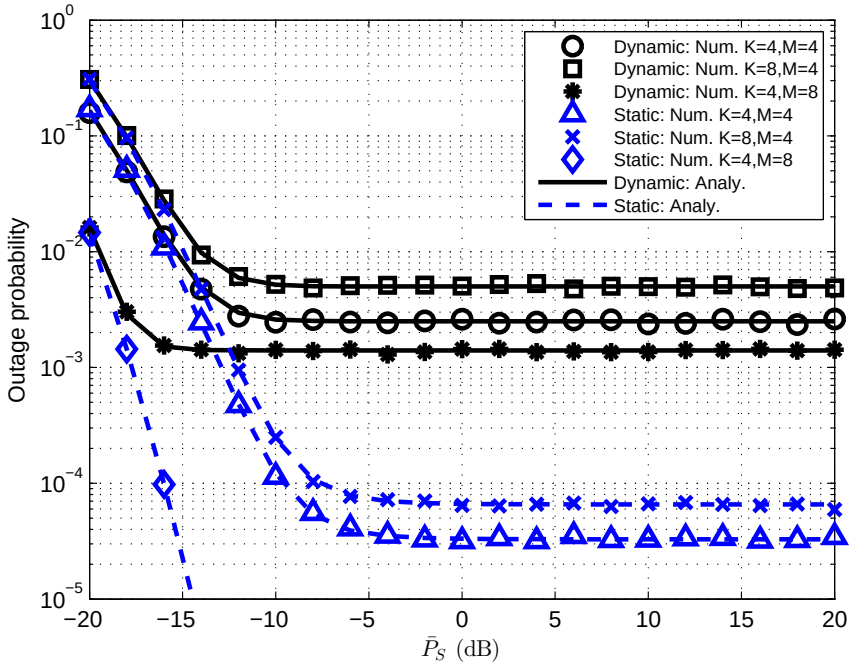
and vary this transmit power limit to substantiate (5.22), (5.37), (5.40) and (5.43). The simulation results are shown in Figure 5.2 for bulk and per-subcarrier selection schemes with different numbers of subcarriers and relays.

From Figure 5.2, we can see that the theoretical results perfectly match the numerical results, which validate the correctness of our analysis given in **Section 5.4**. In addition, the per-subcarrier selection scheme outperforms the bulk selection scheme in terms of outage probability when $\bar{P}_S$ and $\bar{P}_R$ are small. However, with the increase of $\bar{P}_S$ and $\bar{P}_R$, outage probabilities corresponding to both selection schemes become close when dynamic power control mechanism is applied, which indicates that the dynamic power control mechanism dominates the outage performance as long as $\bar{P}_S$ and $\bar{P}_R$ are sufficiently large, instead of relay selections. On the contrary, this is not the case for the static power control mechanism, as the correlation term $\bar{g}(k)$ is out of consideration, which will result in a significant performance improvement by using per-subcarrier selection.

Meanwhile, some important features of the proposed full-duplex relay-assisted OFDM D2D system can also be shown in Figure 5.2. First, the power control mechanisms constrain the improvement of outage performance by increasing $\bar{P}_S$ and $\bar{P}_R$, as it is dominated by the interference to cellular communications when $\bar{P}_S$ and $\bar{P}_R$ are large. Second, both dynamic and static power control mechanisms share similar outage performance when $\bar{P}_S$ and $\bar{P}_R$ are small, but will have a performance gap when $\bar{P}_S$ and $\bar{P}_R$ increase. The performance gap is mainly determined by the static power control factor κ. Besides, increasing the number of subcarriers K will lead to a larger outage probability, as the SIRs of all subcarriers should be larger than the preset outage threshold in order to prevent outage (c.f. **Definition 1**). On the other hand, increasing the number of relays M will yield a lower outage probability, because the DUE transmitter can have more options when performing multi-carrier relay selections. Moreover, the positive effect on outage performance by increasing M for the static power control mechanism is much more obvious than



(a) Bulk selection scheme



(b) Per-subcarrier selection scheme

Figure 5.2: Outage probability of D2D communications vs. $\bar{P}_S$ for bulk and per-subcarrier selection schemes, given $\bar{P}_R = \bar{P}_S$.

that for the dynamic power control mechanism, since there is one less correlation term when the static power control mechanism is applied. These results provide guidelines for the design of OFDM D2D systems, when coexisting with traditional cellular systems in an underlay manner.

5.6.2 Performance Benefits by Relay Selections and Comparisons

5.6.2.1 Effects of μ_{SR} and μ_{RD}

In order to study the effects of the D2D transmission links, we focus on μ_{SR} and μ_{RD} in this subsection, which are directly related to the quality of relay-assisted D2D communications. To simulate, we normalize $\bar{P}_S = \bar{P}_R = 1$, set $M = K = 4$, and maintain other settings as the same in the last subsection. Then, we assume $\mu_{RD} = \mu_{SR}$, and vary them to obtain the relation between the outage probability and the quality of the D2D transmission links. Meanwhile, to illustrate the performance benefits brought by relay selections, we also take random relay selection as a comparison benchmark in our simulations. The numerical results are illustrated in Figure 5.3. By these numerical results, it is clear that the outage performance yielded by bulk and per-subcarrier selections will become close with increasing μ_{SR} and μ_{RD} when the dynamic power control mechanism is applied, while this does not happen for the case of static power control mechanism. This is because with increasing μ_{SR} and μ_{RD}, the outage event is dominated by the deepest fade over all subcarriers. Therefore, when the dynamic power control mechanism is applied, the relay selected to forward the deepest faded subcarrier (i.e., with the minimum SIR) will be the same for bulk and per-subcarrier selections. Furthermore, compared to the random selection scheme, both bulk and subcarrier selection schemes own outage performance gains, which validate the effectiveness of multi-carrier relay selections in full-duplex relay-assisted OFDM D2D systems.

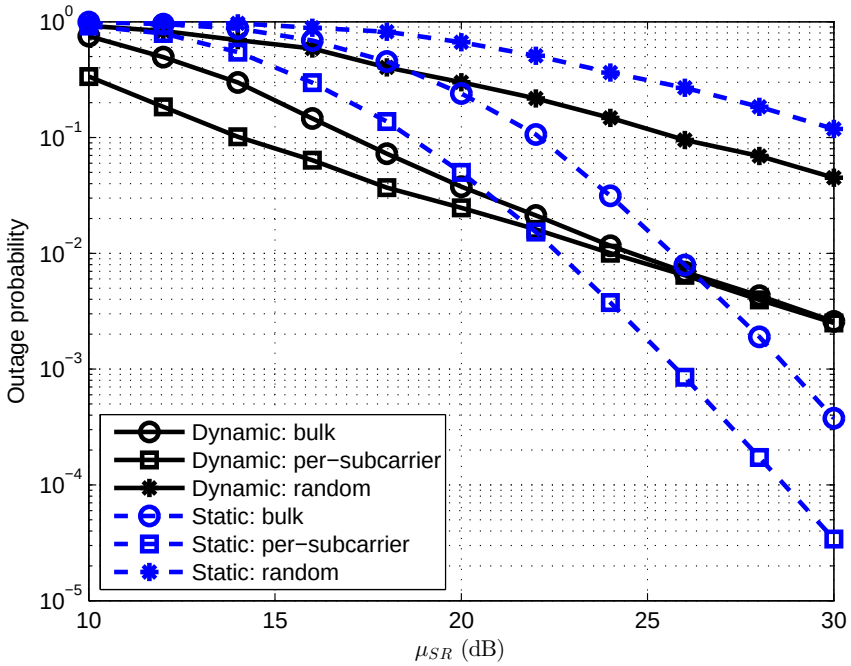


Figure 5.3: Outage probability of D2D communications vs. the average channel power gain μ_{SR}, given $\mu_{RD} = \mu_{SR}$ and $M = K = 4$.

5.6.2.2 Effects of μ_{SB} and μ_{RB}

The channels between BS and DUE transmitter as well as relays are important, as they are related to the power control mechanisms. Here, we also investigate them via μ_{SB} and μ_{RB}. By taking similar simulation configurations as above, and fixing $\mu_{SR} = \mu_{RD} = 30$ dB, we assume $\mu_{RB} = \mu_{SB}$, and vary them to illustrate how the qualities of these channels affect the outage performance of D2D communications. The numerical results are given in Figure 5.4. We can find from this figure that increasing μ_{SB} and μ_{RB} will yield a negative impact on the outage performance, because on average, less transmit power will be allowed for D2D communications when μ_{SB} and μ_{RB} become large. Meanwhile, because of the correlation term $\bar{l}(k)$, bulk and per-subcarrier selections have similar outage performance when μ_{SR} and μ_{RD} are large.

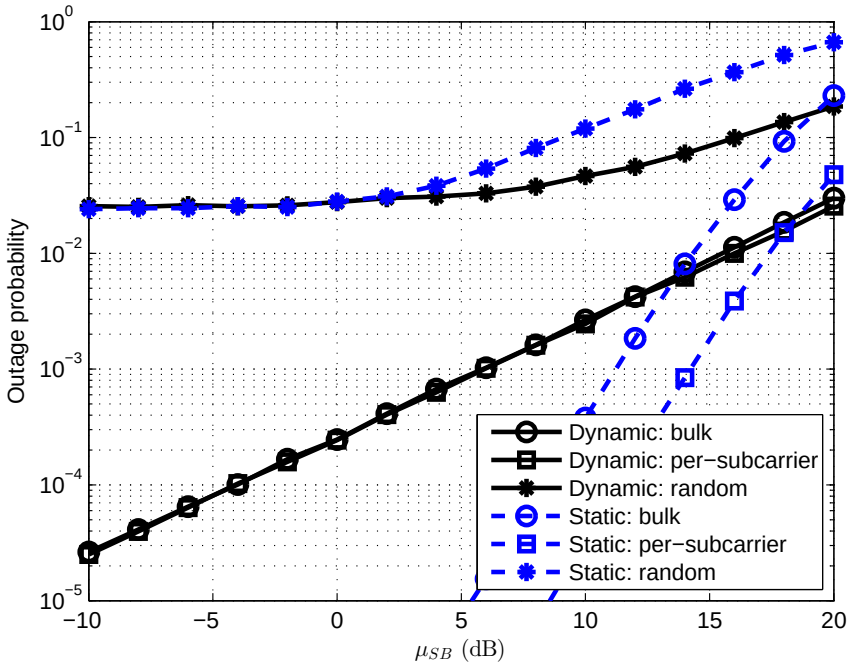


Figure 5.4: Outage probability of D2D communications vs. the average channel power gain μ_{SB}, given $\mu_{RB} = \mu_{SB}$ and $M = K = 4$.

5.6.2.3 Effects of μ_{CR} and μ_{CD}

Additionally, the channels between CUE and relay as well as the DUE receiver determine the quality of the signal reception, as the transmitted signals from CUEs are regarded as interference to relays and the DUE receiver. Here, we let $\mu_{CD} = \mu_{CR}$, and change them to observe their impacts on the D2D signal reception. The numerical results are shown in Figure 5.5. The numerical results demonstrated in Figure 5.5 are aligned with our expectation that increasing μ_{CR} and μ_{CD} will produce a destructive effect on outage performance, as a large interference from cellular communications will exist at the relays and the DUE receiver. Meanwhile, because of the correlation term $\bar{h}(k)$, with decreasing μ_{CR} and μ_{CD}, the performance curves of bulk and per-subcarrier selections become close to one another.

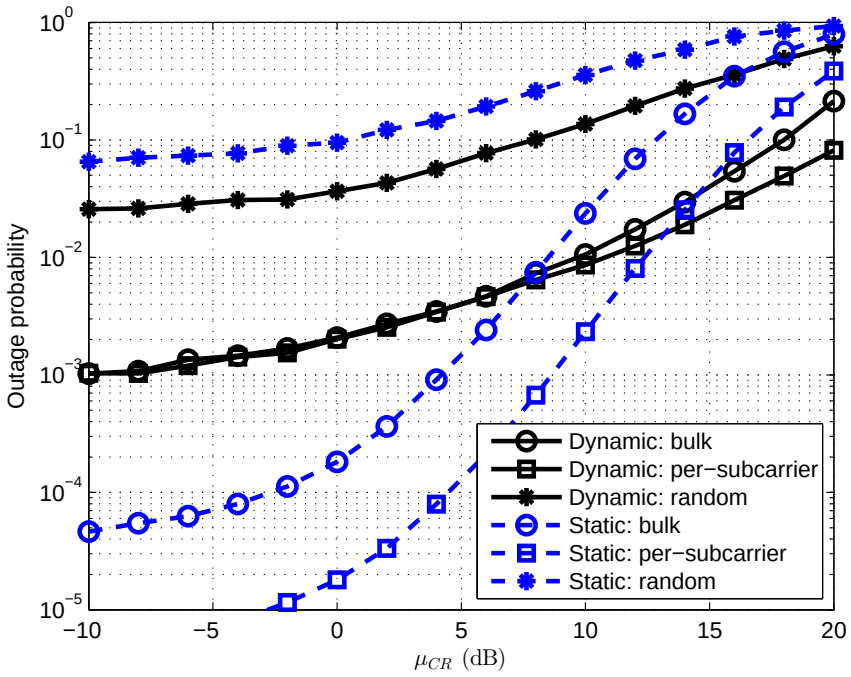
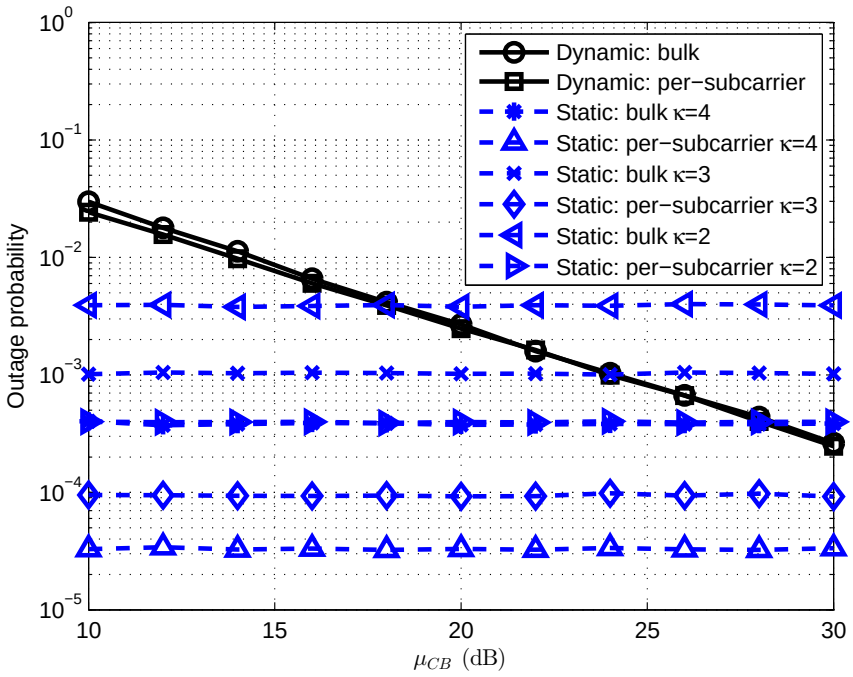


Figure 5.5: Outage probability of D2D communications vs. the average channel power gain μ_{CR}, given $\mu_{CD} = \mu_{CR}$ and $M = K = 4$.

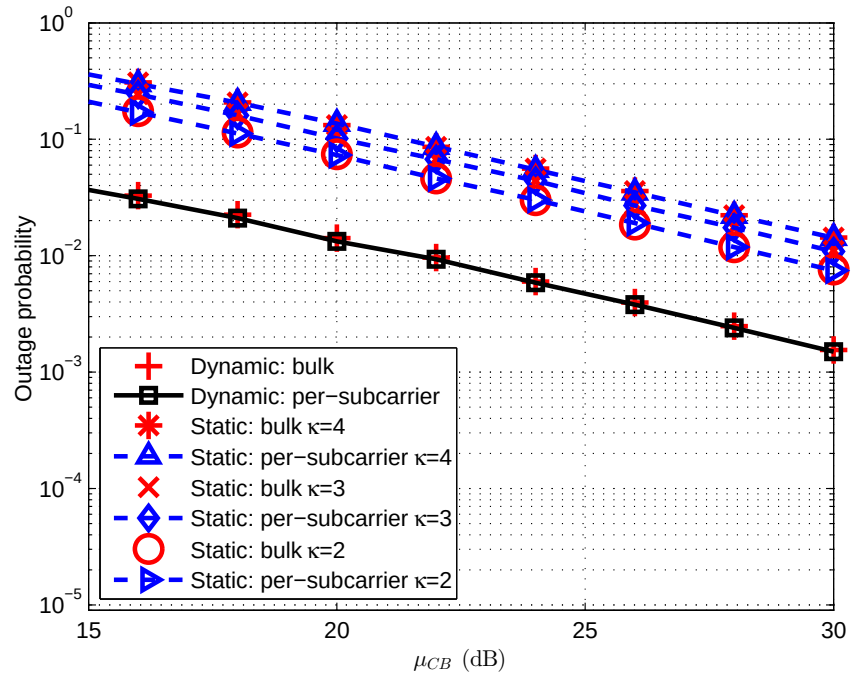
5.6.3 Comparison between Dynamic and Static Power Control Mechanisms

The performance difference between dynamic and static power control mechanisms mainly depends on μ_{CB} and κ. In this subsection, we study the relation between μ_{CB} and outage performance for different κ. To provide a comprehensive analysis of the effects of μ_{CB} on both D2D and cellular communications, we should take the outage probabilities from both sides into consideration. Taking the same simulation configurations specified in **Section 5.6.1** and normalizing $\bar{P}_S = \bar{P}_R = 1$, we carry out the numerical simulations and present the numerical results in Figure 5.6 for both D2D and cellular communications.

From Figure 5.6 (a), we can observe that the outage probabilities regarding bulk and per-subcarrier selections become close at high μ_{CB}, which indicates that the correlation term $\bar{g}(k)$ plays a dominant role in the relay selection process, and produces a deleterious impact on the performance gain. This subfigure also provides



(a) D2D communications.



(b) Cellular communications.

Figure 5.6: Outage probability vs. μ_{CB} for D2D and cellular communications, given $M = K = 4$.

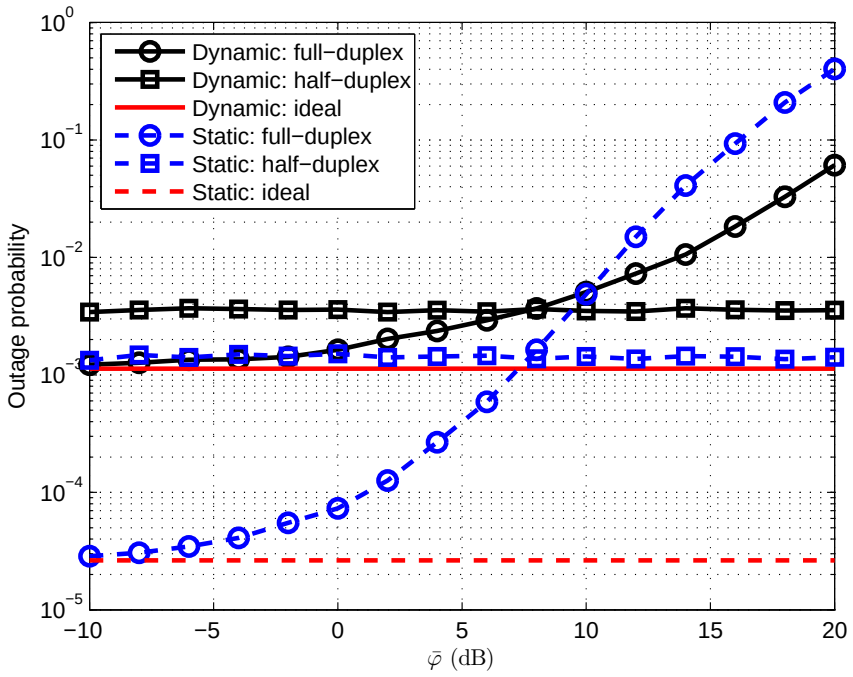
a hint to choose appropriate power control mechanisms. Meanwhile, when the static power control mechanism is applied, a lower κ will lead to a lower outage probability, and the performance is independent of μ_{CB}, as $\bar{g}(k)$ is not taken into consideration for static power control. On the other hand, by observing Figure 5.6 (b), the numerical results verify our analysis that the potential performance gain in D2D communications brought by the static power control mechanism comes at the price of the performance loss in cellular communications. Besides, as we can also see, the relay selection schemes adopted by DUEs does not matter in the cellular communications, because on average, all relays are viewed equivalently to the BS, and so is their interference.

5.6.4 Comparison between Full-Duplex and Half-Duplex Transmissions

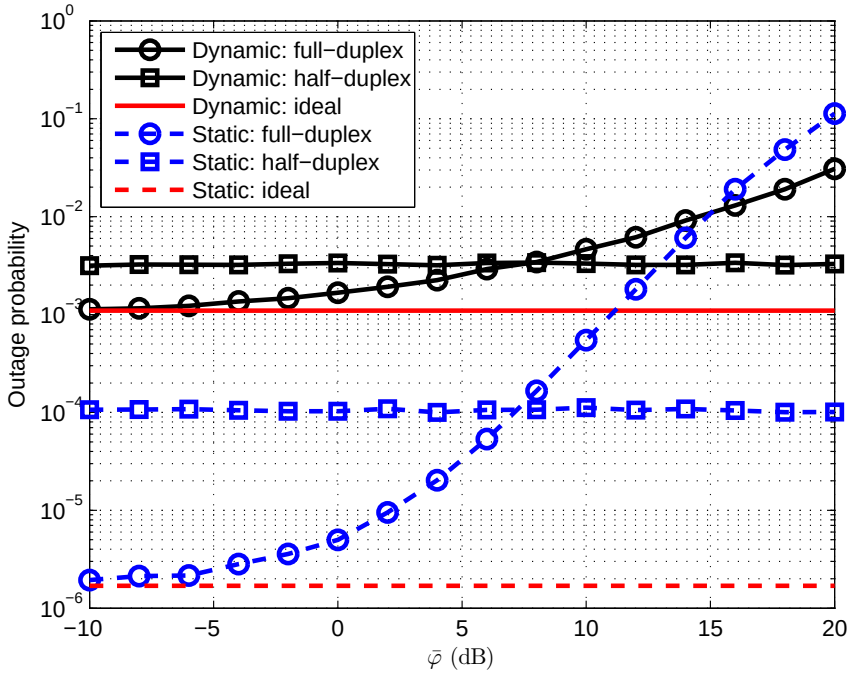
As it is well known that full-duplex transmission does not always outperform half-duplex transmission [62], the performance difference between them is mainly dependent on the average power of the residual SI term, i.e., $\bar{\varphi}$. Therefore, we study $\bar{\varphi}$ in this subsection and compare the outage performance provided by full-duplex and half-duplex transmissions (c.f. (5.7) and (5.8)). Meanwhile, we also provide an ideal case that the power of residual SI can be mitigated to a noise level and is thus negligible to show the ideal scenario of full-duplex transmission for comparison purposes. This ideal case can be produced by

$$P_{out}^{ideal}(s) = \lim_{\bar{\varphi}\to 0} P_{out}(s). \tag{5.52}$$

Taking the same simulation configurations given in **Section 5.6.1** and normalizing $\bar{P}_S = \bar{P}_R = 1$, we carry out the numerical simulations and all simulation results are shown in Figure 5.7. From this figure, it is obvious that the priority of transmission protocols depends on $\bar{\varphi}$, and full-duplex transmission does have the potential to provide a lower outage probability, as long as a satisfactory SI elimination technology



(a) Bulk selection scheme.



(b) Per-subcarrier selection scheme.

Figure 5.7: Outage probability of D2D communications vs. $\bar{\varphi}$ for bulk and per-subcarrier selection schemes, given $M = K = 4$.

can be utilized to reduce $\bar{\varphi}$ below a certain level.

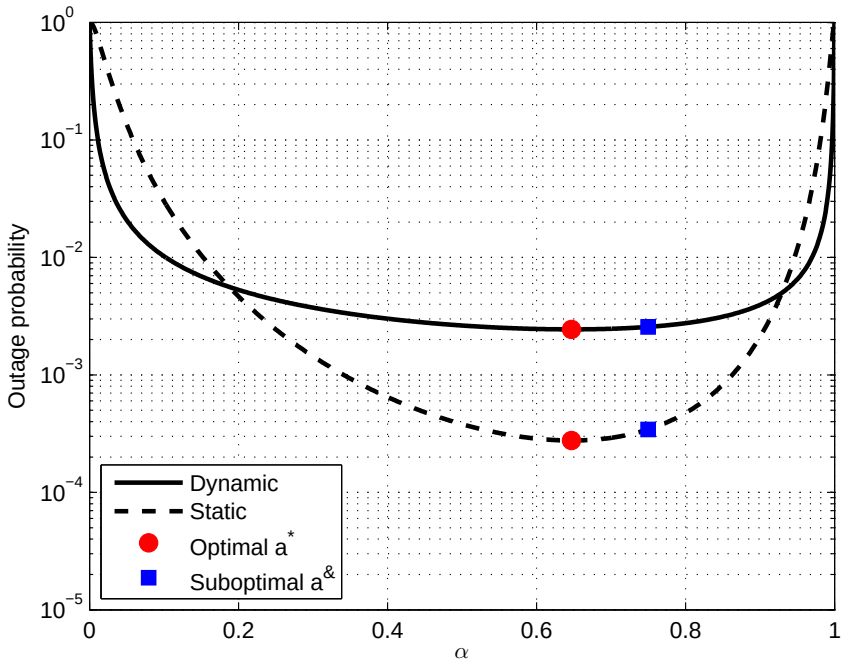
5.6.5 Verification of Outage Performance Optimization Strategies

To verify the effectiveness of the suboptimal solutions to the original optimization problem formulated in (5.45), we carry out simulations to investigate the relation between α and outage probability in this subsection. Here we adopt the same simulation configurations as set in **Section 5.6.1** and normalize $\bar{P}_S = \bar{P}_R = 1$. Simulation results are shown in Figure 5.8. Compared with the optimal[4] and suboptimal power coordination factors α^* and $\alpha^{\&}$ (highlighted by red circles and blue squares), our proposed suboptimal solutions can yield close outage probabilities to those by the optimal solutions, which validate the feasibility of our proposed suboptimal algorithms for both dynamic and static power control cases. Therefore, we can employ these algorithms to efficiently coordinate transmit power among DUE transmitter and relays to yield a lower outage probability.

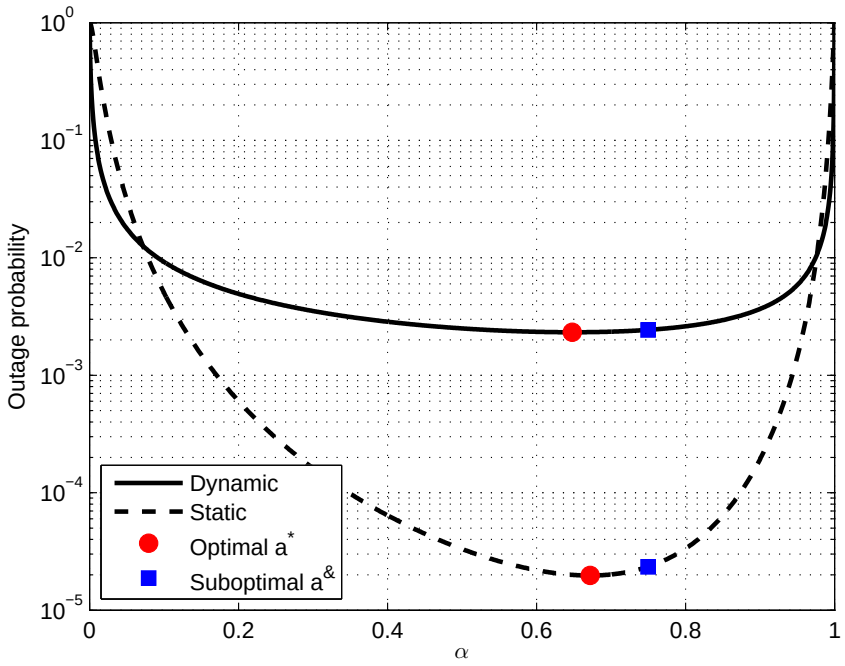
5.7 Summary

In this chapter, we proposed a full-duplex relay-assisted OFDM D2D system, and considered applying multi-carrier relay selections in this system. Meanwhile, power control mechanisms were also taken into consideration in order to efficiently mitigate the interference from D2D communications to cellular communications. Then, we analyzed the outage performance of the proposed system. We obtained the single integral expressions of the outage probabilities when the dynamic power control mechanism was applied, and these expressions can be further simplified to closed forms when the static power control mechanism was utilized. Meanwhile, by assuming two ideal conditions, the outage floors for the static power control mechanism were derived in neat and closed forms, which clearly reveal the relations

[4]Here, the optimal α^* in simulations is produced by a brute-force method searching over the full set of α with a small increment from zero to one.



(a) Bulk selection scheme.



(b) Per-subcarrier selection scheme.

Figure 5.8: Outage probability of D2D communications vs. α for bulk and per-subcarrier selection schemes, given $M = K = 4$.

among outage performance and system parameters. After that, we studied the outage performance optimization problem by coordinating transmit power among DUE transmitter and relays. Due to the mathematical intractability of the original optimization problem, we proposed two alternative optimization problems, which are capable of providing suboptimal solutions for both dynamic and static power control cases. From the analytical and numerical results provided in this chapter, we can have an insight into the full-duplex relay-assisted OFDM D2D system, and understand its characteristics in most aspects thoroughly. Moreover, as a number of comparisons are given, this chapter can also provide a guideline for implementing relay-assisted D2D communications and the relevant technologies in next generation networks.

5.8 Appendices

5.8.1 Proof of Equivalence of Optimization Problems Formulated in (5.45) and (5.46)

According to the theorem of Lebesgue-Stieltjes integration, for an arbitrary random variable X with CDF $F_X(x)$, we can derive its expectation as follows [134]:

$$\mathbb{E}\{X\} = \int_0^\infty (1 - F_X(x))\mathrm{d}x - \int_{-\infty}^0 F_X(x)\mathrm{d}x. \tag{5.53}$$

In our case, because X is the end-to-end SIR and $F_X(x)$ is the outage probability, it is obvious that $F_X(x) = 0$ for $x < 0$, and thus (5.53) can be simplified to

$$\mathbb{E}\{X\} = \int_0^\infty (1 - F_X(x))\mathrm{d}x. \tag{5.54}$$

Considering $F_X(x)$ is a monotone increasing function of x, the relation given in (5.54) validates the equivalence between $\min\limits_{\alpha}\{P_{out}(s)\}$ and $\max\limits_{\alpha}\{\mathbb{E}\{\mathsf{SIR}(m,k)\}\}$, for $0 < \alpha < 1$.

5.8.2 Proof of Quasi-Concavity of the Optimization Problem Formulated in (5.47)

To prove the quasi-concavity of the formulated problem in (5.47), we first propose a lemma as follows:

Lemma 3. Given a bounded, continuous and real piecewise function

$$f(x) = \begin{cases} f_1(x), & x \in (x_{\min}, x_c) \\ f_2(x), & x \in [x_c, x_{\max}) \end{cases}, \tag{5.55}$$

if $f_1(x)$ is a monotone increasing function of x, and $f_2(x)$ is a monotone decreasing function of x, $f(x)$ is a quasi-concave function of x and the maximum $f(x)$ is achieved when $x = x_c$.

■

Proof. This lemma is straightforward to prove by elementary algebraic derivations and the definition of a quasi-concave function. Therefore, we omit a detailed proof here, and comprehensive analysis of the relation between quasi-concavity and monotonicity can be found in [135].

■

As a result of **Lemma 3**, we can transfer the exploration of quasi-concavity to the explorations of continuity and monotonicity. It is obvious from (5.48b) and (5.48c) that $\omega_1(\alpha)$ and $\omega_2(\alpha)$ are continuous over $\alpha \in (0, \varrho)$ and $\alpha \in [\varrho, 1)$. Now, we can examine the continuity of both $\omega_1(\alpha)$ and $\omega_2(\alpha)$ at the boundary point $\alpha = \varrho$ by

$$\lim_{\alpha \to \varrho^-} \omega_i(\alpha) = \lim_{\alpha \to \varrho^+} \omega_i(\alpha), \tag{5.56}$$

where $i \in \{1, 2\}$. This relation indicates that both $\omega_1(\alpha)$ and $\omega_2(\alpha)$ are continuous at the boundary point $\alpha = \varrho$. Therefore, both $\omega_1(\alpha)$ and $\omega_2(\alpha)$ are continuous over the entire domain of definition $\alpha \in (0, 1)$.

To investigate the monotonicity of $\omega_1(\alpha)$ and $\omega_2(\alpha)$, we propose another two lemmas as follows:

Lemma 4. $f(x) = Ax\left(1 - e^{-\frac{B}{x}}\right)$, where A and B are bounded and positive constants, is a monotone increasing function of x, $\forall\ x \in (0, 1)$.

■

Proof. We derive the first and second order derivatives of $f(x)$ with respect to x as follows:

$$f'(x) = \frac{\mathrm{d}f(x)}{\mathrm{d}x} = A\left(1 - \frac{B+x}{x}e^{-\frac{B}{x}}\right) \tag{5.57}$$

and

$$f''(x) = \frac{\mathrm{d}^2 f(x)}{\mathrm{d}x^2} = -\frac{AB^2}{x^3}e^{-\frac{B}{x}} < 0. \tag{5.58}$$

From (5.58), we know that $f'(x)$ is a monotone decreasing function of x and therefore

$$\min_x\{f'(x)\} > \lim_{x\to 1} f'(x) = Ae^{-B}\left(e^B - B - 1\right) > 0. \tag{5.59}$$

Because the first order derivative $f'(x) > 0$, $\forall\ x \in (0, 1)$, $f(x)$ is a monotone increasing function of x.

■

Lemma 5. $t(x) = A(1-x)\left(1 - e^{-\frac{B}{1-x}}\right)$, where A and B are bounded and positive constants, is a monotone decreasing function of x, $\forall\ x \in (0, 1)$.

■

Proof. We can express $t(x) = f(1 - x)$. By **Lemma 4**, $f(x)$ is a monotone increasing function of x, and $f'(x) > 0$, $\forall\ x \in (0, 1)$. Then, we can obtain the first order derivative of $t(x)$ with respect to x by

$$t'(x) = \frac{\mathrm{d}t(x)}{\mathrm{d}x} = \frac{\mathrm{d}f(1-x)}{\mathrm{d}x} = -f'(x) < 0, \tag{5.60}$$

and therefore $t(x) = f(1 - x)$ is a monotone decreasing function of x, $\forall\ x \in (0, 1)$.

■

According to **Lemma 4** and **Lemma 5**, we can easily see that $\omega_1(\alpha)$ and $\omega_2(\alpha)$ are monotone increasing functions of α when $0 < \alpha < \varrho$ and monotone decreasing functions of α when $\varrho \leq \alpha < 1$. As a result of **Lemma 3**, we prove that $\omega_1(\alpha)$ and $\omega_2(\alpha)$ are quasi-concave functions of x, $\forall\ x \in (0,1)$, and so as the quasi-concavity of the formulated problem in (5.47).

5.8.3 Proof of Quasi-Concavity of the Optimization Problem Formulated in (5.49)

It can be easily seen that $\gamma_1(\alpha)$ is a bounded, continuous and monotone increasing function of α, while $\gamma_2(\alpha)$ is a bounded, continuous and monotone decreasing function of α. To prove $\gamma(\alpha)$ to be a quasi-concave function of α, we first divide the formulated problem into three cases:

1. Case 1: $\gamma_1(\alpha) > \gamma_2(\alpha)$, $\forall\ \alpha \in (0,1)$.
2. Case 2: $\gamma_1(\alpha) < \gamma_2(\alpha)$, $\forall\ \alpha \in (0,1)$.
3. Case 3: $\gamma_1(\alpha) < \gamma_2(\alpha)$, for $\alpha \in (0,\epsilon)$, and $\gamma_1(\alpha) > \gamma_2(\alpha)$, $\forall\ \alpha \in (\epsilon,1)$, where ϵ is a critical point, in which $\gamma_1(\epsilon) = \gamma_2(\epsilon)$.

For Case 1 and Case 2, it is straightforward that $\gamma(\alpha) = \gamma_1(\alpha)$ and $\gamma(\alpha) = \gamma_2(\alpha)$. Because of the monotonicity of $\gamma_1(\alpha)$ and $\gamma_2(\alpha)$, it is easy to derive the relation infra for both cases

$$\begin{aligned} &\forall\ \alpha_1, \alpha_2 \in (0,1) \text{ and } \lambda \in (0,1), \\ &\quad \exists\ \gamma(\lambda\alpha_1 + (1-\lambda)\gamma_2) \geq \min\left\{\gamma(\alpha_1), \gamma(\gamma_2)\right\}. \end{aligned} \tag{5.61}$$

Hence, according to the definition of a quasi-concave function [106], we have proved $\gamma(\alpha)$ to be quasi-concave for Case 1 and Case 2. For Case 3, we suppose $0 < \alpha_1 < \alpha_2 < 1$ without losing generality and further divide Case 3 into another three subcases as follows:

1. Case 3-1: $0 < \alpha_1 < \alpha_2 < \epsilon$

2. Case 3-2: $\epsilon < \alpha_1 < \alpha_2 < 1$

3. Case 3-3: $0 < \alpha_1 < \epsilon < \alpha_2 < 1$

Case 3-1 and Case 3-2 are simply special cases of Case 2 and Case 1, respectively. Therefore, the quasi-concavity of Case 3-1 and Case 3-2 can be proven in a similar manner to above. For Case 3-3, we need to discuss λ in the range of $\left(0, \frac{\alpha_2-\epsilon}{\alpha_2-\alpha_1}\right)$ and $\left(\frac{\alpha_2-\epsilon}{\alpha_2-\alpha_1}, 1\right)$, respectively. When $\lambda \in \left(0, \frac{\alpha_2-\epsilon}{\alpha_2-\alpha_1}\right)$, we can derive

$$\gamma(\lambda\alpha_1 + (1-\lambda)\alpha_2) = \gamma_1(\lambda\alpha_1 + (1-\lambda)\alpha_2) \geq \gamma_1(\alpha_1) = \gamma(\alpha_1) \geq \min\{\gamma(\alpha_1), \gamma(\alpha_2)\}. \tag{5.62}$$

Similarly, when $\lambda \in \left(\frac{\alpha_2-\epsilon}{\alpha_2-\alpha_1}, 1\right)$, we can derive

$$\gamma(\lambda\alpha_1 + (1-\lambda)\alpha_2) = \gamma_2(\lambda\alpha_1 + (1-\lambda)\alpha_2) \geq \gamma_2(\alpha_2) = \gamma(\alpha_2) \geq \min\{\gamma(\alpha_1), \gamma(\alpha_2)\}. \tag{5.63}$$

By (5.62) and (5.63), we have proved $\gamma(\alpha)$ to be a quasi-concave function of α for Case 3. Now we have proved $\gamma(\alpha)$ to be a quasi-concave function of α for all cases and thus the quasi-concavity of the formulated optimization problem.

Chapter 6

Adaptive OFDM with Index Modulation for Relay Networks

In previous chapters, we have not yet fully explored the encoding and decoding processes in OFDM-based relay systems, as well as the corresponding error performance. In addition to practical application scenarios, to have a comprehensive understanding of OFDM-based relay systems and provide a holistic analysis in a system level, the encoding and decoding processes of OFDM-based relay systems must be taken into consideration. Classic modulation schemes, e.g., PSK and QAM, map a sequence of information bits to a modulated data symbol with a certain amplitude and phase, and such a modulated data symbol can be represented by a point in the two-dimensional constellation diagram [71]. With rapid increasing demands for reliability and data transmission rate, however, these classic modulation schemes might not be able to satisfy the challenging communication requirements for next generation networks in terms of spectrum and energy efficiency [136]. As a result, there has been a growing interest in design and optimization of modulation schemes that can achieve a high spectrum and/or energy efficiency [137]. One of the most promising schemes is the OFDM-IM, which is capable of adding one extra modulation dimension in addition to the conventional amplitude and phase dimen-

sions [138], and is now being regarded as an attractive modulation methodology for 5G networks [139].

In the meantime, due to the maturity and benefits of multi-carrier relay systems, it is of an increasingly high interest to integrate it with OFDM-IM, which is still an open issue. Therefore, an analytical framework integrating the merits of both is expected. Also, motivated by a variety of adaptive modulation schemes proposed for other novel modulation schemes and proven to be capable of greatly enhancing system performance [140–142], the adaptive modulation mechanism in OFDM-IM for relay networks would also be worth investigating.

Based on these considerations, we propose an adaptive OFDM-IM for two-hop relay networks in this chapter. In this proposed adaptive OFDM-IM, the mapping schemes between a bit stream and indices of active subcarriers for the first and second hops are adaptively selected by a certain criterion. As a result, the active subcarriers for the same bit stream in the first and second hops can be varied in order to combat slow frequency-selective fading. This adaptive mechanism can be regarded as a good alternative to multi-carrier relay selection and is particularly helpful when there is only one relay and relay selection is not feasible. The analyses of average outage probability, end-to-end capacity and SER are given in closed form for DF relaying networks.

6.1 System Framework

Consider a two-hop OFDM-IM system with one source, one relay, one destination and N_T subcarriers, which is operating in slow frequency-selective Rayleigh fading channels. Also, N_S out of the N_T subcarriers will be selected by a certain criterion to form a *mapping scheme* (a.k.a. a *codebook*) for OFDM-IM, where $1 \leq N_S < N_T$. In each instant, there is a variable-length equiprobable stream $[\mathbf{b}_S(k), \mathbf{b}_M(m_1), \mathbf{b}_M(m_2), \ldots, \mathbf{b}_M(m_{N_A(k)})]$, required to be transmitted at the source,

where $m_t \in \mathcal{M} = \{1, 2, \ldots, M\}$ denotes the index of the chosen amplitude and phase modulation (APM) constellation symbol for the tth active subcarrier and M is the order of APM; $k \in \mathcal{K} = \{1, 2, 3, \ldots, 2^{N_S}\}$ denotes the index of the subcarrier activation pattern and $N_A(k)$ is the corresponding number of active subcarriers. Supposing that the lengths of $\mathbf{b}_S(k)$ and $\mathbf{b}_M(m_t)$ are B_S and B_M, the length of the entire variable-length stream is $B(k) = B_S + N_A(k)B_M$. The B_S-bit stream $\mathbf{b}_S(k)$ is modulated by the subcarrier activation pattern, and $N_A(k)$ out of N_S subcarriers will be activated to convey the APM symbols generated according to these B_M-bit streams $\mathbf{b}_M(m_1)$, $\mathbf{b}_M(m_2)$,...,$\mathbf{b}_M(m_{N_A(k)})$ by the conventional M-ary APM scheme (e.g., M-PSK or M-QAM). Note that normally the mapping scheme is preset in classic OFDM-IM systems and remains fixed, but in this chapter, we assume it can be dynamically selected according to the instantaneous CSI. More details of the mapping scheme and its adaptation mechanisms will be given latter in **Section 6.2**.

Meanwhile, we assume that a single bit in $\mathbf{b}_S(k)$ represents the activation state of a given subcarrier in an on-off keying (OOK) manner. In other words, for a given B_S-bit stream $\mathbf{b}_S(k)$, the selected subcarriers having the same sequence numbers with bits '1' will be activated, on which $N_A(k)$ different APM symbols are transmitted. That is to say, $N_S = B_S$ and the number of active subcarriers $N_A(k)$ is equal to the *Hamming weight* of the B_S-bit stream $\mathbf{b}_S(k)$. More specifically, the activation state matrix can be designed as

$$\mathbf{S}(k) = \text{diag}\{b_S(k,1), b_S(k,2), \ldots, b_S(k,N_S)\}, \tag{6.1}$$

where $b_S(k,n)$ is either '0' or '1' denoting the nth entry in $\mathbf{b}_S(k)$, $\forall\, n \in \{1, 2, \ldots, N_S\}$. As a result, by OFDM-IM, the information contained in the entire $B(k)$-bit stream is now conveyed by both of $N_A(k)$ M-ary constellation symbols $\{\chi_{m_t}\}$ and the activation state matrix $\mathbf{S}(k)$. Both will be jointly estimated by maximum-likelihood (ML) detection method at the relay and destination.

Here we further assume that there is no direct transmission link between source

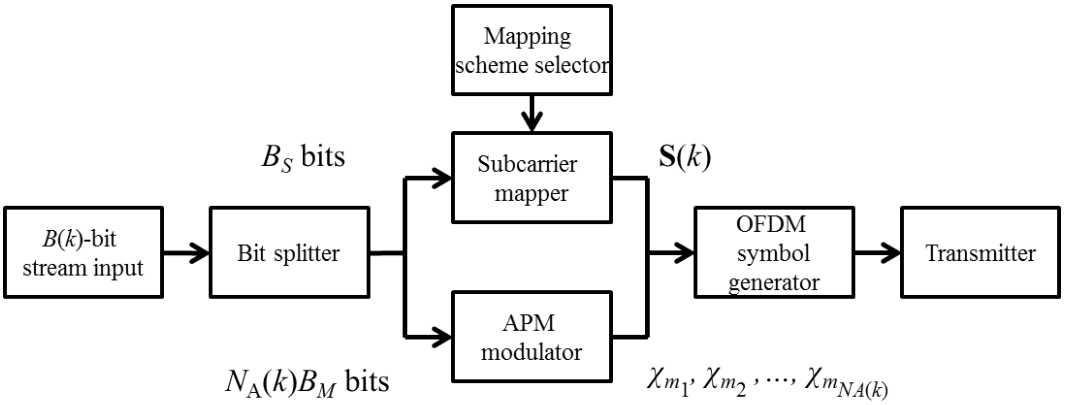


Figure 6.1: System block diagram of the source (similar to the transmission part of the relay).

and destination due to deep fading or severe propagation attenuation and a half-duplex forwarding protocol is adopted at the relay, so that two orthogonal temporal phases are required for a complete symbol transmission from the source to the destination. In the first phase, the generated OFDM-IM symbol at the source is transmitted to the relay in slow frequency-selective Rayleigh fading channels. Because DF relaying protocol and ML detection are adopted at the relay, once the distorted symbol is received by the relay, it will be first decoded and regenerated according to the relay's own mapping scheme for the second hop. Then the relay transmits the regenerated symbol to the destination. Finally, the distorted version of the new symbol is received by the destination and then decoded to retrieve the complete $B(k)$-bit stream. For clarity, the system block diagram of the source is illustrated in Figure 6.1, which is also highly similar to the transmission part of the relay.

As for the channel model, we assume the wireless channels in the first and second hops are slow frequency-selective faded and their gains to be exponentially distributed but with different means μ_1 and μ_2 due to different propagation attenuations. Note that the slow or quasi-static property referred to here indicates that the channel gains are random but would remain unchanged for a sufficiently large period of time [111]. Based on such an assumption, the overheads caused by

transmitting the selected mapping scheme via feedforward links to relay and destination for decoding purposes are negligible [140]. This justifies the feasibility of our proposed adaptive OFDM-IM in practice. Denoting the set of all subcarriers as $\mathcal{N} = \{1, 2, \ldots, N_T\}$, the PDF $f_i(s)$ and the CDF $F_i(s)$ of the channel gain $|h_i(n)|^2$, $\forall\ n \in \mathcal{N}$, can be written as the same as given in (5.3) with mean μ_i for $i \in \{1, 2\}$ denoting the index of the first or second hop. Meanwhile, because of the fundamental assumptions of OFDM, it is supposed that these N_T channel gains in each hop are statistically independent (refers to **Section 2.2** for more details).

In terms of the APM scheme, we adopt M-PSK as the APM scheme. As has been proven for SM systems and similarly for OFDM-IM systems, a constant-envelope APM is preferable over a non-constant-envelope APM when the spatial or frequency indices are employed for information transmission, since it can offer a higher power efficiency and a reduced-complexity decoding process [143, 144]. In other words, M-PSK outperforms M-QAM. This is the reason for using M-PSK in this chapter. Without loss of generality, we normalize the data symbol by $\chi_{m_t}\chi^*_{m_t} = 1$, $\forall\ m_t \in \mathcal{M}$.

6.2 Mapping Scheme Selections and Performance Evaluation Metrics

Now let us focus on the key property of the proposed system, i.e., a dynamical mapping scheme selection according to CSI. First, here we assume CSI can be perfectly known at source and relay without delay and overhead. Then, the set of all mapping schemes is denoted by $\mathcal{C}$ and the cardinality of $\mathcal{C}$, i.e., the total number of possible mapping schemes is given by $\mathrm{Card}(\mathcal{C}) = \binom{N_T}{N_S}$, where $\binom{\cdot}{\cdot}$ denotes the binomial coefficient. It should be noted that the OFDM blocks are normally generated by IFFT, which will require $N_T = 2^\zeta$, $\zeta \in \mathbb{N}^+ = \{1, 2, \ldots\}$.

6.2.1 Signal Model and Dual-Mode Transmission Protocol

In order to perform mapping scheme selection, we have to construct the signal model and transmission protocol as well as some important performance metrics. Now, let us first focus on the construction of the transmit OFDM block (a.k.a. transmit signal vector) before adopting a certain mapping scheme. Assuming a CP with sufficient length is applied to the time-domain transmit OFDM block produced by a N_T-point IFFT, the OFDM signaling model can be considered at a subcarrier level. A general form of the $N_T \times 1$ transmit OFDM block in the frequency domain without interblock interference can be written as

$$\mathbf{x} = [x(1), x(2), \ldots, x(N_T)]^T \in \mathbb{C}^{N_T \times 1}, \tag{6.2}$$

where $(\cdot)^T$ denotes the matrix transpose operation.

When selecting an arbitrary cth mapping scheme, $c \in \mathcal{C}$, which selects N_S out of N_T subcarriers to form a subset $\mathcal{N}_S(c) \subset \mathcal{N}$ for OFDM-IM, the reduced OFDM block determined by the $B(k)$-bit stream is given by

$$\mathbf{x}(k) = [x(m_1, 1), x(m_2, 2), \ldots, x(m_{N_S}, N_S)]^T \in \mathbb{C}^{N_S \times 1}, \tag{6.3}$$

where

$$x(m_n, n) = \begin{cases} \chi_{m_n}, & n \in \mathcal{N}_A(k) \\ 0, & \text{otherwise} \end{cases} \tag{6.4}$$

corresponds to the data symbol transmitted on the nth subcarrier, and $\mathcal{N}_A(k) \subseteq \mathcal{N}_S(c)$ is the subset of $N_A(k)$ active subcarriers out of N_S selected subcarriers when $\mathbf{b}_S(k)$ is transmitted.

Now, in order to avoid the *zero-active subcarrier dilemma*, which is defined as the case when all selected subcarriers are required to be inactive (i.e., $\mathbf{b}_S(1) = \{0, 0, \ldots, 0\}$ and thus $N_A(1) = 0$), we propose a *dual-mode transmission protocol*, which consists of the regular transmission mode and the complementary transmission mode.

If $\mathbf{S}(k) \neq \mathbf{0}_{N_S \times N_S}$, i.e., $\mathbf{b}_S(k)$ is not an all-zero bit stream, consequently, the regular transmission mode is activated and the received signal for the ith hop can be expressed by [145]

$$\mathbf{y}_i(k) = [y_i(m_1, 1), y_i(m_2, 2), \ldots, y_i(m_{N_S}, N_S)]^T = \sqrt{\frac{P_t}{N_A(k)}}\mathbf{H}_i(c)\mathbf{x}(k) + \mathbf{w}_i \in \mathbb{C}^{N_S \times 1}, \tag{6.5}$$

where $\mathbf{H}_i(c) = \text{diag}\{h_i(c, 1), h_i(c, 2), \ldots, h_i(c, N_S)\} \in \mathbb{C}^{N_S \times N_S}$ is a $N_S \times N_S$ diagonal channel state matrix for the ith hop when the cth mapping scheme is selected; $\mathbf{w}_i = [w_i(1), w_i(2), \ldots, w_i(N_S)]^T \in \mathbb{C}^{N_S \times 1}$ is the vector of independent complex AWGN samples on each subcarrier at the ith hop, whose entries obey $\mathcal{CN}(0, N_0)$, and N_0 is the noise power; P_t is a uniform transmit power adopted at both source and relay. Due to the normalization of APM symbols, we obtain the received SNR in the ith hop for the nth subcarrier as

$$\gamma_i(k, n) = \frac{P_t}{N_A(k)N_0} b_S(k, n)|h_i(c, n)|^2, \qquad \forall\ n \in \mathcal{N}_S(c). \tag{6.6}$$

However, for $\mathbf{S}(1) = \mathbf{0}_{N_S \times N_S}$ (we denote $k = 1$ for this case), i.e., $\mathbf{b}_S(1)$ is an all-zero bit stream, one of those $N_T - N_S$ unselected subcarriers $\tilde{n}_i$ will all be activated to undertake the transmission of data symbol $\chi_{m_{\tilde{n}}}$ in the ith hop. In this case, the received signal transmitted on the complementary subcarrier in the ith hop becomes

$$y_i(1, \tilde{n}_i) = h_i(\tilde{n}_i)\chi_{m_{\tilde{n}}} + w_i(\tilde{n}_i), \tag{6.7}$$

where $w_i(\tilde{n}_i)$ is a complex AWGN on the complementary subcarrier, and the SNRs of the complementary subcarrier as well as other selected subcarriers become

$$\gamma_i(1, \tilde{n}_i) = \frac{P_t}{N_0}|h_i(\tilde{n}_i)|^2 \ \text{ and } \ \gamma_i(1, n) = 0,\ \forall\ n \in \mathcal{N}_S(c). \tag{6.8}$$

We term this special case *complementary transmission* mode, so that at least one data symbol $\chi_{m_{\tilde{n}}}$ can still be transmitted on the standby subcarrier $\tilde{n}_i$ when all selected subcarriers are inactive[1]. Based on the above specification for the dual-

[1]The information conveyed by $\chi_{m_{\tilde{n}}}$ can be crucial for system coordination, e.g., synchronization.

mode transmission protocol, we can have the average transmission rate in bit per channel use (bpcu) as follows

$$\begin{aligned}\bar{B} &= \log_2\left(2^{N_S}\right) + \mathop{\mathbb{E}}_{k\in\mathcal{K}}\left\{\max\left\{1, N_A(k)\right\}\log_2(M)\right\} \\ &= N_S + \frac{\log_2(M)}{2^{N_S}}\left(1 + \sum_{n=1}^{N_S}\binom{N_S}{n}n\right) \\ &= N_S + \frac{\log_2(M)}{2^{N_S}}\left(1 + 2^{N_S-1}N_S\right) \qquad \text{[bpcu]},\end{aligned} \tag{6.9}$$

where $\mathbb{E}\{\cdot\}$ denotes the expected value of the random variable enclosed.

6.2.2 Decentralized Mapping Scheme Selection

Here, we propose two feasible mapping scheme selection methodologies, which can be applied depending on the design specification of the relay node, i.e., whether the relay is capable of performing mapping scheme selection or not. We first introduce the decentralized mapping scheme as follows. When both source and relay can get access to perfect CSI and carry out the subcarrier adaptation process, in order to optimize the outage performance and error performance, the mapping scheme selections are independently performed at the source and relay according to the criterion[2]

$$\hat{c}_i = \mathop{\arg\max}_{c\in\mathcal{C}}\left\{\sum_{n\in\mathcal{N}_S(c)}\gamma_i(2^{N_S}, n)\right\}, \tag{6.10}$$

where $\hat{c}_i$ denotes the index of the optimal mapping scheme selected for the ith hop. Because the mapping scheme selections are independently performed at both source and relay, we term this selection methodology the *decentralized mapping scheme selection*.

Subsequently, for the ith hop, the selection criterion of the complementary subcarrier is given by

$$\tilde{n}_i = \mathop{\arg\max}_{n\in\mathcal{N}\setminus\mathcal{N}_S(\hat{c}_i)} |h_i(n)|^2. \tag{6.11}$$

[2]We denote the index of all-one B_S-bit stream as $k = 2^{N_S}$, i.e., $\mathbf{b}_S(2^{N_S}) = [1, 1, \ldots, 1]$. Obviously, by this selection criterion, it is equivalent to select the N_S best subcarriers out of the N_T subcarriers in terms of SNR for the ith hop.

6.2.3 Centralized Mapping Scheme Selection

However, the decentralized mapping scheme selection methodology will result in a high system complexity at the relay node, which might not be practical as the relay is normally an idle user mobile device with relatively limited processing capability [57]. We thereby propose an alternative suboptimal mapping scheme selection methodology, which is performed only at the source and thus relaxes the design requirements of the relay. Because the mapping scheme selection is only performed at the source, we term this the *centralized mapping scheme selection*. Specifically, the mapping scheme is only selected at the source and will be simply followed by the relay. The mapping scheme selection criterion is given by

$$\hat{c} = \arg\max_{c \in \mathcal{C}} \left\{ \sum_{n \in \mathcal{N}_S(c)} \min\left\{ \gamma_1(2^{N_S}, n), \gamma_2(2^{N_S}, n) \right\} \right\}, \tag{6.12}$$

which is equivalent to choose the N_S best links from the N_T links in terms of end-to-end SNR.

In a similar manner to the decentralized case, we can select the contemporary subcarrier for a whole link by the criterion

$$\tilde{n} = \arg\max_{n \in \mathcal{N} \setminus \mathcal{N}_S(\hat{c})} \min\left\{ |h_1(n)|^2, |h_2(n)|^2 \right\}. \tag{6.13}$$

The two-hop systems with decentralized and centralized mapping scheme selections are illustrated in Figure 6.2 for clarity.

By either the decentralized or centralized mapping scheme selection methodology, as long as the cth mapping scheme is selected, the B_S-bit stream $\mathbf{b}_S(k)$ will be mapped to activate a subset of $\mathcal{N}_A(k)$ from $\mathcal{N}_S(c)$ subcarriers. To achieve this, we first need to relabel the subcarriers in $\mathcal{N}_S(c)$ by the new indices in ascending order. To be clear, the indices in the original full set $\mathcal{N}$ are termed *absolute indices*, whereas the indices in the selected subset $\mathcal{N}_S(c)$ are termed *relative indices*[3]. An

[3]Because the values of indices *per se* do not affect the mathematical analysis, with a slight abuse of notation, we do not specifically distinguish them and denote a generic subcarrier index as n in this chapter.

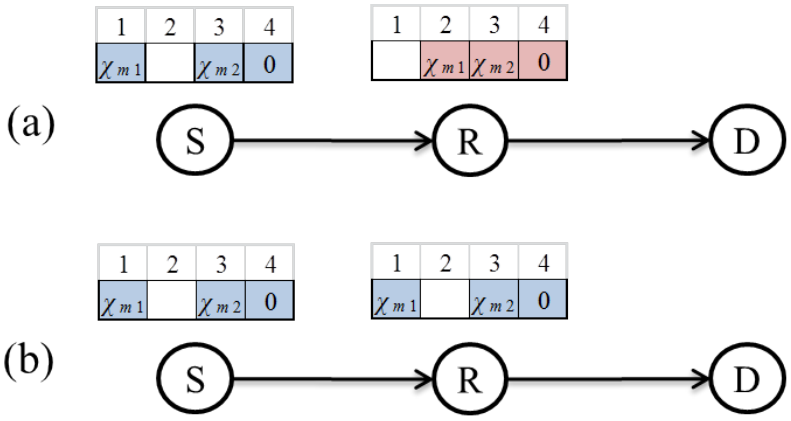


Figure 6.2: An example of (a): a two-hop system with the decentralized mapping scheme selection; (b): a two-hop system with the centralized mapping scheme selection, when $N_T = 4$, $N_S = 3$ and $N_A(k) = 2$.

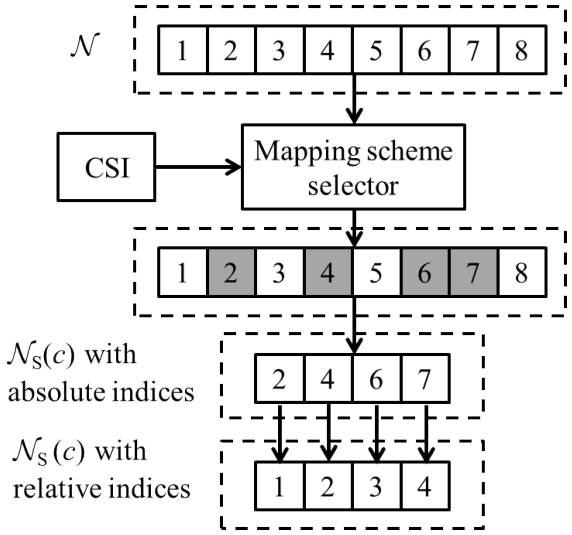


Figure 6.3: An example of mapping scheme selection process from $\mathcal{N}$ to $\mathcal{N}_S(c)$, when $N_T = 8$ and $N_S = 4$.

example of the mapping scheme selection process from $\mathcal{N}$ to $\mathcal{N}_S(c)$ can be observed in Figure 6.3, given $N_T = 8$ and $N_S = 4$. Furthermore, for clarity, an example of the OFDM-IM mapping table when $B_M = 1$ and $B_S = 2$ is given in Table 6.1 (Because $B_M = 1$, BPSK is adopted for APM and here we stipulate that data symbols $+1$ and -1 correspond to bit '1' and '0', respectively).

Table 6.1: An example of the OFDM-IM mapping table when $B_M = 1$ and $B_S = N_S = 2$.

$\mathbf{b}_S(k)$	$\mathcal{N}_A(k)$	$[\mathbf{b}_M(m_1), \ldots, \mathbf{b}_M(m_{N_A(k)})]$	$\mathbf{S}(k)$	$\mathbf{x}(k)$	$\chi_{m_{\tilde{n}}}$
$[0,0]$	$\varnothing$	$[0]$	$\text{diag}\{0,0\}$	$[0,0]^T*$	-1
$[0,0]$	$\varnothing$	$[1]$	$\text{diag}\{0,0\}$	$[0,0]^T*$	+1
$[0,1]$	$\{1\}$	$[0]$	$\text{diag}\{0,1\}$	$[0,-1]^T$	0
$[0,1]$	$\{1\}$	$[1]$	$\text{diag}\{0,1\}$	$[0,+1]^T$	0
$[1,0]$	$\{2\}$	$[0]$	$\text{diag}\{1,0\}$	$[-1,0]^T$	0
$[1,0]$	$\{2\}$	$[1]$	$\text{diag}\{1,0\}$	$[+1,0]^T$	0
$[1,1]$	$\{1,2\}$	$[0,0]$	$\text{diag}\{1,1\}$	$[-1,-1]^T$	0
$[1,1]$	$\{1,2\}$	$[0,1]$	$\text{diag}\{1,1\}$	$[-1,+1]^T$	0
$[1,1]$	$\{1,2\}$	$[1,0]$	$\text{diag}\{1,1\}$	$[+1,-1]^T$	0
$[1,1]$	$\{1,2\}$	$[1,1]$	$\text{diag}\{1,1\}$	$[+1,+1]^T$	0

* The complementary transmission mode will be activated in this case.

6.2.4 Performance Evaluation Metrics

6.2.4.1 Average Outage Probability

By **Definition 1** for the outage event in OFDM systems and fundamental probability theory, we can determine the conditional outage probability when $\mathbf{b}_S(k)$ is transmitted by

$$P_o(s|k) = \begin{cases} \mathbb{P}\left\{ \bigcup\limits_{i=1,2} \{\gamma_i(1,\tilde{n}_i) < s\} \right\}, & \text{if } k = 1 \\ \mathbb{P}\left\{ \bigcup\limits_{i=1,2} \left\{ \bigcup\limits_{n \in \mathcal{N}_A(k)} \{\gamma_i(k,n) < s\} \right\} \right\}, & \text{if } k > 1 \end{cases} \tag{6.14}$$

where $\mathbb{P}\{\cdot\}$ denotes the probability of the event enclosed. Therefore, the *average outage probability* over k can be written as

$$\bar{P}_o(s) = \mathop{\mathbb{E}}_{k \in \mathcal{K}} \{P_o(s|k)\}, \tag{6.15}$$

which is an important metric used in this chapter to characterize the system reliability.

6.2.4.2 Average End-to-End Capacity

To jointly consider throughput and reliability, we should also take end-to-end capacity into consideration to further investigate the performance of the proposed systems. According to the max-flow min-cut theorem [146], the *average end-to-end capacity* in two-hop networks is given by

$$\bar{C} = \underset{\substack{\mathbf{H}_i(\hat{c}_i), h_i(\tilde{n}_i) \\ i\in\{1,2\}, k\in\mathcal{K}}}{\mathbb{E}} \{C(k)\} \quad [\text{bit/s/Hz}], \tag{6.16}$$

where $C(k)$ is the end-to-end capacity when $\mathbf{b}_S(k)$ is transmitted and can be written as

$$C(k) = \begin{cases} \frac{1}{2}\min\left\{\log_2\left(1+\gamma_1(1,\tilde{n}_1)\right), \log_2\left(1+\gamma_2(1,\tilde{n}_2)\right)\right\}, & \text{if } k=1 \\ \sum\limits_{n\in\mathcal{N}_A(k)} \frac{1}{2}\min\left\{\log_2\left(1+\gamma_1(k,n)\right), \log_2\left(1+\gamma_2(k,n)\right)\right\}, & \text{if } k>1 \end{cases} \tag{6.17}$$

6.2.4.3 Average Symbol Error Rate

To analyze the error performance, we have to first specify the ML detection method used in our proposed systems. Due to the dual-mode transmission protocol adopted in this chapter, the ML detection method has to be tailored accordingly. In order to effectively perform detection, we first need to construct a concatenated symbol block by $\mathbf{x}(k)$ and $\chi_{m_{\tilde{n}}}$ as $\mathbf{X}(k) = \langle \mathbf{x}(k), \chi_{m_{\tilde{n}}} \rangle$, where $\langle \cdot, \cdot \rangle$ represents the vector/diagonal matrix concatenation operation[4]. The set of all possible $\mathbf{X}(k)$ is denoted as $\mathcal{X}$ and $\text{Card}(\mathcal{X}) = M + \sum_{n=1}^{N_S} \binom{N_S}{n} M^n$. Subsequently, the detection criterion of the ML detector for the received concatenated signal $\dot{\mathbf{Y}}_i(\dot{k}) = \langle \dot{\mathbf{y}}_i(\dot{k}), y_i(1,\tilde{n}_i) \rangle$ distorted from the authentic transmitted concatenated OFDM-IM symbol $\dot{\mathbf{X}}(\dot{k})$ in the ith hop is given by

$$\hat{\mathbf{X}}(\hat{k}) = \underset{\mathbf{X}(k)}{\arg\min} \left\| \dot{\mathbf{Y}}_i(\dot{k}) - \sqrt{\tfrac{P_t}{N_A(k)}} \langle \mathbf{H}_i(\hat{c}_i), h_i(\tilde{n}_i) \rangle \mathbf{X}(k) \right\|_F, \tag{6.18}$$

[4]Here we define: for arbitrary vectors $\mathbf{u}_1 = [u_1(1), u_1(2), \ldots, u_1(n)]^T$ and $\mathbf{u}_2 = [u_2(1), u_2(2), \ldots, u_2(m)]^T$, $\langle \mathbf{u}_1, \mathbf{u}_2 \rangle = [u_1(1), u_1(2), \ldots, u_1(n), u_2(1), u_2(2), \ldots, u_2(m)]^T$; for arbitrary diagonal matrices $\mathbf{U}_1 = \text{diag}\{u_1(1), u_1(2), \ldots, u_1(n)\}$ and $\mathbf{U}_2 = \text{diag}\{u_2(1), u_2(2), \ldots, u_2(m)\}$, $\langle \mathbf{U}_1, \mathbf{U}_2 \rangle = \text{diag}\{u_1(1), u_1(2), \ldots, u_1(n), u_2(1), u_2(2), \ldots, u_2(m)\}$.

where $\left\|.\right\|_F$ denotes the Frobenius norm of the enclosed matrix/vector.

Hence, the conditional SER for the ith hop can be written as

$$P_{e:i}(\dot{\mathbf{X}}(\dot{k})|\mathbf{H}_i(\hat{c}_i), h_i(\tilde{n}_i)) = \sum_{\hat{\mathbf{X}}(\hat{k})\neq\dot{\mathbf{X}}(\dot{k})} P_{e:i}(\dot{\mathbf{X}}(\dot{k}) \to \hat{\mathbf{X}}(\hat{k})|\mathbf{H}_i(\hat{c}_i), h_i(\tilde{n}_i)). \tag{6.19}$$

Subsequently, the unconditional SER can be expressed as

$$P_{e:i}(\dot{\mathbf{X}}(\dot{k})) = \mathop{\mathbb{E}}_{\mathbf{H}_i(\hat{c}_i), h_i(\tilde{n}_i)} \left\{ P_{e:i}(\dot{\mathbf{X}}(\dot{k})|\mathbf{H}_i(\hat{c}_i), h_i(\tilde{n}_i)) \right\}. \tag{6.20}$$

Due to the bottleneck effect of two-hop DF relay networks, the end-to-end SER can be approximated by[5]

$$P_e(\dot{\mathbf{X}}(\dot{k})) \approx P_{e:1}(\dot{\mathbf{X}}(\dot{k})) + P_{e:2}(\dot{\mathbf{X}}(\dot{k})) - P_{e:1}(\dot{\mathbf{X}}(\dot{k}))P_{e:2}(\dot{\mathbf{X}}(\dot{k})). \tag{6.21}$$

Now, we can define the average SER as

$$\bar{P}_e = \mathop{\mathbb{E}}_{\dot{\mathbf{X}}(\dot{k})\in\mathcal{X}} \left\{ P_e(\dot{\mathbf{X}}(\dot{k})) \right\}, \tag{6.22}$$

which will be used in this chapter to evaluate the fidelity of the proposed systems.

6.2.5 Comparison Benchmarks

6.2.5.1 Conventional OFDM-IM

Without mapping scheme adaptation, the conventional OFDM-IM system will activate $N_T/2$ out of N_T subcarriers in each instant to convey information [95]. The transmission rate of the conventional OFDM-IM is given by

$$B_{classic} = \frac{N_T}{2}\log_2(M) + \lfloor \log_2 \binom{N_T}{N_T/2} \rfloor \qquad \text{[bpcu]}, \tag{6.23}$$

where $\lfloor\cdot\rfloor$ represents the floor function.

It can be seen by comparing (6.9) with (6.23) that the transmission rate of the conventional OFDM-IM scheme without mapping scheme adaptation is higher

[5]For simplicity, we neglect the circumstance that an erroneously estimated and retransmitted signal at the relay can be again 'erroneously' estimated to the correct signal at the destination, as the probability is small.

than that with mapping scheme adaptation. Another merit of the conventional OFDM-IM is that it always activates $N_T/2$ subcarriers, so that the zero-active subcarrier dilemma does not exist. However, because the conventional OFDM-IM utilizes the index of subcarrier set to convey information, it is expected that some possible subcarrier sets will never be used in this scheme and therefore the spectral efficiency is degraded without any benefit [95]. Also, without subcarrier selection, the reliability of the systems will be much lower than that with our proposed adaptive scheme.

6.2.5.2 FPSK

As a well known modulation scheme [147], we also take frequency and phase shift keying (FPSK) as a comparison benchmark in this chapter. In FPSK, only one subcarrier will be activated and the index of the active subcarrier is used for conveying information. The transmission rate is given by

$$B_{FPSK} = \log_2(M) + \lfloor \log_2(N_T) \rfloor \qquad \text{[bpcu]}. \tag{6.24}$$

The FPSK scheme would lead to a low-complexity system, since the detection process is much simpler than our proposed adaptive OFDM-IM scheme and the zero-active subcarrier dilemma does not exist either. On the other hand, the transmission rate of the systems using FPSK might be much lower than that of systems using our proposed schemes, because the spectral efficiency of FPSK in frequency dimension is too low by activating only a single subcarrier in each instant. To clearly illustrate the mapping processes of the benchmarks and our proposed adaptive scheme, we plot the subcarrier activation patterns with $N_T = 4$ and $B_S = 2$ for all three schemes in Figure 6.4.

Detailed numerical comparisons in terms of outage performance, end-to-end capacity and error performance for the adaptive OFDM-IM scheme and these two benchmarks will be given in **Section 6.5**. The transmission rates of these three schemes are plotted in Figure 6.5 for illustration purposes. From this figure, it can

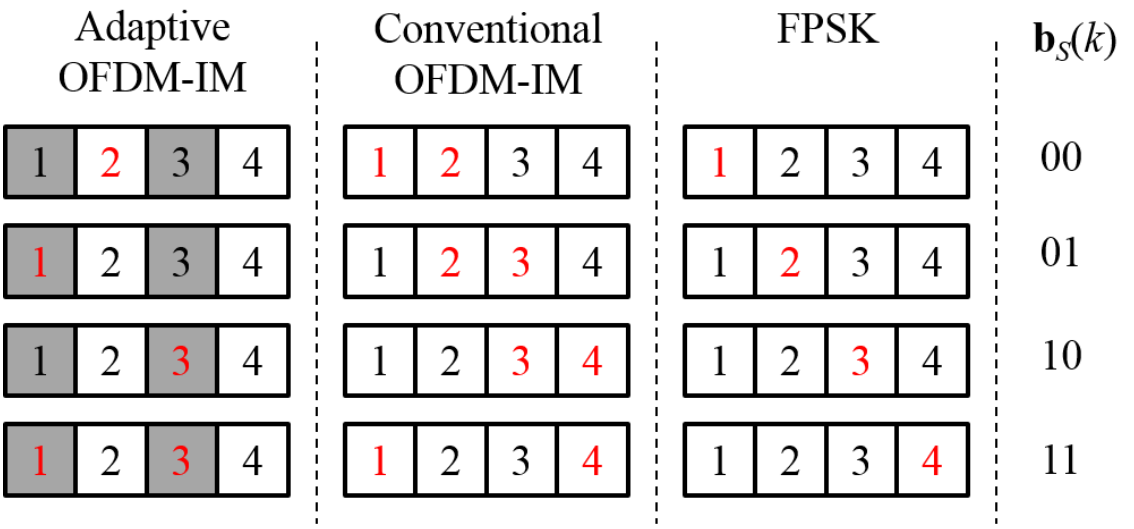


Figure 6.4: Activation patterns for the proposed adaptive OFDM-IM, conventional OFDM-IM and FPSK with $N_T = 4$ and $B_S = 2$. The numbers in boxes are corresponding to the sequence numbers of subcarriers. The grey boxes are corresponding to subcarriers are selected by the adaptive mechanism and red numbers indicate the corresponding subcarriers are active.

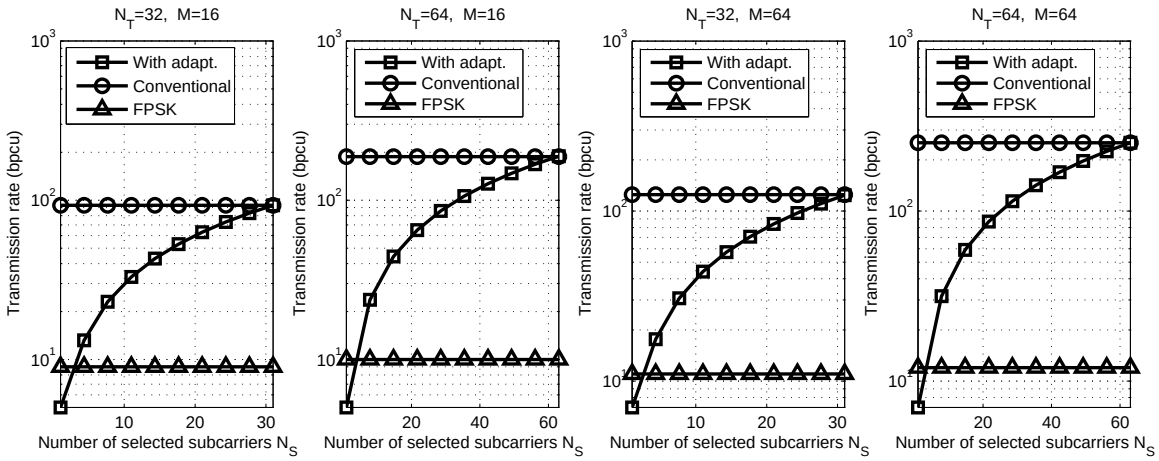


Figure 6.5: Transmission rates of different schemes vs. N_S.

be found that the adaptive OFDM-IM has a much better rate with a moderate N_S than that of FPSK, but lower than that of conventional OFDM-IM. When $N_S = N_T - 1$, any subcarrier is likely to be activated by the adaptive OFDM-IM without selection. Therefore, statistically, the rate of the adaptive OFDM-IM with $N_S = N_T - 1$ will be almost the same as the conventional OFDM-IM. As a consequence, there will be no diversity anymore.

6.3 Performance Analysis for Decentralized Mapping Scheme Selection

6.3.1 Outage Performance Analysis

When $\mathbf{b}_S(1) = [0, 0, \ldots, 0]$ is required to be transmitted, the complementary transmission mode will be activated and the standby subcarrier $\tilde{n}_i$ will be employed to convey the APM symbol $\chi_{m_{\tilde{n}}}$. By (6.11), the standby subcarrier $\tilde{n}_i$ is the $(N_T - N_S)$th worst among all N_T subcarriers and the only one active subcarrier in the complementary transmission mode. Therefore, the outage probability regarding the subcarrier $\tilde{n}_i$ in the ith hop is given by

$$P_{o:i}(s|k=1) = F_{i(N_T-N_S)}\left(\frac{sN_0}{P_t}\right), \tag{6.25}$$

where

$$F_{i(\xi)}(s) = \sum_{n=\xi}^{N_T} \binom{N_T}{n} \left(F_i(s)\right)^n \left(1 - F_i(s)\right)^{N_T-n} \tag{6.26}$$

denotes the outage probability of the ξth order statistic of the channel gain among N_T subcarriers in the ith hop [148]. Hence, the outage probability of the complementary transmission mode is

$$P_o(s|k=1) = P_{o:1}(s|k=1) + P_{o:2}(s|k=1) - P_{o:1}(s|k=1)P_{o:2}(s|k=1). \tag{6.27}$$

In order to analyze the outage performance when $k \neq 1$, we propose and prove a lemma as follows[6].

Lemma 6. For $k \neq 1$, the generic conditional outage probability for the ith hop can be determined by

$$P_{o:i}(s|k) = \sum_{\xi=N_T-N_S+1}^{N_T-N_A(k)+1} \Upsilon(k,\xi) F_{i(\xi)}\left(\frac{sN_0N_A(k)}{P_t}\right), \tag{6.28}$$

where $\Upsilon(k,\xi) = \binom{N_T-\xi}{N_A(k)-1} \Big/ \binom{N_S}{N_A(k)}$.

■

[6]See Appendix 6.7.1 for a proof.

Due to the DF forwarding protocol, the conditional outage probability considering two hops is derived by

$$P_o(s|k) = P_{o:1}(s|k) + P_{o:2}(s|k) - P_{o:1}(s|k)P_{o:2}(s|k). \tag{6.29}$$

Because $\mathbf{b}_S(k)$ is equiprobable, the average outage probability is given by

$$\bar{P}_o(s) = \frac{1}{2^{N_S}} \sum_{k \in \mathcal{K}} P_o(s|k). \tag{6.30}$$

By employing a power series expansion at $P_t/N_0 \to \infty$, we can obtain the asymptotic expression of $\bar{P}_o(s)$ as

$$\bar{P}_o(s) \sim \frac{\binom{N_T}{N_T-N_S}}{2^{N_S}} \left[\left(\frac{1}{\mu_1} \right)^{N_T-N_S} + \left(\frac{1}{\mu_2} \right)^{N_T-N_S} \right] \left(\frac{sN_0}{P_t} \right)^{N_T-N_S}, \tag{6.31}$$

by which we can find the diversity order to be $N_T - N_S$. This aligns with our expectation that N_T will always have a positive impact on the outage performance. The effects of N_S is indeterminate and dependent on other factors, but asymptotically it yields a destructive impact on the outage performance.

6.3.2 End-to-End Capacity Analysis

By (6.17), we can reduce the expression of the end-to-end capacity of the complementary transmission mode to

$$C(1) = \frac{1}{2} \log_2 \left(1 + \min \left\{ \gamma_1(1, \tilde{n}_1), \gamma_2(1, \tilde{n}_2) \right\} \right), \tag{6.32}$$

in which the PDF of $\min \left\{ \gamma_1(1, \tilde{n}_1), \gamma_2(1, \tilde{n}_2) \right\}$ after performing mapping scheme selections can be expressed as $\psi_{(N_T-N_S, N_T-N_S)} \left(\frac{sN_0}{P_t} \right)$ and

$$\psi_{(\xi,\eta)}(xs) = x f_{1(\xi)}(xs) \left(1 - F_{2(\eta)}(xs) \right) + x f_{2(\eta)}(xs) \left(1 - F_{1(\xi)}(xs) \right), \tag{6.33}$$

where

$$f_{i(\xi)}(s) = \frac{\mathrm{d}F_{i(\xi)}(s)}{\mathrm{d}s} = \frac{N_T! \left(F_i(s) \right)^{\xi-1} \left(1 - F_i(s) \right)^{N_T-\xi} f_i(s)}{(\xi-1)!(N_T-\xi)!}. \tag{6.34}$$

Therefore, the average capacity over $h_1(\tilde{n}_1)$ and $h_2(\tilde{n}_2)$, for the complementary transmission mode can be obtained as

$$\begin{aligned}\bar{C}(1) &= \mathop{\mathbb{E}}_{h_1(\tilde{n}_1),h_2(\tilde{n}_2)}\{C(1)\} \\ &= \int_0^\infty \frac{1}{2}\log_2(1+s)\,\psi_{(N_T-N_S,N_T-N_S)}\left(\frac{sN_0}{P_t}\right)\mathrm{d}s \\ &= \Lambda_G\left(N_T-N_S, N_T-N_S, \frac{N_0}{P_t}\right).\end{aligned} \tag{6.35}$$

Here, $\Lambda_G(\xi,\eta,x)$ is a defined special function, which can be explicitly written as

$$\begin{aligned}\Lambda_G(\xi,\eta,x) = &\underbrace{\int_0^\infty \frac{x}{2}\log_2(1+s)f_{1(\xi)}(xs)\mathrm{d}s}_{\lambda_1(\xi,x)} - \underbrace{\int_0^\infty \frac{x}{2}\log_2(1+s)f_{1(\xi)}(xs)F_{2(\eta)}(xs)\mathrm{d}s}_{\nu_{1,2}(\xi,\eta,x)} \\ &+ \underbrace{\int_0^\infty \frac{x}{2}\log_2(1+s)f_{2(\eta)}(xs)\mathrm{d}s}_{\lambda_2(\eta,x)} - \underbrace{\int_0^\infty \frac{x}{2}\log_2(1+s)f_{2(\eta)}(xs)F_{1(\xi)}(xs)\mathrm{d}s}_{\nu_{2,1}(\eta,\xi,x)}.\end{aligned} \tag{6.36}$$

The expressions $\lambda_i(\xi,x)$ and $\nu_{i,j}(\xi,\eta,x)$ can be derived in closed form as

$$\lambda_i(\xi,x) = \frac{N_T!\sum_{b=0}^{\xi-1}\left[\binom{\xi-1}{b}(-1)^{b+1}\exp\left(\frac{x}{\mu_i}\left(N_T-\xi+1+b\right)\right)\mathrm{Ei}\left(-(N_T-\xi+1+b)\right)\right]}{(2\ln 2)(\xi-1)!(N_T-\xi)!} \tag{6.37}$$

and

$$\nu_{i,j}(\xi,\eta,x) = \frac{N_T!\sum_{n=\eta}^{N_T}\sum_{d=0}^{n}\sum_{b=0}^{\xi-1}\binom{N_T}{n}\binom{n}{d}\binom{\xi-1}{b}(-1)^{b+d+1}\frac{\exp(x\kappa_{i,j}(\xi,n,d,b))\mathrm{Ei}(-x\kappa_{i,j}(\xi,n,d,b))}{\kappa_{i,j}(\xi,n,d,b)}}{\mu_i(2\ln 2)(\xi-1)!(N_T-\xi)!}, \tag{6.38}$$

where $(i,j)\in\{(1,2),(2,1)\}$; $\mathrm{Ei}(x) = -\int_{-x}^{\infty}\frac{e^{-u}}{u}\mathrm{d}u$ is the exponential integral function and $\kappa_{i,j}(\xi,n,d,b) = \frac{N_T-\xi+1+b}{\mu_i} + \frac{N_T+d-n}{\mu_j}$ represents an intermediate coefficient.

For $k\neq 1$, there will be $N_A(k)$ active subcarriers at each hop, whose orders are denoted by $\boldsymbol{\Xi}_1(k) = \{\xi_1,\xi_2,\ldots,\xi_{N_A(k)}\}$ and $\boldsymbol{\Xi}_2(k) = \{\eta_1,\eta_2,\ldots,\eta_{N_A(k)}\}$, where $\xi_i\neq\xi_j$ and $\eta_i\neq\eta_j$ for $i\neq j$ and $N_T-N_S+1\leq\xi_i,\eta_i\leq N_T$, $\forall\ 1\leq i\leq N_A(k)$. The set of permutations of $\boldsymbol{\Xi}_1(k)$ and $\boldsymbol{\Xi}_2(k)$ is denoted as $\mathcal{D}(k)$ and $\mathrm{Card}(\mathcal{D}(k)) = N_S!/(N_S-N_A(k))!$. Therefore, in order to determine the conditional average capacity over $\mathbf{H}_1(\hat{c}_1)$ and $\mathbf{H}_2(\hat{c}_2)$, we propose and prove a lemma as follows[7].

[7]See Appendix 6.7.2 for a proof.

Lemma 7. For $k \neq 1$, the conditional average capacity over $\mathbf{H}_1(\hat{c}_1)$ and $\mathbf{H}_2(\hat{c}_2)$ is given by

$$\begin{aligned}\bar{C}(k) &= \underset{\mathbf{H}_1(\hat{c}_1),\mathbf{H}_2(\hat{c}_2)}{\mathbb{E}}\{C(k)\} \\ &= \sum_{\boldsymbol{\Xi}_1(k)\in\mathcal{D}(k)} \sum_{\boldsymbol{\Xi}_2(k)\in\mathcal{D}(k)} \left(\frac{(N_S - N_A(k))!}{N_S!}\right)^2 \sum_{n\in\mathcal{N}_A(k)} \Lambda_G\left(\xi_n, \eta_n, \frac{N_0 N_A(k)}{P_t}\right).\end{aligned} \tag{6.39}$$

■

As a result of the equiprobable assumption of $\mathbf{b}_S(k)$, the average end-to-end capacity can be obtained by

$$\bar{C} = \underset{k\in\mathcal{K}}{\mathbb{E}}\left\{\bar{C}(k)\right\} = \frac{1}{2^{N_S}} \sum_{k\in\mathcal{K}} \bar{C}(k). \tag{6.40}$$

6.3.3 Error Performance Analysis

According to [149], we can determine the conditional SER in the ith hop as

$$P_{e:i}(\dot{\mathbf{X}}(\dot{k}) \to \hat{\mathbf{X}}(\hat{k}) | \mathbf{H}_i(\hat{c}_i), h_i(\tilde{n}_i)) = Q\left(\sqrt{\frac{P_t}{N_0}\left\|\langle \mathbf{H}_i(\hat{c}_i), h_i(\tilde{n}_i)\rangle \left(\frac{\dot{\mathbf{X}}(\dot{k})}{\sqrt{N_A(\dot{k})}} - \frac{\hat{\mathbf{X}}(\hat{k})}{\sqrt{N_A(\hat{k})}}\right)\right\|_F^2}\right), \tag{6.41}$$

where $Q(x) = \frac{1}{\sqrt{2\pi}} \int_x^\infty \exp\left(-u^2/2\right) \mathrm{d}u$ is the Q-function. Subsequently, in order to remove the conditions on $\mathbf{H}_i(\hat{c}_i)$, $h_i(\tilde{n}_i)$ and obtain an accurate closed-form approximation, we first need to approximate the Q-function by [150]

$$Q(x) \approx (1/12)\exp\left(-x^2/2\right) + (1/4)\exp\left(-2x^2/3\right), \tag{6.42}$$

which becomes accurate when x is large, and has been proven to be effective in obtaining the approximate SER for traditional OFDM-IM as shown in [95]. Also,

we define a function $\Theta_{G_i}\left(\dot{\mathbf{X}}(\dot{k}), \hat{\mathbf{X}}(\hat{k}), \mathbf{\Xi}_i\right)$ and simplify it by

$$
\begin{aligned}
&\Theta_{G_i}\left(\dot{\mathbf{X}}(\dot{k}), \hat{\mathbf{X}}(\hat{k}), \mathbf{\Xi}_i\right) \\
&= \underbrace{\int_0^{\infty}\int_0^{\infty}\cdots\int_0^{\infty}}_{(N_S+1)-\text{fold}} Q\left(\sqrt{\frac{P_t}{N_0}\left\|\text{diag}\{u_1, u_2, \ldots, u_{N_S+1}\}\left(\frac{\dot{\mathbf{X}}(\dot{k})}{\sqrt{N_A(\dot{k})}} - \frac{\hat{\mathbf{X}}(\hat{k})}{\sqrt{N_A(\hat{k})}}\right)\right\|_F^2}\right) \\
&\qquad\qquad \times \left(f_{i(N_T-N_S)}(u_{N_S+1})\prod_{n=1}^{N_S} f_{i(\xi_n)}(u_n)\right) \mathrm{d}u_1\,\mathrm{d}u_2\ldots\mathrm{d}u_{N_S+1} \\
&\approx \frac{1}{12}\left(\frac{N_T!\Gamma\left(N_S+1+\frac{\mu_i P_t}{2N_0}\left|\dot{\chi}_{\dot{m}_{\tilde{n}}} - \hat{\chi}_{\hat{m}_{\tilde{n}}}\right|^2\right)}{N_S!\Gamma\left(N_T+1+\frac{\mu_i P_t}{2N_0}\left|\dot{\chi}_{\dot{m}_{\tilde{n}}} - \hat{\chi}_{\hat{m}_{\tilde{n}}}\right|^2\right)}\right) \\
&\qquad\qquad \times \prod_{n=1}^{N_S}\left(\frac{N_T!\Gamma\left(N_T-\xi_n+1+\frac{\mu_i P_t}{2N_0}\left|\frac{\dot{x}(\dot{m}_n,n)}{\sqrt{N_A(\dot{k})}} - \frac{\hat{x}(\hat{m}_n,n)}{\sqrt{N_A(\hat{k})}}\right|^2\right)}{(N_T-\xi_n)!\Gamma\left(N_T+1+\frac{\mu_i P_t}{2N_0}\left|\frac{\dot{x}(\dot{m}_n,n)}{\sqrt{N_A(\dot{k})}} - \frac{\hat{x}(\hat{m}_n,n)}{\sqrt{N_A(\hat{k})}}\right|^2\right)}\right) \\
&\quad + \frac{1}{4}\left(\frac{N_T!\Gamma\left(N_S+1+\frac{2\mu_i P_t}{3N_0}\left|\dot{\chi}_{\dot{m}_{\tilde{n}}} - \hat{\chi}_{\hat{m}_{\tilde{n}}}\right|^2\right)}{N_S!\Gamma\left(N_T+1+\frac{2\mu_i P_t}{3N_0}\left|\dot{\chi}_{\dot{m}_{\tilde{n}}} - \hat{\chi}_{\hat{m}_{\tilde{n}}}\right|^2\right)}\right) \\
&\qquad\qquad \times \prod_{n=1}^{N_S}\left(\frac{N_T!\Gamma\left(N_T-\xi_n+1+\frac{2\mu_i P_t}{3N_0}\left|\frac{\dot{x}(\dot{m}_n,n)}{\sqrt{N_A(\dot{k})}} - \frac{\hat{x}(\hat{m}_n,n)}{\sqrt{N_A(\hat{k})}}\right|^2\right)}{(N_T-\xi_n)!\Gamma\left(N_T+1+\frac{2\mu_i P_t}{3N_0}\left|\frac{\dot{x}(\dot{m}_n,n)}{\sqrt{N_A(\dot{k})}} - \frac{\hat{x}(\hat{m}_n,n)}{\sqrt{N_A(\hat{k})}}\right|^2\right)}\right),
\end{aligned}
\tag{6.43}
$$

where $\mathbf{\Xi}_i \in \mathcal{D}$ is the vector of ordered indices of the channel gains regarding N_S selected subcarriers in the ith hop and $\mathcal{D}$ is the permutation set; $\Gamma(x) = \int_0^{\infty} u^{x-1}\exp(-u)\mathrm{d}u$ is the gamma function.

By (6.19), (6.20) and (6.21), we can obtain the unconditional end-to-end SER by

$$
P_e(\dot{\mathbf{X}}(\dot{k})) = \Omega_{G_1}(\dot{\mathbf{X}}(\dot{k})) + \Omega_{G_2}(\dot{\mathbf{X}}(\dot{k})) - \Omega_{G_1}(\dot{\mathbf{X}}(\dot{k}))\Omega_{G_2}(\dot{\mathbf{X}}(\dot{k})), \tag{6.44}
$$

where $\Omega_{G_i}(\dot{\mathbf{X}}(\dot{k}))$ is defined as follows:

$$
\Omega_{G_i}(\dot{\mathbf{X}}(\dot{k})) = \frac{1}{N_S!}\sum_{\hat{\mathbf{X}}(\hat{k})\neq\dot{\mathbf{X}}(\dot{k})}\sum_{\mathbf{\Xi}_i\in\mathcal{D}}\Theta_{G_i}\left(\dot{\mathbf{X}}(\dot{k}), \hat{\mathbf{X}}(\hat{k}), \mathbf{\Xi}_i\right). \tag{6.45}
$$

Therefore, by (6.22), the average SER can be determined by

$$\bar{P}_e = \sum_{\dot{\mathbf{X}}(\dot{k})\in\mathcal{X}} \varphi(\dot{\mathbf{X}}(\dot{k}))P_e(\dot{\mathbf{X}}(\dot{k})), \tag{6.46}$$

where $\varphi(\dot{\mathbf{X}}(\dot{k}))$ represents the probability that $\dot{\mathbf{X}}(\dot{k})$ is transmitted, and can be written as

$$\varphi(\dot{\mathbf{X}}(\dot{k})) = \binom{N_S}{N_A(k)} \Big/ \left(2^{N_S} M^{\max\{1,N_A(k)\}}\right). \tag{6.47}$$

6.4 Performance Analysis for Centralized Mapping Scheme Selection

6.4.1 Outage Performance Analysis

Because the mapping schemes used at the source and relay are the same by the centralized mapping scheme selection, we have to integrate the channels in two hops into a whole, which is termed a *link*. When DF forwarding protocol is adopted, due to the bottleneck effect, the PDF $\phi(s)$ and CDF $\Phi(s)$ of the gain regarding a certain unsorted link can be similarly written as (5.3) with mean $\mu_\Sigma = \mu_1\mu_2/(\mu_1+\mu_2)$.

In a similar manner to the decentralized case, we can have the outage probability of the complementary transmission mode as

$$P_o(s|k=1) = \Phi_{(N_T-N_S)}\left(\frac{sN_0}{P_t}\right), \tag{6.48}$$

where

$$\Phi_{(\xi)}(s) = \sum_{n=\xi}^{N_T} \binom{N_T}{n} (\Phi(s))^n (1-\Phi(s))^{N_T-n} \tag{6.49}$$

denotes the outage probability of the ξth order statistic of the link gain among N_T links.

Now, let us generalize the analysis to an arbitrary case when $k \neq 1$, and similarly obtain the generic conditional average outage probability by

$$P_o(s|k) = \sum_{\xi=N_T-N_S+1}^{N_T-N_A(k)+1} \Upsilon(k,\xi)\Phi_{(\xi)}\left(\frac{sN_0N_A(k)}{P_t}\right). \tag{6.50}$$

Then, by (6.15) and the assumption of equiprobable $\mathbf{b}_S(k)$, the average outage probability can be calculated by (6.30) as well. By employing a power series expansion at $P_t/N_0 \to \infty$, we can obtain the asymptotic expression of $\bar{P}_o(s)$ as

$$\bar{P}_o(s) \sim \frac{1}{2^{N_S}} \binom{N_T}{N_T - N_S} \left(\frac{sN_0}{\mu_\Sigma P_t}\right)^{N_T - N_S}, \tag{6.51}$$

by which we can find the diversity order to be $N_T - N_S$. Seemingly, the centralized mapping scheme selection method will result in the same diversity as its distributed counterpart, but with a lower coding shift.

6.4.2 End-to-End Capacity Analysis

We can express the end-to-end capacity of the complementary mode by modifying (6.32) and determine the PDF of $\min\{\gamma_1(1,\tilde{n}), \gamma_2(1,\tilde{n})\}$ by $\phi_{(N_T-N_S)}\left(\frac{sN_0}{P_t}\right)$, where

$$\phi_{(\xi)}(xs) = \frac{\mathrm{d}\Phi_{(\xi)}(xs)}{\mathrm{d}s} = \frac{x(N_T)!(\Phi(xs))^{\xi-1}(1-\Phi(xs))^{N_T-\xi}\phi(xs)}{(\xi-1)!(N_T-\xi)!}. \tag{6.52}$$

Subsequently, the average capacity of the complementary mode can be determined by

$$\bar{C}(1) = \mathop{\mathbb{E}}_{h_1(\tilde{n}),h_2(\tilde{n})}\{C(1)\} = \int_0^\infty \frac{1}{2}\log_2(1+s)\,\phi_{(N_T-N_S)}\left(\frac{sN_0}{P_t}\right)\mathrm{d}s = \Lambda_L\left(N_T - N_S, \frac{N_0}{P_t}\right), \tag{6.53}$$

where $\Lambda_L(\xi, x)$ can be similarly defined as (6.37) by replacing μ_i with μ_Σ.

For $k \neq 1$, we can derive the conditional average capacity similarly as for the decentralized case by

$$\bar{C}(k) = \mathop{\mathbb{E}}_{\mathbf{H}_1(\hat{c}),\mathbf{H}_2(\hat{c})}\{C(k)\} = \sum_{\mathbf{\Xi}(k)\in\mathcal{D}(k)} \left(\frac{(N_S - N_A(k))!}{N_S!}\right) \sum_{n\in\mathcal{N}_A(k)} \Lambda_L\left(\xi_n, \frac{N_0 N_A(k)}{P_t}\right). \tag{6.54}$$

Then, by (6.40), the average end-to-end capacity for the centralized case can be derived.

6.4.3 Error Performance Analysis

Following the concept of a link as explained in **Section 6.4.1**, we can let

$$\begin{aligned}\mathbf{L}(\hat{c}) &= \text{diag}\{l(\hat{c},1), l(\hat{c},2), \ldots, l(\hat{c},N_S)\} \\ &= \text{diag}\{\min\{h_1(\hat{c},1), h_2(\hat{c},1)\}, \min\{h_1(\hat{c},2), h_2(\hat{c},2)\}, \ldots, \min\{h_1(\hat{c},N_S), h_2(\hat{c},N_S)\}\},\end{aligned} \tag{6.55}$$

and

$$l(\tilde{n}) = \min\{h_1(\tilde{n}), h_2(\tilde{n})\}. \tag{6.56}$$

Then, when applying the centralized mapping scheme selection, we can similarly obtain the unconditional end-to-end SER by

$$P_e(\dot{\mathbf{X}}(\dot{k})) = \Omega_L(\dot{\mathbf{X}}(\dot{k})), \tag{6.57}$$

where

$$\Omega_L(\dot{\mathbf{X}}(\dot{k})) = \frac{1}{N_S!} \sum_{\hat{\mathbf{X}}(\hat{k}) \neq \dot{\mathbf{X}}(\dot{k})} \sum_{\boldsymbol{\Xi} \in \mathcal{D}} \Theta_L \left(\dot{\mathbf{X}}(\dot{k}), \hat{\mathbf{X}}(\hat{k}), \boldsymbol{\Xi} \right) \tag{6.58}$$

and $\Theta_L \left(\dot{\mathbf{X}}(\dot{k}), \hat{\mathbf{X}}(\hat{k}), \boldsymbol{\Xi} \right)$ can be similarly defined and approximated as (6.43) by replacing μ_i with μ_Σ. As a result, substituting (6.57) into (6.46) yields the average SER for the centralized mapping scheme selection case.

6.5 Numerical Simulations and Discussion

To verify the analyses presented in the above sections, we normalize $\mu_1 = \mu_2 = 1$, $s = 1$ as well as $N_0 = 1$ and let $N_T = 4$. Then we carry out the simulations with different numbers of selected subcarriers N_S regarding average outage probability, end-to-end capacity and SER, respectively. The simulation results are shown and discussed as follows.

6.5.1 Outage Performance

The relations between average outage probability and the ratio of transmit power to noise power P_t/N_0 for different transmission schemes were numerically simulated by

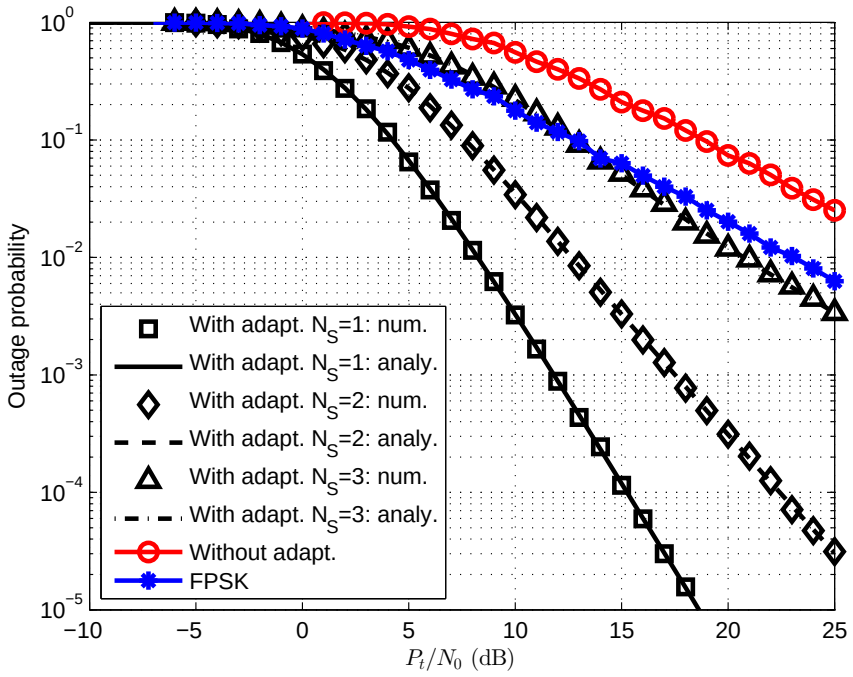
Monte Carlo methods and are shown in Figure 6.6. From this figure, the numerical results match the analytical results, which verifies our analysis in **Section 6.3.1** and **Section 6.4.1**. Meanwhile, from these two figures, some important features of adaptive OFDM-IM are revealed. First, the systems with decentralized and centralized mapping scheme selections share the same diversity order[8], but have different coding gains. This aligns with our analytical results given in (6.31) and (6.51).

Second, our proposed schemes always have a better outage performance compared to the scheme without adaptation, and this performance advantage is brought by reducing the number of subcarriers used for OFDM-IM. Besides, our proposed schemes with any N_S will enjoy a better outage performance than that of FPSK, as long as P_t/N_0 is relatively large. Also, a larger N_S will result in a larger average number of active subcarriers, which will degrade the outage performance, as all active subcarriers need to be ensured not in outage as specified in **Definition 1**. Therefore, when N_S approaches N_T, the outage performance of the adaptive schemes will be close to that of the conventional OFDM-IM. This reflects a diversity-multiplexing trade-off in terms of N_S in adaptive OFDM-IM[9].

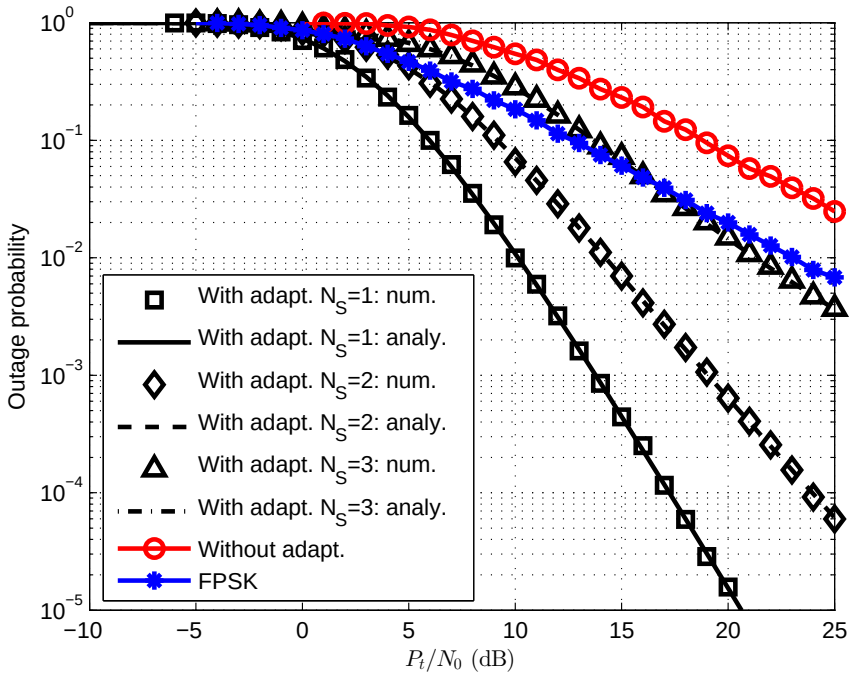
Furthermore, we have plotted the average outage probabilities and the asymptotic expressions at high SNR for both decentralized and centralized cases in Figure 6.7, which further verifies the derived asymptotic relations in **Section 6.3.1** and **Section 6.4.1** and the diversity discussion above.

[8] We can take $N_S = 2$ as an example to explore this property. In Figure 6.6 (a), when P_t/N_0 increases from 15 to 25 dB, the outage probability decreases from about $10^{-2.6}$ to $10^{-4.6}$ and the diversity gain is thereby $4.6 - 2.6 = 2$. Similarly, in Figure 6.6 (b), when P_t/N_0 increases from 15 to 25 dB, the outage probability decreases from about $10^{-2.2}$ to $10^{-4.2}$ and the diversity gain can be read as $4.2 - 2.2 = 2$. Therefore, the same diversity gain is achieved by both decentralized and centralized mapping scheme selections.

[9] A similar trade-off for MIMO systems has been found and analyzed in [151].

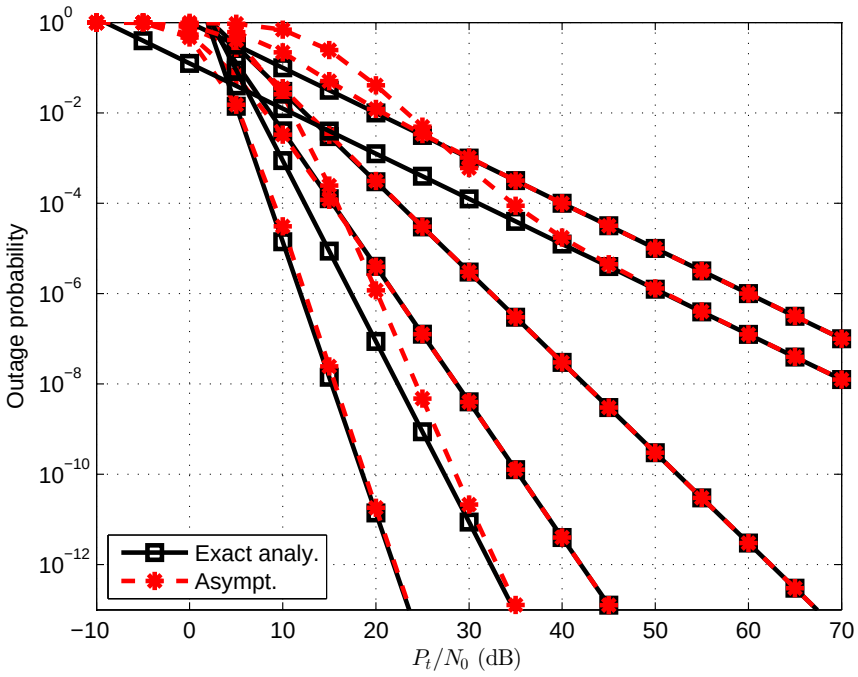


(a) Decentralized mapping scheme selection

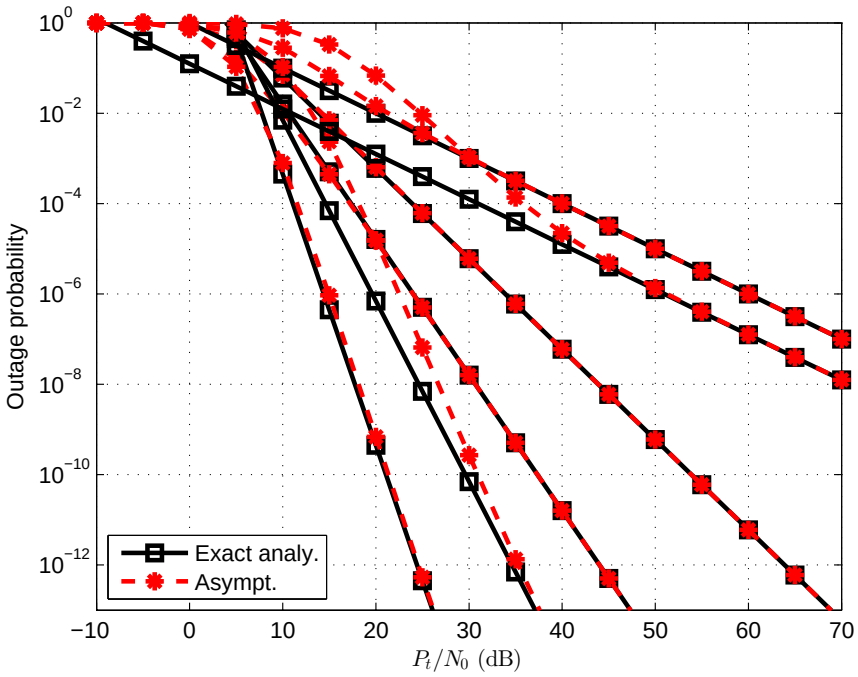


(b) Centralized mapping scheme selection.

Figure 6.6: Average outage probability vs. ratio of transmit power to noise power P_t/N_0 for different schemes.



(a) Decentralized mapping scheme selection



(b) Centralized mapping scheme selection.

Figure 6.7: Exact expressions and asymptotic expressions of outage probability for decentralized and centralized mapping scheme selections.

6.5.2 End-to-End Capacity

By taking the same settings for the simulations of outage probability, we carried out Monte Carlo simulations to study the average end-to-end capacity for different transmission schemes and present the results in Figure 6.8. The numerical results verify our analysis in **Section 6.3.2** and **Section 6.4.2**. Therefore, they can be used as effective tools to estimate the average end-to-end capacity of systems applying adaptive OFDM-IM in two-hop networks. Meanwhile, it is expected that the system using the decentralized mapping scheme selection always outperforms the system using the centralized mapping scheme selection in terms of average end-to-end capacity. For the effects of N_S, the situation becomes complicated and interesting. On the one hand, with a small P_t/N_0, a smaller N_S will lead to a higher average end-to-end capacity, since the power allocated in each subcarrier matters and has a significant impact on the capacity. Therefore, when N_S is small, the average transmit power allocated to each active subcarrier will be large, which yields a positive impact on the end-to-end capacity. On the other hand, when P_t/N_0 is large, because of the logarithmic function (c.f. (6.17)), the power allocated in each subcarrier only has a small impact on the capacity, while the number of terms taken in the summation operation matters. Therefore, as long as P_t/N_0 is sufficiently large, a larger N_S will lead to a higher end-to-end capacity.

Besides, both decentralized and centralized adaptive schemes outperform FPSK in terms of average end-to-end capacity. However, the proposed adaptive schemes do not always outperform the conventional OFDM-IM when P_t/N_0 is large. This indicates that if the end-to-end capacity is regarded as a major system performance metric, our proposed adaptive schemes are particularly useful for cell-edge communications with a relatively small average SNR. The ratio of transmit power to noise power, by which the capacity without adaptation is equal to that with adaptation (i.e., the crossing point) is termed the *threshold power ratio*. We have numerically simulated the relation between threshold power ratio and N_S with different N_T for

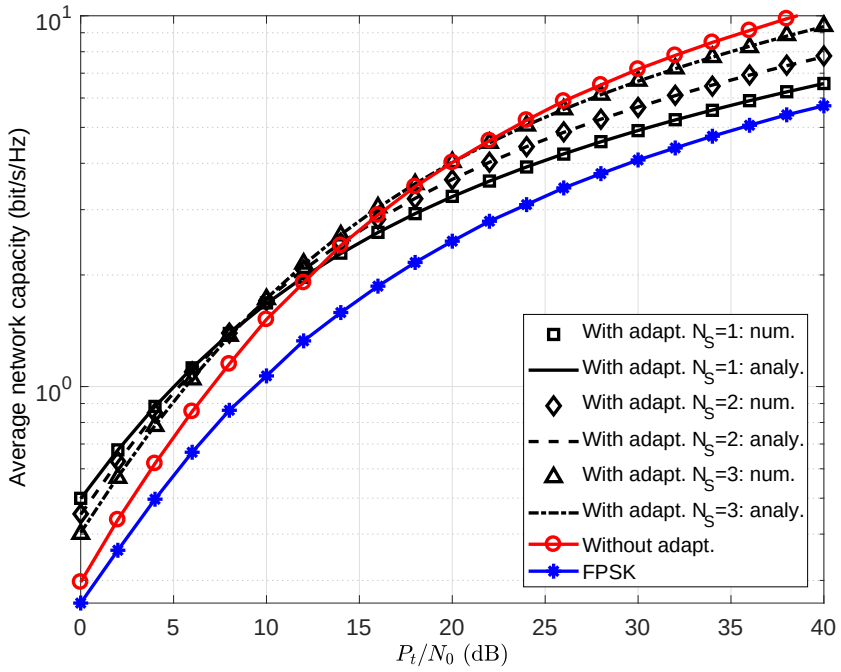
both decentralized and centralized cases and have presented the results in Figure 6.9. From this figure, we can see that the system without adaptation would require a large transmit power in order to have a higher end-to-end capacity than that with adaptation, especially when N_S is large. Therefore, this further confirms the applicability of our proposed adaptive schemes in practice.

6.5.3 Error Performance

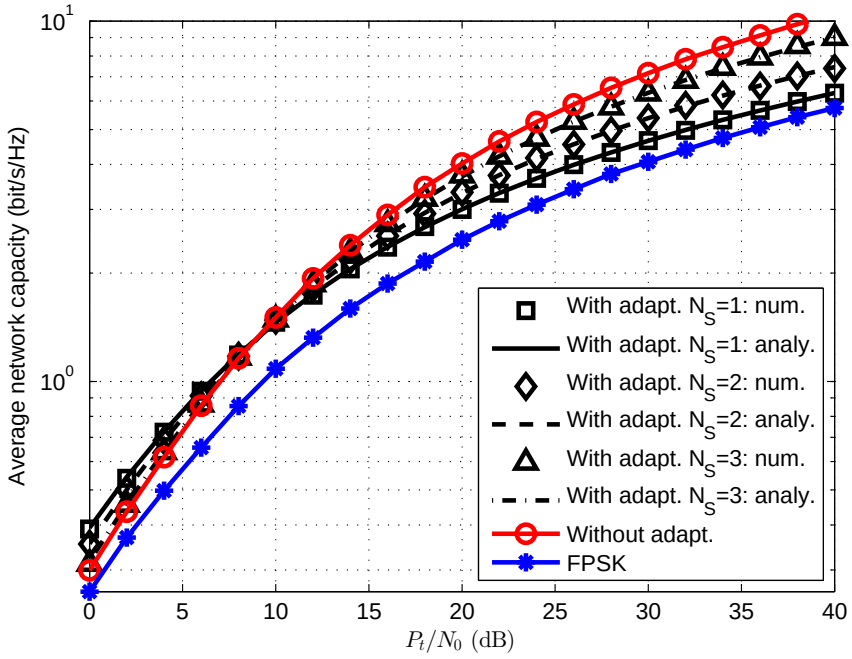
Fixing the total number of subcarrier $N_T = 4$ and the APM order $M = 4$ (i.e., quadrature PSK (QPSK)), we adopted different numbers of selected subcarriers N_S, and numerically simulated the relations between average SER and the ratio of transmit power to noise power P_t/N_0 for both decentralized and centralized mapping scheme selections. The simulation results are plotted in Figure 6.10. From this figure, we can see that the derived approximations based on (6.42) can effectively estimate the SER at high SNR. Also, the diversity orders shown in the simulation results align with our expectation, and are equal to $N_T - N_S$, which is the same as the average outage probabilities. A smaller N_S will lead to a better error performance as expected. Compared with conventional OFDM-IM and FPSK schemes, our proposed schemes always exhibit a better error performance when P_t/N_0 is relatively large, because of their adaptive mechanisms. Also, OFDM-IM with the decentralized mapping scheme selection outperforms OFDM-IM with the centralized mapping scheme selection in terms of error performance, as an extra degree of freedom is obtainable by changing the mapping scheme at the relay in the former case.

6.5.4 Effects of CSI accuracy on Error Performance

Meanwhile, the assumption of perfect CSI would not be realistic, and the imperfect CSI could affect the mapping scheme selection and OFDM-IM symbol estimation processes. Therefore, we also numerically investigate the effects of imperfect CSI in



(a) Decentralized mapping scheme selection.



(b) Centralized mapping scheme selection.

Figure 6.8: Average end-to-end capacity vs. ratio of transmit power to noise power P_t/N_0 for different schemes.

this subsection. To quantify the effects of imperfect CSI, we involve the circularly-symmetric Gaussian random variables with variance δ_S, δ_R and δ_D to mimic the

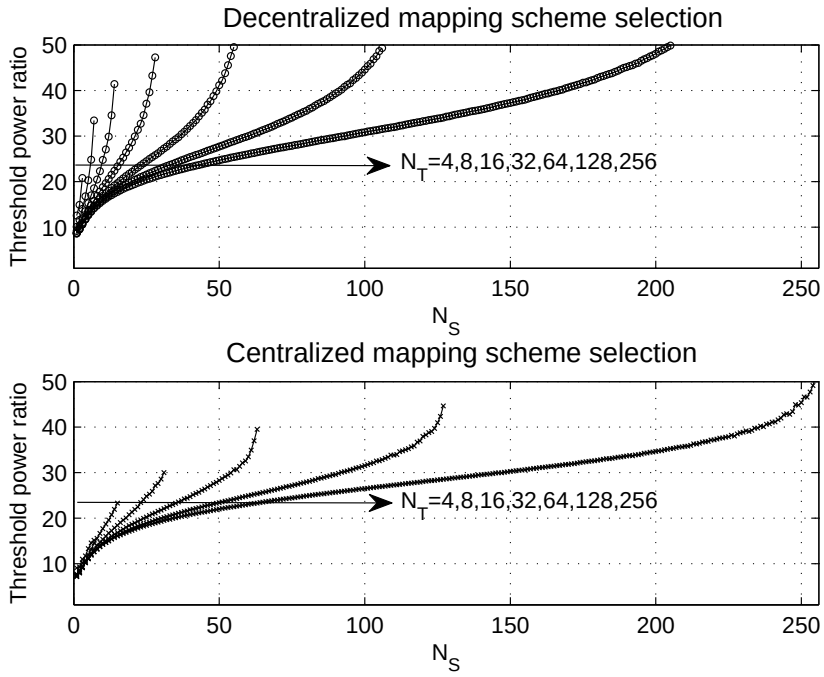
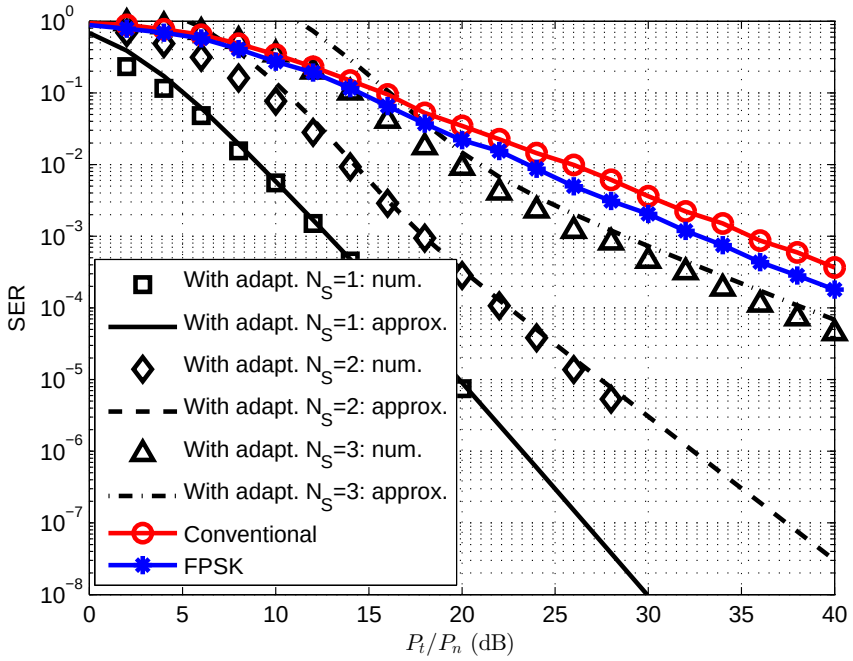
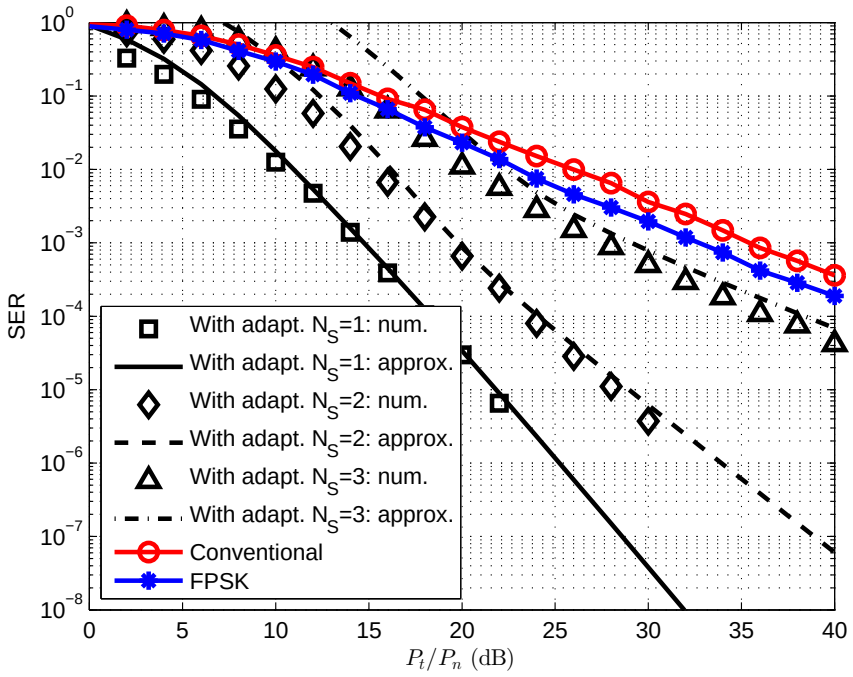


Figure 6.9: Threshold power ratio ratio vs. the number of selected subcarriers N_S with different N_T for decentralized and centralized mapping scheme selections.

estimation errors at the source, relay and destination, respectively. To be specific, we model the channel variable with estimation errors by $h_{i:\mathcal{T}}(n) = h_i(n) + \Delta_{\mathcal{T}}(n)$ where $\Delta_{\mathcal{T}}(n) \sim \mathcal{CN}(0, \delta_{\mathcal{T}})$ and $\mathcal{T} \in \{S, R, D\}$. Because the system applying decentralized mapping scheme selection requires CSI at the relay, and is thereby more generic for exploring the effects of imperfect CSI, we simulate the case of decentralized mapping scheme selection and fix $N_T = 4$, $N_S = 1$ and $M = 4$. The simulation results are shown in Figure 6.11. From these numerical results, we can observe that error floors are inevitable at high SNR for cases utilizing imperfect CSI. Also, the imperfect CSI at the relay will yield a more severe impact on the fidelity, as the CSI is required for both mapping scheme selection and symbol estimation at the relay. Meanwhile, it can also be observed that the impact of imperfect CSI at the destination for symbol estimation is more significant than that at the source for mapping scheme selection. Therefore, the priority order for obtaining accurate CSI is: relay>destination>source, which provides a hint for analyzing and optimizing



(a) Decentralized mapping scheme selection.



(b) Centralized mapping scheme selection.

Figure 6.10: Average SER vs. ratio of transmit power to noise power P_t/N_0 for different schemes.

the proposed system with imperfect CSI.

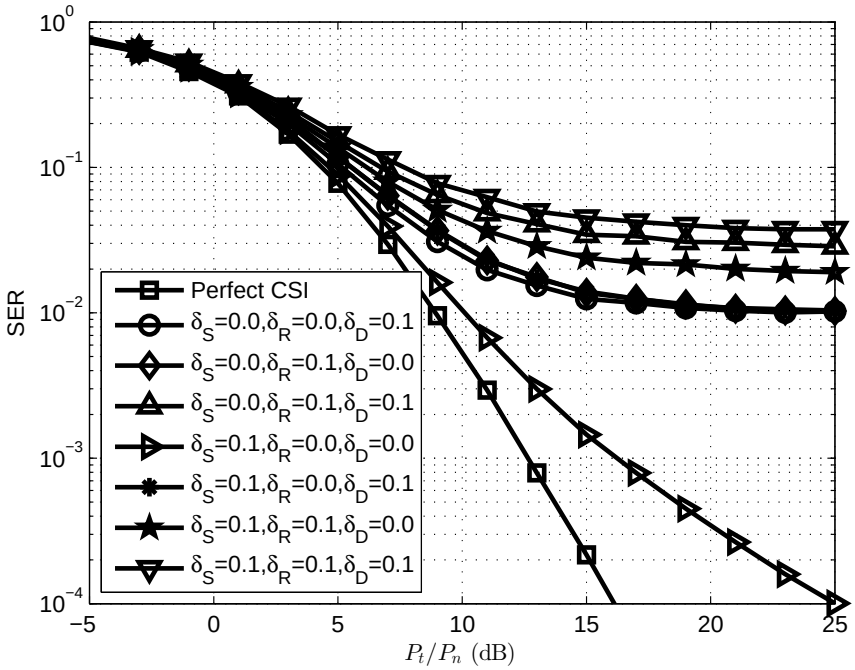


Figure 6.11: Average SER vs. ratio of transmit power to noise power P_t/N_0 with different δ_S, δ_R and δ_D.

6.6 Summary

In this chapter, we proposed an adaptive OFDM-IM scheme for two-hop DF relay networks, which is capable of obtaining diversity gains by adaptively selecting a portion of the total available OFDM subcarriers, instead of using all for OFDM-IM. This provides a possible mechanism allowing reducing throughput for gaining reliability. Considering the complexity and processing capability of relays, we also raised two mapping scheme selection methodologies, which can be applied to different network scenarios. We analyzed a series of important performance metrics of the two-hop relay networks with OFDM-IM, including average outage probability, end-to-end capacity and SER. The average outage probability and end-to-end capacity can be determined in closed form, and the asymptotic expressions of average outage probability at high SNR were also given in closed form, by which the diversity gain is revealed. Meanwhile, the average SER can be approximated by closed-form expressions, and the approximations are accurate at high SNR. The

numerical results substantiated our analysis and also verified the feasibility of the proposed schemes in practice compared to conventional OFDM-IM without adaptation as well as FPSK. From the analytical and numerical results provided in this chapter, a comprehensive framework for analyzing adaptive OFDM-IM in relay networks has been constructed, which can be modified to analyze other extended cases with more complicated channel models and transmission protocols.

On the other hand, through the simulations regarding imperfect CSI, it is worth pointing out that the superior performance of the adaptive OFDM-IM proposed in this chapter relies on the acquisition of accurate CSI, which is used for mapping scheme selection and symbol estimation. Consequently, the practicality of the adaptive OFDM-IM in a fast fading environment would be weakened, since the instantaneous CSI would be difficult to obtain or a high signaling overhead will be caused.

6.7 Appendices

6.7.1 Proof of Lemma 6

When $\mathbf{b}_S(k)$ is transmitted, we need to activate $N_A(k)$ subcarriers from N_S selected subcarriers. Suppose that the worst subcarrier among these $N_A(k)$ active subcarriers in terms of channel gain is the ξth worst in the total ordered N_T subcarriers. Because of the mapping scheme selection, it is easy to derive the relation $N_T - N_S + 1 \leq \xi \leq N_T - N_A(k) + 1$. As a result, by (6.26), the outage probability when the worst subcarrier among these $N_A(k)$ active subcarriers is the ξth worst in the total ordered N_T subcarriers can be written as $F_{i(\xi)}\left(\frac{sN_0N_A(k)}{P_t}\right)$.

The total number of combinations of $N_A(k)$ active subcarriers is $\binom{N_S}{N_A(k)}$, and the number of possible combinations, in which the worst subcarrier among these $N_A(k)$ active subcarriers is the ξth worst is $\binom{N_T-\xi}{N_A(k)-1}$. Consequently, the probability that the worst subcarrier among these $N_A(k)$ active subcarriers is the ξth worst can be

determined by

$$\Upsilon(k,\xi) = \binom{N_T - \xi}{N_A(k) - 1} \Big/ \binom{N_S}{N_A(k)} \tag{6.59}$$

Finally, when $\mathbf{b}_S(k)$ is transmitted, the weighted average of the conditional outage probability over ξ gives (6.28).

6.7.2 Proof of Lemma 7

Because $\boldsymbol{\Xi}_1$ and $\boldsymbol{\Xi}_2$ are independently, discretely and uniformly distributed over domain $\mathcal{D}(k)$, the joint probability mass function (PMF) with respect to $\boldsymbol{\Xi}_1$ and $\boldsymbol{\Xi}_2$, i.e., the probability that the ith element in $\mathcal{D}(k)$ is chosen for $\boldsymbol{\Xi}_1$ and the jth element in $\mathcal{D}(k)$ is chosen for $\boldsymbol{\Xi}_2$ is thereby

$$p(i,j) = \left(\frac{1}{\mathrm{Card}(\mathcal{D}(k))}\right)^2 = \left(\frac{(N_S - N_A(k))!}{N_S!}\right)^2, \ \forall\ i,j, \tag{6.60}$$

in which the corresponding end-to-end capacity can be written as

$$\bar{C}(k|i,j) = \sum_{n \in \mathcal{N}_A(k)} \Lambda_G\left(\xi_n, \eta_m, \frac{N_0 N_A(k)}{P_t}\right). \tag{6.61}$$

Hence, the weighted average of $\bar{C}(k|i,j)$ over $\boldsymbol{\Xi}_1$ and $\boldsymbol{\Xi}_2$ is

$$\bar{C}(k) = \sum_{\boldsymbol{\Xi}_1(k) \in \mathcal{D}(k)} \sum_{\boldsymbol{\Xi}_2(k) \in \mathcal{D}(k)} p(i,j)\bar{C}(k|i,j), \tag{6.62}$$

which yields (6.39).

Chapter 7

Conclusions

7.1 Thesis Summary

In this thesis, we have introduced the fundamentals of OFDM-based relay systems and analyzed four novel OFDM-based relay systems in detail. These four examples cover a wide range of application scenarios in next generation networks with different performance requirements. By the insightful analyses and findings provided in this thesis, a full picture and the outlook on the OFDM-based relay technology can be illustrated, and key properties of the associated systems were revealed.

To be specific, we briefly discussed the status quo of current wireless communication networks and introduced the motivations for OFDM-based relay systems in **Chapter 1**. Then, we provided a research overview in **Chapter 2**, covering the fundamentals of relay technology, OFDM and relevant research topics. The first technical chapter for OFDM-based relay systems with bulk and per-subcarrier selections in spatially random networks refers to **Chapter 3**, in which PPP is employed to model the randomness of relays. The second main technical contribution was presented in **Chapter 4**, in which a satisfactory solution to the performance-complexity trade-off in multi-carrier relay selection was provided and proven to be optimal in the high SNR region. Furthermore, the spatial correlation among

channels was also considered in this chapter in order to provide a more realistic analysis. Subsequently, we analyzed multi-carrier relay selections for full-duplex relay-assisted OFDM D2D systems in **Chapter 5**, which refer to more complicated application scenarios in next generation networks. Finally, in **Chapter 6**, in order to have a comprehensive understanding of OFDM-based relay systems and integrate state-of-the-art modulation schemes, we proposed the adaptive OFDM-IM for relay networks, by which we can provide reliability enhancement when there is only one relay and relay selection is thereby impossible. All the analyses given in this thesis constitute a comprehensive analytical framework for OFDM-based relay systems in next generation networks.

7.2 Outlook on OFDM-Based Relay Technology

From the theoretical analyses presented in this thesis, we develop a general outlook on OFDM-based relay technology and its place in future communication networks. First, due to the high power and spectrum efficiency brought by OFDM-based relay systems, their implementations in 5G networks are inexorable. In particular, the high spectrum efficiency of OFDM due to the overlap of subcarriers is capable of mitigating the scarcity of spectrum resource, which is one of the main issues restricting the improvement of communication service. Also, by cooperative communications via relays, the performance of the entire communication network can be improved without consuming too much transmit power. This advantage is crucial for WSNs, in which nodes are non-rechargeable. Moreover, the bright future and development trend of OFDM-based relay technology are guaranteed by its mature standards, which have been in use in many scenarios. OFDM has been included in the IEEE 802.11a standard and utilized in wireless local area networks (WLANs), as well as one of the core technologies in the Third Generation Partnership Project (3GPP) and LTE systems. OFDM is thereby the best option for the transmission

technique for 5G networks [79]. Albeit a latecomer, relay technology has been standardized in IEEE 802.16j and in IEEE 802.16m as a solution for extending network coverage and enhancing capacity. Therefore, we are confident that OFDM-based relay technology will continue to play a key role in future communication networks for the next decade.

Also, let us go beyond wireless cellular communications, we can also find that OFDM-based relay systems suit applications of IoT well. As we previously mentioned, a relay is more of a functional concept than a special kind of device, which allows relays to be defined in a very broad way. Therefore, for applications of IoT, a large number of nodes, which are able to transmit and receive would form a mesh relay network, and each node can be regarded as a relay communicating on different parallel subchannels. In this regard, the OFDM-based relay technology designed for wireless cellular communications can be easily transplanted to applications of IoT to enhance their performance. Considering the secrecy and security of applications of IoT, AF relaying could be helpful, as decoding of the original message is not required.

7.3 Future Work

From the research of OFDM-based relay systems in this thesis, we also find a number of potential research directions, which can be used as a fingerpost for advanced research activities. Their details are presented in the following subsections.

7.3.1 Incentives for OFDM-Based Cooperative Communications

Incentive mechanisms are the key to implement OFDM-based relay systems, especially in the commercialized stage [152]. In theoretical analyses, of course, researchers can simply assume 'there are M AF/DF relays' without considering where

these quixotic relays come from and why they are so kind to share their limited resources to assist others' transmissions. Although such a resource sharing mechanism will benefit the holistic network in the long term, telecommunication operators and service subscribers might focus on short-term interest and thereby refuse to provide their communication devices as relays. To promote the implementation of OFDM-based relay systems, currently, three incentive mechanisms exist: 1) energy harvesting-based incentive, 2) spectrum resource-based incentive and 3) monetary incentive. Admittedly, incentives for cooperative communications have been analyzed in some specific scenarios, e.g., OFDM-based cooperative cognitive radio (CR) networks [153] and large-scale commercial access networks [152], but a comprehensive analysis of incentives for OFDM-based relay systems is still lacking. Moreover, the incentive policy combining the above three kinds of incentives shall be interesting, and explorations of new incentives are still underway. Some economic and marketing analytical tools, e.g., auction-theoretic strategies [154] and PESTEL analysis[1] [155], would be helpful for designing incentives in OFDM-based relay systems.

7.3.2 Novel Multi-Carrier Relay Selection Criterion Design

Although there have existed a huge number of multi-carrier relay selection schemes suited for many different applications, it is believed that the realm of multi-carrier relay selection has not been fully exploited. Therefore, further performance enhancement brought by multi-carrier relay selection criterion design is still possible. For example, currently most multi-carrier relay selection criteria treat SNR/SIR/SINR on each individual subcarrier as a selection metric, which assume all subcarriers are mutually independent. However, this might not be true in practice, and a more practical selection metric e.g., the sum of mutual information over all subcarri-

[1]The terminology 'PESTEL' in marketing and business represents six key factors completely describing the external business environment: political, economic, sociological, technological, environmental, and legal.

ers would be taken as the selection metric instead [156]. Meanwhile, the novel selection metric should also consider the power budget as well as the processing capability constraint of different relays, instead of assuming they are homogeneous. Meanwhile, extensions of multi-carrier relay selection criteria to multi-hop cooperative networks are still challenging, especially for AF relaying [114]. This challenge is results from the mathematical intractability of the statistics of end-to-end SNR/SIR/SINR in multi-hop AF relay networks. To provide an insight into multi-hop AF relay networks, some approximation and asymptotic techniques might be worth exploring.

Also, for almost all works dedicated to relay selections, there is a widely applied assumption: transmission is not possible among relays. To further enhance the network reliability, it might be worth considering the transmission among relays, which might bring another degree of freedom. On the other hand, this variable-hop transmission scenario could bring extra difficulties to higher layer protocol designs and implementations. These are still unknown and the hop-relay joint selection problem could be of interest, especially for super dense networks.

In addition, for multi-user multi-carrier relay selections, most works treat the selection problems as special cases of resource allocations, and optimization techniques dominate the league table to deal with multi-carrier relay selection in multi-user scenarios. It cannot be denied that these optimization techniques are powerful for assigning relays and subcarriers to multiple users, but no analytical result can be provided by this way. To provide an insight into multi-user multi-carrier relay selections, novel selection criteria and mathematical tools, e.g., game-theoretical approaches are worth investigating.

7.3.3 OFDM-Based Relay Systems in Spatially Random Networks

In **Chapter 3**, multi-carrier relay selections are analyzed in spatially random networks where relay nodes are homogeneously Poisson distributed over a two-dimensional region. It can be found in this chapter that even though the analysis is fundamental, there are only closed-form analytical results for some special cases. To fill this gap between the OFDM-based relay technology and spatially random networks, more contributions would be required. First, more advanced mathematical tools for analyzing the spatially random networks should be explored so that some key quantitative relations between performance and network parameters, e.g., path loss, node density, distribution region, shape and boundary can be well explained. Second, instead of homogeneous PPP, more node distribution models (e.g., binomial point process (BPP) and Poisson cluster process (PCP) etc.) suited for different application scenarios should also be applied to model the geographical distribution of relay nodes. Third, irregular node distribution regions and boundary effects should be considered in order to fit the theoretical analysis to realistic situations [157, 158]. Last but not least, considering the satellite and underwater acoustic communications, the distribution space might not be restricted to a two-dimensional plane, and thereby a generalized analysis with arbitrary higher dimensions for OFDM-based relay systems over spatially random networks would be interesting.

7.3.4 Relay-Assisted OFDM with Index Modulation

In **Chapter 6**, the OFDM-IM is combined with relay systems. By applying an adaptive mapping scheme selection in the proposed system, a diversity gain can be obtained. However, as preliminary research, the analyses given in this chapter are relatively simple, and only a classic three-node cooperative network paradigm is considered. Therefore, more attention could be paid to the analysis of more

complicated scenarios, e.g., with an arbitrary number of relays between source and destination. Meanwhile, the application of relay-assisted OFDM-IM in multi-hop scenarios would also be interesting, as this could be a potential approach to alleviate the bottleneck effect in multi-hop DF cooperative networks. Furthermore, the analysis and comparison between AF and DF forwarding protocols for OFDM-IM are also required in order to provide a full picture of this new technology. Most importantly, the design of space-frequency activation patterns consisting of the activation states of both relay and subcarrier would be the key to greatly improve the spectrum efficiency of relay-assisted OFDM-IM, which is still an open question.

7.3.5 OFDM-Based Relay Systems with Energy Harvesting

Wireless power transfer has been regarded as one of most powerful approaches to extend the lifetime of WSNs, in which sensor nodes are normally non-rechargeable. To facilitate wireless power transfer in future communication networks, the energy harvesting incorporating cooperative relaying shows its potential [159]. Due to the popularity of OFDM-based relay systems, the energy harvesting technology has also been extended to help OFDM-based relay nodes, which results in the simultaneous wireless information and power transfer (SWIPT) protocol [153]. A comprehensive protocol design and optimization of energy harvesting in OFDM-based relay systems are presented in [160], where a power-splitting relaying scheme is proposed to enable power transfer from the source to relay [161]. On the other hand, relays can also transfer power to 'rootless' sources when relays are fixed and supported by stable power sources. Such a scenario of OFDM-based relay systems is analyzed in [162]. On the other hand, the system models adopted in aforementioned papers are relatively simple, and the potential of energy harvesting in OFDM-based relay systems has not been fully exploited. Meanwhile, all subcarriers are homogenized in these works. However, in practice subcarriers have different properties as well as data/power transfer efficiencies depending on their frequency bands. That

is, some subcarriers might be suitable for data transfer and the other subcarriers are good for power transfer, which should be considered when designing a realistic SWIPT-OFDM protocol. In addition, energy harvesting can also provide an incentive mechanism to encourage cooperative transmissions, which has not been properly addressed in the current literature.

7.3.6 NOMA-OFDM Relay Systems

Non-orthogonal multiple access (NOMA) is one of the latest research topics for 5G networks, which greatly enhances multi-user transmissions by applying successive interference cancellation (SIC). Meanwhile, it has been shown that in non-cooperative networks, applying OFDM can further enhance the performance by facilitating SIC via co-channel user selection [163–165]. Due to the merits of cooperative communications, it is worth extending NOMA-OFDM transmission to cooperative scenarios. Meanwhile, by involving multiple relays in the resource allocation process for NOMA-OFDM systems, an extra degree of freedom is obtainable, so that the overall system performance could be further improved. Besides, the subcarrier permutation mechanism can also be applied at relays to exploit the frequency diversity gain and enhance the reliability of NOMA-OFDM systems. All these issues regarding NOMA-OFDM relay systems are believed to be powerful for enabling 5G communications containing a huge number of users, and are awaiting investigations.

7.3.7 Relay Systems Using New Waveforms

Some state-of-the-art waveforms might hold the potential to yield better performance than OFDM, which could be introduced to relay systems and cooperative communications. For example, the filter-bank based multi-carrier (FBMC) applies a filter to each subcarrier to diminish sidelobes and is able to have a smaller ICI than OFDM. As a result, the insertions of CP and guard interval would be omitted.

Moreover, because by FBMC, strictly orthogonal relations among subcarriers (c.f. (2.4)) are not necessary anymore, a flexible bandwidth control for each subcarrier is possible [166]. Some primary performance comparisons between FBMC and OFDM in relay networks are presented in [167–170], by which performance advantages of FBMC over OFDM can be illustrated. FBMC-based DF and AF relay systems are analyzed in [171] and [172], respectively. However, all these analyses are fundamental and more realistic scenarios should be considered. Besides, to mitigate the destructive effect of the Doppler shift caused by high-speed nodes and reduce the PAPR in OFDM, generalized frequency-division multiplexing (GFDM) could be another potential candidate for future communication systems, which uses circular filtering for pulse shaping [166]. However, so far, there is still no work on analyzing GFDM-based relay systems, and the alliance of these two promising technologies would be worth investigating.

References

[1] A. Gupta and R. K. Jha, "A survey of 5G network: architecture and emerging technologies," *IEEE Access*, vol. 3, pp. 1206–1232, 2015.

[2] J. G. Andrews, S. Buzzi, W. Choi, S. V. Hanly, A. Lozano, A. C. K. Soong, and J. C. Zhang, "What will 5G be?," *IEEE Journal on Selected Areas in Communications*, vol. 32, pp. 1065–1082, Jun. 2014.

[3] Z.-m. Jiang, "Development of IT industry in China in the new age," *Journal of Shanghai Jiaotong University (Science)*, vol. 14, no. 1, pp. 1–24, 2009.

[4] J. S.-B. Orange, A. G. Armada, B. Evans, A. Galis, and H. Karl, "White paper for research beyond 5G," *Accessed*, vol. 23, p. 2016, 2015.

[5] Ofcom-UK, "Communications market report," *UK Mobile Phone Usage Statistics, London, UK*, 2016.

[6] I. Cisco, "Cisco visual networking index: forecast and methodology, 2016–2021," *CISCO White paper*, 2017.

[7] Z. Lv, T. Yin, Y. Han, Y. Chen, G. Chen, *et al.*, "Webvrweb virtual reality engine based on P2P network," *Journal of Networks*, vol. 6, no. 7, pp. 990–998, 2011.

[8] A. Osseiran and et al, "Scenarios for 5G mobile and wireless communications: the vision of the METIS project," *IEEE Communications Magazine*, vol. 52, pp. 26–35, May 2014.

[9] V. Stankovic, A. Host-Madsen, and Z. Xiong, "Cooperative diversity for wireless ad hoc networks," *IEEE Signal Processing Magazine*, vol. 23, pp. 37–49, Sept. 2006.

[10] S. Ma, Y. Yang, and H. Sharif, "Distributed MIMO technologies in cooperative wireless networks," *IEEE Communications Magazine*, vol. 49, pp. 78–82, May 2011.

[11] W. C. Chung, N. J. August, and D. S. Ha, "Signaling and multiple access techniques for ultra wideband 4G wireless communication systems," *IEEE Wireless Communications*, vol. 12, pp. 46–55, Apr. 2005.

[12] S. Dang, J. P. Coon, and G. Chen, "Outage performance of two-hop ofdm systems with spatially random decode-and-forward relays," *IEEE Access*, vol. 5, pp. 27514–27524, Nov. 2017.

[13] S. Dang, J. P. Coon, G. Chen, and D. E. Simmons, "Outage performance analysis of multicarrier relay selection for cooperative networks," in *Proc. IEEE ISCC*, (Heraklion, Greece), Jul. 2017.

[14] S. Dang, J. P. Coon, and G. Chen, "An equivalence principle for OFDM-based combined bulk/per-subcarrier relay selection over equally spatially correlated channels," *IEEE Transactions on Vehicular Technology*, vol. 66, pp. 122–133, Jan. 2017.

[15] S. Dang, J. P. Coon, and D. E. Simmons, "Combined bulk/per-subcarrier relay selection in two-hop OFDM systems," in *Proc. IEEE VTC Spring*, (Nanjing, China), May 2016.

[16] S. Dang, D. E. Simmons, and J. P. Coon, "Comparison of multicarrier relay selection schemes in super dense networks," in *Proc. IEEE CAMAD*, (Guildford, UK), Sept. 2015.

[17] S. Dang, J. P. Coon, and D. E. Simmons, "Combined bulk and per-tone relay selection in super dense wireless networks," in *Proc. IEEE ICC*, (London, UK), Jun. 2015.

[18] S. Dang, G. Chen, and J. P. Coon, "Outage performance analysis of full-duplex relay-assisted device-to-device systems in uplink cellular networks," *IEEE Transactions on Vehicular Technology*, vol. 66, pp. 4506–4510, May 2017.

[19] S. Dang, J. P. Coon, and G. Chen, "Resource allocation for full-duplex relay-assisted device-to-device multicarrier systems," *IEEE Wireless Communications Letters*, vol. 6, pp. 166–169, Apr. 2017.

[20] S. Dang, G. Chen, and J. P. Coon, "Multicarrier relay selection for full-duplex relay-assisted OFDM D2D systems," *arXiv preprint arXiv:1708.03295*, 2017.

[21] S. Dang, G. Chen, and J. P. Coon, "Outage performance of two-hop OFDM with index modulation and multi-carrier relay selection," *IEEE Wireless Communications Letters*, 2017 (under review).

[22] S. Dang, J. Coon, and G. Chen, "Adaptive OFDM with index modulation for two-hop relay-assisted networks," *IEEE Transactions on Wireless Communications*, 2017.

[23] S. Dang, G. Chen, and J. P. Coon, "Power allocation for adaptive OFDM index modulation in cooperative networks," in *Proc. IEEE GLOBECOM*, (Singapore), Dec. 2017.

[24] E. C. Van Der Meulen, "Three-terminal communication channels," *Advances in Applied Probability*, vol. 3, no. 1, pp. 120–154, 1971.

[25] A. Chandra, C. Bose, and M. K. Bose, "Wireless relays for next generation broadband networks," *IEEE Potentials*, vol. 30, pp. 39–43, Mar. 2011.

[26] M. Dohler and Y. Li, *Cooperative Communications: Hardware, Channel and PHY*. Wiley, 2010.

[27] P. Murphy and A. Sabharwal, "Design, implementation, and characterization of a cooperative communications system," *IEEE Transactions on Vehicular Technology*, vol. 60, pp. 2534–2544, Jul. 2011.

[28] J. N. Laneman, D. N. C. Tse, and G. W. Wornell, "Cooperative diversity in wireless networks: efficient protocols and outage behavior," *IEEE Transactions on Information Theory*, vol. 50, pp. 3062–3080, Dec. 2004.

[29] B. M. C. Silva, J. J. P. C. Rodrigues, N. Kumar, and G. Han, "Cooperative strategies for challenged networks and applications: a survey," *IEEE Systems Journal*, 2017.

[30] M. Pejanovic-Djurisic, E. Kocan, and R. Prasad, *OFDM based relay systems for future wireless communications*. River Publishers, 2012.

[31] A. Neskovic, N. Neskovic, and G. Paunovic, "Modern approaches in modeling of mobile radio systems propagation environment," *IEEE Communications Surveys Tutorials*, vol. 3, pp. 2–12, Third 2000.

[32] B. Timus, "Cost analysis issues in a wireless multihop architecture with fixed relays," in *Proc. IEEE VTC*, (Stockholm, Sweden), May 2005.

[33] A. Nosratinia, T. E. Hunter, and A. Hedayat, "Cooperative communication in wireless networks," *IEEE Communications Magazine*, vol. 42, pp. 74–80, Oct. 2004.

[34] M. Salem, A. Adinoyi, M. Rahman, H. Yanikomeroglu, D. Falconer, Y. D. Kim, E. Kim, and Y. C. Cheong, "An overview of radio resource management in relay-enhanced OFDMA-based networks," *IEEE Communications Surveys Tutorials*, vol. 12, pp. 422–438, Third 2010.

[35] N. Esseling, B. H. Walke, and R. Pabst, "Performance evaluation of a fixed relay concept for next generation wireless systems," in *Proc. IEEE PIMRC*, vol. 2, (Barcelona, Spain), Sept. 2004.

[36] G. Li and H. Liu, "On the capacity of broadband relay networks," in *Proc. IEEE ACSSC*, vol. 2, (Pacific Grove, CA, USA), Nov. 2004.

[37] K. Doppler and A. Hottinen, "Integration of amplify and forward relays in an OFDM network," in *Proc. IEEE ACSSC*, (Pacific Grove, CA, USA), Oct. 2005.

[38] G. Li and H. Liu, "Resource allocation for OFDMA relay networks," in *Proc. IEEE ACSSC*, vol. 1, (Pacific Grove, CA, USA), Nov. 2004.

[39] G. Li and H. Liu, "Resource allocation for OFDMA relay networks with fairness constraints," *IEEE Journal on Selected Areas in Communications*, vol. 24, pp. 2061–2069, Nov. 2006.

[40] W. Ying, Q. Xin-chun, W. Tong, and L. Bao-ling, "Power allocation and subcarrier pairing algorithm for regenerative OFDM relay system," in *Proc. IEEE VTC Spring*, (Dublin, Ireland), Apr. 2007.

[41] C. K. Ho, R. Zhang, and Y. C. Liang, "Two-way relaying over OFDM: optimized tone permutation and power allocation," in *Proc. IEEE ICC*, (Beijing, China), May 2008.

[42] D. Chen and J. N. Laneman, "Joint power and bandwidth allocation in multihop wireless networks," in *Proc. IEEE WCNC*, (Las Vegas, NV, USA), Mar. 2008.

[43] C. R. N. Athaudage, M. Saito, and J. Evans, "Performance analysis of dual-hop OFDM relay systems with subcarrier mapping," in *Proc. IEEE ICC*, (Beijing, China), May 2008.

[44] E. Kocan, M. Pejanovic-Djurisic, D. S. Michalopoulosy, and G. K. Karagiannidisy, "BER performance of OFDM amplify-and-forward relaying system with subcarrier permutation," in *Proc. IEEE Wireless VITAE*, (Aalborg, Denmark), May 2009.

[45] H. A. Suraweera and J. Armstrong, "Performance of OFDM-based dual-hop amplify-and-forward relaying," *IEEE Communications Letters*, vol. 11, pp. 726–728, Sept. 2007.

[46] V. K. Y. Wu, Y. G. Li, M. Green, T. Reid, and P. Wang, "Error rate performance in OFDM-based cooperative networks," in *Proc. IEEE GLOBECOM*, (Washington, DC, USA), Nov. 2007.

[47] B. Can, M. Portalski, H. S. D. Lebreton, S. Frattasi, and H. A. Suraweera, "Implementation issues for OFDM-based multihop cellular networks," *IEEE Communications Magazine*, vol. 45, pp. 74–81, Sept. 2007.

[48] K. S. Woo and et al, "Synchronization and channel estimation for OFDM systems with transparent multi-hop relays," in *Proc. IEEE VTC Spring*, (Dublin, Ireland), Apr. 2007.

[49] H. Mheidat, M. Uysal, and N. Al-Dhahir, "Equalization techniques for distributed space-time block codes with amplify-and-forward relaying," *IEEE Transactions on Signal Processing*, vol. 55, pp. 1839–1852, May 2007.

[50] B. Can, H. Yomo, and E. D. Carvalho, "Hybrid forwarding scheme for cooperative relaying in OFDM based networks," in *Proc. IEEE ICC*, vol. 10, (Istanbul, Turkey), Jun. 2006.

[51] Y. Yan, C. Gan, C. Zuo, S. Wu, and S. Dang, "Analysis of uniform and optimal power allocation strategies for decode-and-forward relay considering direct transmit link," in *Proc. IEEE ICEIT*, (Marrakech, Morocco), Mar. 2015.

[52] R. Zhang, L. Wang, and et al, "Advances in base- and mobile-station aided cooperative wireless communications: an overview," *IEEE Vehicular Technology Magazine*, vol. 8, pp. 57–69, Mar. 2013.

[53] F. Mansourkiaie and M. H. Ahmed, "Cooperative routing in wireless networks: a comprehensive survey," *IEEE Communications Surveys Tutorials*, vol. 17, pp. 604–626, Secondquarter 2015.

[54] F. Gomez-Cuba, R. Asorey-Cacheda, and F. J. Gonzalez-Castano, "A survey on cooperative diversity for wireless networks," *IEEE Communications Surveys Tutorials*, vol. 14, pp. 822–835, Third 2012.

[55] D. Soldani and S. Dixit, "Wireless relays for broadband access [radio communications series]," *IEEE Communications Magazine*, vol. 46, pp. 58–66, Mar. 2008.

[56] P. Guo, Y. Bai, Z. Ma, S. Wu, and S. Dang, "Relay technology for multicarrier systems: a research overview," in *Proc. IEEE C3IT*, (Hooghly, India), Feb. 2015.

[57] X. Tao, X. Xu, and Q. Cui, "An overview of cooperative communications," *IEEE Communications Magazine*, vol. 50, pp. 65–71, Jun. 2012.

[58] M. Xia and S. Aissa, "Underlay cooperative af relaying in cellular networks: performance and challenges," *IEEE Communications Magazine*, vol. 51, pp. 170–176, Dec. 2013.

[59] C. Hoymann, W. Chen, J. Montojo, A. Golitschek, C. Koutsimanis, and X. Shen, "Relaying operation in 3GPP LTE: challenges and solutions," *IEEE Communications Magazine*, vol. 50, pp. 156–162, Feb. 2012.

[60] Y. Li, "Distributed coding for cooperative wireless networks: an overview and recent advances," *IEEE Communications Magazine*, vol. 47, pp. 71–77, Aug. 2009.

[61] T. Riihonen, S. Werner, and R. Wichman, "Comparison of full-duplex and half-duplex modes with a fixed amplify-and-forward relay," in *Proc. IEEE WCNC*, (Budapest, Hungary), Apr. 2009.

[62] T. K. Baranwal, D. S. Michalopoulos, and R. Schober, "Outage analysis of multihop full duplex relaying," *IEEE Communications Letters*, vol. 17, pp. 63–66, Jan. 2013.

[63] Z. Zhang, X. Chai, K. Long, A. V. Vasilakos, and L. Hanzo, "Full duplex techniques for 5G networks: self-interference cancellation, protocol design, and relay selection," *IEEE Communications Magazine*, vol. 53, pp. 128–137, May 2015.

[64] A. Sabharwal, P. Schniter, D. Guo, D. W. Bliss, S. Rangarajan, and R. Wichman, "In-band full-duplex wireless: challenges and opportunities," *IEEE Journal on Selected Areas in Communications*, vol. 32, pp. 1637–1652, Sept. 2014.

[65] L. Li, H. V. Poor, and L. Hanzo, "Non-coherent successive relaying and cooperation: principles, designs, and applications," *IEEE Communications Surveys Tutorials*, vol. 17, pp. 1708–1737, thirdquarter 2015.

[66] G. Liu, F. R. Yu, H. Ji, V. C. M. Leung, and X. Li, "In-band full-duplex relaying: a survey, research issues and challenges," *IEEE Communications Surveys Tutorials*, vol. 17, pp. 500–524, Secondquarter 2015.

[67] K. Liu, A. Sadek, W. Su, and A.Kwasinski, *Cooperative Communications and Networking*. Cambridge University Press, 2009.

[68] D. E. Simmons and J. P. Coon, "Two-way OFDM-based nonlinear amplify-and-forward relay systems," *IEEE Transactions on Vehicular Technology*, vol. 65, pp. 3808–3812, May 2016.

[69] Q. Zhang, F. Shu, M. Wang, and J. Sun, "Relay selection schemes for precoded cooperative OFDM and their achievable diversity orders," *IEEE Signal Processing Letters*, vol. 18, pp. 231–234, Apr. 2011.

[70] W. Zhang, Y. Li, X. g. Xia, P. C. Ching, and K. B. Letaief, "Distributed space-frequency coding for cooperative diversity in broadband wireless ad hoc networks," *IEEE Transactions on Wireless Communications*, vol. 7, pp. 995–1003, Mar. 2008.

[71] J. Proakis and M. Salehi, *Digital Communications*. McGraw-Hill, 2008.

[72] J. Y. Chang and Y. W. Chen, "A cluster-based relay station deployment scheme for multi-hop relay networks," *Journal of Communications and Networks*, vol. 17, pp. 84–92, Feb. 2015.

[73] G. Berardinelli, L. A. M. R. de Temino, S. Frattasi, M. I. Rahman, and P. Mogensen, "OFDMA vs. SC-FDMA: performance comparison in local area IMT-A scenarios," *IEEE Wireless Communications*, vol. 15, pp. 64–72, Oct. 2008.

[74] S. W. Peters and R. W. H. Jr., "The future of WiMAX: multihop relaying with IEEE 802.16j," *IEEE Communications Magazine*, vol. 47, pp. 104–111, January 2009.

[75] R. Pabst and et al, "Relay-based deployment concepts for wireless and mobile broadband radio," *IEEE Communications Magazine*, vol. 42, pp. 80–89, Sept. 2004.

[76] F. Drake, "Mobile phone masts: protesting the scientific evidence," *Public understanding of science*, vol. 15, no. 4, pp. 387–410, 2006.

[77] Y. W. Hong, W. J. Huang, F. H. Chiu, and C. C. J. Kuo, "Cooperative communications in resource-constrained wireless networks," *IEEE Signal Processing Magazine*, vol. 24, pp. 47–57, May 2007.

[78] M. Peng, C. Yang, Z. Zhao, W. Wang, and H. H. Chen, "Cooperative network coding in relay-based IMT-advanced systems," *IEEE Communications Magazine*, vol. 50, pp. 76–84, Apr. 2012.

[79] I. k. Fu, Y. s. Chen, P. Cheng, Y. Yuk, R. Y. Kim, and J. S. Kwak, "Multicarrier technology for 4G WiMAX system [WiMAX/LTE update]," *IEEE Communications Magazine*, vol. 48, pp. 50–58, Aug. 2010.

[80] S. Berger, M. Kuhn, A. Wittneben, T. Unger, and A. Klein, "Recent advances in amplify-and-forward two-hop relaying," *IEEE Communications Magazine*, vol. 47, pp. 50–56, Jul. 2009.

[81] T. Hwang, C. Yang, G. Wu, S. Li, and G. Y. Li, "OFDM and its wireless applications: a survey," *IEEE Transactions on Vehicular Technology*, vol. 58, pp. 1673–1694, May 2009.

[82] C. Alexandre and R. Fernandes, "Outage performance of cooperative amplify-and-forward OFDM systems with nonlinear power amplifiers," in *Proc. IEEE SPAWC*, (Cesme, Turkey), Jun. 2012.

[83] H. Mu, M. Tao, W. Dang, and Y. Xiao, "Joint subcarrier-relay assignment and power allocation for decode-and-forward multi-relay OFDM systems," in *Proc. IEEE ChinaCom*, (Xi'an, China), Aug. 2009.

[84] L. Dai, B. Gui, and L. J. C. Jr., "Selective relaying in OFDM multihop cooperative networks," in *Proc. IEEE WCNC*, (Kowloon, Hong Kong, China), Mar. 2007.

[85] J. P. Coon and M. Sandell, "Combined bulk and per-tone transmit antenna selection in OFDM systems," *IEEE Communications Letters*, vol. 14, pp. 426–428, May 2010.

[86] B. Gui, L. Dai, and L. J. C. Jr., "Selective relaying in cooperative OFDM systems: two-hop random network," in *Proc. IEEE WCNC*, (Las Vegas, NV, USA), Mar. 2008.

[87] Y. Li, W. Wang, and F. C. Zheng, "Combined bulk and per-tone relay selection in cooperative OFDM systems," in *Proc. IEEE ICCC*, (Beijing, China), Aug. 2012.

[88] W. Yang and Y. Cai, "Distributed relay selection in OFDM-based cooperative wireless networks," in *Proc. IEEE WiCOM*, (Chengdu, China), Sept. 2010.

[89] M. Kaneko, K. Hayashi, P. Popovski, K. Ikeda, H. Sakai, and R. Prasad, "Amplify-and-forward cooperative diversity schemes for multi-carrier systems," *IEEE Transactions on Wireless Communications*, vol. 7, pp. 1845–1850, May 2008.

[90] M. Haenggi, J. G. Andrews, F. Baccelli, O. Dousse, and M. Franceschetti, "Stochastic geometry and random graphs for the analysis and design of wireless networks," *IEEE Journal on Selected Areas in Communications*, vol. 27, pp. 1029–1046, Sept. 2009.

[91] A. Agarwal and A. K. Jagannatham, "Distributed estimation in homogenous Poisson wireless sensor networks," *IEEE Wireless Communications Letters*, vol. 3, pp. 90–93, Feb. 2014.

[92] S. Sun, T. S. Rappaport, T. A. Thomas, A. Ghosh, H. C. Nguyen, I. Z. Kovcs, I. Rodriguez, O. Koymen, and A. Partyka, "Investigation of prediction accuracy, sensitivity, and parameter stability of large-scale propagation path loss models for 5G wireless communications," *IEEE Transactions on Vehicular Technology*, vol. 65, pp. 2843–2860, May 2016.

[93] H. Wang, S. Ma, T. S. Ng, and H. V. Poor, "A general analytical approach for opportunistic cooperative systems with spatially random relays," *IEEE Transactions on Wireless Communications*, vol. 10, pp. 4122–4129, Dec. 2011.

[94] G. Chen, J. P. Coon, and M. D. Renzo, "Secrecy outage analysis for downlink transmissions in the presence of randomly located eavesdroppers," *IEEE Transactions on Information Forensics and Security*, vol. 12, pp. 1195–1206, May 2017.

[95] E. Basar, U. Aygolu, E. Panayrc, and H. V. Poor, "Orthogonal frequency division multiplexing with index modulation," *IEEE Transactions on Signal Processing*, vol. 61, pp. 5536–5549, Nov. 2013.

[96] C. Y. Wong, R. S. Cheng, K. B. Lataief, and R. D. Murch, "Multiuser OFDM with adaptive subcarrier, bit, and power allocation," *IEEE Journal on Selected Areas in Communications*, vol. 17, pp. 1747–1758, Oct. 1999.

[97] S. Yin and Z. Qu, "Resource allocation in multiuser OFDM systems with wireless information and power transfer," *IEEE Communications Letters*, vol. 20, pp. 594–597, Mar. 2016.

[98] G. Chen, D. Liang, M. Ghoraishi, P. Xiao, and R. Tafazolli, "Optimum user selection for hybrid-duplex device-to-device in cellular networks," in *Proc. IEEE ISWCS*, (Brussels, Belgium), Aug. 2015.

[99] Y. J. Zhang and K. B. Letaief, "Multiuser adaptive subcarrier-and-bit allocation with adaptive cell selection for OFDM systems," *IEEE Transactions on Wireless Communications*, vol. 3, pp. 1566–1575, Sept. 2004.

[100] Y. S. Soh, T. Q. S. Quek, M. Kountouris, and H. Shin, "Energy efficient heterogeneous cellular networks," *IEEE Journal on Selected Areas in Communications*, vol. 31, pp. 840–850, May 2013.

[101] C. Rose and R. Yates, "Location uncertainty in mobile networks: a theoretical framework," *IEEE Comms. Mag.*, vol. 35, pp. 94–101, Feb 1997.

[102] Y. Xu, S. E. Elayoubi, E. Altman, R. El-Azouzi, and Y. Yu, "Flow-level QoE of video streaming in wireless networks," *IEEE Transactions on Mobile Computing*, vol. 15, pp. 2762–2780, Nov. 2016.

[103] L. Atzori, A. Iera, and G. Morabito, "The internet of things: A survey," *Computer networks*, vol. 54, no. 15, pp. 2787–2805, 2010.

[104] S. H. Lee, S. Lee, H. Song, and H. S. Lee, "Wireless sensor network design for tactical military applications: Remote large-scale environments," in *IEEE MILCOM*, (Boston, MA, USA), Oct. 2009.

[105] B. Thomson, J. Bruckner, and A. Bruckner, *Elementary Real Analysis, Second Edition.* www.classicalrealanalysis.com., 2008.

[106] K. J. Arrow and A. C. Enthoven, "Quasi-concave programming," *Econometrica: Journal of the Econometric Society*, pp. 779–800, 1961.

[107] B. Nguyen, R. Afolabi, and K. Kim, "Dependence of outage probability of cooperative systems with single relay selection on channel correlation," *IEEE Communications Letters*, vol. 17, pp. 2060–2063, Nov. 2013.

[108] Y. Chen and C. Tellambura, "Distribution functions of selection combiner output in equally correlated Rayleigh, Rician, and Nakagami-m fading chan-

nels," *IEEE Transactions on Communications*, vol. 52, pp. 1948–1956, Nov. 2004.

[109] A. Ghasemi and E. Sousa, "Fundamental limits of spectrum-sharing in fading environments," *IEEE Transactions on Wireless Communications*, vol. 6, pp. 649–658, Feb. 2007.

[110] K. Hamdi, W. Zhang, and K. Ben Letaief, "Power control in cognitive radio systems based on spectrum sensing side information," in *Proc. IEEE ICC*, (Glasgow, UK), June 2007.

[111] D. Tse and P. Viswanath, *Fundamentals of Wireless Communication*. Wiley series in telecommunications, Cambridge University Press, 2005.

[112] M. Haenggi, *Stochastic Geometry for Wireless Networks*. Stochastic Geometry for Wireless Networks, Cambridge University Press, 2013.

[113] D. Simmons, D. Halls, and J. P. Coon, "OFDM-based nonlinear fixed-gain amplify-and-forward relay systems: SER optimization and experimental testing," in *Proc. IEEE EuCNC*, (Bologna, Italy), Jun. 2014.

[114] G. Huang, Y. Wang, and J. Coon, "Performance of multihop decode-and-forward and amplify-and-forward relay networks with channel estimation," in *Proc. IEEE PacRim*, (Victoria, BC, Canada), Aug. 2011.

[115] M. Abramowitz and I. Stegun, *Handbook of Mathematical Functions: With Formulas, Graphs, and Mathematical Tables*. Dover Publications, 1964.

[116] M. Hasna and M.-S. Alouini, "A performance study of dual-hop transmissions with fixed gain relays," *IEEE Transactions on Wireless Communications*, vol. 3, pp. 1963–1968, Nov. 2004.

[117] A. Asadi, Q. Wang, and V. Mancuso, "A survey on device-to-device communication in cellular networks," *IEEE Communications Surveys Tutorials*, vol. 16, pp. 1801–1819, Fourthquarter 2014.

[118] Y. Cao, T. Jiang, and C. Wang, "Cooperative device-to-device communications in cellular networks," *IEEE Wireless Commun.*, vol. 22, pp. 124–129, Jun. 2015.

[119] M. Sheng, Y. Li, X. Wang, J. Li, and Y. Shi, "Energy efficiency and delay tradeoff in device-to-device communications underlaying cellular networks," *IEEE J. Sel. Areas in Commun.*, vol. 34, pp. 92–106, Jan. 2016.

[120] P. Mach, Z. Becvar, and T. Vanek, "In-band device-to-device communication in OFDMA cellular networks: a survey and challenges," *IEEE Communications Surveys Tutorials*, vol. 17, pp. 1885–1922, Fourthquarter 2015.

[121] M. Hasan and E. Hossain, "Resource allocation for network-integrated device-to-device communications using smart relays," in *Proc. IEEE GLOBECOM*, (Atlanta, GA, USA), Dec. 2013.

[122] Y. Ni, X. Wang, S. Jin, K. K. Wong, H. Zhu, and N. Zhang, "Outage probability of device-to-device communication assisted by one-way amplify-and-forward relaying," *IET Communications*, vol. 9, no. 2, pp. 271–282, 2015.

[123] X. Xiao, X. Tao, and J. Lu, "A QoS-aware power optimization scheme in OFDMA systems with integrated device-to-device (D2D) communications," in *Proc. IEEE VTC Fall*, (San Francisco, CA, USA), Sept. 2011.

[124] G. Zhang, K. Yang, P. Liu, and J. Wei, "Power allocation for full-duplex relaying-based D2D communication underlaying cellular networks," *IEEE Transactions on Vehicular Technology*, vol. 64, pp. 4911–4916, Oct. 2015.

[125] B. Zhong, J. Zhang, Q. Zeng, and X. Dai, "Coverage probability analysis for full-duplex relay aided device-to-device communications networks," *China Communications*, vol. 13, pp. 60–67, Nov. 2016.

[126] B. Kaufman and B. Aazhang, "Cellular networks with an overlaid device-to-device network," in *Proc. IEEE ACSSC*, (Pacific Grove, CA), Oct. 2008.

[127] G. Chen, Y. Gong, P. Xiao, and J. A. Chambers, "Dual antenna selection in secure cognitive radio networks," *IEEE Transactions on Vehicular Technology*, vol. 65, pp. 7993–8002, Oct. 2016.

[128] I. Krikidis, "Relay selection for two-way relay channels with MABC DF: A diversity perspective," *IEEE Transactions on Vehicular Technology*, vol. 59, pp. 4620–4628, Nov. 2010.

[129] Z. Zhang, K. Long, A. V. Vasilakos, and L. Hanzo, "Full-duplex wireless communications: challenges, solutions, and future research directions," *Proceedings of the IEEE*, vol. 104, pp. 1369–1409, Jul. 2016.

[130] R. Merris, *Combinatorics*. Wiley Series in Discrete Mathematics and Optimization, Wiley, 2003.

[131] F.-C. Chang, "Recursive formulas for the partial fraction expansion of a rational function with multiple poles," *Proceedings of the IEEE*, vol. 61, pp. 1139–1140, Aug. 1973.

[132] H. Kung and D. Tong, "Fast algorithms for partial fraction decomposition," *SIAM Journal on Computing*, vol. 6, no. 3, pp. 582–593, 1977.

[133] P. Sun, K. G. Shin, H. Zhang, and L. He, "Transmit power control for D2D-underlaid cellular networks based on statistical features," *IEEE Transactions on Vehicular Technology*, vol. 66, pp. 4110–4119, May 2017.

[134] B. Hajek, "Notes for ECE 534 an exploration of random processes for engineers," *Univ. of Illinois at Urbana–Champaign*, 2009.

[135] A. Guerraggio and E. Molho, "The origins of quasi-concavity: a development between mathematics and economics," *Historia Mathematica*, vol. 31, no. 1, pp. 62–75, 2004.

[136] M. D. Renzo, H. Haas, A. Ghrayeb, S. Sugiura, and L. Hanzo, "Spatial modulation for generalized MIMO: challenges, opportunities, and implementation," *Proceedings of the IEEE*, vol. 102, pp. 56–103, Jan. 2014.

[137] P. Banelli, S. Buzzi, G. Colavolpe, A. Modenini, F. Rusek, and A. Ugolini, "Modulation formats and waveforms for 5G networks: Who will be the heir of OFDM?: An overview of alternative modulation schemes for improved spectral efficiency," *IEEE Signal Processing Magazine*, vol. 31, pp. 80–93, Nov. 2014.

[138] E. Basar, "Multiple-input multiple-output OFDM with index modulation," *IEEE Signal Processing Letters*, vol. 22, pp. 2259–2263, Dec. 2015.

[139] E. Basar, "Index modulation techniques for 5G wireless networks," *IEEE Communications Magazine*, vol. 54, pp. 168–175, Jul. 2016.

[140] P. Yang, Y. Xiao, Y. Yu, and S. Li, "Adaptive spatial modulation for wireless MIMO transmission systems," *IEEE Communications Letters*, vol. 15, pp. 602–604, Jun. 2011.

[141] X. Wu, M. D. Renzo, and H. Haas, "Adaptive selection of antennas for optimum transmission in spatial modulation," *IEEE Transactions on Wireless Communications*, vol. 14, pp. 3630–3641, Jul. 2015.

[142] R. Rajashekar, K. V. S. Hari, and L. Hanzo, "Antenna selection in spatial modulation systems," *IEEE Communications Letters*, vol. 17, pp. 521–524, Mar. 2013.

[143] M. D. Renzo and H. Haas, "Bit error probability of SM-MIMO over generalized fading channels," *IEEE Transactions on Vehicular Technology*, vol. 61, pp. 1124–1144, Mar. 2012.

[144] M. Wen, X. Cheng, M. Ma, B. Jiao, and H. V. Poor, "On the achievable rate of OFDM with index modulation," *IEEE Transactions on Signal Processing*, vol. 64, pp. 1919–1932, Apr. 2016.

[145] N. Ishikawa, S. Sugiura, and L. Hanzo, "Subcarrier-index modulation aided OFDM - will it work?," *IEEE Access*, vol. 4, pp. 2580–2593, 2016.

[146] W. Wang and R. Wu, "Capacity maximization for OFDM two-hop relay system with separate power constraints," *IEEE Transactions on Vehicular Technology*, vol. 58, pp. 4943–4954, Nov. 2009.

[147] Y. Wang, W. Liu, M. Jin, S. Jang, and J. M. Kim, "FQAM/FPSK modulation for spatial modulation systems," in *Proc. IEEE ICTC*, (Jeju, Korea), Oct. 2016.

[148] G. Chen, O. Alnatouh, and J. Chambers, "Outage probability analysis for a cognitive amplify-and-forward relay network with single and multi-relay selection," *IET Communications*, vol. 7, pp. 1974–1981, Nov. 2013.

[149] M. S. Alouini and A. J. Goldsmith, "A unified approach for calculating error rates of linearly modulated signals over generalized fading channels," *IEEE Transactions on Communications*, vol. 47, pp. 1324–1334, Sept. 1999.

[150] M. Chiani and D. Dardari, "Improved exponential bounds and approximation for the Q-function with application to average error probability computation," in *Proc. IEEE GLOBECOM*, Nov. 2002.

[151] L. Zheng and D. N. C. Tse, "Diversity and multiplexing: a fundamental tradeoff in multiple-antenna channels," *IEEE Transactions on Information Theory*, vol. 49, pp. 1073–1096, May 2003.

[152] A. Bader, "Commercial multihop networks," in *Proc. IEEE ICT*, (Doha, Qatar), April 2010.

[153] Z. Gao and B. Wang, "User cooperation in OFDM-based cognitive radio networks with simultaneous wireless information and power transfer," in *Proc. IEEE WCSP*, (Nanjing, China), Oct. 2015.

[154] A. Mukherjee and H. M. Kwon, "General auction-theoretic strategies for distributed partner selection in cooperative wireless networks," *IEEE Transactions on Communications*, vol. 58, pp. 2903–2915, Oct. 2010.

[155] Y. Sun, P. Guo, Z. Ma, T. Li, and S. Dang, "UK-based external business environment analysis of outdoor adventure clothing using the PESTEL tool and its future outlook," in *Proc. IEEE ICITSI*, (Bandung, Indonesia), Nov. 2014.

[156] J. P. Coon, D. E. Simmons, and M. D. Renzo, "Approximating the outage probability of parallel fading channels," *IEEE Communications Letters*, vol. 19, pp. 2190–2193, Dec. 2015.

[157] J. Coon, C. P. Dettmann, and O. Georgiou, "Full connectivity: corners, edges and faces," *Journal of Statistical Physics*, vol. 147, no. 4, pp. 758–778, 2012.

[158] J. Coon, C. P. Dettmann, and O. Georgiou, "Impact of boundaries on fully connected random geometric networks," *Physical Review E*, vol. 85, no. 1, p. 011138, 2012.

[159] G. Chen, P. Xiao, J. R. Kelly, B. Li, and R. Tafazolli, "Full-duplex wireless-powered relay in two way cooperative networks," *IEEE Access*, vol. 5, pp. 1548–1558, Jan. 2017.

[160] Y. Liu and X. Wang, "Information and energy cooperation in OFDM relaying: Protocols and optimization," *IEEE Transactions on Vehicular Technology*, vol. 65, pp. 5088–5098, Jul. 2016.

[161] F. Wang and X. Zhang, "Resource allocation for multiuser cooperative overlay cognitive radio networks with RF energy harvesting capability," in *Proc. IEEE GLOBECOM*, (Washington, DC, USA), Dec. 2016.

[162] X. Huang and N. Ansari, "Data and energy cooperation in relay-enhanced OFDM systems," in *Proc. IEEE ICC*, (Kuala Lumpur, Malaysia), May 2016.

[163] P. Parida and S. S. Das, "Power allocation in OFDM based NOMA systems: a DC programming approach," in *Proc. IEEE GLOBECOM*, (Austin, TX, USA), Dec. 2014.

[164] X. Li, C. Li, and Y. Jin, "Dynamic resource allocation for transmit power minimization in OFDM-based NOMA systems," *IEEE Communications Letters*, vol. 20, pp. 2558–2561, Dec. 2016.

[165] W. Cai, C. Chen, L. Bai, Y. Jin, and J. Choi, "Subcarrier and power allocation scheme for downlink OFDM-NOMA systems," *IET Signal Processing*, vol. 11, pp. 51–58, Feb. 2017.

[166] Y. Tao, L. Liu, S. Liu, and Z. Zhang, "A survey: several technologies of non-orthogonal transmission for 5G," *China Communications*, vol. 12, pp. 1–15, Oct. 2015.

[167] M. Shaat and F. Bader, "Comparison of OFDM and FBMC performance in multi-relay cognitive radio network," in *Proc. IEEE ISWCS*, (Paris, France), Aug. 2012.

[168] F. Bader, M. Shaat, and Y. Medjahdi, "New opportunities for spectrum coexistence using advanced multicarrier scheme," in *Proc. IEEE MCC*, (St.-Malo, France), Oct. 2013.

[169] J. Zhang, A. Nimr, and M. Haardt, "Joint design of multi-tap filters and power control for FBMC/OQAM based two-way decode-and-forward relaying systems in highly frequency selective channels," in *Proc. IEEE ICASSP*, (Brisbane, Australia), Apr. 2015.

[170] M. Woltering, M. Zhang, D. Wuebben, and A. Dekorsy, "Comparison of general multi-carrier schemes in two way relaying channels," in *Proc. IEEE WSA*, (Munich, Germany), Mar. 2016.

[171] M. G. S. Sriyananda and N. Rajatheva, "Performance of an asymmetric and asynchronous decode-and-forward FBMC relay system," in *Proc. IEEE WCNC*, (Istanbul, Turkey), Apr. 2014.

[172] D. Gregoratti and X. Mestre, "AF relaying for FBMC signals," in *Proc. IEEE EuCNC*, (Bologna, Italy), Jun. 2014.